ALT`22

INTERNATIONAL CONFERENCE

Advanced Laser Technologies

BOOK OF ABSTRACTS

September 11-16, 2022

MOSCOW, RUSSIA

УДК 535.21; 535.23; 535. 33; 535.37
ББК 22.343.4; 22.344; 22.345

Abstracts of the 29th International Conference on Advanced Laser Technologies – 2022. – 224 c.

The book contains abstracts of ALT`22 conference reports devoted to fundamental and applied aspects of innovative laser technologies, laser-matter interaction, biomedical photonics, laser systems and materials, laser diagnostics and spectroscopy, nonlinear and terahertz photonics. The book contains abstracts of plenary, invited, oral and poster presentations. The official language of the conference is English.

ALT`22 Conference Book of Abstracts are on the conference website
https://altconference.org/proceedings

ISBN 978-5-6045474-6-5

BOOK OF ABSTRACTS

ALT`22

The 29th International Conference on Advanced Laser Technologies

September 11-16, 2022 / Moscow, Russia

Contents

Organizers and Sponsors

Prokhorov General Physics Institute
of the Russian Academic of Science Russia

Department of Physical Sciences
of the Russian Academy of Sciences

Institute of Spectroscopy of
the Russian Academy of Sciences (ISAN)

Center of Laser Technology
and Material Science

Lomonosov Moscow State University
Russia

National Research Nuclear University
MEPhI, Russia

FRC "Crystallography and Photonics"
of the Russian Academic of Science
Russia

Physics of Wave Phenomena
journal Russia

Conference Chairman

Ivan SHCHERBAKOV (Russia)

Program Committee Chair

Vitaly KONOV (Russia)

International Program Committee

Mukhsin ASHUROV (Republic of Uzbekistan)

Sagdulla BAKHRAMOV (Republic of Uzbekistan)

Aladar CZITROVSKY (Hungary)

Boris DENKER (Russia)

Thomas GRAF (Germany)

Sergey GARNOV (Russia)

Leonid GOLOVAN (Russia)

Pavel KASHKAROV (Russia)

Sergey KLIMENTOV (Russia)

Yuri KULCHIN (Russia)

Vladimir MAKAROV (Russia)

Tofig MAMMADOV (Republic of Azerbaijan)

Attila NAGY (Hungary)

Beat NEUENSCHWANDER (Switzerland)

Kyung Hyun PARK (Korea)

Alexander PRIEZZHEV (Russia)

Alexander SHKURINOV (Russia)

Valery TUCHIN (Russia)

Vadim VEIKO (Russia)

Haohai YU (China)

Irina ZAVESTOVSKAYA (Russia)

Jiyang WANG (China)

Organizing Committee Chair

Vladimir PUSTOVOY (Russia)

PLENARY SESSION

DOI: 10.24412/cl-35039-2022-22-8-8

Single-molecule spectroscopy and nanoscopy: advantages and new horizons

Andrey V. Naumov

Lebedev Physical Institute RAS, Troitsk Branch, Moscow, Russia
Institute for Spectroscopy RAS, Moscow, Russia
Moscow Pedagogical State University, Moscow, Russia
a_v_naumov@mail.ru

The lecture discusses the experimental technique of fluorescence spectromicroscopy of single molecules, and quantum emitters in general, the history of the development of this field, as well as applications for studying the photophysical properties of colloidal semiconductor quantum dots (QDs), organic single molecules (SMs), color centers in diamonds, incl. at cryogenic temperatures. The microscopic nature of the blinking photoluminescence effect of single QDs, the results of studies of local field effects, as well as the processes of spectral diffusion and electron-phonon coupling in impurity polymer media with quantum dots and organic molecules are considered. The results of a comparative analysis with data obtained by other methods (photon echo, Raman scattering, electron microscopy) are presented. The capabilities of the three-dimensional (3D-) fluorescence nanoscopy technique implemented according to the scheme of the double-helix point spread function (DHPSF) with the use of adaptive optics tools are demonstrated.

The lecture presents the results obtained by the team of authors of the Leading Scientific School of Russia headed by RAS Corr. Memb. A.V. Naumov (NSh-776.2022.1.2, www.single-molecule.ru). Researches were supported by State Contract of MPGU (AAAA-20-120061890084-9).

[1] A.V. Naumov et al. **Physics Uspekhi** 56, 605 (2013); Nano Letters 18, 6129 (2018)
[2] I.Y. Eremchev et al. **Physics Uspekhi** 62, 294 (2019); 65 (2022)
[3] E.P. Kozhina et al. **Bull. RAS: Physics** 84, 1465 (2020)
[4] I.Y. Eremchev et al. **J. Phys. Chem.** C 125, 17774 (2021)
[5] A.I. Arzhanov et al. **Photonics Russia** 15, 622 (2021); 16, 96 (2022)

DOI: 10.24412/cl-35039-2022-22-9-9

Nonlinear singular polarization optics of wave beams and pulses

V.A. Makarov

M.V. Lomonosov Moscow State University, Faculty of Physics, Leninskie Gory, Moscow 119991
vamakarov@phys.msu.ru

In the middle of 70's the first experimental evidence of the nonlinear optical activity came to light, giving the impulse to the development of nonlinear polarization optics. The subsequent theoretical and experimental investigations assure that the polarization self-action and interaction of waves are fine and widespread phenomena in nonlinear optics. Despite the popularity and wide range of the considered problems, investigations of the origin and dynamics of the polarization singularities in nonlinear optical processes are virtually absent. The present report focuses on the study of formation of *L*-type *C*-type polarization singularities in the signal beam cross section generated in various nonlinear optical processes.

The conditions of appearance and the behavior of polarization singularities in the cross-section of light beam arising due to nonlinear interaction of elliptically polarized laser beams with a medium with nonlocality of quadratic and cubic optical responses are discussed. The formation dynamics and propagation features of *C*-points, including pairwise creation and annihilation, for sum-frequency and second harmonic generation, beams self-action and interaction and other nonlinear optical processes are presented. The ranges of the parameters of an elliptically polarized Gaussian beam and a medium with local and nonlocal nonlinearity are determined, at which the lines of circular polarization singularity appear in cross sections of propagated beam. The specific features of nonlinear optics with laser beams containing polarization singularities are also discussed.

Analytically found expressions, which relate the values of two parameters characterizing the topological type of linear and circular polarization singularities in nonparaxial light fields to the values of the complex amplitude components of the electric field and their first spatial derivatives are also discussed.

The numerically investigate the interaction of a plane elliptically polarized monochromatic wave on a spherical nanoparticle. In the resulting light field near the particle, the topology of strips, formed by the axes of the polarization ellipses and the normal vectors to their planes, is studied. The strips may have one half-twist only if they enclose a circular polarization singularity line, while almost all other strips, even enclosing the linear polarization singularity lines, are trivial. The correlation between the twisting indices of different strips is found, and their relation to the topological features of points of the singular lines is analyzed.

The found laws of transformation of the total topological indices allow one to get an idea of the fine details of these nonlinear optical processes and may be of interest for creating light beams and pulses with an inhomogeneous distribution of the electric field containing polarisation singularities of a given type by methods of nonlinear optics. The latter are promising for use in quantum information optical systems and can be used in problems of nonlinear bulk and surface spectroscopy of nonlinear media.

I take this opportunity to acknowledge many key contributions to this report by former students and postgraduate students of M.V. Lomonosov Moscow State University. I am indeed grateful to Prof. Dr. A.A. Golubkov, Dr. K.S. Grigoriev, Dr. I.A. Perezhogin, Dr. N.N. Potravkin, and M.P.S. N.Yu. Kuznetsov, G.M. Shishkov, P.S. Ryzhikov, and G.A. Gryaznov.

DOI: 10.24412/cl-35039-2022-22-10-10

Optical Coherence Elastography: Past, Present, and Future

Vladimir Yu. Zaitsev

Institute of Applied Physics, RAS, Nizhniy Novgorod, Russia
vyuzai@ipfran.ru

Over two decades passed after the seminal work by J. Schmitt in which, by analogy with medical ultrasound, he proposed Optical Coherence Elastography (OCE) for evaluation of microscopic strains and characterization of elastic properties of biological tissues. However, only during ~5-7 recent years there appeared practically workable realizations OCT-based imaging of strains, as well as quantitative OCT-based techniques for assessment of elastic properties of biological tissues based on the compression principle and measurements of shear-wave velocities.

These techniques have demonstrated previously unavailable prospects for various applications, where imaging of strains is required (from fairly rapidly varying thermo-mechanical strains, osmotically-induced strains to slow strains due to drying, relaxation, etc.)

Furthermore, quantitative assessment of tissue elasticity beyond conventional linear paradigm has become possible. For oncologic applications, novel possibilities have been demonstrated, in particular feasible in vivo morphological segmentation of tumors with an accuracy very close to results of morphological segmentation of conventional histological images, the obtaining of which requires laborious and invasive procedures. In application to freshly excised samples of breast-cancer tissues, OCT-based elastography opened previously unavailable possibilities of accurate assessment of clean resection boundary. Furthermore, intraoperatively feasible OCE-based differentiation of molecular/morphological subtypes of tumors has been demonstrated. The report gives an overview of these topics.

ALT'22

LASER-MATTER INTERACTION

DOI: 10.24412/cl-35039-2022-22-12-12

From Color Laser Marking to Laser Painting

V. Veiko, G. Odintsova, V. Luong, D. Lutoshina

ITMO University
vadim.veiko@mail.ru

Light is the main source of art around us. It allows us to see colors, and moreover, light itself can be a tool for creating unique pieces of art and designs. Here we demonstrate that a laser acts as a multifunctional and effective tool for creation of masterpieces in a way similar to that of classical paints and brushes. To make analogies between the processes of an artist creating a canvas and laser painting an artwork, we investigate the interaction between focused laser irradiation and metallic surfaces and analyze deeply the optical effects in thin oxide films. For this, we describe the nature of three main artistic operations, which are color making, multiple color change, and erasing managed by a nanosecond laser. These processes are possible due to the material heating above the evaporation point and are proved to be dependent on the cooling rate according to the obtained experimental and theoretical results. Therefore, our work is the first attempt to present the concept of interference-based laser paintbrush, which sets new perspectives for modern art and design.

DOI: 10.24412/cl-35039-2022-22-13-13

Ultrafast excitation of silicon by mid-IR tightly focused laser radiation

F. V. Potemkin

M.V. Lomonosov Moscow State University, Moscow, Russia
potemkin@physics.msu.ru

Silicon (Si) is one of the most important materials for modern electronics and photonics. However, due to low band-gap (~1.1 eV) and high refractive index (~3.3), it is challenging to perform the three-dimensional (3D) femtosecond micromachining of its volume. Novel photonics platform for high-speed data transfer and optical memory demands higher flexibility of the silicon modification, including on-chip and in-bulk inscription regimes. These are deepness, three-dimensionality, controllability of sizes and morphology of created modifications. The two-photon absorption[1], aberrations induced by refractive index mismatch, and plasma delocalization in the pre-focal volume[2] drastically spread the energy of the femtosecond pulse across a large volume and drop the deposited energy density below the threshold of micromodification formation[3]. Shifting central wavelength of a driving pulse into the mid-IR can make the process of photoionization[4] dominant in semiconductors, avoid two- and three-photon absorption, and create single-shot femtosecond micromodification in a bulk Si for a broad range of energies. In this paper, we demonstrate that the tightly focused mid-IR femtosecond pulses are capable of micromodification creation due to overcoming deposited energy density threshold, determined by the latent heat of fusion (about 4 kJ/cm^3) (see Fig.1).

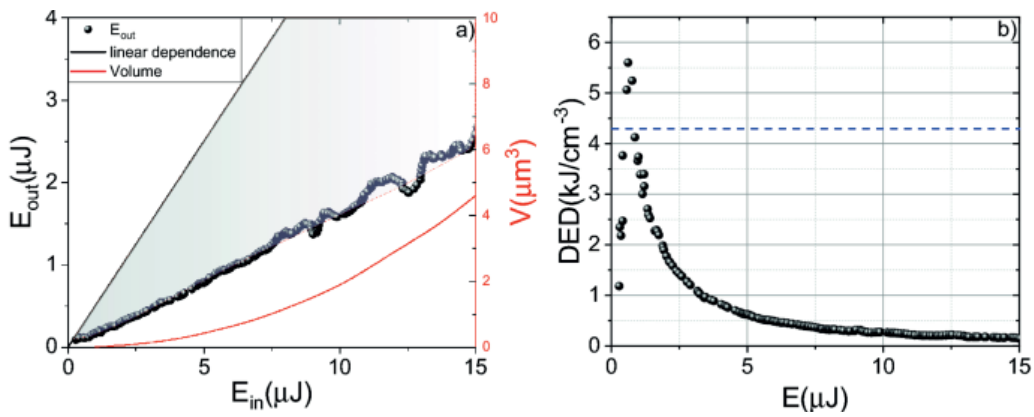

Fig.1 a) Energy dependence of nonlinear transmission (black dots) and interaction volume (solid red line). The shaded area shows the absorbed energy region. b) Dependence of DED on the laser pulse energy. The dotted line shows the threshold of micromodification formation

In such a regime, we successfully performed single-shot bulk microstruturing of silicon. Using third-harmonic and near-IR microscopy, and molecular dynamics, we demonstrated that there is a low-density region in the center of a micromodification, surrounded by a "ring" with higher density, that could be an evidence of its micro-void structure. The formation of created micromodification could be controlled in situ using third-harmonic generation microscopy. The numerical simulation indicates that single-shot damage becomes possible due to electrons heating in the conduction band up to 8 eV (mean thermal energy) and the subsequent generation of microplasma with an overcritical density of 8.5×10^{21} cm^{-3}. These results promise to be the foundation of a new approach of deep three-dimensional single-shot bulk micromachining of silicon[5].

1. E. V. Zavedeev, V. V. Kononenko, and V. I. Konov, «Delocalization of femtosecond laser radiation in crystalline Si in the mid-IR range,» Laser Physics **26**(1), 016101 (2016).
2. E. I. Mareev, K. V Lvov, B. V Rumiantsev, E. A. Migal, I. D. Novikov, S. S. Yu, and P. F.V., «Effect of pulse duration on the energy delivery under nonlinear propagation of tightly focused Cr : forsterite laser radiation in bulk silicon,» Laser Phys. Lett. **17**, 015402 (2019).
3. V. V. Kononenko, V. V. Konov, and E. M. Dianov, «Delocalization of femtosecond radiation in silicon,» Optics Letters **37**(16), 3369 (2012).
4. E. Migal, E. Mareev, E. Smetanina, G. Duchateau, and F. Potemkin, «Role of wavelength in photocarrier absorption and plasma formation threshold under excitation of dielectrics by high-intensity laser field tunable from visible to mid-IR,» Scientific Reports **10**(1), 1–10 (2020).
5. E. Mareev, A. Pushkin, E. Migal, K. Lvov, S. Stremoukhov, and F. Potemkin, «Single-shot femtosecond bulk micromachining of silicon with mid-IR tightly focused beams,» Scientific Reports 2022 12:1 **12**(1), 1–12 (2022).

DOI: 10.24412/cl-35039-2022-22-14-14

Laser synthesis of linear carbon: new route of molecular optics

A. Kucherik[1], S. Kutrovskaya[1,2], A. Osipov[1], V. Samyshkin[1], A. Abramov[1], A. Povolotskiy[3]

1 - Department of Physics and Applied Mathematics, Stoletov Vladimir State University, 600000 Gorkii street, Vladimir, Russia
2 - Skolkovo Institute of Science and Technology, 30 Bolshoy Boulevard, bld. 1, 121205 Moscow, Russia
3 - Institute of Chemistry, St. Petersburg State University,198504, Ulianovskaya str. 5, St. Petersburg, Russia
kucherik@vlsu.ru

Here we study stable elongated carbon chains synthesized by the laser ablation technique in a colloidal solution [1]. The mechanical stabilisation of carbyne is achieved due to the electron bonding of carbon chains to gold nanoparticles (NPs) [2]. When deposited on a substrate, the stabilized chains demonstrate straight parts whose lengths significantly exceed the theoretical limit for a free stable monoatomic carbon chain. The high-resolution transmission electron microscopy (HR TEM) of our samples shows straight linear carbon chains of the lengths that sometimes exceed 5 nm. The time-resolved photoluminescence (TRPL) spectra show that the radiative life-time of the observed transitions is of the order of 1 ns, that is similar to the data reported for excitons in CNTs. The exciton radiative lifetime decreases with the decrease of the length of the chain. We refer to the Su-Schrieder-Heeger model [3] to argue that the transition that dominates low temperature PL spectra is based on the edge electronic states that form the HOMO-LUMO pair in carbon chains stabilized by gold NPs.

The study was carried out using the equipment of the interregional multispecialty and interdisciplinary center for the collective usage of promising and competitive technologies in the areas of development and application in industry/ mechanical engineering of domestic achievements in the field of nanotechnology (Agreement No. 075-15-2021-692 of August 5, 2021). This work was also partially supported by the framework of the state task of VlSU № 0635-2020-0013

[1] A. Kucherik, S.M Arakelian et al Two-stage laser-induced synthesis of linear carbon chains, Quantum Electronics 46, 627 (2016).
[2] S. Kutrovskaya, I. Chestnov et al Electric field assisted alignment of monoatomic carbon chain, Scientific Reports 10(1) (2020)
[3] W. P. Su, J. R. Schrieffer, and A. J. Heeger, Solitons in polyacetylene, Phys. Rev.Lett. 42, 1698 (1979).

DOI: 10.24412/cl-35039-2022-22-15-15

Laser-Induced Forward Transfer of CVD Graphene for Electronic Applications

M. Komlenok, N. Kurochitsky, P. Pivovarov, M. Rybin, E. Obraztsova, V. Konov

Prokhorov General Physics Institute of the Russian Academy of Sciences, st. Vavilova 38, Moscow, 119991 Russia
Main author email address: komlenok@nsc.gpi.ru

The patterning and transfer of a graphene film without damaging its original structure is an urgent and difficult task for realizing the unique physical properties of a two-dimensional material in nanotechnology. For this purpose, we propose the use of the laser-induced forward transfer (LIFT), which has proven itself in the selective transfer of such delicate materials. The ease of implementation of laser techniques reduces the number of intermediate manipulations with a graphene film, increasing its safety. The work demonstrates the promise of LIFT of single-layer graphene from a metal surface to an arbitrary substrate at room temperature and in an ambient environment. The effect of the parameters of this method on the structure of transferred graphene islands is investigated. The relevance of reducing the distance between irradiating and receiving substrates for the transfer of free-lying graphene is demonstrated. The reasons for the damage to the integrity of the carbon film observed in the experiments are discussed. The preservation of the original crystal structure of transferred graphene under optimized conditions is confirmed by Raman spectroscopy. The proposed technique allows the formation of emitting crumpled graphene patterns without loss of the quality of initially synthesized graphene. Electron field emission properties of crumpled graphene imprints 1x1 mm^2 in size are studied. The transferred graphene flakes demonstrate competitive adhesion and emission characteristics.

The research was funded by the Russian Science Foundation, grant number 18-72-10158.

DOI: 10.24412/cl-35039-2022-22-16-16

Magnetic fields generated by light in dielectric particles

B.S. Lukiyanchuk

Faculty of Physics, Lomonosov Moscow State University
lukiyanchuk@nanolab.phys.msu.ru

In 2010, it was theoretically demonstrated in [1] that a plane wave incident on a dielectric nanosphere with a high refractive index excites a large magnetic moment in it. This phenomenon was confirmed experimentally [2] and became the basis for creating resonant dielectric nanostructures with a high refractive index [3]. Resonant scattering of electromagnetic waves is a widely studied phenomenon with a vast range of applications that span completely different fields, from astronomy or meteorology to spectroscopy and optical circuitry. Despite being subject of intensive research for many decades, new fundamental aspects are still being uncovered, in connection with emerging areas, such as metamaterials and metasurfaces or quantum and topological optics, to mention some. We show that weakly dissipating dielectric spheres made of materials such as glass, quartz, etc. can support high order Fano resonances associated with internal Mie modes [4]. These resonances, happening for specific values of the size parameter, yield field-intensity enhancement factors on the order of 10^4–10^7, which can be directly obtained from analytical calculations. Associated to these "super-resonances", we analyze the emergence of magnetic nanojets with giant magnetic fields, which might be attractive for many photonic applications. We show experimentally [5] that GHz radiation illuminating a high refractive index ceramic sphere creates instant magnetic near-fields comparable to those in neutron stars, opening up a new paradigm for creation of giant magnetic fields on the millimeter's scale. Recently we demonstrated the ability to create big magnetic fields in photonic lenses with whispering gallery waves at Janus particles [6].

[1] A. B. Evlyukhin et al.// *Phys. Rev. B.* **82**, 045404, (2010).
[2] A. I. Kuznetsov et al.// *Scientific Reports* **2**, 492 (2012).
[3] A. I. Kuznetsov et al.// *Science* **354**, aag2472 (2016).
[4] Z. B. Wang et al.// *Scientific Reports* **9**, 20293 (2019).
[5] B. Luk`yanchuk et al.// *Scientific Reports* **11**, 23453 (2021).
[6] I. V. Minin et al.// *Opto-Electron Science* **1**, 210008 (2022).

DOI: 10.24412/cl-35039-2022-22-17-17

3D inflection and 1D-3D attenuation of initially planar shock wave generated by femtosecond laser pulse

V. Shepelev[1], Y. Petrov[2,3], N. Inogamov[2,4], V. Zhakhovsky[4,5], E. Perov[5], S. Fortova[1]

1- Institute for Computer-Aided Design of the Russian Academy of Sciences, 19/18, 2nd Brestskaya st., Moscow 123056, Russia
2- Landau Institute for Theoretical Physics of the Russian Academy of Sciences, 1a, Akademika Semyonova st., Chernogolovka, Moscow region 142432, Russia
3- Moscow Institute of Physics and Technology, 9, Institutskiy per., Dolgoprudny, Moscow Region 141701, Russia
4- Dukhov All-Russian Research Institute of Automation, 22, Sushchevskaya st., Moscow 127055, Russia
5- Joint Institute for High Temperatures of the Russian Academy of Sciences, 13 Bldg.2, Izhorskaya st., Moscow 125412, Russia
nailinogamov@gmail.com

Evolution of wavefront geometry during propagation and attenuation of initially planar shock waves generated by femtosecond laser pulses in aluminum is studied. We demonstrate that three stages of shock front inflection take place in consistent hydrodynamics and molecular dynamics simulations [1].

During the first stage, the distance (D) traveled by a near-planar shock wave (SW) DSW $\lesssim$ RL is smaller than the radius of heated laser spot RL. Wave attenuation is associated with one-dimensional plane (1D) rarefaction wave coming from the free surface. Such rarefaction wave shapes the shock wave to a 1D triangular pressure profile along direction normal to target surface with a shock front followed by an unloading tail. The second transitional stage starts after propagation of DSW $\sim$ RL, at which the unloading lateral waves begin to arrive to a symmetry axis of flow and initiate inflection of the initially planar shock front. Next at the third stage, the wavefront geometry is finally rounded and rapid attenuation of shock pressure begins at DSW $\gtrsim$ RL.

It is shown that such divergent shock wave cannot generate plastic deformations in aluminum shortly after propagation of DSW $\sim$ RL. Thus, we may estimate the maximal laser shock peening (LSP) depth as a radius of focal spot, which sets an upper limit for the laser shock peening.

The cessation of plastic deformation is caused by the fall of the shockwave amplitude below the Hugoniot elastic limit (HEL). Value of the HEL is much larger for ultrashort SWs than is usually supposed [2,3]. When SW amplitude becomes less than HEL, then the laser elastic-plastic wave transits to a purely elastic mode of propagation [1,4,5]. For large-sized light spots, this transition ends in the 1D mode of propagation.

[1] V. Shepelev et al., Attenuation and inflection of initially planar shock wave generated by femtosecond laser pulse, Optics & Laser Technology, vol. 152, 108100, (2022). https://doi.org/10.1016/j.optlastec.2022.108100
[2] V. Zhakhovsky and N. Inogamov, Elastic-plastic phenomena in ultrashort shock waves, JETP Lett., vol. 92(8), pp. 521-526, (2010). DOI: 10.1134/S0021364010200063
[3] S. Ashitkov et al., Behavior of Aluminum near an Ultimate Theoretical Strength in Experiments with Femtosecond Laser Pulses, JETP Lett., vol. 92(8), pp. 516-520, (2010). https://doi.org/10.1134/S0021364010200051
[4] N. Inogamov et al., Laser Shock Wave: The Plasticity and Thickness of the Residual Deformation Layer and the Transition from the Elastoplastic to Elastic Propagation Mode, JETP Lett., vol. 115, pp. 71-78, (2022). Doi 10.1134/S0021364022020047
[5] В. Хохлов и др., Плавление титана ударной волной, вызванной мощным фемтосекундным лазерным импульсом, Письма ЖЭТФ, том 115(9), сс. 576-584, (2022). DOI: 10.31857/S1234567822090051

DOI: 10.24412/cl-35039-2022-22-18-18

Mechanisms of femtosecond ablation of optical crystals depending on free electron lifetime

Sergey Klimentov [1], Stéphane Guizard[2], Nikita Fedorov[3], Allan Bildé[2], Alexandros Mouskeftraras[4], Anton Popov[1]

1 National Research Nuclear University "MEPhI", Moscow, Russia
2 Laboratoire des Solides Irradiés, Ecole Polytechnique, Palaiseau, France,
3 Centre Lasers Intenses et Applications, Université Bordeaux I, Talence, France
4 Laboratoire LP3, Aix-Marseille University, CNRS, UMR 7341, 13009 Marseille, France.
smklimentov@mephi.ru

Intense ultrashort laser pulses have proven to be a versatile tool for today technologies of wide band gap materials including precision modification, ablative micromachining and fabrication of nanomaterials for biomedical applications [1]. The effect of laser exposure and the particular sequence of stages, or mechanisms, resulting in modification and ablation are critically dependent not only on characteristics of the incident laser pulse but also on the nature of irradiated materials, primarily on the fast photo-electron kinetics playing the clue role in deposition of energy into the lattice of the dielectric. In our study, we focus in interaction of femtosecond IR, visible and UV pulses with the conventional optical materials, namely the crystalline quartz, sapphire, magnesium oxide and alkali halides, the model materials featured by the high initial transparency and the lifetime of free electrons covering the range form tens of femtoseconds to hundreds of picoseconds.

The pump-probe experimental approach employing three synchronized ultrashort laser pulses have been used in several kinds of complementary measurements, when the first pump pulse in the trio was tailored to generate free electrons via multiphoton absorption, the second pump aimed to boost their energy via the induced intraband absorption, while the third one was used to probe the transient absorption and refraction index modification, brought on by the first and the second pulses, aiming to observe and quantify possible multiplication of the charge carriers via impact ionization mechanism. The automated experimental setup allowed to choose pulse-width, wavelength and delay between the first two pulses which was then fixed during the measurement. The third one, usually the shortest, arrived at variable delay to trace the fast electron kinetics. Variety of ablation thresholds was measured in the same two pump experimental conditions with the reference to a particular electron concentration induced by the first pulse. The geometry of interaction was kept unchanged as much as possible in the different kinds of measurements. Energy of the electrons within the conduction band was estimated in similar configuration in two-pulse photo-electron spectroscopy experiments. This way, the complete set of direct measurements was performed for quantitative characterization of all stages of the kinetics ending up at the surface ablation in these materials.

The obtained experimental data and the results of theoretical modeling indicate the cascade intraband absorption, occurring simultaneously with electron-phonon coupling, to play the clue role in laser ablation of optical crystals known for long free electron lifetime (Al_2O_3 and MgO) which happens through the mechanism of thermal instability of the lattice, in spite of the short pulses involved in the excitation process. The evidences of free electron multiplication via impact ionization were revealed only in SiO_2 and alkali halides known for the fast trapping of electrons with formation of self-trapped excitons [2]. In spite of popular opinion, electron multiplication or the avalanche was not the main cause of optical breakdown in any of the studied cases. The research received partial financial support from LASERLAB-EUROPE (the grant agreement 654148).

[1] A. Popov, G. Tikhonovski, P. Shakhov, E. Popova-Kuznetsova, G. Tselikov, R. Romanov, A. Makeev, S. Klimentov, A. Kabashin, Synthesis of Titanium Nitride Nanoparticles by Pulsed Laser Ablation in Different Aqueous and Organic Solutions, Nanomaterials, vol. 12(10), p. 1672 (2022)
[2] S. Guizard, S. Klimentov, A. Mouskeftaras, N. Fedorov, G. Geoffroy, C. Vilmart, Ultrafast Breakdown of dielectrics: Energy absorption mechanisms investigated by double pulse experiments, Applied Surface Science, vol. 336, pp. 206-211 (2015)

DOI: 10.24412/cl-35039-2022-22-19-19

Ultrafast laser processing of photosensitive planar junctions in graphene and carbon nanotube field-effect transistors

A.V. Emelianov[1,2], N.P. Nekrasov[1], I.I. Bobrinetskiy[1,3]

1- National Research University of Electronic Technology, 1 Shokin square, Moscow, Zelenograd, Russia
2- P. N. Lebedev Physical Institute of the Russian Academy of Sciences, 53 Leninsky Prospect, Moscow, Russia
3- BioSense Institute, University of Novi Sad, 1 Dr Zorana Djindjica, Novi Sad, Serbia
Main author email address: emmsowton@gmail.com

The ultrafast laser processing of low-dimensional materials is a new powerful tool for tailoring the electronic, optical and mechanical properties of matter via interaction with low energy photons. When the ultrashort laser pulse interacts with free electrons in the hexagonal carbon lattes the different dynamics of hot electronics can occur resulting in the different effect of atomic structure as well as chemical properties of materials. Even the ablation of carbon lattice can have different mechanism when irradiated with femtoseconds laser pulses. We have shown that depending on the accumulated fluence managed by number of picoseconds laser pulses the graphene ablation can happen by two different mechanisms [1]: thermo-acoustical layer detachment and photochemical oxidative etching. The physical mechanism behind these effect can lay in the integration of hot electrons and photons on different time scales. While pulses are separated in time for low frequencies the only higher energies can lead to braking the C-C bonds and detaching the carbon lattice resulting in "conventional" ablation. At a high repetition rate of low-intensity pulses with a period shorter than the decay time of optical photons, hot electrons are excited and the surrounding molecules are activated, which leads to photochemical processes, such as oxidation in the presence of oxygen molecules [2].

In this report we demonstrate the using of photochemical interaction of femtosecond laser pulses with the channel of field-effect transistors made of graphene or carbon nanotubes to produce planar junction sensitive to visible light. Pristine graphene and carbon nanotubes show a very weak response to visible light; while are activly studied for IR application.The fabrication of planar junctions in carbon nanomaterials is a promising way to increase the optical sensitivity of optoelectronic nanometer-scale devices in photonic connections, sensors, and photovoltaics [3, 4]. Utilizing a unique lithography approach based on direct femtosecond laser processing, a fast and easy technique for modification of graphene and single-walled carbon nanotube (SWCNT) optoelectronic properties through localized two-photon oxidation is developed. It results in a novel approach of quasi-metallic to semiconducting nanotube conversion so that metal/semiconductor planar junction is formed via local laser patterning. The fabricated planar junction in the field-effect transistors based on individual SWCNT drastically increases the photoresponse of such devices. The broadband photoresponsivity of the two-photon oxidized structures reaches the value of 2×10^7 A/W per single SWCNT at 1 V bias voltage and zero gate votage. The SWCNT-based transistors with induced metal/semiconductor planar junction can be applied to detect extremely small light intensities with high spatial resolution. We also had demonstrated that the photocurrent generation in $p–p^+$ junctions formed in single-layer graphene is related to the photothermoelectric effect. The photoresponsitivity of laser patterned single-layer graphene junctions is shown to be as high as 100 mA/W with noise equivalent power less than 6 kW/cm^2. These results open a path to a low-cost maskless technology for fabrication of graphene-based optoelectronic devices with tunable properties for spectroscopy, signal processing, and sesning applications.

[1] I. Bobrinetskiy, A. Emelianov, A. Nasibulin, I. Komarov, N. Otero, P.M. Romero, Photophysical and photochemical effects in ultrafast laser patterning of CVD graphene, Journal of Physics D: Applied Physics, vol. 49(41), pp. 41LT01 (2016).
[2] J. Aumanen, A. Johansson, J. Koivistoinen, P. Myllyperkiö, M. Pettersson, Patterning and tuning of electrical and optical properties of graphene by laser induced two-photon oxidation, Nanoscale, vol. 7, pp. 2851, (2015).
[3] A.V. Emelianov, D. Kireev, A. Offenhäusser, N. Otero, P.M. Romero, I.I. Bobrinetskiy, Thermoelectrically Driven Photocurrent Generation in Femtosecond Laser Patterned Graphene Junctions, ACS Photonics, vol. 5(8), pp. 3107-3115, (2018)
[4] A.V. Emelianov, N.P. Nekrasov, M.V. Moskotin, G.E. Fedorov, N. Otero, P.M. Romero, V.K. Nevolin, B.I. Afinogenov, A.G. Nasibulin, I.I. Bobrinetskiy, Individual SWCNT Transistor with Photosensitive Planar Junction Induced by Two-Photon Oxidation. Adv. Electron. Mater., vol. 7, pp. 2000872(1-11), (2021).

DOI: 10.24412/cl-35039-2022-22-20-20

Specific mechanisms of nonlinear absorption of intense ultrashort mid-infrared laser pulses in transparent semiconductors

V. Gruzdev

Department of Physics and Astronomy, University of New Mexico,
210 Yale Blvd. NE, Albuquerque, NM, 87106, USA
Main author email address: vgruzdev@unm.edu

Since discovery of generation of very-high order harmonics by high-power femtosecond laser pulses in semiconductors [1, 2], increasing research efforts are being focused on ultrafast laser-semiconductor interactions at mid-infrared wavelengths. Absorption of laser radiation is the basic effect that triggers a broad range of those interactions. For the semiconductors transparent to low-intensity laser pulses, the traditional models [3-5] suggest domination of nonlinear multiphoton absorption due to inter-band multiphoton or tunneling electron excitation and linear absorption by laser-generated free carriers. However, they miss some special effects characterisitc of the ultrafast mid-infrared laser-semiconductor interactions. First, reduced photon energy (as compared to near-infrared wavelength range) supports generation of free electrons at a near-bottom part of conduction band that favors reduced electron-phonon collision rate. Second, extended wavelengths of the mid-infrared range suggest feasibility of transferring large amounts of ponderomotive energy from laser radiation to electrons via laser-driven electron oscillations. The energy is enough for specific intra-band free-electron excitatiosn even at moderate intensity, but may exceed band gap at higher intenisty. Third, complicated band structure of typical semiconductors suggest feasibility of specific intra-band and inter-band excitations with contributions from multiple energy bands. Finally, the special features of laser-driven free-carrier dynamics suggest significnat contribution of the absorption mechanisms that are considered as not effective at shorter wavelengths of near-infrared radiation.

In this talk, we overview the major mechanisms and specific physical effects of inter-band and intra-band electron excitations produced in typical semiconductors by mid-infrared laser pulses that contain a few (from 3 to 10) opticall cycles. Estimations are reported GaAs, GaP, GaN, and ZnSe at peak intensity varying from 10 GW/cm^2 to damage and ablation thresholds. Of major focus are the special features of inter-band electron transitions driven by the laser pulses with significant spectrum width, contributions of multiple bands to the laser-driven free-carrier generation, the free-carrier absorption influenced by inter-conduction-band and inter-valley transitions, and special mechanisms of mid-infrared absorption, e. g., Brunel-type absorption and free-carrier multiphoton absorption. We discuss the fundamental limitations of the traditional models of light absorption and compare theoretical predictions against available experimental data.

This work is supported by Research Technology & Laboratory Directorate / Basic Research Office of the US Department of Defense via Newton Award for Transformative Ideas during the COVID-19 Pandemic No. HQ00342010028 and the Air Force Office of Scientific Research under award number FA9550-15-1-0254.

[1] S. Ghimire, A. D. DiChiara, et al, «Observation of high-order harmonic generation in a bulk crystal,» *Nat. Phys.* **7**, 138 (2011).
[2] S. Ghimire, D. A. Reis, "High-harmonic generation from solids", *Nat. Phys.* **15**, 10-16 (2019).
[3] A. Kaiser, et al, "Microscopic processes in dielectrics under irradiation by subpicosecond laser pulses", *Phys. Rev. B* **61**, 11437 (2000).
[4] S.S.Mao, F.Quere, S.Guizard, X.Mao, R.E.Russo, et al, *Appl. Phys. A* **79**, 1695 (2004).
[5] P. Balling and J. Schou, *Rep. Prog. Phys.* **76**, 036502 (2013).

DOI: 10.24412/cl-35039-2022-22-21-21

Role of the leaf epidermis in the interaction of low-intensity laser radiation with the plant regulatory system

Yu.N. Kulchin[1], E.P. Subbotin[1], A.S. Kholin[1], D.O. Gol'tsova[1], S.O. Kozhanov[2], E.I. Markovetc[2]

[1]Institute of Automation and Control Processes Far Eastern Branch of the Russian Academy of Sciences (IACP FEB RAS), Far Eastern Branch of the Russian Academy of Sciences, 5 Radio str., Vladivostok, 690041, Russia
[2]Far Eastern Federal University, 10 Ajax Bay, Russky Island, Vladivostok 690922, Russia
kulchin@iacp.dvo.ru

Among the many factors that affect the life of all plant organisms and crops in particular, solar energy is one of the most significant. Nutrients, sufficient air and moisture cannot fully ensure the harmonious development of plants. It is photons, particles of light, that are the energy source of photosynthesis – the most important process that occurs in plants, as a result of which organic compounds are formed from carbon dioxide, water and minerals. In addition, plants use sunlight as a source of information.

As a result of long-term experiments and observations, scientists were able to establish that by regulating such high-quality indicators of light radiation as spectral composition, intensity, exposure time (photoperiod), dose and nature (pulse or continuous light) of radiation, an increase in crop yield by 30% can be stimulated. It was also noted that radiation polarization also has a certain biostimulatory effect on plants. But beyond understanding, mechanisms remained to determine the effect of radiation polarization on plants. We drew attention to the fact that plant leaves are a complex multilayer and multicellular structure with a certain anisotropy of mechanical stress, which can cause anisotropy of their optical properties. A special place in this system is occupied by the layer of the epidermis of plant leaves [1].

The purpose of this report is to discuss issues aimed at understanding the role of the leaf epidermis in the interaction of low-intensity polarized laser radiation with plants, which may cause the regulation of some stages of their development.

Financial support was provided by the Russian Science Foundation, grant № 20-16-00016.

[1] Yu.N. Kulchin, A.A. Sergeev, Yu.A. Zinin, D.O. Gol'tsova, S.O. Kozhanov, E.P. Subbotin Simulation of interaction of polarised laser light with plant leaves. Quantum Electronics 51 (10) 947–952 (2021).

DOI: 10.24412/cl-35039-2022-22-22-22

Laser-ablative synthesis of multimodal nanoparticles for nuclear nanoteranostics

Irina N. Zavestovskaya[1,2]

[1]P.N. Lebedev Physical Institute, Moscow, Russia;
[2]MEPHI, Moscow, Russia
E-mail address: Zavestovskayain@lebedev.ru

Recent data which we have in realization of the joint project with LPI, MEPHI and Tsyb Radiological Center show that the field of nuclear medicine can be significantly expanded by integrating with nanomedicine, which utilizes nanoparticles (NPs) as carriers of radionuclides or as radiosensitizers for radiation therapy and/or active agents for imaging (radiopharmaceutical medicines in situ). The synergy of laser nanotechnology with nuclear medicine opens up a new direction of cancer imaging and therapy - nuclear nanotheranostics.

Laser ablation has appeared as a new non-chemical pathway for the synthesis of nanomaterials, which is free of limitations of conventional chemical approaches and makes possible the synthesis of ultrapure nanostructures. In this approach, small nanoscale clusters are naturally formed during laser ablation from a solid target, and then released into a liquid ambient to form a colloidal nanoparticle solution. Laser ablation can provide nanomaterials exhibiting unique properties and functionalities.

The properties of NPs as an increased ratio of surface area to volume, the ability of passive/active guidance and high load capacity, a large cross-section of interaction with biological tissues, unique properties of the surface of nanomaterials, easy giving of many functions to nanomaterials, etc. are used. All these properties of laser-synthesized nanomaterials promise their successful employment in theranostics.

We propose different types of NPs synthesized by promising laser-based approaches as a NPs for nanotheranostics. One can use these methods to make stable colloidal dispersions of nanoparticles in both organic and aqueous media, which are suitable for a multitude of applications across the important fields of health care. For example, size tailoring allows production of Si*NPs with efficient photoluminescence that can be tuned across a broad spectral range from the visible to near-IR by varying particle size and surface functionalization. These applications encompass several types of bioimaging and various therapies, including phototherapy, RF thermal therapy, and radiotherapy. In addition, in contrast to nanostructures prepared by conventional chemical or electrochemical routes, laser-synthesized NPs have ideal round shape, controllable size with low size dispersion, and are free of any toxic impurities, which promises a better transport in vivo and the absence of side effects.

We demonstrate the possibility for fast PEGylization and conjugation of laser-synthesized Si*NPs with Rhenium-188 (188Re) radionuclide, which is one of most promising generator-type therapeutic beta-emitters with the energy of positron emission of 1.96 MeV (16.7%) and 2.18 MeV (80%) and half-decay time of 17 hours. Our tests on rat survival demonstrate excellent therapeutic effect (72% survival compared to 0% of the control group). Combined with a series of imaging and therapeutic functionalities based on unique intrinsic properties of Si*NPs, the proposed biodegradable complex promises a major advancement of nuclear nanomedicine.

Technologies of targeted proton therapy technologies using promising nanoparticles and systems based on them as therapy sensitizers and active agents for diagnostics are considered. The latter direction involves a significant expansion of the field of modern nuclear medicine through integration with nanotheranostics, which uses nanoparticles for the diagnosis and therapy of cancer, using their unique properties. The introduction of non-radioactive materials that can be activated from the outside using various external sources of nuclear particles to produce radioactivity in situ is one of the new directions of activation of nano-drugs at the site of a cancerous tumor, which can be considered as in situ production of radiopharmaceuticals. Such binary radiotherapy technologies become especially efficient when one can achieve a high tumor/non-tumor action contrast, which enables to minimize side effects related to the irradiation of healthy issues.

The study is supported by the Ministry of Science and Higher Education of RF (project No 075-15-2021-1347), RFBR (project No 20-20-00861).

DOI: 10.24412/cl-35039-2022-22-23-23

Laser functionalization of titanium surface for medical applications

G. Odintsova, V. Veiko, Yu. Karlagina

ITMO University, Kronverksky Pr. 49, bldg. A, St. Petersburg, 197101, Russia
Main author email address: gvodintsova@itmo.ru

The past year has convincingly shown how important healthcare is in modern society. Improving the quality of medical services, development of new medicines, medical equipment and instruments is a critical condition for maintaining the health, ability to work, longevity and quality of life of the population of our country. One of the well-known examples is dental implantology. The installation of dental implants can not only fully restore all the functions of the teeth like mechanical processing and retention of food, participation in the formation of speech sounds and aesthetic function, but also prevent bone tissue atrophy.

As science and technology develop, new areas of application are revealed and new materials and methods of their processing appear, which states a new problem as how to the control of surface properties (at micro- and nano-level). With the advent of laser technologies, it has become possible to locally control the surface geometry and partly its chemical composition (during processing in various media) in order to impart certain properties to it.

In this work, we propose to give the following properties to implants and other medical metal products: improvement of biocompatibility (implants for various purposes); increase in bacterial resistance (medical instruments, orthopedic components: abutments, screws, membranes, etc.); product identification (medical instruments, orthopedic components: abutments, screws, membranes, etc.).

As an example, we present an ideal implant consisting of three functional zones (Fig. 1). The first zone is an implant screw in contact with a trabecular bone, which we treated with a "Groove" type structure with a cell size comparable to one of the bone tissue. The second zone is a collar of the implant in contact with the compact bone, on which we recreated the biomimetic structure of the bone tissue - "Osteon".

The first two zones showed improved cell proliferation, differentiation, and migration.

The third zone is an abutment in contact with an epithelium tissue, on which we created an oxide film exhibit high photoactivity when irradiated with UV light, which leads to the formation of hydroxyl radicals, which gradually destroy bacterial membranes, which leads to their death.

Authors acknowledge the support of the Ministry of Science and Higher Education of the Russian Federation research agreement No. 075-11-2021-045 of 24.06.2021, project title "Development of high-tech production of equipment and technologies for laser functionalization of the surface of medical products" (within the framework of decree of the Government of the Russian Federation No. 218 of 09.04.2010).

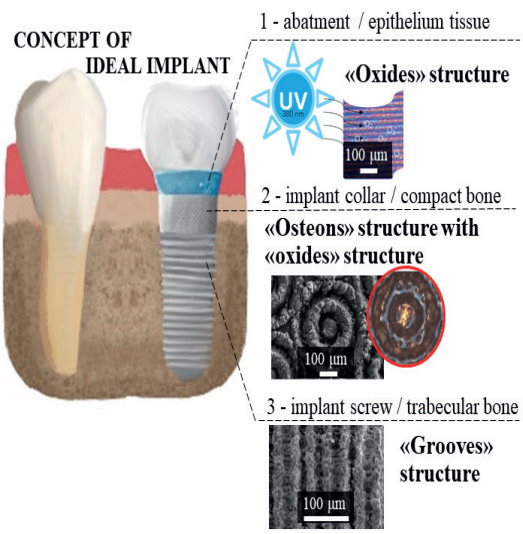

Fig. 1. Concept of ideal dental implant

DOI: 10.24412/cl-35039-2022-22-24-24

Laser synthesis of colloidal nanomaterials for biomedicine

Anton Popov

Institute of Engineering Physics for Biomedicine (Phys-Bio), Moscow Engineering Physics Institute
aapopov1@mephi.ru

Pulsed laser ablation in liquids is a "green" physical technique for NPs synthesis, which offers an exceptional purity level of the nanomaterials. This method profits from natural generation of nanoclusters under ablation of a solid target by laser irradiation in various liquids. The technique does not require any specific chemicals for the synthesis. Therefore, it can avoid any residual contamination of NPs surface and solvent itself. This feature of the laser ablative synthesis makes the produced nanomaterials very perspective for various applications including catalysis and biomedicine. Here we present our recent results in synthesis of various functional colloidal nanomaterials by methods of pulsed laser ablation in liquids for biomedical applications.

DOI: 10.24412/cl-35039-2022-22-25-25

Direct laser writing of copper micropatterns from deep eutectic solvents: chemical and physical aspects

Lev Logunov [1], Ekaterina A. Avilova [1], Evgeniia M. Khairullina [2], Andrey Yu. Shishov [2], Aleksandra Levshakova [2], Dmitry A. Sinev [1], Ilya I. Tumkin[2]

[1]School of Physics and Technology, ITMO University, 197101 St. Petersburg, Russia;
[2]Institute of Chemistry, Saint Petersburg University, SPbU, 7/9 Universitetskaya nab., St. Petersburg 199034, Russia
e-mail: i.i.tumkin@spbu.ru, +7 911 127 9134

In comparison with traditional methods such as photolithography and processes occurring at high vacuum, additive technologies are promising and rather cheap for fabrication of materials on different surfaces, including polymers. It is known that recently the demand for various optoelectronic devices such as liquid crystal displays (LCDs), touch screens, solar cells, organic light-emitting diodes (OLED) and electrochromic devices has been significantly increasing [1].

In this work, we present a new approach based on deep eutectic solvents (DES)-assisted synthesis of conductive copper structures using regular technique of laser-induced liquid deposition of metals (LCLD). The main benefits of such a modified LCLD are no need to use vacuum chamber or photomasks and simplicity of the step that includes DES preparation.

Along with this, the vector of modern industrial microelectronics technologies is shifting annually towards the development and application of more environmentally friendly approaches. Deep eutectic solvents have been gaining popularity for the last 10 years as "green" solvents. Thus, the use of such systems seems extremely relevant, taking into account the replacement of traditional approaches with more environmentally friendly ones. At the same time, working with DES is hampered by the high lability of these compounds. In turn, the covering process is also associated with adhesion to the substrate surface, which is affected by the chemical affinity of the components and the substrate material. For example, it was shown that the process of film covering on the substrate or membrane surfaces is usually stepwise and includes heating, covering of a film using spin coating and final annealing (depends on the composition of DES).

The current work is focused on modification of the LCLD method, in which deposition of metallic layers and structures from solutions containing cheap and simple components occurs upon cw or pulsed radiation. The advantages of this method are simplicity, low reagent consumption, the ability to control the shape and size of structures with an optical circuit and the low cost of reagents. The main limitation of this method was the speed of fabrication, which did not allow scaling this technology. However, recently, it was shown that it is possible to increase the deposition rate of copper by an order of magnitude by using deep eutectic solvents (DESs) as a medium for laser synthesis [2].

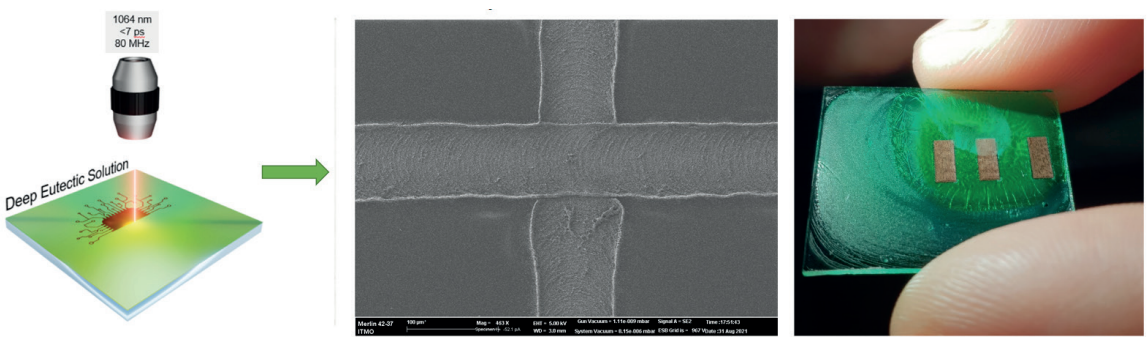

Figure 1. Copper patterns deposited from DES.

I. I. T., E. M. K., and A.S.L. acknowledge Russian Science Foundation (grant 20-79-10075). The authors would like to thank the SPbSU Nanotechnology Interdisciplinary Centre, Centre for Physical Methods of Surface Investigation, Centre for Innovative Technologies of Composite Nanomaterials, Centre for Optical and Laser Materials Research and Centre for X-ray Diffraction Studies.

references:

[1] Bhuiyan, M. E. H.; Behroozfar, A.; Daryadel, S.; Moreno, S.; Morsali, S.; Minary-Jolandan, M. A Hybrid Process for Printing Pure and High Conductivity Nanocrystalline Copper and Nickel on Flexible Polymeric Substrates. Sci. Rep. 2019, 9 (1), 1–10. https://doi.org/10.1038/s41598-019-55640-7.

[2] Shishov, A.; Gordeychuk, D.; Logunov, L.; Tumkin, I. High rate laser deposition of conductive copper microstructures from deep eutectic solvents. Chem. Commun., 55, 9626–9628, (2019).

DOI: 10.24412/cl-35039-2022-22-26-26

An insight into property-process parameters correlation of laser additive manufactured TiC precipitates in Ti-Al composite

M.D. Khomenko[1], F.Kh. Mirzade[1], J. D. Majumdar[2]

1- Institute on laser and information technologies RAS - branch of FSRC "Crystallography and photonics" RAS, 1, Svyatoozerskaya str., Shatura, Russia, 140700
2- Department of Metallurgical and Materials Engineering, Indian Institute of Technology Kharagpur, India
hmd@laser.ru

The correlation of properties and process parameters in laser additive manufacturing requires an understanding of the related phenomena in order to make the right choice in optimization. The complex nature of these technologies is reflected in the multitude of processing parameters involved, high temperatures and flow rates, making direct examination inefficient or even impossible. Direct numerical simulation has proven to be a reliable method for confirming experimental results and obtaining valuable information about phenomena. For example, our macro model shows very good performance and has already been calibrated and validated for homogeneous materials [1]. We present a numerical model that predicts solute transport and precipitation phenomena for Ti-Al composite samples reinforced with TiC particles and fabricated by laser metal deposition (LMD). We use published experimental data to calibrate the precipitation model [2]. It is shown that the dynamics and distribution of the temperature field affect the size of deposited TiC particles in Ti-Al/TiC composite samples. We are trying to isolate the most valuable processing parameters for optimization.

[1] M.D. Khomenko, N.W. Makoana, F.K. Mirzade, S. Pityana, Coupled heat transfer, fluid flow and solidification kinetics for laser additive manufacturing applications. Journal of Manufacturing Processes, 67, 611-618. (2021).
[2] A. Weisheit, A. Dutta, S. K. Rittinghaus, and J. D. Majumdar, Structure-property-process parameters correlation of laser additive manufactured TiC dispersed titanium aluminide (Ti45Al5Nb0. 5Si) composite. Intermetallics, 134, 10718 (2021).

DOI: 10.24412/cl-35039-2022-22-27-27

Laser-induced topological quantum states in thin films on solid surface: the functional characteristics controlling for cluster systems

D. Bukharov, T. Khudaiberganov, A. Putilov, A. Antipov, S. Arakelian

Vladimir state university named after Nikolay and Alexander Stoletovs
Main author email address: arak@vlsu.ru

1. Fundamental dimensional phenomena of topological quantum nanophotonics in surface solid-state structures and the prospect of using these effects in different applications are under study in laser experiment and by laser technologies.
2. Development of approaches and conditions for the use of laser methods that make it possible to experimentally obtain cluster systems from different materials - semiconductor, metallic and hybrid (metal-carbon and silicon - with noble metals - compounds) with a controlled topology on a solid surface (with granule sizes for metal particles - about 5-20nm, for silicon - 100-200nm), which are promising for creating components and systems of topological photonics and optoelectronics based on new physical principles, including under conditions of excitation of quantum bound states of light with a medium (quasiparticles of different nature) in granular and periodic / microcavity systems.
3. The subject of the paper is also the creation of dynamic models and algorithms for evaluating the characteristics and control methods of nanocluster structures / island nanofilms with a given topology, including fractal objects and dimensional quantum states of nanocluster structures induced by laser action on a solid surface.
4. Revealing the conditions for the realization of various mechanisms of quantum electrical conductivity with localized and delocalized quantum states of electrons in nanocluster systems (tunneling and hopping processes between different clusters and under thermal activation conditions) and establishing the dependence of the electrophysical parameters of such objects on their topological features arising in a laser experiment and taking into account the appropriate boundary conditions and surface inhomogeneities is principal advantages of the study.

DOI: 10.24412/cl-35039-2022-22-28-28

Porosity reduction and structural features of 316L stainless steel fabricated using combined laser metal deposition with laser remelting

A. V. Dubrov, Y. N. Zavalov, P. S. Rodin, E. S. Makarova and V. D. Dubrov

ILIT RAS – Branch of the FSRC «Crystallography and Photonics» RAS,
Svyatoozerskaya 1, 140700, Shatura, Moscow Region, Russia
dubrov.av@mail.ru

Laser metal deposition (LMD) is one of the additive manufacturing technologies. In order to achieve the required quality and defect-free LMD part, it is necessary to ensure the maintenance of optimal solidification conditions of the material at each point of the build trajectory. However, when creating objects of complex geometries, for example, including full-bodied, thin-walled and overhanging elements, thermodynamic conditions along the construction path can vary greatly, which becomes a significant challenge in terms of determining optimal technological parameters and/or their dynamic adjustment. If the thermodynamic regime does not correspond to the target one, defects are likely to form in the material, for example, areas of incomplete fusion, cracks, etc. [1]. A possible way to solve this problem is to modify the original LMD technology by adding an auxiliary laser remelting (LR) stage after depositing each LMD layer [2].

In this paper, a parametric experimental study of the combined LMD+LR technology was carried out using 316L stainless steel powder. The possibility of correcting defects that occur at the LMD stage when the thermodynamic regime deviates from the optimal one by adding the LR stage was considered. Attention was paid to the evolution of various types of defects in the material, the influence of the LR process on the properties of the material, as well as processes occurring at the micro-level. The mechanisms that play a role in reducing the defect of the material were analyzed. The influence of LR on the microhardness and structural features of the material was considered. It was found that the use of the LR stage leads to a marked decrease in the interlayer porosity. In this case, there may be a slight increase in the intralayer porosity. It is also demonstrated that the structure of the material of samples obtained by the LMD+LR technology, under certain technological parameters, is layered, in which layers with different properties formed at the LMD and LR stages alternate.

The work was supported by the Russian Foundation for Basic Research (grant No 20-21-00158).

[1] Sun, Guifang, Rui Zhou, Jinzhong Lu, and Jyotirmoy Mazumder. "Evaluation of defect density, microstructure, residual stress, elastic modulus, hardness and strength of laser-deposited AISI 4340 steel." Acta Materialia, 84, pp. 172-189, (2015).
[2] dos Santos Paes, Luiz Eduardo, et al. "Understanding the behavior of laser surface remelting after directed energy deposition additive manufacturing through comparing the use of iron and Inconel powders." Journal of Manufacturing Processes, 70, pp. 494-507, (2021).

DOI: 10.24412/cl-35039-2022-22-29-29

Modeling of Laser-Induced Surface Structures Generation due to Surface Plasmon-Polariton Excitation

D. S. Ivanov[1,2], P.N. Tetekhin[3], M.E. Garcia[4], B. Rethfeld[3], I.N. Zavestovskaya[1], A. Kabashin[2], and S. Klimentov[2]

[1] Lebedev Physical Institute, 119991 Moscow, Russia
[2] Moscow Engineering Physics Institute, 115409 Moscow, Russia
[3] Technical University of Kaiserslautern, 67663 Kaiserslautern, Germany
[4] University of Kassel, 34132 Kassel, Germany
Presenting author e-mail address: ivanov@uni-kassel.de

Ultrashort laser pulses, focused on metal surfaces, can produce Laser-Induced Periodic Surface Structures (LIPSS), which have found a lot of applications in IT- and Bio- technologies. During the laser energy deposition Surface Plasmon Polaritons (SPP) [1] can be excited on a rough material surface. The interference of the plasmons wave and the incoming pulse leads to the redistribution of the laser intensity across the material's surface and the subsequent formation of LIPSS. In this work we propose a combined atomistic-continuum Molecular Dynamics based numerical approach for investigation of LIPSS formation mechanism on metals in super-large simulations [2]. We introduce the corresponding source term description due to SPP in the combined model [3]. The simulation results are directly compared with the experimental data, generated on the same temporal and spatial scales, and analyzed. This allowed to extract the main mechanisms of LIPSS formation. The performed research allows for a possibility for the structures generation with predesigned topological, morphological, and optical properties.

[1] S.A. Maier, *Plasmonics, Fundamentals and Applications* (Springer, Berlin) (2007).
[2] P.N. Terekhin, J. Oltmanns, A. Blumenstein, D.S. Ivanov, F. Kleinwort, M.E. Garcia, B. Rethfeld, J. Ihlemann, and P. Simon, "Plasmonic nature of periodic surface structures following single laser pulse irradiation", *Nanophotonics* **11**, 359-367 (2022).
[3] O. Benhayoun, P. N. Terekhin, B. Rehfeld, D. S. Ivanov, and M. E. Garcia, "Theory for heating of metals assisted by Surface Plasmon Polaritons", *Appl. Sur. Sci.* **569**, 150427 (2021).

DOI: 10.24412/cl-35039-2022-22-30-30

Synthesis of copper nanoparticles by high-energy laser pulses in liquid

A.G. Putilov[1,2], A.E Shepelev[1], A.A. Antipov[1,2]

[1] ILIT RAS — Branch of FSRC "Crystallography and Photonics" RAS, Shatura, Russia
[2] Vladimir State University named after Alexander Grigorievich and Nikolai Grigorievich Stoletovs, Vladimir, Russia
e-mail: antiplit@yandex.ru

The study of the synthesis of copper nanoparticles is due to their unique properties compared to bulk materials and their application in various fields. Recently, copper nanoparticles have found application in the formation of conductive films, the creation of nonlinear devices, and bactericidal agents [1]. The laser ablation method has advantages over chemical synthesis methods. By this method, the synthesis occurs in a short time, chemically pure substances are formed, and hybrid materials of dissimilar metals can also be obtained. The synthesized nanoparticles are also highly active and almost immediately ready for use [2].

Colloidal solutions of copper were formed by laser ablation of the material into a liquid. A copper target was placed into the liquid: distilled water and glycerin. The energy density of laser radiation on a copper target ranged from 33 to 52 J/cm2 [3]. The scanning speed did not exceed 2 mm/s. Under laser action on a target with a frequency of 5 Hz, the average particle size is about 20 nm, and an increase in the laser radiation frequency to 15 Hz leads to an increase in the average particle size to 150 nm. Such an increase is associated with a change in the laser beam profile, since an increase in frequency leads to an increase in the thermal lens. The absorption spectrum for colloidal solutions with synthesized copper nanoparticles was in the region of ~520 nm.

Further experimental studies are aimed at the formation of thin cluster films. Cluster films were formed on a solid dielectric substrate by drop deposition. In the first series, the experiments were carried out under natural conditions at a temperature of 25 °C. In the process of drying, a cluster thin film is formed with a clearly defined boundary and evenly deposited particles in the center. The second series of experiments is devoted to the forced evaporation of a liquid medium using laser radiation. The deposited surface is an island film, since there is a competition between two processes of diffusion of nanoparticles from the heating region and a hydrodynamic flow into the heating region.

Copper nanoparticles of the smallest size are synthesized at an energy of 52 J/cm2, a repetition rate of 5 Hz, and a scan rate of 2 mm/s. Increasing the frequency leads not only to a change in the beam profile, but also to an increase in the average particle size. The formation of cluster films during natural and forced evaporation of the liquid phase is demonstrated.

The reported study was funded by RFBR No. 20-32-90052, partly within the framework of RFBR projects No. 19-29-10022, 20-02-00515.

[1] Fernández-Arias, M., Boutinguiza, M., del Val, J., Covarrubias, C., Bastias, F., Gómez, L., Maureira, M., Arias-Gonzalez, F., Riveiro, A., & Pou, J. Copper nanoparticles obtained by laser ablation in liquids as bactericidal agent for dental applications. Applied Surface Science, 507, 145032. (2020).
[2] Kucherik, A. O., Ryabchikov, Y. V., Kutrovskaya, S. V., Al-Kattan, A., Arakelyan, S. M., Itina, T. E., & Kabashin, A. V.. Cavitation-Free Continuous-Wave Laser Ablation from a Solid Target to Synthesize Low-Size-Dispersed Gold Nanoparticles. Chemphyschem : a European journal of chemical physics and physical chemistry, 18(9), 1185–1191. (2017)
[3] Антипов А.А., Путилов А.Г., Осипов А.В., Шепелев А.Е., Лазерная абляция металлических мишеней в жидкости цугами наносекундных импульсов, Известия Российской академии наук. Серия физическая. Т. 86. № 6. С. 853-858.(2022).

DOI: 10.24412/cl-35039-2022-22-31-31

Femtosecond laser plasma driven nanoparticle formation in Au aqueous solution

V.V. Kononenko, K.H. Ashikkalieva, N.R. Arutyunyan and V.I. Konov

Prokhorov General Physics Institute of the Russian Academy of Sciences, Moscow, Russia
e-mail: vitali.kononenko@nsc.gpi.ru

One of the most interesting laser application based on the plasma-assisted processes in aqueous solutions is a photochemical reduction of metal salts. The intense femtosecond laser excitation of water is known to be a quite effective tool to ionize solution and drive the formation of metal nanoparticles (NPs) [1]. This technique requires no chemical catalysts in order the reaction to run and enables precise control over the size and shape of synthesized nanoparticles. Here we present an experimental study of laser induced plasma in the gold aqueous solution ($HAuCl_4$) and explore the correlation between its properties and a gold NPs synthesis.

Ionization of water was provided in a strong optical field of the Ti:sapp femtosecond laser (pulse duration ~ 100 fs, wavelength 800 nm, intensity > 10^{12} W/cm^2). The laser induced processes, including ionization of water, solvation of excess electrons, geminate recombination of plasma and development of cavitation, were visualized and characterized with the pump-probe interferometry. Besides interferometric measurements the scattering of pump radiation on aqueous plasma was studied.

For the photochemical experiments the salt solutions were irradiated during ≈10-100 minutes. The kinetics of Au ions reduction and formation of Au NPs was measured at varied pulse energy during and after the laser treatment. The absorption spectra of the irradiated solutions and particle size distribution monitoring by a dynamic light scattering technique were studied. We discuss the relationship between the different regimes of water ionization and productivity of the metal ions reduction in laser-induced plasma. Presented data provide an experimental basis for theoretical models that describe the plasma-assisted processes in aqueous media.

This work was supported by the Russian Science Foundation (grant 19-12-00255).

DOI: 10.24412/cl-35039-2022-22-32-32

Laser synthesis of thin-film memristor structures based on tantalum and niobium oxides

O. Novodvorsky, O. Khramova, L. Parshina, D. Gusev*, A. Polyakov, V. Mikhalevsky, E. Cherebilo

1- Institute on Laser and Information Technologies of Russian Academy of Sciences — Branch of Federal Scientific Research Center "Crystallography and Photonics" of Russian Academy of Sciences, Svyatoozerskaya 1, 140700, Shatura, Moscow Region.
. Corresponding author.*
E-mail address:dagiet04@gmail.com (D.Gusev).

In the present work, thin films of niobium and tantalum oxides are obtained and investigated [1,2]. The effect of the O_2 gas pressure and the laser radiation energy on the target on the composition, structure, and optical properties of the deposited NbO_x and TaO_x films is considered. It was found that, at different oxygen pressures, NbO_x films are formed by various nanocrystallites, the size and structure of which depend on the wavelength of the ablating radiation. In this case, the band gap of NbO_x films depends on the energy of particles deposited by PLD. The behavior of bifurcations and attractor type in the transmission curves of NbO_x films was found as a function of the oxygen pressure, which is associated with the formation of NbO_2 nanocrystallites. Switching of memristor devices based on tantalum oxides is associated, in particular, with a change in the degree of oxidation in a TaO_x thin film, which affects its structural and electrical characteristics. In this work, we investigate the possibility of tuning the resistive switching of the $Pt/TaO_x/Ta_2O_5/Pt/c\text{-}Al_2O_3$ memristors in crossbar geometry by changing the oxygen pressure from 0.5 to 50 mTorr during the low-temperature laser synthesis. X-ray diffraction studies of the TaO_x films with high resolution made it possible to determine the conditions for obtaining the active region of the memristor with the formation of certain size nanocrystallites. The $Pt/TaO_x/Ta_2O_5/Pt/c\text{-}Al_2O_3$ memristor showed very reliable resistive switching performance over 100 DC cycles with the memory window performance of $R_{ON}/R_{OFF} \sim 10^3$ at RESET operating voltage of ~ 2.3 V. Memristors $Me/NbO_x/Me$ with a lower electrode of a noble metal and an upper one of a noble or reactive metal have been obtained and investigated. Volatile memristors of $Nb/NbO_x/Nb_2O_5/Pt/c\text{-}Al_2O_3$ ($x \leq 2.5$) in cross-bar geometry were created demonstrating long-term stability of operation for 60 DC cycles with $\Delta R_{HRS}/R_{HRS} < 8\%$ at an operating switching voltage of ~ 0.5 V. All memristor layers were deposited by PLD in a drop-free mode using an excimer KrF laser or a second harmonic of a YAG:Nd^{3+} laser. The influence of the energy of deposited particles on the characteristics of memristors with different types of upper electrode and different compositions of the oxide NbO_x layer is investigated.

[1] L. Parshina, O. Novodvorsky, O. Khramova, D. Gusev, A. Polyakov, V. Mikhalevsky, E. Cherebilo Laser synthesis of non-volatile memristor structures based on tantalum oxide thin films Chaos, Solitons and Fractals vol.142, pp. 110460-5, (2021).
[2] O. Novodvorsky, L. Parshina, O. Khramova, D. Gusev, A. Polyakov, V. Mikhalevsky, E. Cherebilo Laser synthesis of volatile memristors based on niobium oxide thin films Surfaces and Interfaces vol. 30, pp101891-7, (2022).

DOI: 10.24412/cl-35039-2022-22-33-33

Laser-Induced Phase Transitions Dynamics of GeTe and $Ge_2Sb_2Te_5$ Thin Films

A.V. Kiselev, A.A. Burtsev, V.V. Ionin, N.N. Eliseev, V.A. Mikhalevsky, A.A. Nevzorov, M.D. Khomenko and A.A. Lotin

ILIT RAS — Branch of FSRC "Crystallography and Photonics" RAS,
140700, Shatura, Svyatoozerskaya Str., 1, Moscow Region, Russia
Main author email address: lotin_82@mail.ru

Thin film chalcogenide materials based on germanium telluride (GeTe, $Ge_2Sb_2Te_5$) are widely used in photonic and optoelectronic devices [1]. These alloys have very small amorphization and crystallization times in the order of nanoseconds, which combined with large cyclability and a pronounced property contrast between the crystalline and amorphous phases [2].

In this paper, the dynamics of changes in the optical transmission and reflection coefficients of thin 100 nm GeTe and $Ge_2Sb_2Te_5$ films during crystallization and amorphization induced by nano- and femtosecond laser pulses are studied. It is shown that the change in optical coefficients in the subnanosecond time scale during crystallization and amorphization induced by fs pulses is mainly determined by the photoexcitation of charge carriers. On the nano-microsecond time scale, the processes of crystallization and amorphization are determined by thermal processes and described by the mathematical model of thermal conductivity and the Stefan problem. The progress of the phase transition can be monitored using the increase in reflectance upon crystallization and analyzed using the Johnson–Mehl–Avrami–Kolmogorov model [3].

Reproducible multi-level modulation of optical constants of samples is demonstrated. The modulation magnitude is limited by the Booger absorption. Results demonstrate different mechanisms of crystallization for nano- [4-6] and femtosecond laser pulses.

[1] K.V. Sreekanth, M. ElKabbash, V. Caligiuri, R. Singh, A. De Luca, G. Strangi. New Directions in Thin Film Nanophotonics, ch. 3 (2019).
[2] P. Guo, A. M. Sarangan and I. Agha. A Review of Germanium-Antimony-Telluride Phase Change Materials for Non-Volatile Memories and Optical Modulators. Applied Sciences, 9, 3, 530 (2019).
[3] V. Weidenhof, I. Friedrich, S. Ziegler, and M. Wuttig. Laser induced crystallization of amorphous $Ge_2Sb_2Te_5$ films. Journal of Applied Physics, 89, pp. 3168-3176 (2001).
[4] V. V. Ionin, A. V. Kiselev, N. N. Eliseev, V. A. Mikhalevsky, M. A. Pankov, A. A. Lotin, Multi-level reversible laser-induced phase transitions in GeTe thin films. Applied Physics Letters, 117, 011901 (2020).
[5] A.V. Kiselev, V.A. Mikhalevsky, A.A. Burtsev, V.V. Ionin, N.N. Eliseev, A.A. Lotin, Transmissivity to reflectivity change delay phenomenon observed in GeTe thin films at laser-induced reamorphization, Optics and Laser Technology, 143, 107305 (2021)
[6] A.V. Kiselev, V.V. Ionin, A.A. Burtsev, N.N. Eliseev, V.A. Mikhalevsky, N.A. Arkharova, D.N. Khmelenin and A.A. Lotin, Dynamics of reversible optical properties switching of Ge2Sb2Te5 thin films at laser-induced phase transitions, Optics and Laser Technology, 147 107701 (2022)

DOI: 10.24412/cl-35039-2022-22-34-34

LIPSS Fabrication on Large Areas of Amorphous Silicon Under Multi-Pulse Femtosecond Laser Action

S. Zabotnov[1], D. Shuleiko[1], D. Presnov[1], M. Martyshov[1], E. Kuzmin[2], P. Danilov[2], A. Serdobintsev[3], P. Kashkarov[1]

1- M.V. Lomonosov Moscow State University, Faculty of Physics, 1/2 Leninskie Gory, Moscow, 119991, Russia
2- P.N. Lebedev Physical Institute of RAS, 53 Leninsky Ave., Moscow, 119991, Russia
3- Saratov State University, 83 Astrakhanskaya St., Saratov, 410012, Russia
zabotnov@physics.msu.ru

Direct laser writing is an effective technique to fabricate surface structures with wavelength and subwavelength accuracy. One of realizations of such approach is the laser-induced periodic surface structures (LIPSS) formation via femtosecond laser irradiation where intensive surface photoexcitation results to surface plasmon-polariton generation not only in metals but also in semiconductors due to electron-hole plasma generation [1,2]. Such surface electromagnetic waves give a contribution to the periodical relief modulation and corresponding ripple formation at the irradiated surfaces. In particular, because of femtosecond laser pulses irradiation of amorphous silicon films and corresponding LIPSS formation, strong optical [3] and electrophysical anisotropy [4] may emerge in plane of a sample. Thus, it is a promising way to fabricate compact devices of optical memory and photovoltaic which are polarization and applied current sensitive, respectively.

The present work describes main features of the LIPPS formation at amorphous silicon surfaces under femtosecond laser action with the wavelength of 1030 nm or 1250 nm when the pulses number are varied in the range of 50–1000 at different energy fluences. It allows to fabricate ripples with the period from 880 to 1250 nm and the orientation perpendicular or parallel relative to the laser radiation polarization. Using mechanical translators and a galvanometric scanner we obtained relatively large areas (1 mm x 1 mm and more) with LIPSS and a good quality for the applications.

To explain the observed ripple evolution, we used the model proposed by J.E. Sipe [5] where the efficacy factor depends on the real and imaginary parts of the dielectric constant and defines the LIPSS wave vector on the irradiated surface [2]. In turn, according to the Drude model the dielectric constant complex value is varied due to concentration change for the nonequilibrium electrons excited by different number of high-power femtosecond laser pulses.

The modified surfaces are characterized by the high level of nanocrystallization. According to Raman spectra analysis the volume fraction of nanocrystals in the irradiated films ranges from 17% to 70% depending on the treatment conditions. The silicon nanocrystal presence leads to growth of the specific conductivity up to 3 orders for the irradiated samples in comparison with nonirradiated ones. The in-plane conductivity anisotropy was revealed also [4]. This result is in a good agreement with the Bruggeman model [6] and spectra of absorption for the surface possessing form anisotropy.

The investigation was funded by the Russian Science Foundation grant # 22-19-00035, https://rscf.ru/project/22-19-00035/.

[1] J. Bonse and S. Gräf, Maxwell meets Marangoni–A review of theories on laser-induced periodic surface structures, Laser Photonics Rev., 14, 2000215, (2020).
[2] J. Bonse, A. Rosenfeld, J. Krüger, On the role of surface plasmon polaritons in the formation of laser-induced periodic surface structures upon irradiation of silicon by femtosecond-laser pulses, J. Appl. Phys., 106, 104910, (2009).
[3] R. Drevinskas, M. Beresna, M. Gecevičius, et al., Giant birefringence and dichroism induced by ultrafast laser pulses in hydrogenated amorphous silicon, Appl. Phys. Lett., 106, 171106, (2015).
[4] D. Shuleiko, M. Martyshov, D. Amasev, et al., Fabricating femtosecond laser-induced periodic surface structures with electrophysical anisotropy on amorphous silicon, Nanomaterials, 11, 42 (2021).
[5] J. Sipe, J.F. Young, J. Preston, H. van Driel, Laser-induced periodic surface structure. I. Theory. Phys. Rev. B, 27, 1141–1154 (1983).
[6] A.K. Sarychev and V.M. Shalaev, Electrodynamics of Metamaterials (Singapore: World Scientific), Ch. 2.2 Conductivity and dielectric constant: Effective medium theory, (2007).

DOI: 10.24412/cl-35039-2022-22-35-35

Anisotropic femtosecond laser-induced modification of doped amorphous silicon films

D. Shuleiko[1], S. Zabotnov[1,2], D. Presnov[1,3,4], M. Martyshov[1], P. Kashkarov[1,4]

1- Faculty of Physics, Lomonosov Moscow State University, Leninskie Gory, 1/2, Moscow, Russia;
2- National Research Centre «Kurchatov Institute», Academika Kurchatova sq., 1, Moscow, Russia
3- Quantum Technology Centre, Faculty of Physics, Lomonosov Moscow State University, Leninskie Gory, 1/2, Moscow, Russia
4- Skobeltsyn Institute of Nuclear Physics, Lomonosov Moscow State University, Leninskie Gory, 1/2, Moscow, Russia.
shuleyko.dmitriy@physics.msu.ru

Ultrafast laser irradiation is a perspective tool for modification of thin amorphous silicon (a-Si) films' properties to improve their performance in thin-film photovoltaics and optics [1]. Application of femtosecond laser pulses allows achieving simultaneous crystallization in the bulk and "ripples" or laser-induced periodic surface structures (LIPSS) formation on the surface of the a-Si film. The LIPSS formed due to the excitation of surface plasmon-polaritons (SPP), induce electrical anisotropy of a-Si film [2], as well as birefringence and dichroism, which can be potentially applied in polarization-sensitive devices [3].

In this work we irradiated a-Si films with various thickness (400–1200 nm) and doping type (phosphorous-doped n-a-Si or boron-doped p-a-Si) by femtosecond laser pulses (λ = 1250 nm, τ = 150 fs, ν = 10 Hz) in scanning mode at various moving speeds. The laser fluence was 0.15 – 0.3 J/cm^2.

In all cases on the irradiated surfaces, we observed formation of LIPSS orthogonal to the laser polarization. The LIPSS period was close to λ and decreased from 1100±100 to 840±70 nm with decreasing scanning speed. Such effect can be caused by increase of the relief height from 150±50 to 300±100 nm which was simultaneously observed when the film was modified at lower scanning speeds. The higher surface relief leads to a shift in the value of the SPP resonant period [4]. An additional contribution to this effect may be given by excessive electron emission from the surface, assuming that the a-Si film is heated more at low scanning speed.

The Raman spectra demonstrated formation of crystalline silicon (c-Si) phase within irradiated films with the volume fraction up to 82±13% for p-a-Si, and up to 19±3% for n-a-Si.

Dark conductivity of irradiated a-Si films increased by up to 7 orders (up to $1.2 \cdot 10^{-2}$ S/cm) compared to initial films, due to the crystalline Si phase formation. The conductivity dependence of irradiated a-Si films was nonlinear due to nonuniform c-Si phase distribution within film depth, which was confirmed by Raman measurements.

Electrophysical anisotropy induced by LIPSS formation was observed in all samples: the dark conductivity was up to 10 times higher along the LIPSS ridges. Observed anisotropy may be explained by LIPSS depolarizing influence, ablated surface relief and uneven crystalline phase distribution within a-Si films.

The investigation was funded by the Russian Science Foundation (grant 22-19-00035), https://rscf.ru/project/22-19-00035/

[1] L. Hong, X.C. Wang, H.Y. Zheng, et al. Femtosecond laser induced nanocone structure and simultaneous crystallization of 1.6 μm amorphous silicon thin film for photovoltaic application. J. Phys. D Appl. Phys., vol. 46, art. 195109, (2013)
[2] D. Shuleiko, M. Martyshov, D. Amasev, et al. Fabricating femtosecond laser-induced periodic surface structures with electrophysical anisotropy on amorphous silicon. Nanomaterials, vol. 11, art. 42, (2020)
[3] R. Drevinskas, M. Beresna, M. Gecevičius, et al. Giant birefringence and dichroism induced by ultrafast laser pulses in hydrogenated amorphous silicon. Appl. Phys. Lett., Vol. 106, art. 171106, (2015)
[4] M. Huang, F. Zhao, Y. Cheng, et al. Origin of laser-induced near-subwavelength ripples: interference between surface plasmons and incident laser. ACS Nano, vol. 3(12), pp. 4062–4070, (2009)

DOI: 10.24412/cl-35039-2022-22-36-36

Investigation of a composite of laser reduced graphene oxide and polymers for implant applications

E.G. Abyzova, E.M. Dogadina, E.N. Bolbasov, R.D. Rodriguez , E.S. Sheremet

Federal State Autonomous Educational Institution for Higher Education National Research Tomsk Polytechnic University, Tomsk, Russian Federation
[1]abyzovaeg@gmail.com

Currently, the need for medical implants is increasing, which means that it is necessary to monitor their condition. Standard monitoring methods have limitations, in particular, there is a need for frequent visits to the clinic. In addition, they can be effective only in the late stages of implant malfunction. The development of an electronic element for remote monitoring would make it possible to monitor the condition of the implant with convenience for doctors and patients [1] and an extra benefit of early diagnosis of the issues.

Carbon nanomaterials have great prospects in the field of medicine, including drug delivery systems and tissue scaffolds [2]. The introduction of graphene-like materials increases the mechanical strength and electrical conductivity of composites [3]. In addition, the presence of graphene increases the attachment of cells and their growth on the surface of biomaterials. One of the new and promising materials is graphene oxide, which has a low cost, high conductivity, as well as ease of preparation and the ability to create flexible structures. By chemical, thermal, or photonic reduction, graphene oxide is converted from a dielectric into reduced graphene oxide (rGO), an electrically conductive material. Currently, there is a lot of research in the field of synthesis of new polymers. However, these polymers have limitations in application due to their mechanical properties. Graphene has such distinctive properties as high thermal conductivity, excellent mechanical properties, and high electrical conductivity [4], which allow it to be integrated into polymer matrices to create new functional composites.

It is proposed to develop and investigate composite materials fabricated by laser-induced composite formation based on reduced graphene oxide and biodegradable polymers. The study of chemical and mechanical properties showed a change in its conductivity. The composite turned out to be biocompatible, which will allow it to continue developing an electronic element for monitoring the state of the implant based on it.

The subsequent development and implementation of the electronic element will make it possible to remotely monitor the condition of the implant to prevent complications and control some important physiological parameters.

The work was supported by Russian Science Foundation grant № 22-12-20027, https://rscf.ru/project/22-12-20027/ and the funding from Tomsk region administration.

[1] J. Artico, M. Zecchin, A. Zorzin Fantasia, G. Skerl, B. Ortis, S. Franco, S. Albani, G. Barbati, J. Cristallini, A. Cannata, G. Sinagra, Long-term patient satisfaction with implanted device remote mon-itoring: a comparison among different systems, Journal of Cardiovascular Medicine, 20(8), pp. 542–550, (2019).
[2] G. Rajakumar, X.-H. Zhang, T. Gomathi, S.-F. Wang, M. A. Ansari, G. Mydhili, G. Nirmala, M. A. Alzohairy, I.-M. Chung, Association of Inpatient Use of Angiotensin-Converting Enzyme Inhibitors and Angiotensin II Receptor Blockers With Mortality Among Patients With Hypertension Hospitalized With COVID-19, Circulation Research, 8(3), p. 355, (2020).
[3] W.K. Chee, H.N. Lim, N.M. Huang, I. Harrison, RSC Advances, 5, p. 68014, (2015).
[4] T. Kuila, S. Bhadra, D. Yao, N.M. Kim, S. Bose, J.H. Lee, Recent Advances in Fabrication and Characterization of Graphene-Polymer Nanocomposites, Progress in Polymer Science, 35 (11), pp. 1350-1375, (2010).

DOI: 10.24412/cl-35039-2022-22-37-37

Thermo-mechanical effect of eye-tissue laser modification.

O.I. Baum

Institute of Photon Technologies, Federal Scientific Research Centre 'Crystallography and Photonics' of Russian Academy of Sciences, Troitsk, 108840 Moscow, Russia
baumolga@gmail.com

Laser-indused thermo-mechanical effect is a basis of new methods for laser modification of the biological tissue structure. This effect can be useful in normalizing intraocular pressure in correction of refraction [1], treatment of glaucoma [2], laser reshaping of rib cartilage for larynx stenosis surgery [3] and for regeneration processes [4]. The common problem for all these new laser methods is achieving the predicted and stable result.

Earlier the assumption that in the places of the sample, where the greatest thermal stresses were created, is the epicenter of pore formation, was confirmed. In this work the theoretical calculation of thermal stresses was compared with the laser-induced pore-distribution along the direction perpendicular to the laser radiation axis. The experimentally obtained width and position of the maximum size distribution of laser-induced pores in bio-tissue repeated the dynamics obtained theoretically. The obtained verification of the theoretical model demonstrates its potential and will allow it to be further used to predict the result obtained under laser irradiation.

The novelty of the developed approach is associated with the development of the foundations for a new method of diagnosing and monitoring the treatment method for advanced open-angle glaucoma.

References

O. Baum, A. Yuzhakov, A. Bolshunov, et.al., "New laser technologies in ophthalmology for normalisation of intraocular pressure and correction of refraction," Quantum electronics, 47(9), p.860, 2017.

O. Baum, S. Wachsmann-Hogiu, T. Milner, E. Sobol, "Laser-assisted formation of micropores and nanobubbles in sclera promote stable normalization of intraocular pressure," Laser Physics Letters, 14 (6), p.065601, 2017.

O. Baum, Y. Soshnikova, E. Sobol, "Laser reshaping of costal cartilage for transplantation," Lasers in surgery and medicine, 43 (6), pp.511-515 (2011).

Alexandrovskaya, Y. M., Baum, O. I., Shekhter, A. B., Petersen, E. V., Tiflova, O. A., Dmitriev, A. K. & Sobol, E. N. Mechanisms of laser activation of chondrocytes in osteoarthritis healing. Laser Physics Letters, 15(8), 085601 (2018).

DOI: 10.24412/cl-35039-2022-22-38-38

Direct Laser Writing of Helical Bragg Grating in Vortex Fiber

V.V. Likhov[1,2], S.L. Semjonov[1], S.A. Vasiliev[1], G.K. Alagashev[1], A.G. Okhrimchuk[1,2]

1- Prokhorov General Physics Institute of the Russian Academy of Sciences, 38 Vavilova Str. Moscow, Russia
2- Mendeleev University of Chemical Technology of Russia, 9 Miusskaya Sq, Moscow, Russia
okhrim@fo.gpi.ru

Ring core fibers, also known as vortex fibers, are a perspective solution to increase capacity of optical communication systems with mode division multiplexing [1]. Modes carrying orbital angular momentum (OAM) draw attention in this concern due to low cross talk in the ring core fibers. We consider that helical structures integrated in the fiber systems are a natural solution for generating and filtering OAM modes. However, no such devices were known up to now.

Direct laser writing (DLW) by femtosecond laser pulses is widely used to pattern the refractive index of optical materials. The high spatial resolution of this 3D patterning method, comparable to the light wavelength, in combination with high-precision positioners, makes it possible to form high quality phase structures in crystals and glasses, including helical Bragg gratings (HBG) that reflect visible and near-IR light [2,3]. Here, we applied DLW with lenticular beam waist performing helical movement to inscribe third order HBG reflecting at wavelength region of 1550 nm [3]. Uniform helical pattern with refractive index modulation of about 10^{-3} was inscribed in the Ge-doped core of home-made ring-core fiber by femtosecond laser beam (Fig.1). Laser wavelength, pulse duration and repetition rate were 1030 nm, 180 fs and 250 Hz correspondingly. Grating length was 3 mm. Positioning of the beam waist inside the fiber core was controlled by multiphoton excitation of the blue luminescence of the germanium oxygen deficient centers (GODC) under laser pulse energy below modification threshold. HBG reflectance spectra was recorded with single frequency tunable laser light coupled into the vortex fiber core (Fig.2).

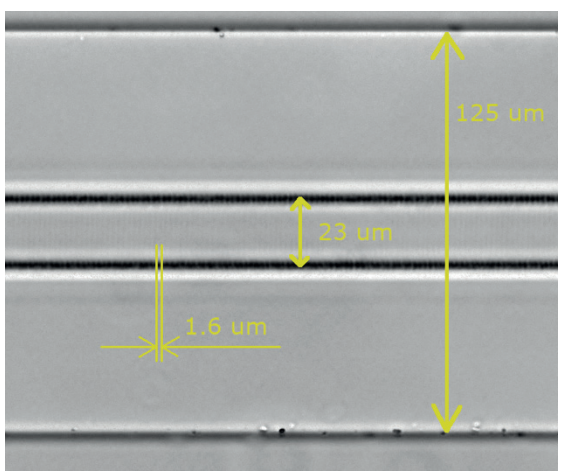

Fig.1. Bright filed microscopic picture of HBG in ring-core fiber.

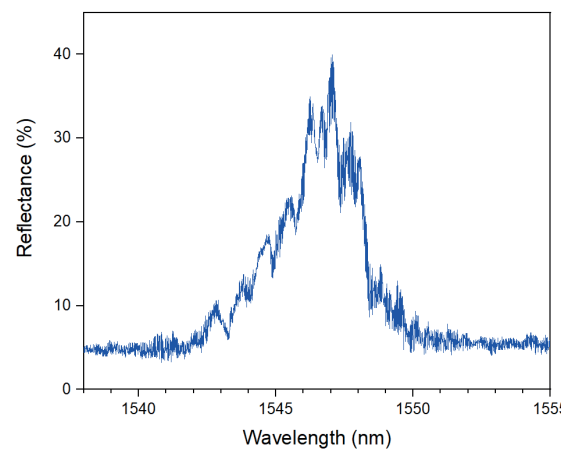

Fig.2. Reflectance spectra of HBG. Background is due to Fresnel reflection from the fiber ends.

According to our calculations the investigated fiber supports twenty six cylindrical vector modes with the same radial index equaled to unity and different azimuthal indices (HE_{m1} and EH_{m1}). The modes can form vortex modes with OAM as high as 7. We suppose that the written HBG provides resonance couplings of counter-propagating OAM modes (Fig.2). Different peaks within the reflection band correspond to coupling of OAM modes with different topological charges [3].

The study was supported by Russian Science Foundation, grant #22-29-01187.

[1]. H. Wang, Y. Liang, X. Zhang, S. Chen, L. Shen, L. Zhang, J. Luo, and J. Wang, "Low-Loss Orbital Angular Momentum Ring-Core Fiber: Design, Fabrication and Characterization," J. Light. Technol. 38, 6327–6333 (2020).
[2] J. He, J. He, X. Xu, B. Du, B. Xu, C. Liao, Z. Bai, and Y. Wang, "Single-mode helical Bragg grating waveguide created in a multimode coreless fiber by femtosecond laser direct writing," Photonics Res. 9, 2052 (2021).
[3] A. G. Okhrimchuk, V. V. Likhov, S. A. Vasiliev, and A. D. Pryamikov, "Helical Bragg gratings: experimental verification of light orbital angular momentum conversion," J. Light. Technol. 40, 2481–248 (2022).

DOI: 10.24412/cl-35039-2022-22-39-39

Direct writing of conductive patterns with pulsed near-IR laser irradiation of deep eutectic solvents

D.A. Sinev[1], E.A. Avilova[1], E.A. Eltysheva[1], M.A.Zaikina[1], E.M. Khairullina[1,2], A.Yu.Shishov[2], I.I.Tumkin[2]

1 - ITMO University, 197101 St. Petersburg, Russia
2 - Saint Petersburg State University, 199034 St. Petersburg, Russia
sinev@itmo.ru

The laser-induced deposition method is a powerful tool for providing the localized metallization of flexible and rigid dielectric materials for the purposes of functional materials engineering, surface modification, electronics, and sensory applications. Direct laser writing of conductive micropatterns was recently improved by implementation of the eutectic solvents, that are characterized by an increased thermal and yielding efficiency of the copper reduction chemical reaction [1-2].

The experiments on the formation of conductive elements by laser-induced copper deposition were carried out in this work in an eutectic solvent medium with the composition of copper (II) acetate 2 g, choline chloride 1 g, tartaric acid 1.07 g. In this study we show the ways of forming conductive structures of an arbitrary topology by means of a single exposure using near-infrared radiation at speeds of up to 2 mm/s (Figure 1). The productivity increasing methods are discussed, including the pre-preparation of the substrate by the laser-induced microplasma [3], multiple exposure patterning, and usage of an auxiliary cover glass.

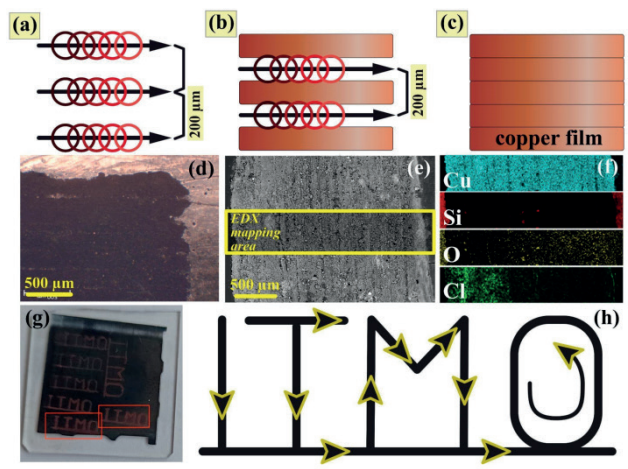

Fig.1. (a–c) The continuous -coating recording scheme, (d) optical and (e) scanning electron microphotography, and (f) EDX analysis of the recorded coating structure. (g) Photo and (h) recording scheme for the structures of arbitrary topology [2].

I.I.T. and E.M.K. acknowledge the Russian Science Foundation's (grant 20-79-10075) support for the design of chemical compositions for the selective metallization and laser fabrication of patterns. D.A.S. and E.A.A. acknowledge the Russian Science Foundation's (grant 21-79-10241) support for direct laser recording, surface structuring, and LIPSSs formation studies.

[1] A.S. Levshakova, E.M. Khairullina, L.S. Logunov, M.S. Panov, A.S. Mereshchenko, V.B. Sosnovsky, D.I. Gordeychuk, A.Yu. Shishov, I.I. Tumkin, Highly rapid direct laser fabrication of Ni micropatterns for enzyme-free sensing applications using deep eutectic solvent, Materials Letters, vol. 308, Part A, pp. 131085 (2022).
[2] E.A. Avilova, E.M. Khairullina, A.Yu. Shishov, E.A. Eltysheva, V. Mikhailovskii, D.A. Sinev, I.I. Tumkin, Direct Laser Writing of Copper Micropatterns from Deep Eutectic Solvents Using Pulsed near-IR Radiation, Nanomaterials, vol. 12, pp.1127 (2022).
[3] V.S. Rymkevich, M.M. Sergeev, R.A. Zakoldaev, Laser microplasma as a spot tool for glass processing: Focusing conditions, J. Mater. Process. Technol., vol. 292, pp. 117061 (2021).

DOI: 10.24412/cl-35039-2022-22-40-40

Capillary instability of a keyhole and pore formation mechanism during laser additive manufacturing

R. D. Seidgazov*[1], F. Kh. Mirzade[1]

[1] ILIT RAS - Branch of the FSRC "Crystallography and Photonics" RAS,
Svyatoozerskaya, 1, 140700, Shatura, Moscow Region, Russia.
** Corresponding author E-mail: seidgazov@mail.ru*

The deep penetration mode is widely used in laser welding, and it has begun to be used in additive manufacturing by melting powder layers with a laser beam in recent years. In contrast to conduction mode with its characteristic shallow melt pool, a deep penetration regime differs by a significant surface depression as a cavity, due to which the beam penetrates deep into the metal, forming a melting zone narrow and deep. The unstable cavity behavior causes defects (pores), which significantly degrade the structural integrity and performance of products, limiting the potential of technologies. A fundamental understanding of pore formation is key to a practical pore reduction strategy.

The report presents a study of capillary oscillations inside a cavity leading to pores formation. The amplitude and frequency of these oscillations determine the volume and frequency of pore appearance. The change of pores volume (Fig. 1) and appearance frequency (Fig.2) depending on the beam scanning speed is analyzed. Scanning speed values at which the amplitude and frequency of capillary oscillations (i.e., the pores volume and frequency of pores appearance) reach their maximum values are obtained. The correspondence between the calculated curves and experimental data (Fig.1, 2) confirms the capillary nature of cavity oscillations leading to pores formation, as well as the predictive capabilities of presented analysis.

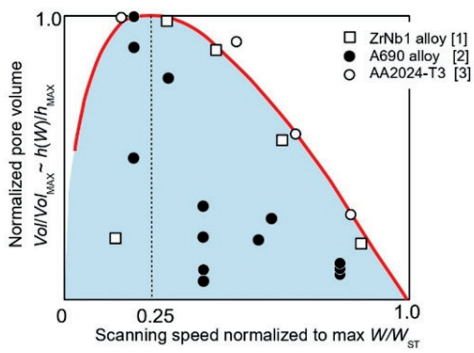

Fig. 1. Distribution of pore volume value (normalized to max) $Vol(W)/Vol_{MAX}$ and change in molten layer thickness (normalized to max value) $h(W)/h_{MAX}$ versus the scan speed (normalized to max) W/W_{PF}. The solid line corresponds to calculation and has the maximum at W=0.25W_{PF}.
Dots are the measured pore volume in experiments [1-3].

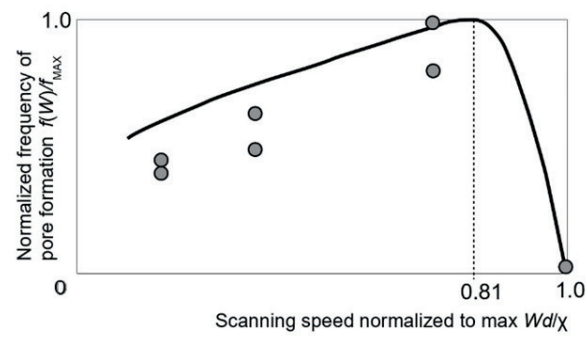

Fig. 2. Variation of the frequency of pore formation with the beam scan speed. The solid line is a frequency calculation. All data are normalized to their maximum values and presented in relative units. Points are experimental data [4]. The frequency of capillary oscillations and pore formation tends to zero at pore-free scan speed W/W_{PF} = 1. The maximum $f(W)$ corresponds to scan speed W=0.81W_{PF}

Results obtained can help in choosing the optimal value of scanning speed W in designing of pore-free technology with a deep penetration mode. To minimize pore formation, it is proposed to use the ratio $W_{PF} = \chi/d$, which allows for a metal with thermal diffusivity χ to choose the value of the scanning speed W_{PF} for a given focal spot size d or, conversely, to choose a focusing mode with a spot size d for a given scanning speed W_{PF}.

[1] K. Harald, T. Jürgen, Z. Harald. Einfluß verschiedener Schweißdaten auf die Porosität von Elektronenstrahl-schweißnähten in der Zirkoniumlegierung ZrNb1. Schweißtechnik, Berlin, 36, No 8 (1986) 358-360 (in German)
[2] J. D. Tucker, T. K. Nolan, A. J. Martin, G. A. Young. Effect of Travel Speed and Beam Focus on Porosity in Alloy 690 Laser Welds. JOM, Vol. 64, No. 12, 2012 DOI: 10.1007/s11837-012-0481-3
[3] O. T. Ola, F. E. Doern. Keyhole-induced porosity in laser-arc hybrid welded aluminum. Int J Adv Manuf Technol (2015) 80:3–10 DOI 10.1007/s00170-015-6987-4
[4] T. Omae, Y. Yoshida, T. Hirozane, S. Suzuki. Fundamental Study of CO2 Laser welding. *Misubisi juko guho,* 20, No 4 (1983) 435-440 (in Japanese)

DOI: 10.24412/cl-35039-2022-22-41-41

Laser-assisted design of graphene-glass conductive surfaces for electronics and sensing

R. D. Rodriguez*[1], A. Garcia[1], M. Fatkullin[1], S. Shchadenko[1], I. Petrov[1], L. Lu[2], A. Averkiev[1], A. Lipovka*[1], R. Wang[3], J. Sun[3], Q. Li[4], X. Jia[2], C. Cheng[4], O. Kanoun[5], E. Sheremet[1]

1- Tomsk Polytechnic University, Lenin ave. 30, Tomsk, Russia,634050
2- Shihezi University, Shihezi 832003, People's Republic of China
3 - Institute of Ceramics, Chinese Academy of Sciences, Shanghai 200050, China
4 - College of Polymer Science and Engineering, State Key Laboratory of Polymer Materials Engineering, Sichuan University, Chengdu, 610065, China
5- Chemnitz University of Technology, 09111 Chemnitz, Germany
Main author email address: raul@tpu.ru, lipovka.a@gmail.com

Smart and functional electronics designed on the base of daily used objects is an attractive research direction to contribute to the Internet-of-Things. Glass, being a widespread material, which we interact with every day is highly desirable to turn electrically conductive. Especially helpful is to make it within the specific shapes allowing fabrication of electrical circuits and specific sensor geometries, leaving intact and optically transparent the rest and inactive surface (Fig. 1). For this task to be solved the conventional ways to induce the conductivity in glass (such as conductive oxide or metal coatings) are not the most optimal and straightforward [1].

In this work, we propose an elegant way to selectively integrate graphene into glass using the laser-induced backward transfer (LIBT). We use graphene oxide (GO) water suspension as a graphene source, and the LIBT route transfers laser-reduced GO into glass. This way does not only allow making arbitrary shapes, but it also allows the transfer of the lightest and highly reduced rGO sheets contributing to the improved quality of the structures. Finally, our method leads to robust integration with the formation of graphene-glass composites (Fig. 2).

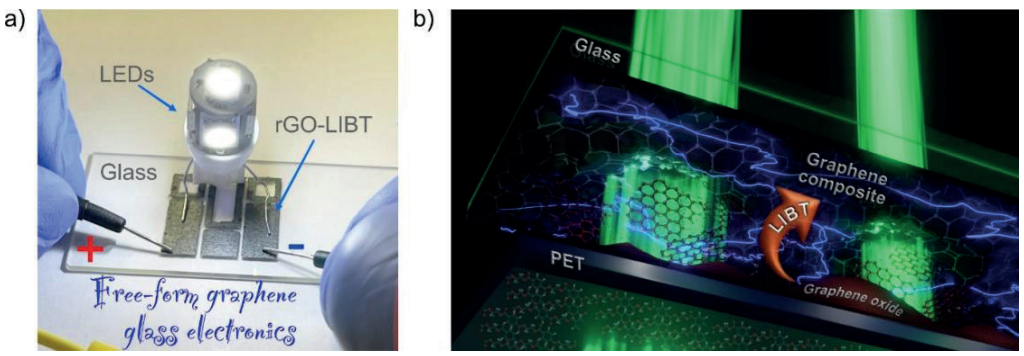

Fig. 1. a) Arbitrary-shaped conductive pattern for lighting LED using our novel graphene-glass composite. b) Concept of LIBT for graphene-glass robust integration.

The structures we get are highly conductive (160 Ohm sq^{-1}), robust enough to survive sonication and mechanical scratching without degradation of performance, and could be functionalized with other materials like silver to improve the performance in electrochemical and plasmonic sensing. Ag-functionalized graphene-glass composites showed the limit of detection of the model analyte down to the nanomolar range.

Our technology does not require comprehensive equipment, is inexpensive, adjustable, and opens multiple opportunities in modern smart electronics and ultrasensitive detection of analytes including drugs and pesticide leftovers.

The reported study was funded by RFBR and DFG, project number 21-51-150001. The research was carried out using the core facilities of TPU's "Physics and Chemical methods of analysis".

[1] W. Xuan, M. He et.al., Fast Response and High Sensitivity ZnO/glass Surface Acoustic Wave Humidity Sensors Using Graphene Oxide Sensing Layer, Sci. Rep., 4, 7206 (2014).

DOI: 10.24412/cl-35039-2022-22-42-42

Laser processing mechanisms of graphene oxide

G. Murastov[1], M. Fatkullin[1], A. Averkiev[1], D. Cheshev[1], L. Kim[1], R.D. Rodriguez[1], E. Sheremet[1].

1- Tomsk Polytechnic University, 30 Lenin Ave, 634050, Tomsk, Russia
Main author email address: esheremet@tpu.ru

Among all the methods of graphene oxide (GO) reduction, the effect of laser radiation on suspensions and films is the most environmentally friendly, both in terms of the reagents used and in terms of energy consumption [1]. Moreover, such a method is spatially controlled (compared to thermal annealing in ovens), which makes it possible to implement reduction locally in the zone of laser beam impact [2]. Thus, by scanning the GO film surfaces with a laser beam, it is possible to create structures of strictly specified sizes and shapes [3]. This approach is easily integrated into modern technological processes of photolithography (compared to the methods of atomic force microscopy (AFM) and scanning electron microscopy (SEM) lithography that require complex expensive equipment) [4].

In the current work, the laser reduction was carried out by irradiating GO films deposited on different substrates such as glass, polyethylene terephthalate (PET), and indium tin oxide (ITO) with photon fluxes of continuous laser with different wavelengths and power densities. Raman spectroscopy and AFM scanning were used to confirm the presence of reduced GO (rGO) (Fig. 1a). We also have created the computational model of GO laser heating based on the finite element method (FEM) to determine the temperature distribution, profile, and maximum that we could reach with particular parameters of laser power, irradiation time, substrate, etc. (Fig. 1b, c). For model verification, experiments with silicon nanowires (NWs) were performed. In this experiment, the temperature was determined indirectly by the correlation of the Raman spectra shift with different power densities of the laser. Finally, the temperatures obtained from the computational model and from the Raman peak shift of Si NWs under the laser irradiation were compared to find the minimum temperature reached at the sample, and therefore the laser parameters for rGO formation.

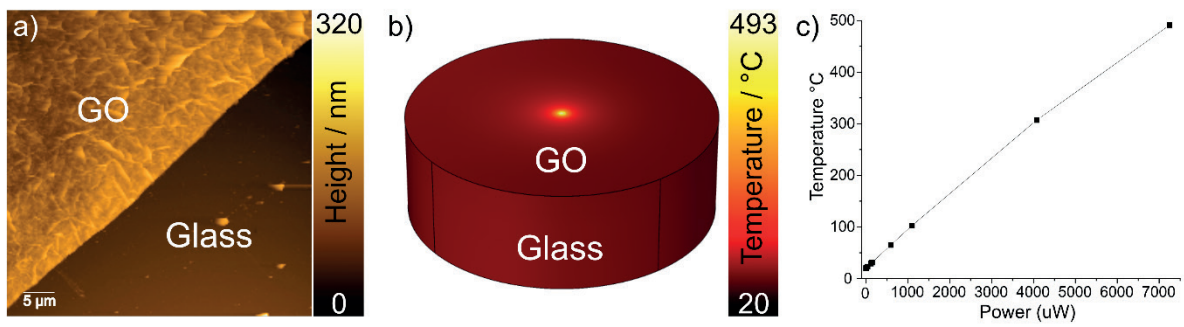

Fig. 1. a) AFM topography image of the GO film/glass interface. b) Simulation GO/glass model image of the temperature distribution after 40 seconds of laser heating with the 7.25 mW power. c) Maximum temperature after 40 seconds of laser heating of GO/glass sample at different laser powers.

The work was supported by Russian Science Foundation grant № 22-12-20027, https://rscf.ru/project/22-12-20027/ and the funding from Tomsk region administration.

[1] Zhang Y.-L., Chen Q.-D., Xia H., Sun H.-B. Designable 3D Nanofabrication by Femtosecond Laser Direct Writing. Nano Today, 5 (5), 435–448, (2010).
[2] Rodriguez R. D., Khalelov A., Postnikov P. S., Lipovka A., Dorozhko E., Amin I., Murastov G. V., Chen J.-J., Sheng W., Trusova M. E., Chehimi M. M., Sheremet E. Beyond Graphene Oxide: Laser Engineering Functionalized Graphene for Flexible Electronics. Mater. Horiz., 7 (4), 1030–1041, (2020).
[3] Lipovka A., Petrov I., Fatkullin M., Murastov G., Ivanov A., Villa N. E., Shchadenko S., Averkiev A., Chernova A., Gubarev F., Saqib M., Sheng W., Chen J.-J., Kanoun O., Amin I., Rodriguez R. D., Sheremet E. Photoinduced Flexible Graphene/polymer Nanocomposites: Design, Formation Mechanism, and Properties Engineering. Carbon N. Y., 194, 154–161, (2022).
[4] Jiang H.-B., Zhang Y.-L., Han D.-D., Xia H., Feng J., Chen Q.-D., Hong Z.-R., Sun H.-B. Bioinspired Fabrication of Superhydrophobic Graphene Films by Two-Beam Laser Interference. Adv. Funct. Mater., 24 (29), 4595–4602, (2014).

DOI: 10.24412/cl-35039-2022-22-43-43

Drilling of micro-hole grids in quartz crystals with ultraviolet picosecond laser

E.M. Ibragimova[1,2], A.A. Sapaeva[1], N.E. Iskandarov[1], F.M. Tojinazarov[1], B.R. Sobirov[1], K.T. Nazarov[1] and Z.T. Azamatov[1]

[1]Center for Advanced Technologies, Tashkent, Uzbekistan;
[2]Institute of Nuclear Physics Academy of Sciences, Tashkent, Uzbekistan
ibragimova@inp.uz

Ultrafast laser pulse of a few μJ energy tightly focused inside the bulk of a transparent solid generates ~ MJ/cm^3 energy density within a micro-scale focal volume; ultraviolet femtosecond lasers are used for patterning micro-grooves in glass substrates by means of laser ablation [1]. However we found that profiles of micro- and nano-holes drilled in silica glass with ultraviolet picosecond laser were changing during a few months due to viscosity of glass network [2]. To eliminate the negative effect of viscous flow, a crystalline dielectric is required for drilling stable micromembranes.

We studied various modes of drilling micro-hole grids in piezoelectric quartz crystal plates of 1 mm thickness with 10 picosecond pulses of diode pumped Nd:YAG laser at the 4th harmonics 266 nm (PL2231-50, Ekspla, Litvania). For intensive UV-absorption the samples were irradiated with ^{60}Co γ-quanta. The surface morphology of the obtained micro- and nano-holes and temporal stability of the hole profiles were studied with scanning electron microscope (SEM EVO-MA10, Zeiss) after deposition of 5 nm Ag film for removing an induced charge. Figure 1 shows profiles and sizes of one micro-hole (a) and 6×6 grid (b), and also profiles of shock waves around each hole (a).

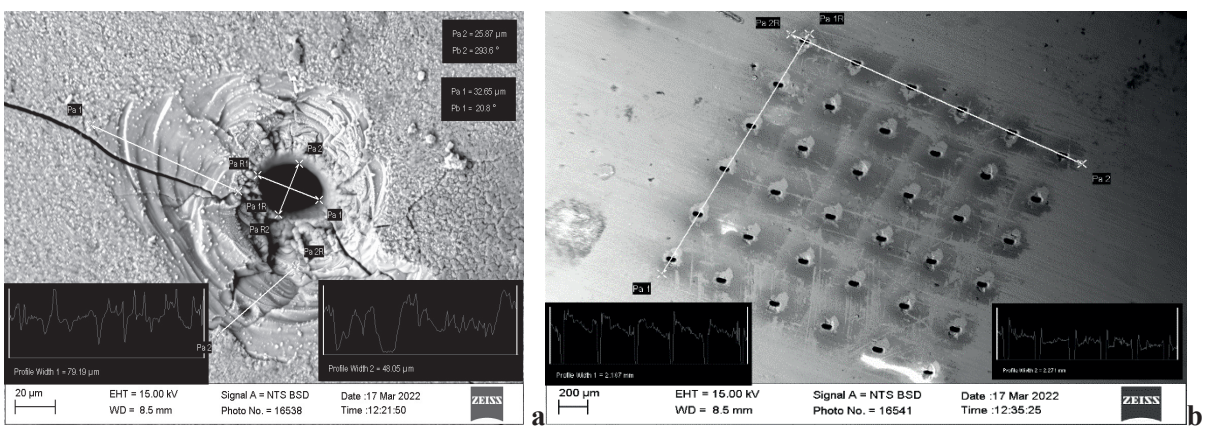

Fig. 1. Profiles of micro-holes drilled in piezo-quartz crystal with 4-th harmonics 266 nm at a pulse energy 3 mJ (a), 14 mJ (b)

Photos taken at higher and lower magnification show an elliptic shape of each hole and asymmetric damage area around it. The local element composition (Energy Dispersion Spectrometer installed in SEM) around the holes was found to deviate from that of the reference sample: the concentration of Si decreases from 45 to 25 w%, while Carbon increases from 8 to 35w%. This effect depends on the laser pulse energy and maybe due to processes in the plasma generated in SiO_2 by the focused laser beam. Fig.1a revealed radial shockwaves with the period of 5 mm. Varying the energy and number of pulses allowed us to obtain through holes in the range of diameters ∅ 5-50 μm, which are suitable for grid membranes filtering or separating liquid mixtures [1]. The crystal lattice of quartz retains the shape of laser holes and frozen radial shock waves, which will allow using the picosecond laser processing to make nano-ribbed and micro-ribbed structures in the near-surface layer about a few microns for resonant tunneling photonic filters.

The research is supported by Ministry of innovation development of Republics Uzbekistan.

[1] V.P. Veiko, V.I. Konov Ed. Fundamentals of laser-assisted micro- and nanotechnologies. 2014, Springer Series in materials science, vol.195.

[2] E.M. Ibragimova, A.A. Sapaeva, V.V. Kim, N.E. Iskandarov, Z.T. Azamatov. 20th Internat. Conf on Radiation Effects in Insulators. 19-23 August, 2019, Nur_Sultan Kazakhstan, Book of Abstract, p.161.

DOI: 10.24412/cl-35039-2022-22-44-44

Laser processing as an approach for an inexpensive, green, and scalable dual-channel pesticide sensor fabrication

M. Fatkullin, A. Lipovka, A. Averkiev, A. Ivanov, J. Kolesnikova, R. Rodriguez, E. Sheremet

Tomsk Polytechnic University, Lenina ave. 30, 634034, Tomsk, Russia
fatkullin.262@gmail.com

The demand of humanity to have clean and safe food and water raised to a critical point during the last century as the concern for the environment, which is hardly affected by humankind. That is why all over the world scientists tend to research how to preserve and minimize damage we are making to the environment and ourselves. The American Chemical Society partially summarized this trend in their 12 principles of green chemistry, one of which is formulated as "Real-time analysis for pollution prevention" [1]. To fulfill this principle, there is a huge need for a new generation of sensors and methods, which would be able to detect targeted analytes fast, selective, and in very small concentrations.

In this work, we are expanding our laser processing technology, for the time shown on aluminum nanoparticles [2], towards the creation of stable high-performance pesticides sensors. We implemented this approach for the integration of silver nanoparticle films on polyethylene terephthalate (PET) substrate to create a plasmonic laser-induced metal/polymer composite (AgLIMPc) (Fig. 1a). This sensor was used to detect organophosphate pesticides by surface-enhanced Raman spectroscopy (SERS) and electrochemistry (Fig. 1b).

We choose the combination of these two methods since SERS is highly selective and sensitive, but often could not be used to make a quantitative analysis. On the other hand, electrochemistry allows quantitative analysis. Also combining these two methods in a single platform gives the opportunity to enhance each other performance [3].

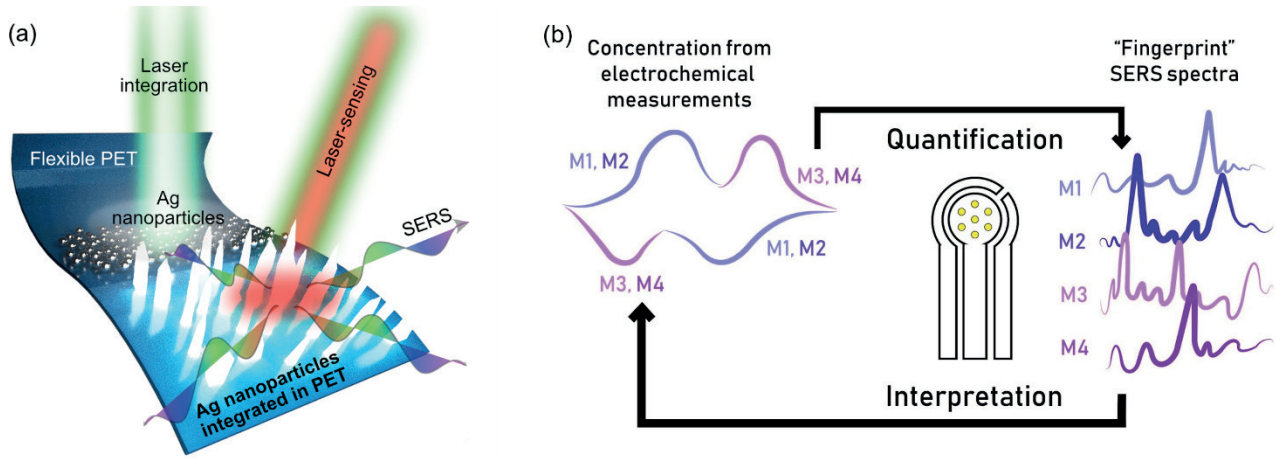

Fig. 1 (a) Sketch of manufacturing of plasmonic sensor based on AgLIMPc; (b) concept art of dual-channel detection.

The reported study was funded by RFBR and DFG, project number 21-51-150001. The research was carried out using the core facilities of TPU's "Physics and Chemical methods of analysis".

[1] Jessop PG, Trakhtenberg S, Warner J. The twelve principles of green chemistry, Innovations in Industrial and Engineering Chemistry. Washington, DC: American Chemical Society, pp. 401–436, (2008)
[2] Rodriguez RD, Shchadenko S, Murastov G, Lipovka A, Fatkullin M, Petrov I, et al. Ultra-robust flexible electronics by laser-driven polymer-nanomaterials integration, Adv Funct Mater.; 2008818, (2021)
[3] Lipovka A, Fatkullin M, Averkiev A, Pavlova M, Adiraju A, Weheabby S, et al. Surface-Enhanced Raman Spectroscopy and Electrochemistry: The Ultimate Chemical Sensing and Manipulation Combination, Crit Rev Anal Chem, pp. 1–25, (2022)

DOI: 10.24412/cl-35039-2022-22-45-45

Coulomb explosion in metals under the influence of fs-laser pulses

V.I. Mazhukin, M.M. Demin, A.V. Shapranov, A.V. Mazhukin

Keldysh Institute of Applied Mathematics of RAS, Moscow, Russia

An ultrashort super-powerful laser action on metal targets leads to the appearance of strongly nonequilibrium states in them, characterized by a large difference in the temperatures of the electron Femi gas T_e and the crystal lattice T_i, $T_e >> T_i$ due to the release of laser radiation energy in the electronic component of the metal. The impact is also accompanied by a powerful transfer of matter, which is characterized by high temperatures, speeds and pressures. It is known that at the metal-vacuum interface there is a thin surface layer of spatially separated electric charges of the opposite sign - a double electric layer (EDL), resulting from the displacement of the electron gas outside the positively charged crystal lattice. EDL is electrically neutral under normal conditions.

The description of the processes of ultrashort fs-ps laser ablation of metals was carried out within the framework of a nonequilibrium combined continuum-atomistic model. The continuum representation was used to describe processes in the electronic component of the metal and EDL in the hydrodynamic approximation [1]. The state of a metal lattice heated by energy exchange with an electron gas was displayed within the framework of an atomistic model. The developed nonequilibrium combined model, which takes into account the influence of the electric field, was used to simulate the fs effects in the Al target.

Mathematical modeling of laser action with duration τ = 100 fs and fluence F = 0.5 J cm^{-2} made it possible to determine two ablation mechanisms, which were noticed earlier in experimental works [2-3]. The first is a fast non-thermal mechanism, the second is a slow thermal ablation mechanism. The appearance of a nonthermal mechanism is related to the fact, as shown by the simulation results, that nonequilibrium laser heating causes a rapid increase in the temperature Te and the electron pressure p_e. The excess electron pressure pene, which acts only inside the electron gas, leads to the violation of the quasi-neutrality of the DEL and the generation of an additional Coulomb force F^{ne}, which exerts a stretching effect on the lattice ions. Upon reaching a sufficient value, the force F^{ne} leads to the breakdown of thin surface layers forming a flow of rapidly expanding ions and clusters at a speed of ~ (8-14) km/s. Non-thermal removal of matter occurs and continues during the duration of the laser pulse. With the end of the laser pulse, the degree of thermodynamic nonequilibrium rapidly decreases, which manifests itself in the equalization of temperatures $T_e \approx T_i$ and pressures $p_e \approx p_e^{eq}$, as well as in the disappearance of the nonequilibrium electron pressure p_e^{ne} and the excess Coulomb force F^{ne}. As the thermodynamic nonequilibrium decreases, the mechanism of fast nonthermal ablation associated with electric fields is replaced by the mechanism of relatively slow thermal ablation, where thermal and HD processes play the main role.

Acknowledgements: This work was supported by Russian Science Foundation (project No. 18-11-00318).

[1] V.I. Mazhukin, M.M. Demin, A.V. Shapranov, A.V. Mazhukin. Appl.Sur.Sct., 530, 2020, 147227
[2]H. Dachraoui, W. Husinsky, G. Betz. Appl. Phys. A, 83(2) (2006) 333–336.
[3]H. Dachraoui and W. Husinsky. Appl. Phys. Lett. 89, (2006) 104102 doi:10.1063/1.2338540

DOI: 10.24412/cl-35039-2022-22-46-46

Anisotropic structuring of $Ge_2Sb_2Te_5$ thin films by femtosecond laser pulses

A.V. Kolchin[1], S. V. Zabotnov[1], D. V. Shuleiko[1], L. A. Golovan[1], M. N. Martyshov[1], A. I. Efimova[1], V. B. Glukhenkaya[2], P. I. Lazarenko[2], T. S. Kunkel[3,4], S. A. Kozyukhin[4], E. V. Kuzmin[5], P. K. Kashkarov[1]

1-Lomonosov Moscow State University, Faculty of Physics, Moscow, Russia
2-National Research University of Electronic Technology, Zelenograd, Russia
3-Moscow Institute of Physics and Technology, Dolgoprudniy, Russia
4-Kurnakov Institute of General and Inorganic Chemistry of RAS, Moscow, Russia
5- Lebedev Physical Institute of RAS, Moscow, Russia
avkolchin@physics.msu.ru

Phase-change material $Ge_2Sb_2Te_5$ (GST225) is widely used for development of memory and nanophotonical devices [1]. In turn, femtosecond laser irradiation allows to fabricate structures which possesses optical [2] and electrophysical properties [3]. Thus, such technology may be used for improvement of GST225-based applications.

Amorphous GST225 thin films with the thickness 200±20 nm on the dielectric substrates (SiO_2/c-Si) were formed by magnetron sputtering. The area with the sizes 3x3 mm^2 was irradiated by femtosecond laser system Avesta (wavelength 1250 nm, pulse duration 135 fs, repetition rate 10 Hz, energy fluence 0.2 J/cm^2, pulse number 240) at the scanning mode. Surface morphology was investigated by optical (OM; Olympus BX41) and scanning electron microscopies (SEM; Carl Zeiss Supra 40). Experimental and theoretical studies of ultrafast phase transition were provided by Raman (Horiba Jobin Yvon HR800; excitation wavelength 488 nm) and energy-dispersive X-ray (EDX; Tuscan Vega 3) spectroscopies, as well two-temperature model (TTM) calculations [4], consequently. In turn, optical and electrophysical properties were studied by IR-Fourie-spectroscopy (Bruker IFS-66/v) and picoampermeter Keitheley 6487 with ARS DE-204SE nitrogen cryostat.

OM- and SEM-images show formation of so-called laser-induced periodic surface structures (LIPSS). Such ripples exhibit the period 1050-1150 nm. As well, the surface gratings are directed orthogonally to the laser polarization. These structural properties can indicate surface plasmon-polariton excitation [3]. In turn, Raman spectra demonstrate transition to face-centered cubic (fcc) crystalline phase [1]. TTM calculations confirm such suggestion. Furthermore, EDX spectroscopy data exhibit that femtosecond laser structuring doesn't influence on GST225 stoichiometry.

Anisotropy of the optical reflectance was observed in the range (800-2000 nm). Such behavior can be explained as alternating of amorphous and crystalline stripes [2]. In turn, conductivity alongside the scanlines is higher on 1-5 order than same value in orthogonal direction. The heterogeneous crystallization most likely emerge electrophysical anisotropy [3].

The observed results can improve memory and nanophotonical devices which is based on GST225.

This work was supported by Russian Foundation for Basic Research (grants №20-32-90111).

[1] B. Gerislioglu et al., Mater. Today Phys., vol. 12, pp. 100178, (2020).
[2] R. Drevinskas et al., Appl. Phys. Lett., vol. 106, pp. 171106, (2015).
[3] D. Shuleiko et al., Nanomaterials, vol. 11., pp. 42, (2021).
[4] N.A. Inogamov et al., High Temperature, vol. 58., pp. 632-646, (2020).

DOI: 10.24412/cl-35039-2022-22-47-47

Modification of $Ge_2Sb_2Te_5$ Thin Film by Femtosecond Laser Pulses under Different Irradiation Modes

M. Smayev[1], P. Lazarenko[2], Yu. Vorobyov[3], T. Kunkel[4], S. Kozyukhin[5]

[1]Lebedev Physical Institute of the Russian Academy of Sciences, Moscow, Russia
[2]National Research University of Electronic Technology, Zelenograd, Russia
[3]Ryazan State Radio Engineering University, Ryazan, Russia
[4]Moscow Institute of Physics and Technology, Dolgoprudny, Russia
[5]Kurnakov Institute of General and Inorganic Chemistry, RAS, Moscow, Russia
sergkoz@igic.ras.ru

The simplicity of switching between the crystalline and amorphous phases of the $Ge_2Sb_2Te_5$ (GST225) thin film, along with the significant differences between the electrical and optical properties for these phases, provides interest in this material for various applications. Multiple reversible phase switching can be observed when GST225 film is subjected to thermal, low-frequency or optical electromagnetic fields. Upon action of ultrashort laser pulses, the formation of a laser-induced periodic surface structure (LIPSS) consisting of alternating lines of a crystalline or amorphous phase is possible [1]. In this work, we study the different types of the laser-induced periodic structures obtained as a result of crystallization and ablation of the initially amorphous Ge2Sb2Te5 thin films as well as the scale them up by a scanning laser beam.

The 130-nm-thick films of amorphous GST225 were produced by a dc magnetron sputtering. The films were deposited on W (200 nm)/TiN (50 nm)/SiO2 (1 μm)/Si multilayer structures. We used a Yb:KGW laser system with a wavelength of 1030 nm. The pulse duration was τ = 185 fs; the repetition rate was in the range 1÷1000 kHz. The films were placed on the translational stage, which made it possible precise positioning and smooth movement of the sample. The light beam diameter on the film surface was about 140 μm ($1/e^2$). The possibility of scaling up the LIPSS was demonstrated by single-pass scanning of the sample with respect to a laser beam. High-quality periodic structures up to 1 mm long were obtained in this way, consisting of about 50 parallel amorphous-crystalline lines with a period of about 1 μm, oriented perpendicular to the light polarization [2]. It has been shown that the recorded extended LIPSS are reflective diffraction gratings due to the large optical contrast between the amorphous and crystalline phases.

We demonstrate that laser ablation is also a convenient way to create spatially ordered surface nanostructures. By irradiating of $Ge_2Sb_2Te_5$ thin films with more energetic femtosecond laser pulses we achieved the formation of organized nanospheres and ripples with pronounced morphology. First pulses generate a surface plasmon-polariton (SPP) wave propagating along the surface. Further irradiation is followed by interference between SPP and incident light; that leads to spatially modulated melting in the interference maxima. The surface represents periodically distributed threads of molten material oriented perpendicular to the polarization vector of laser beam and with a period equal to its wavelength. Plateau-Rayleigh instability modulates the threads into equidistance droplets, which solidify in the form of glassy spheres. Numerical solution of the Fourier equation shows that irradiation of surface covered with regular distributed spheres creates lateral temperature gradient from spheres to film. Due to thermo-capillary (Marangoni) forces arising opposite to the temperature gradient material moves from hot to colder areas, and it leads to the formation of regular structures on the surface.

The study was supported by RFBR (20-03-00379).

[1] S. Kozyukhin, M. Smayev, V. Sigaev, Y. Vorobyov, Y. Zaytseva, A. Sherchenkov, P. Lazarenko, "Specific features of formation of laser-induced periodic surface structures on $Ge_2Sb_2Te_5$ amorphous thin films under illumination by femtosecond laser pulses" Phys. Stat. Sol., v. 257, art. no. 1900617 (2020).

[2] M.P. Smayev, P.I. Lazarenko, I.A. Budagovsky, A.O. Yakubov, V.N. Borisov, Yu.V. Vorobyov, T.S. Kunkel, S.A. Kozyukhin, "Direct Single-Pass Writing of Two-Phase Binary Diffraction Gratings in a $Ge_2Sb_2Te_5$ Thin Film by Femtosecond Laser Pulses" Opt. Laser Technol., v.153, art. no. 108212 (2022).

DOI: 10.24412/cl-35039-2022-22-48-48

Laser assisted synthesis of boron nanoparticles

K.O. Aiyyzhy, E.V. Barmina, G.A. Shafeev

Prokhorov General Physics Institute of the Russian Academy of Sciences,
Vavilova str. 38, 119991 Moscow, Russia

Recently, there has been a great interest in the preparation of elemental boron nanoparticles (NP's). Boron is superior to hydrocarbons in terms of volumetric heat of combustion and in terms of specific mass heat of combustion [1]. These qualities, along with the low toxicity of boron nanoparticles and the possibility of their industrial production, make it possible to consider suspensions of boron nanoparticles in hydrocarbons as promising energy-intensive composite fuels. Studies show that the use of boron nanoparticles as an additive in composite fuel gives a significant increase in temperature in the combustion flame, which affects the energy intensity of the fuel [2, 3]. The burning rate is proportional to the specific surface area of the particles, therefore for efficient combustion the size of the nanoparticles should be as small as possible. Also a decrease size of boron particle lead to an increase in the efficiency of combustion and an expansion of the ignition limits. Industrial powders of Boron are submicron in size. Thus, the aim of this work was to obtain boron nanoparticles with sizes less than 100 nm.

Nanoparticles of elemental Boron are generated by laser ablation of a sintered Boron target in liquid isopropanol and subsequent laser fragmentation of the suspension. For this purpose an ytterbium doped fiber laser with an average power of 20 W, wavelength of 1060-1070 nm, pulse repetition rate of 20 kHz, and pulse duration of 200 ns was used. The size of Boron nanoparticles after ablation and fragmentation of the suspension is around 5-50 nm with maximum of size distribution at 12 nm. Nanoparticles are made mostly of Boron and carbon, some particles have graphitized carbon shell. Crystallographic planes of the shell are visible in Fig. 1. The planes are also projected on the central part of the particle. Their estimated period is 0.34 nm that corresponds to graphitized Carbon. Allotropic composition of nanoparticles differs from that of the initial Boron target. Results of combustion process of hydrocarbon fuels with the addition of Boron NP's showed that during ignition of the composite fuel the temperature in the flame front region increases compared with that in the flame of pure isopropanol.

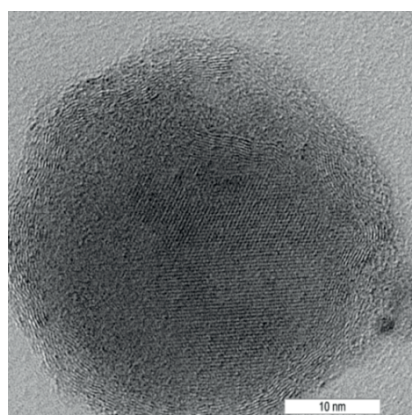

Fig. 1. TEM view of individual Boron nanoparticle

[1] G. Young, K. Sullivan, M. R. Zachariah, K. Yu, Combustion characteristics of boron nanoparticles, Combustion and Flame, vol 156, pp. 322–333, (2009).
[2] S. Karmakar, S. Acharya, K. M. Dooley, Ignition and Combustion of Boron Nanoparticles in Ethanol Spray Flame, Journal of Propulsion and Power, vol. 28, pp. 707-718, (2013).
[3] E.V. Barmina, M.I. Zhilnikova, K.O. Aiyyzhy, V.D. Kobtsev, D.N. Kozlov, S.A. Kostritsa, S.N. Orlov, A.M. Saveliev, V.V. Smirnov, N.S. Titova, G.A. Shafeev, Experimental investigation of diffuse burning of suspension of Boron nanoparticles in isopropanol, Doklady Physics, vol. 67 No. 2, pp. 39–43, (2022).

DOI: 10.24412/cl-35039-2022-22-49-49

Nanostructuring of polymer surfaces mediated by colloidal microparticle lens array by pair of femtosecond laser pulses of different colors

A. Afanasiev, I. Ilyakov, B. Shishkin, A. Pikulin, N. Bityurin

Institute of Applied Physics of Russian Academy of Sciences, 46 Ul'yanov Street, 603950 Nizhny Novgorod, Russia
ava@ipfran.ru

Polymer surfaces covered by the colloidal microparticle lens arrays (polystyrene microspheres, 1mm in diameter) were irradiated by two femtosecond pulses separated in time. The one was at the fundamental frequency of a Ti:sapphire laser and the other was at the second harmonic. Here, about 5 percent of the energy of the fundamental frequency pulse was converted to the second harmonic. Laser irradiation resulted in the elimination of the microspheres and formation of ablation craters of about 100 nanometer size. In our experiments we study the effect of the delay time between the pulses on the nanostructuring results.

Two different polymers were explored. PMMA has a strong linear absorption at the wavelength of the third harmonic of the laser, whereas TOPAS is almost transparent at this wavelength, but it strongly absorbs at the fourth harmonic. We investigated both the dependence of the ablation threshold and the morphology of the craters on the time delay between the pulses. The study of the structures was performed by means of AFM.

We have found that the zero delay time is the most effective for PMMA, as it has been done in our previous paper [1]. On the contrary, the irradiation scheme where the blue pulse comes first proves to be more beneficial for TOPAS.

The explanation relies on the role of the two-photon absorption in the generation of seed electrons in the conduction band. In the case of PMMA, the ω+2ω process dominates, whereas for TOPAS the 2ω+2ω process is preferable. In the most favorable configuration for TOPAS, the seed electrons are generated by the pure second harmonic, whereas the role of the following fundamental frequency pulse is to provide its energy to 'heat' those seed electrons. The simple model of this process is reported.

The laser irradiation through the array of microspheres makes many similar nanostructures at the polymer surface with a single laser shot. What is important is that we obtain a huge amount of realizations of the same laser interaction process simultaneously. This provides a possibility for the statistical filtering of the structure parameters. One can clearly distinguish the observed dependences from artifacts associated with surface inhomogeneities.

When analyzing the ablation nanocraters emerging just beneath the microparticles, one should be aware that the nanostructuring result depends on the environment of the sphere. The recent study shows that the spheres located at the edge of the close-packed array have to be treated in a separate way [2].

This work was financially supported by the Russian Science Foundation grant 22-19-00322.

[1] A. Afanasiev, V. Bredikhin, A. Pikulin, I. Ilyakov, B. Shishkin, R. Akhmedzhanov, N. Bityurin, Two-color beam improvement of colloidal particle lens array assisted surface nanostructuring, Applied Physics Letters, 106, 183102 (2015).
[2] A. Afanasiev, A. Pikulin, I. Ilyakov, B. Shishkin, N. Bityurin, Edge effect at the microsphere colloidal array in near-field particle lithography on polymer surfaces, Surfaces and Interfaces, 29, 101735A (2022).

DOI: 10.24412/cl-35039-2022-22-50-50

Excitation of Rare-Earth Ions Luminescence in Glasses by Satellites of Raman Scattering

G. Malashkevich[1], V. Kouhar[1], A. Sukhodola[1], T. Khottchenkova[1], N. Golubev[2], M. Ziyatdinova[2], V. Sigaev[2]

1 – B.I. Stepanov Institute of Physics of the National Academy of Sciences of Belarus, Minsk, 220072, Belarus
2 – D.I. Mendeleev University of Chemical Technology, Moscow, 125047, Russia
Main author email address: g.malashkevich@ifanbel.bas-net.by

It was recently reported [1] about the luminescence of Yb^{3+} ions in phosphate glasses excited by laser radiation with λ_{exc} = 808 nm which falls outside the $^2F_{7/2} \rightarrow {}^2F_{5/2}$ absorption band of these ions. This effect was explained by the formation of a continuum of the defect centers with the excited states in the field of transparency of a matrix and transfer of excitations from them on the rare-earth activator [2]. Such interpretation for a number of reasons, which are analyzed in the present study, does not seem to be correct. Therefore, we synthesized fused multicomponent glasses and also silica sol-gel ones and studied the luminescence of rare-earth ions (Tb^{3+} and Yb^{3+}) under laser excitation outside their absorption bands. As a result, we found that the dependence of the ions luminescence intensity on the energy gap between the incident quantum and the metastable state of the rare-earth ions excited by it in the glasses correlates with the intensity in the Raman spectrum of the used glass matrices (Fig.).

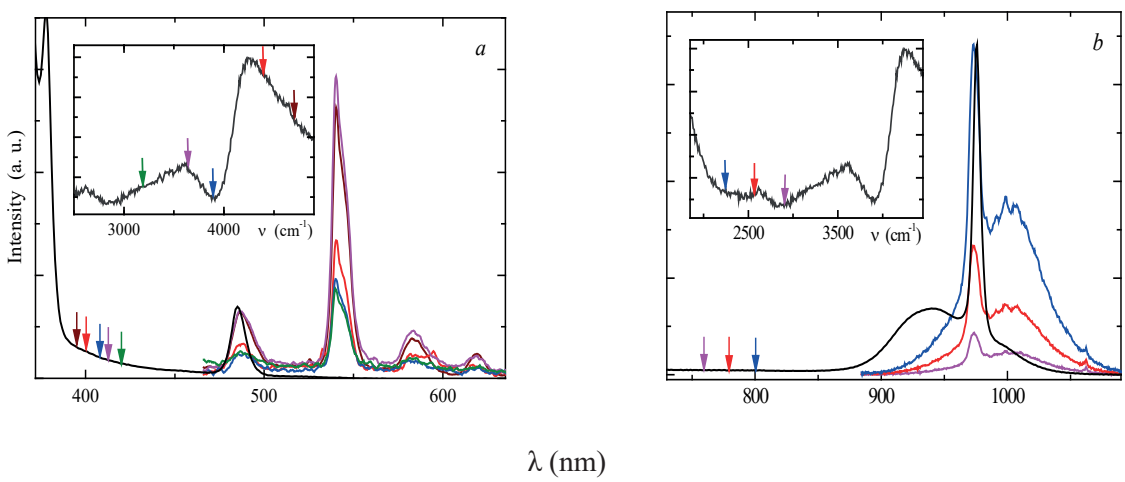

Fig. Absorption (black curve) and luminescence spectra of glasses composition (mol %) $10Tb_2O_3–30Al_2O_3–60B_2O_3$ (*a*) and $2Yb_2O_3–8Y_2O_3–30Al_2O_3–60B_2O_3$ (*b*) at different λ_{exc} (they are marked by arrows, the color of which coincides with the color of the corresponding luminescence spectrum), reduced to the same energy of the excitation pulse, and the Raman spectrum of the matrix (insets).

This correlation made it possible to conclude that the detected effect is due to the emission-free transfer of excitations from Stokes satellites of Raman scattering to the rare-earth activator or, in other words, to the exchange of an incident light quantum for quanta corresponding to excitation of the rare-earth activator and the optical phonon. In this case, the latter can be caused both by vibrations of the matrix structural groupings and vibrations of impurity oscillators, in particular, by hydroxyl (OH^-) groups. It is noted that for Yb-containing phosphate glasses such excitation is possible not only for isolated Yb^{3+} ions, but also through the excited state of paired Yb–Yb centers. Some possibilities of practical use of the described effect are considered.

[1] A.S. Pinheiro, A.M. Freitas, G.H. Silva, M.J.V. Bell, V. Anjos, A.P. Carmo, N.O. Dantas, Laser performance parameters of Yb^{3+} doped UV-transparent phosphate glasses, Chem. Phys. Letters, vol. 592, pp. 164−169, (2014).
[2] W. Stambouli, H. Elhouichet, B. Gelloz, M. Ferid, N. Koshida, Energy transfer induced Eu^{3+} photoluminescence enhancement in tellurite glass, J. Lumin., vol. 132, pp. 205−209, (2012).

DOI: 10.24412/cl-35039-2022-22-51-51

Numerical Simulation and Experimental Validation of Solidification Phenomena in Functionally Graded Inconel625/WC Composite Coatings Fabricated with Laser Metal Deposition

Eyitayo Olatunde Olakanmi[1, 2, 3], Maxim Khomenko[4], Emmanuel Lindsay[1, 2, 3], Idris Akintunde[1, 2, 3], Bathusile Masina[5], Samuel Skhosane[5], Nana Arthur[5], Monnamme Tlotleng[5], Sisa Pityana[5]

[1]Department of Mechanical, Energy & Industrial Engineering,
Botswana international University of Science & Technology, Palapye, Botswana.
[2]UNESCO Chair on Advanced Manufacturing (UCAM) Team,
Botswana International University of Science & Technology, Palapye, Botswana.
[3]Advanced Manufacturing & Engineering Education (AMEE) Research Group,
Botswana International University of Science & Technology, Palapye, Botswana.
[4]Institute on laser and information technologies RAS - branch of FSRC "Crystallography and Photonics" RAS
[5]Laser-Enabled Manufacturing Research Group, Council for Scientific & Industrial Research, Pretoria, South Africa.
[*]Corresponding author: E. O. Olakanmi - UNESCO Chair on Advanced Manufacturing
(olakanmie@biust.ac.bw; +267 742 76012)

Abstract: The three-dimensional (3D) numerical model which predicts solute transport and precipitation phenomena for thin-walled functionally graded (FG) Inconel 625 composite samples reinforced with tungsten carbide (WC-86) particles and fabricated by laser metal deposition (LMD) process is developed via OpenFOAM framework. It elucidates the deposition geometry as well as the conditions of the WC-86 dissolution across the volume of the FG samples as the substrate's preheat temperature is varied. The dynamics and distributions of the temperature field are shown to influence the radius of unmelted WC-86 particles in FG Inconel 625/WC-86 composite thin walls. The increase of substrate's preheat temperature enabled both the thin wall macro parameters and unmelted WC particle radius to increase. The predicted deposition geometry, and the WC-86 dissolution were validated by the experimental data with reasonable accuracy.

Keywords: Functional graded materials (FGM); Inconel 625 composite; Laser metal deposition (LMD); Numerical modelling.

DOI: 10.24412/cl-35039-2022-22-52-52

Pressure pulse in nanosecond laser ablation of mercury due to metal-nonmetal transition: analysis of resent experimental results.

A.A. Samokhin, P.A. Pivovarov

Prokhorov General Physics Institute of the Russian Academy of Sciences, 119991, Moscow, Vavilov str., 38, Russia
e-mail: asam40@mail.ru

In a recent experiment on laser ablation of mercury [1], two features were found in the behavior of the pressure generated in the target: the formation of an additional peak on the pressure pulse and a reduction in the observed delay time Δt for the arrival of the pressure signal from the irradiated region to the piezoelectric sensor. This report presents theoretical estimates confirming the occurrence of these features due to the metal-nonmetal transition (MNT).

With the help of data on the shock compression of mercury [2, 3], the change in the signal delay Δt recorded in [1] was used to determine the shock wave pressure required for this variation. For the cases of Δt = 15 and 50 ns, these pressures are equal to 2630 and 9100 bar, which are approximately 8 times higher than the pressure values indicated in [1] obtained by calibrating the sensor with a conventional thermoacoustic signal in the region of normal boiling temperature. This difference is associated with a change in the calibration coefficient for evaporation pressure signals, the effective area of which is smaller than the thermoacoustic one. An independent estimation of the calibration change can be obtained from the ratio of evaporation pressure (P_2 = 0.56 P_s =560 bar) corresponding to the expected onset of clarification (ρ = 9, T = 1560 K) [4] to the signal value indicated in [1] at a level of ~ 65 bar. This gives about the same correction factor ~8.

Within the framework of the two-wave approach [5], the following estimations were obtained for the speed of the bleaching MNT front d = 165 and 340 m/s, additional pressure ahead of the front P_1 = 2610 and 9100 bar and the required intensity absorbed at the front $I_d = 2.9 \cdot 10^7$ and $5.9 \cdot 10^7$ W/cm^2 for this cases. Estimation of the required total absorbed intensity, taking into account the evaporation process and low absorption in the nonmetal layer for these two cases, gives to the surface absorption coefficient $A \approx 0.62$ and 0.76.

These results are consistent with the assumption about the experimental observation in [1] of the MNT effect during laser ablation of mercury. Further experimental and theoretical studies are needed to elucidate all the main features of the nonequilibrium behavior of metals in the region of their critical parameters, which continue to be insufficiently studied even for mercury.

[1] Samokhin, A.A., Pivovarov, P.A., Shashkov, E.V. et al. On the Metal–Nonmetal Transition under Nanosecond Laser Ablation. Phys. Wave Phen. 29, 204 (2021)
[2] LASL shock Hugoniot data / Stanley P. Marsh, editor. Berkeley; London : University of California Press (1980), 658
[3] A.I. Funtikov, Shock adiabat, phase diagram, and viscosity of mercury at a pressure up to 50 GPa, High Temperature, 47(2) 201 (2009)
[4] I.K. Kikoin, A.P. Senchenkov, S.P. Naurzakov, E.B. Gelman, Perehod metall–nemetall v plotnom metallicheskom pare, Thesis IAE-2310, Moscow 1973 (in Russian)
[5] A.A. Samokhin, P.A. Pivovarov On the mathematical model of combined rarefaction and compression waves in condensed matter Mathematica Montisnigri , 50, 104 (2021).

DOI: 10.24412/cl-35039-2022-22-53-53

Optical Detection of the Glass Transition Temperature of Nanoconfined Polymers Using Plasmon Nanostructures

E. Chernykh, S. Kharintsev

Kazan Federal University, Institute of Physics, Department of Optics and Nanophotonics,
16 Kremlevskaya Street, 420008, Kazan, Russia
elenorchernykh@gmail.com

In the conditions of the modern desire for miniaturization of optoelectronic and photonic devices, the element base of which includes nanosized polymeric materials, the control of their local temperature of phase transitions plays a decisive role. Until now, local detection was carried out by the additional preparation of the sample for the use of methods such as fluorescence spectroscopy [1], which is not always available in the case of polymer film sandwiches. Other existing methods need macroscopic heating of the sample, which can lead to its irreversible destruction of its geometry. As a result, new approaches and methods are require ensuring the registration of the local temperature of phase transitions, since it is handles for the stability of the polymer material, and hence the stability of the device.

We propose to detect the local glass transition temperature using light-induced heat at the nanoscale. Such heating can be generated by plasmonic nanostructures under the action of light under plasmon resonance conditions [2]. However, the increased heat generated by the nanostructure can be dissipated into the substrate with a high thermal conductivity, and as a result, the heating of the nanostructure will be negligible. The creation of enhanced heating of metal nanostructures, which will initiate the glass transition of the polymer, is possible due to the nanostructured surface of the thermostat. We demonstrate that a two-dimensional array of titanium and silicon nitride structures (TiN:Si) allows the creation of localized heating of nanosized polymers, which triggers the glass transition process. The structures are stacked parallelepipeds of titanium and silicon nitride (Figure 1), the latter varying in height. Thermometry of the Raman scattering of light and numerical simulation methods show that with an increase in the height of silicon nanostructures and rise in the temperature of titanium nitride structures is observed. We have determined the glass transition temperature of the nanoconfined polymer PMMA in the form of a thin film for the first time using a tunable plasmonic metasurface and Raman spectroscopy.

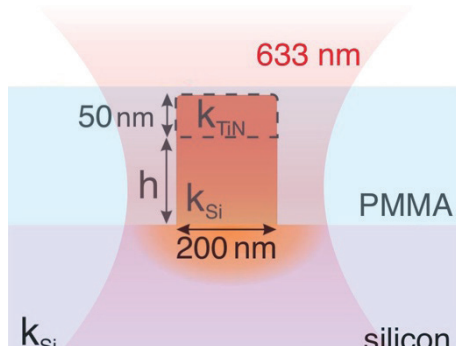

Fig. 1. Scheme of a TiN:Si structure for localized heating of the nanoconfined polymer.

This paper has been supported by the Kazan Federal University Strategic Academic Leadership Program (PRIORITY-2030).

[1] R.R. Baglay and C.B. Roth, Communication: experimentally determined profile of local glass transition temperature across a glassy-rubbery polymer interface with a T_g difference of 80 K, The Journal of Chemical Physics, 143, pp. 111101, (2015).
[2] G. Baffou and R. Quidant, Thermo-plasmonics: using metallic nanostructures as nano-sources of heat, Laser Photonics Review, 7, pp. 171-187, (2013).

DOI: 10.24412/cl-35039-2022-22-54-54

Designing Two-Dimensional Temperature Profiles with Arrays of Tunable TiON:Si Nanostructures

A. V. Kharitonov, S. S. Kharintsev

Department of Optics and Nanophotonics, Institute of Physics,
Kazan Federal University, Kremlevskaya 18, Kazan, 420008, Russia
anvharitonov@kpfu.ru

Optical heat generation and control at the nanoscale play a key role in many applications, including photocatalysis, sensing, thermotics, etc [1]. The heating temperature of a nanostructure is determined by several contributions: the intensity of the incident radiation, the absorption cross section, the heat capacity, and the rate of heat exchange with the thermostat. Tuning the heating temperature can be easily achieved by changing the intensity of the incident light. However, to the best of our knowledge, precise tailoring of the heating temperature at a fixed light intensity is still of no practical implementation. Here, we propose tunable optical nanoheater consisting of titanium oxynitride (TiON) nanocylinder placed on top of Si pillar. The TiON nanostructure acts as a plasmonic antenna that absorbs the incident light. The Si pillar is used to reduce the heat flow from the heated nanostructure to the thermostat (substrate). The designed structure allows for *in situ* adjusting the photoheating temperature at a fixed light intensity. We show, experimentally, that the temperature of TiON:Si nanostructure can be tuned within a broad range 100-700 ^{o}C at the modest incident intensity of 5 MW/cm^2. The temperature is remotely measured using Raman thermometry. Our approach is based on the photoheating-induced oxidation of TiN on air, which leads to formation of a TiON. Typically, preparation of TiON from TiN is not straightforward since the oxidation of TiN quickly leads to the formation of titanium oxide (TiO_2) [2]. We observed a gradual transition from TiN to TiON and then to TiO_2 upon heating at a temperature of 350 ^{o}C. This allowed us to precisely tune the permittivity of TiON. Using this procedure, the absorption cross-section of the TiON nanoantenna can be modified to achieve a desired heating temperature. The proposed TiON:Si nanostructure were used for designing heating surfaces with nonuniform temperature profiles. The heating surface represents a two dimensional array of identical TiON:Si voxels – a three dimensional analogue of pixels. Under uniform illumination all voxels are heated to the same temperature. In order to create a non-uniform temperature profile, we tuned the heating temperature of each voxel through the photoheating-induced oxidation. The results of this study open up new possibilities in photocatalysis and sensing. In particular, the developed TiN:Si nanostructures were used in our recent works for realization of optical sensors for measuring the phase transition temperature of nanosized materials [3, 4].

This paper has been supported by the Kazan Federal University Strategic Academic Leadership Program (PRIORITY-2030).

[1] G.P. Zograf, M.I. Petrov et al., All-dielectric thermonanophotonics, Adv. Opt. Photonics, 13, 643-702 (2021).
[2] L. Braic, N. Vasilantonakis et al., Titanium Oxynitride Thin Films with Tunable Double Epsilon-Near- Zero Behavior for Nanophotonic Applications, ACS Appl. Mater. Interfaces, 9, 29857-29862 (2017).
[3] S.S. Kharintsev, S.G. Kazarian, Nanoscale Melting of 3D Confined Azopolymers through Tunable Thermoplasmonics, J. Phys. Chem. Lett., 13, 5351-5357 (2022)
[4] S.S. Kharintsev, E.A. Chernykh et al, Nanoscale Sensing Vitrification of 3D Confined Glassy Polymers Through Refractory Thermoplasmonics", ACS Photonics, 8, 1477-1488 (2021).

DOI: 10.24412/cl-35039-2022-22-55-55

Influence of Multi-Photon Laser Excitation on Excitons and Free Charge Carriers Dynamics in Lead-Halide Perovskites

D.I. Markina, P.A. Tonkaev, M.A. Masharin, A.P.Pushkarev, S.V. Makarov

ITMO University, Kronverksky pr., 49, St. Petersburg, 197101
Main author email address: daria.markina@metalab.ifmo.ru

Lead halide perovskites are widely known as exciton materials, however, the interplay of excitons and free carriers in them strongly depends on the concentration of charge carriers, temperature, and exciton Bohr radius [1]. The competition between the contributions of excitons and free carriers largely determines the nature of various photophysical processes. It was proved that the contribution of free carriers dominates in solar cells [2], but excitons dominates in light-emitting devices [3]. However, when the carrier concentration becomes extremely high in processes such as lasing [4] and nonlinear upconversion [5], identifying the dominant mechanism becomes a multifactorial problem relevant for modern nanophotonics.

Here the results of a comprehensive study of linear and nonlinear photoluminescence (PL) in CsPbBr3 perovskites depending on the incident excitation energy, temperature, and size of the perovskite structure are presented. It is shown that the dependence of the PL quantum yield on the incident radiation wavelength demonstrates pronounced transitions between different orders of nonlinearity and dependence of output emission intensity on input intensity reveals spectral ranges in which the order of nonlinearity is not equal to the number of photons required for interband absorption. In turn, in the temperature range from 300 K to 6 K, the dependence of the PL on the intensity of the incident radiation shows a decrease in the order of nonlinearity, which corresponds to the exciton response. A similar effect is observed for the case of reduction of the perovskite structures sizes from a 70 nm thick polycrystalline film to nanocrystals (NCs) of 10 nm in diameter. The results obtained are useful for nonlinear nanophotonics, in particular, it is shown that CsPbBr3 NCs introduced in resonant CaCO3 microspheres exhibit two-fold enhanced two-photon PL, which is consistent with the quadratic dependence of the PL signal on the incident light intensity for NCs.

This research was supported by the Presidential Scholarship for Young Scientists and Postgraduates (SP-5169.2021.5) and Priority 2030 Federal Academic Leadership Program Project №922011.

References:

[1] Stranks, S. D, et.al. (2014) Physical Review Applied, 2(3), 034007.
[2] Green, M. A, et.al. (2014) Nature photonics, 8(7), 506-514.
[3] Kim, Y.H., et.al. (2016) PNAS, 113(42), 11694-11702.
[4] D. Yang, et.al. (2018) Optical Letters, 43, 2066.
[5] Zhu, X., et.al. (2019) Advanced Materials, 31(49), 1901240.

DOI: 10.24412/cl-35039-2022-22-56-56

Simulation of microscopic defect formation in layered high-temperature superconducting composites by exposure to ultrashort laser pulses

I. Martirosian, S. Pokrovskii, I. Rudnev

National Research Nuclear University MEPHI, Kashorskoye shosse, 31, Moscow, Russia
Main author email address: mephizic@gmail.com

At present, the most important step in the production of high-temperature superconducting (HTS) materials with high critical current density J_c is the creation of effective magnetic flux pinning centers in the HTS structure. For the HTS, this problem is particularly acute due to the insufficient efficiency of pinning on natural defects and the large contribution of thermal fluctuations at temperatures close to the critical one (T_c). In this regard, the tasks of both determining the conditions for increasing the critical current of materials (the type of defects, their concentration and dispersion) and finding ways to control the creation of additional artificial defects that would act as magnetic flux pinning centers are topical. The main tools for controlled actions on superconductors, leading to a change in their properties, were the introduction of nanosized additives in the solid-state synthesis of high-temperature superconductors [1], surface modification by scratching [2, 3], antidot arrays etching [4, 5], and substrate modification [6 -8], deposition of magnetic islands [9], irradiation with high-energy particles (protons [10], neutrons [11], electrons [12]). Meanwhile, despite some progress in increasing J_c using laser drilling, a number of issues remain unresolved both in terms of optimizing the creating microdefects process and analyzing the mechanisms of defect formation in HTS composites using ultrashort laser pulses.

In this work, pulsed laser action is considered as a method for forming a defect structure of superconducting composites based on REBCO ($REBa_2Cu_3O_{7-x}$, where RE is a rare earth element). A study and numerical analysis of the formation of a defect structure in REBCO HTS films under ultrashort laser irradiation has been carried out. In particular, various laser action regimes and the corresponding local thermal processes leading to heating of the film, melting, and evaporation of the superconducting and the substrate materials are considered. The dependences of the diameter and depth of the defect on the laser radiation energy in a wide energy range (from 50 to 900 nJ) are studied, the features of defect formation are shown for sequences of 2 to 20 laser radiation pulses at one point at different focusing radius of laser radiation (from 1.5 to 3 μm). In the present work, it is shown that the thermal processes occurring under laser irradiation naturally determine the parameters (type, shape, size) of effective pinning centers, and, consequently, the most important fundamental characteristics of HTS materials.

The reported study was funded by RFBR, project number 20-08-00811, and research project № 20-38-90144 (I.V. Martirosian)

[1] B. P. Mikhailov, N. F. Tazetdinova, G. M. Leitus, E. A. Tishchenko, P. E. Kazin, and V. V. Lennikov, Journal of Low Temperature Physics, vol. 105, no. 5, pp. 1553-1557, (1996)
[2] R. Wördenweber, P. Lahl, and J. Einfeld, Applied Superconductivity, IEEE Transactions on, vol. 11, pp. 2812-2815, 04/01 2001.
[3] J. Einfeld, P. Lahl, R. Kutzner, R. Wördenweber, and G. Kästner, Physica C: Superconductivity, vol. 351, no. 2, pp. 103-117, (2001).
[4] A. Crisan et al., Phys. Rev. B, vol. 71, (2005).
[5] A. Palau et al., " p. 35008, (2013)
[6] A. Armenio et al., Superconductor Science and Technology, vol. 33, (2020).
[7] L. Piperno et al., IEEE Transactions on Applied Superconductivity, vol. PP, pp. 1-1, (2018).
[8] W. Bian et al., Journal of the European Ceramic Society, vol. 36, (2016).
[9] D. M. Gillingham, Marina Tselepi, A. Ionescu, Physical review. B, Condensed matter 76(21):214412 (2007)
[10] L. Antonova, T. Demikhov, A. Troitskii, A. Yu. Didyk, Physica Status Solidi (C) Current Topics in Solid State Physics 12(1-2), (2014)
[11] T. Aoki, H. Ueda, A. Ishiyama, N. Miyahara, N. Kashima and S. Nagaya, , IEEE Transactions on Applied Superconductivity, vol. 21, no. 3, pp. 3200-3202, (2011)
[12] T. Nishizaki, T. Naito, S. Okayasu, A. Iwase, and N. Kobayashi, Physical Review B, vol. 61, no. 5, pp. 3649-3654, (2000).

DOI: 10.24412/cl-35039-2022-22-57-57

Atomistic modeling of mobility of solid/liquid interfaces of melting/ crystallization of metals Al, Cu, Fe under deep overheating/undercooling conditions

A.V. Mazhukin, A.V. Shapranov, O.N. Koroleva, V.I. Mazhukin

Keldysh Institute of Applied Mathematics of RAS, Moscow, Russia
vim@modhef.ru

Ultrashort pulsed fs-ps-laser action on various materials leads to consideration of a number of important fundamental problems, which at high heating rates include the features of heterogeneous melting/solidification mechanisms and the associated ultimate overheating and undercooling of matter. The speed of movement of the solid/liquid interface (SLI) $\upsilon s\ell$ plays an important role in crystallization/melting processes, and is one of the fundamental concepts of materials science. Based on the analysis of kinetic models of melting/crystallization with diffusion and collisional-thermal confinement, a modification of the transition state theory is performed, which forms the basis of the Wilson - Frenkel kinetic model developed at the beginning of the 20th century. The modification consists in replacing constant coefficients in the forward and reverse transition rates with a functional temperature dependence of the solid/liquid interface $T_{s\ell}$ [1]. Using 3 EAM interaction potentials for Al, Cu, Fe and the molecular dynamics method, atomistic modeling of melting/ crystallization of metals (Al, Cu, Fe) under conditions of deep overheating/overcooling has been performed.

By comparing the results of atomistic modeling with the data of the modified kinetic model for three metals, the temperature dependences of the response function $\upsilon_{s\ell}$ were plotted in the range of maximum allowable overheating/ overcooling values. The modification of the Wilson - Frenkel model is essentially a new kinetic model [2] and allows one to obtain for metals the temperature diffusion-limited dependences of the velocity of the interface $\upsilon_{s\ell}$, described by the same equation in the entire temperature range.

The temperature dependences of the solid/liquid interface velocity, determined from the results of modeling using both interaction potentials, demonstrate a clear asymmetry with respect to the melting point Tm, which is explained by the strong difference between the solidification kinetics in a strongly undercooled state and the kinetics of melting in a highly superheated state.

This work was supported by Russian Science Foundation (project No. 18-11-00318).

[1] Mazhukin, V.I., Shapranov, A.V., Perezhigin, V.E. et al. Kinetic melting and crystallization stages of strongly superheated and supercooled metals. Math Models Comput Simul. 9, 448–456 (2017). https://doi.org/10.1134/S2070048217040081

[2] Mazhukin, V.I., Shapranov, A.V., Mazhukin, A.V. Atomistic modeling of the dynamics of the solid/liquid interface of Si melting and crystallization taking into account deeply superheated/ supercooled states. Math. Montis, 47, 87-99 (2020). DOI: 10.20948/ mathmontis-2020-47-8.

DOI: 10.24412/cl-35039-2022-22-58-58

Delayed effects in laser ablation

A.A. Samokhin, N.N. Il'ichev, A.V. Sidorin, P.A. Pivovarov

Prokhorov General Physics Institute of the Russian Academy of Sciences, 119991, Moscow, Vavilov str., 38
e-mail: asam40@mail.ru

In a number of experimental works [1-4] on nano- and subnanosecond laser ablation of metals after direct exposure to a laser pulse an additional effect was also observed which was significantly delayed relative to the irradiation pulse. To date, this effect remains without a satisfactory explanation as well as some other aspects of non-equilibrium matter behavior near its critical points of liquid-gaz transition. The multi-microsecond delay is difficult to relate to the delay time of explosive boiling in a highly superheated metastable liquid, which corresponds to picosecond times. It was noted in [5] that, under certain conditions, a large delay can be can be explained as due to the occurrence of explosive boiling in the heating zone and the subsequent cavitation process, for the development of which such long times are usual. However the experimental conditions [1-4] differ significantly from those when cavitation is usually observed during laser action on various liquids [5-8]. The work reports on the influence of various conditions of laser action on the occurrence of cavitation during irradiation of the surface of an absorbing liquid.

The results of the pulse action from a holmium laser (λ = 2.92 μm, τ = 100 ns, E = 0.1–1.5 J/cm^2, $d_{ø}$ = 0.2 cm) on water were recorded by a piezoelectric sensor under various conditions on the irradiated surface. The sensor was located directly under a water layer 0.2 cm thick. The absorption coefficient for such radiation in water is about 10^4 cm^{-1}. In this case only an ablation acoustic signal was observed on the free surface which appeared during the action of the laser pulse. In the presence of a solid transparent cover on the surface (sapphire or quartz with a thicknesses of about 1 cm) a second acoustic signal appeared with a delay of up to hundreds of microseconds with an amplitude comparable to the first signal. The use of a thin (50 μm) fluoroplastic film as a coating led to a decrease in the amplitude and delay of the cavitation signal. These results show that cavitation can develop at shorter absorption lengths than in [6] and with less massive cover than was used in [7, 8]. Observation of such a dependence makes it more probable that under the experimental conditions [1–4] the delayed effect of laser action was caused by the cavitation process that developed after explosive boiling in the liquid layer with an absorption length increased to micrometer values due to metal-nonmetal transition.

[1] A.V. Pakhomov, M.S. Thompson, D.A. Gregory, Laser-induced phase explosions in lead, tin and other elements: microsecond regime and UV-emission, J. Phys. D: Appl. Phys. 36 (2003) 2067
[2] J.H. Yoo, S.H. Jeong, R. Greif, and R.E. Russo, Explosive change in crater properties during high power nanosecond laser ablation of silicon, J. Appl. Phys. 88, 1638 (2000)
[3] J. H. Yoo, S. H. Jeong, X. L. Mao, R. Greif, and R. E. Russo, Evidence for phase-explosion and generation of large particles during high power nanosecond laser ablation of silicon Appl. Phys. Lett., 76(6) 783 (2000)
[4] S.I. Kudryashov, S. Paul, K. Lyon, S.D. Allen, Dynamics of laser-induced surface phase explosion in silicon, Appl. Phys. Lett. 98 254102 (2011)
[5] V.I. Vovchenko, S.M. Klimentov, P.A. Pivovarov, A.A. Samokhin, Effect of submillisecond radiation of the erbium laser on absorbing liquid. Bull. Lebedev Phys. Inst. 34 325–328 (2007)
[6] Phase-change phenomena and acoustic transient generation in the pulsed laser induced ablation of absorbing liquids, Appl. Surf. Sci. 127–129 53-58 (1998)
[7] A.A. Samokhin, N.N. Il'ichev, P. A. Pivovarov, A.V. Sidorin, Laser vaporisation of absorbing liquid under transparent cover Bull. Lebedev Phys. Inst. 43, 156–159 (2016)
[8] A.V. Pushkin, A.S. Bychkov, A.A. Karabutov and F.V. Potemkin Cavitation and shock waves emission on the rigid boundary of water under mid-IR nanosecond laser pulse excitation. Laser Phys. Lett. 15 065401 (2018)

DOI: 10.24412/cl-35039-2022-22-59-59

Enhanced Raman scattering in amorphous carbon films under cw laser irradiation

S. Saparina[1], A. Gazizov [1,2], S. Kharintsev[1,2]

1-Kazan Federal University, Department Optics and Nanophotonics, Kremlevskaya 18, 420008, Kazan, Russia
2- Institute of Applied Research, Tatarstan Academy of Sciences, Bauman 20, 420111, Kazan, Russia
email address: sveta.saparina@yandex.ru

Ultra-thin amorphous carbon (a-C) films (10-100 nm) are well established protective coatings of optical fibers that operate in harsh environment. The formation of hydrogen- and oxygen-containing functional groups reduces the hermeticity of a-C coatings, and therefore, monitoring these impurities is of great importance [1]. In this work, we propose an approach for detecting of the hydrogen- and oxygen- containing functional groups in carbon composites.

In this work we observed anomalous features of Raman spectra of amorphous carbon films as the temperature varied. In particular, the magnitude of I_{aS}/I_S for the *G* band at room temperature was 1/10, whereas the value predicted by the Boltzmann law is 1/600 [2]. Moreover, the profile of the anti-Stokes spectrum is not mirror-symmetric with respect to the Stokes spectrum. We considered that this behavior can be attributed to the resonance Raman scattering and photo-induced heating of the a-C films under continuous wave laser excitation.

We first estimated the contributions of photo-heating in of I_{aS}/I_S ratio by investigating the Raman spectra at different laser power. The resonance Raman scattering was estimated by introducing a resonance factor as a ratio of anti-Stokes to Stokes scattering cross-sections [3]. We attribute the observed resonance Raman scattering with defect-induced modification of joint electronic density of states of a-C [4]. Thus, factor can be used to assess the degree of enrichment/depletion of a-C with functional groups (hydroxyl, epoxy, carbonyl and carboxyl).

Understanding the physical mechanisms of the anomalous anti-Stokes Raman scattering will improve Raman thermometry.

This paper has been supported by the Kazan Federal University Strategic Academic Leadership Program (PRIORITY-2030).

[1] S.V. Saparina, S.S. Kharintsev, A.I. Fishman, et.al., Water enrichment/depletion of amorphous carbon coatings probed by temperature-dependent dc electrical conductivity and Raman scattering, Appl. Surf. Sci., vol. 570, pp. 151052–151058, (2021).
[2] B.J. Kip and R.J. Meier, Determination of the Local Temperature at a Sample During Raman Experiments using Stokes and anti-Stokes Raman Bands, Appl. Spectrosc., vol. 44, pp. 707–711, (1990).
[3] G. Gordeev and S. Reich, Resonant anti-Stokes Raman Scattering in Single-Walled Carbon Nanotubes, Phys. Rev. B., vol. 96, p. 245415, (2007).
[4] P. Johari and V.B. Shenoy, Modulating Optical Properties of Graphene Oxide: Role of Prominent Functional Groups, ACS Nano, vol. 5, pp. 7640–7647, (2011).

DOI: 10.24412/cl-35039-2022-22-60-60

Laser creation of samples to reveal hidden defects in steel products

E. Surmenko, T. Sokolova, D. Bessonov, Yu. Chebotarevskiy, A. Klushev, N. Kulikov

Saratov State Technical University, 77 Polytechnicheskaya st., 410054, Saratov, Russia
surmenko@yandex.ru

In the manufacture of various products, in particular, rolling bearings, hidden surface defects occur that are not detected by visual inspection. Existing methods for detecting such defects, such as the eddy current method, require "standard samples" to identify defects. In the present work, we propose a method for creating such samples by the method of surface modification by laser radiation.

The modification of the surface of stainless steel samples by laser radiation was carried out, followed by a study of the area of laser action ("burns") by the eddy current method and hardness tester.

To create modified layers on the metal surface in order to obtain "standard samples of the defective layer", defocused millisecond radiation was used.

Burns were applied to the sample using various modes. During the experiment, the focal length 110 mm to the treated surface and the duration of laser radiation pulses 4 ms acted as unchangeable modes; the operating voltage of the drives was the variable parametersю Then the hardness was measured and the eddy current method was applied in the center of burns and in the area of the sample without surface defects.

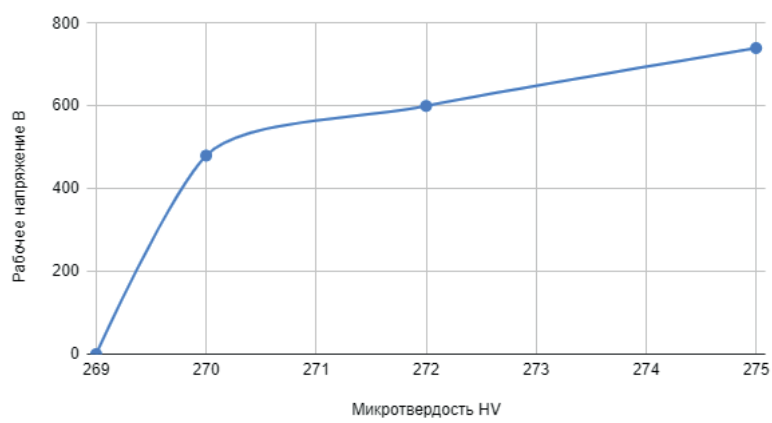

Fig.1. Dependence of microhardness on energy in center of the burn

The eddy current method confirmed the change in the signal in the area of laser action in the absence of visible damage. Based on the data obtained, it can be concluded that the determination of structural changes without external signs is possible using the eddy current method, and samples with laser surface modification can be used as "standard samples".

DOI: 10.24412/cl-35039-2022-22-61-61

Hybrid silicon-based nanoparticles prepared by laser-induced annular plasma

N. Tarasenka[1], V. Kornev[1], S. Gurbatov[2], A. Kuchmizhak[2], N. Tarasenko[1]

1- B. I. Stepanov Institute of Physics, National Academy of Sciences of Belarus, Minsk 220072, Belarus
2- Institute of Automation and Control Processes, Far Eastern Branch of the Russian Academy of Science, Vladivostok 690041, Russia
natalie.tarasenka@dragon.bas-net.by

Recent advances in the field of laser-assisted synthesis show that pulsed laser ablation in liquids (PLAL) has become a versatile tool for nanofabrication providing a possibility of the controlled formation of nanoparticles (NPs) of a given size and composition. In PLAL, particles morphology and structure can be controlled by variation of a number of parameters including target composition, properties of a solvent (for example, temperature), laser parameters as well as laser focusing conditions. The latter approach was used in the present work to produce silicon and hybrid silicon nanostructures decorated with metal NPs. It is noteworthy that despite all the progress, controlled formation of hybrid nanostructures of a given configuration is still challenging and necessitates further development of understanding of the synthesis conditions effect on the NPs parameters. Hereby, to form hybrid NPs, we applied an approach based on laser ablation of a target by laser radiation focused using a combination of an axicon and a converging lens [1]. The idea is to form an annular distribution of light on a target surface with use of the axicon (Fig. 1a). As shown in [2], plasma excitation by laser pulses of an annular profile and its subsequent expansion leads to the formation of a plasma compression layer (stagnation layer) perpendicular to the target surface.

This approach allowed formation of silicon nanospheres as well as hybrid nanoscale silicon decorated with silver and gold NPs. For ablation, the second harmonic of a nanosecond pulsed Nd^{3+}:YAG laser (LOTIS TII, LS 2134D, Belarus) (532 nm, repetition rate 10 Hz, and pulse duration 10 ns, ablation time 30 min) was used. The laser ablation was performed in a mixture of gold and silver colloidal NPs preliminarily prepared by laser ablation of the corresponding targets in acetone. As the results of TEM studies show (Fig. 1b), the developed approach allows obtaining near-spherical particles 30-50 nm in diameter that are decorated with NPs of smaller size. A typical view of the absorption spectra of a colloid obtained by laser ablation of a silicon target in a mixture of Ag and Au colloids is presented in Fig. 1c. As can be seen, the absorption increases in the region of 300–1000 nm, which is promising for application of the prepared samples in nanofluids for photothermal light converters.

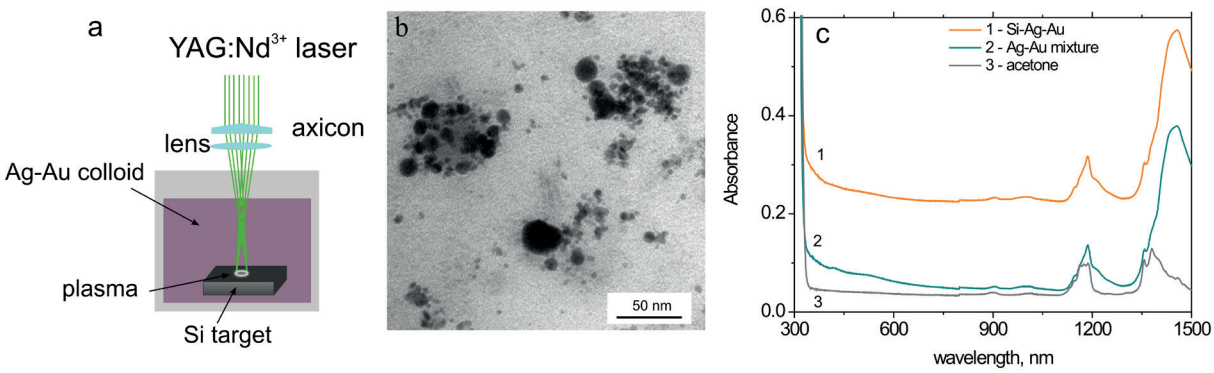

Fig. 1. (a) – Schematic illustration of the hybrid silicon nanoparticles synthesis using an annular beam profile obtained by focusing a Nd:YAG laser beam on a target using a combination of an axicon and a collecting lens; (b) – TEM image of the hybrid Si-Ag-Au nanoparticles obtained; (c) – the absorption spectra of a mixture of silver and gold NPs colloidal solutions in acetone (2), and a colloid synthesized by laser ablation of a pressed silicon target using a ring laser beam (1) in this mixture. The absorption spectrum of acetone (3) is presented for comparison

[1] V. Valenzuela-Villaseca, F. Veloso, G. Muñoz-Cordovez, M. Favre, H. Ruiz, E. Wyndham, Dynamics of laser produced annular plasmas. Journal of Physics: Conference Series. 1043, 012046, (2018).
[2] B. Delaney, P. Hayden, T.J. Kelly, E.T. Kennedy, J.T. Costello, Laser induced breakdown spectroscopy with annular plasmas in vacuo: Stagnation and limits of detection, Spectrochimica Acta Part B: Atomic Spectroscopy, vol. 193, 106430, (2022).

DOI: 10.24412/cl-35039-2022-22-62-62

Picosecond laser-induced micro- and nano-structures on Ti surface

F. Tojinazarov[1,2], E. Ibragimova[1], Kh. Nazarov[1], N. Iskandarov[1]

1- Center for Advanced Technologies, 3A, University st., 100174 Tashkent, Uzbekistan
2- Ajou University in Tashkent, 113, Asalobod street, 100204 Tashkent, Uzbekistan
furqattojinazarov@gmail.com

Enhancement of material surface functionality using short and ultrashort laser pulses has been developed due to their applications in micro- and nanotechnology such as lithography, high-density data storage, micromachining for microelectronics, surface color marking. The surface nano/micro structure was found to exhibit a regular pattern under the appropriate conditions, and this is known as LIPSS (laser induced periodic surface structures). The characteristics of LIPPS as a function of laser parameters such as polarization, fluency, wavelength, and superimposed pulse number have been investigated [1-3]. The micro and nano-structures formed on the surface have a significant impact on optical and mechanical surface properties. The morphology of both microstructures and nanostructures increases the absorption due to the geometric light-trapping effect and generates multiple internal reflections [4].

In this work we present study of LIPPS on titanium surface by dynamic laser processing. Sample is placed on a movable 3D stage allowing vary the scanning speed and step. An electromechanical shutter is used to control the number of laser pulses or to block the laser beam in scanning. A 1064 nm picosecond laser (EKSPLA PL2230) operated with a pulse duration of 28 ps and a repetition rate up to 50 Hz. The beam was focused with a plan-convex lens with the focal length of 75 mm. Laser-induced morphological and composition changes were monitored by scanning electron microscopy (SEM&EDX, EVO MA10, Zeiss). The dependence of the laser parameters on the modified target surface was determined. We also observed structural colourisation on the titanium sample which appears golden and blue. Fig.1 (a) shows SEM image and golden glitter appearance of Ti. Spectral differences between blue and golden titanium as function of wavelength were analysed using a UV-VIS-NIR spectrophotometer (UV-3600 Shimadzu). Fig.1 (b) shows reflectance spectra of Ti before and after processing with laser fluency of 3.75 J/cm^2, the most reduced reflection was about 10% in the range of 300 and 330 nm.

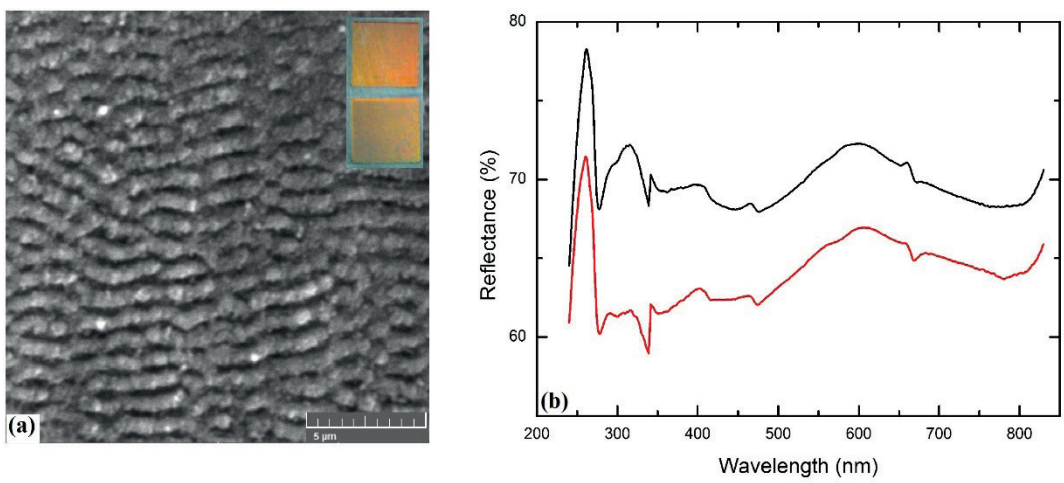

Fig. 1 (a) SEM and inserted optical images of Ti sample modified with 100 mm/min scanning speed at 1064 nm wavelength, (b) Reflectance spectra of Ti: black – before, red – after the laser processing.

[1] S. Maragkaki, et.al.,Wavelength dependence of picosecond laser-induced periodic surface structures on copper, Applied Surface Science, 417, 88-92, (2017).
[2] G.Lazzinia, L. Romolia, F.Tantussib, F.Fuso, Nanostructure patterns on stainless-steel upon ultrafast laser ablation with circular polarization, Optics and Laser Technology, 107, 435-442, (2018).
[3] J. Bonse, S.V. Kirner, J. Krüger, Laser-Induced Periodic Surface Structures (LIPSS) (Springer), (2020).
[4] A. Y. Vorobyev,Chunlei Guo, Multifunctional surfaces produced by femtosecond laser pulses, Journal of Applied Physics 117, 033103 (2015).

BIOMEDICAL PHOTONICS

DOI: 10.24412/cl-35039-2022-22-64-64

In vivo tissue optical clearing as a tool for laser diagnostics and therapeutics

V.V. Tuchin

Science Medical Center, Saratov State University, Astrakhanskaya str. 83, Saratov, 410012, Russia
Laboratory of Laser Molecular Imaging and Machine Learning Tomsk State University, Lenin's av. 36, Tomsk, 634050, Russia
Laboratory of Laser Diagnostics of Technical and Living Systems, Institute of Precision Mechanics and Control, FRC "Saratov Research Centre of Russian Academy of Sciences," Rabochaya str. 24, Saratov, 410028, Russia
e-mail: tuchinvv@mail.ru

The principles and advances in the field of tissue optical clearing, as well as a discussion of new areas of biomedical applications of laser technologies, in particular for multimodal imaging, monitoring of drug delivery and laser therapy are presented [1-3]. Tissue optical clearing is based on the control of the optical properties of tissues by reducing light scattering and improvement of scattering anisotropy factor due to administration of optical immersion agents. The main mechanisms of optical clearing are matching of the refractive indices of tissue components and tissue dehydration with a high impact of constructive interference of scattered waves during temporary and reversible modification of tissue morphology caused by redistribution of refractive index and thicknesses of tissue layers.

Problems of *in vivo* delivery of optical clearing agents, creation of virtual tissue optical windows from UV to THz, multimodal imaging using MRT and CT contrast agents will be discussed. Benefits of a number of laser techniques such as Raman tissue spectroscopy, photoacoustic lymph- and angiography, laser-induced breakdown spectroscopy (LIBS) at using optical clearing will be demonstrated. Laser and optical techniques used for quantification of tissue glycation with the help of diffusion of probing molecules of optical clearing agents in healthy and glycated tissues will be presented. It will be shown that tissue optical clearing is prospective for anticancer and antimicrobial/antifungal/antiviral photodynamic and photothermal therapies.

1. L. Oliveira and V. V. Tuchin, *The Optical Clearing Method: A New Tool for Clinical Practice and Biomedical Engineering*, Springer Nature Switzerland AG, Basel, 2019 – 177 p.
2. V. V. Tuchin, D. Zhu, and E. A. Genina (Eds.), *Handbook of Tissue Optical Clearing: New Prospects in Optical Imaging*, Taylor & Francis Group LLC, CRC Press, Boca Raton, FL, 2022 – 688 p.
3. V.V. Tuchin, E.A. Genina, E.S. Tuchina, A.V. Svetlakova, Y.I. Svenskaya, Optical clearing of tissues: issues of antimicrobial phototherapy and drug delivery, *Advanced Drug Delivery Reviews* **180** (1), 114037 (2022).

DOI: 10.24412/cl-35039-2022-22-65-65

THz solid immersion microscopy: Review and perspectives

N.V. Chernomyrdin[1,2], V.A. Zhelnov[1], M. Skorobogatiy[3], K.I. Zaytsev[1,2]

1- Prokhorov General Physics Institute of the Russian Academy of Sciences, Moscow, Russia
2- Bauman Moscow State Technical University, Moscow, Russia
3- Department of Engineering Physics, Polytechnique Montreal, Montreal, Canada
Main author email address: chernik-a@yandex.ru

Unique effects of terahertz (THz)–wave–matter interaction push rapid progress in THz optoelectronics aimed at bridging the problematic THz gap [1]. However, majority of modern methods of THz spectroscopy and imaging are still hampered by low spatial resolution. Common lens/mirror-based THz optics fails to overcome the Abbe barrier and usually provides resolution larger than a free-space wavelength λ (i.e., hundreds of micrometers or even few millimeters) [2,3]. To mitigate this difficulty, supperresolution THz imaging modalities were introduced recently, among which we particularly underline different methods of THz scanning-probe near-field microscopy. They not only rely on strong light confinement on sub-wavelength probes and provide resolution down to 10^{-1}–10^{-3}λ but also suffer from small energy efficiency or presume an interplay among imaging resolution, signal-to-noise ratio, and performance [4]many research teams working at Terahertz frequencies focused their efforts on surpassing the diffraction limit. Numerous techniques have been investigated, combining methods existing at optic wavelength with THz system such as Time Domain Spectroscopy. The actual development led on one side to a resolution as high as λ/3000 and one the other side to a video-rate recording. The purpose of this paper is to give an overview of the history of the field, to describe the different approaches, to give examples of existing applications and to draw the perspective for this research area. © 2011 The Author(s. In our work, we consider reflection-mode THz solid immersion (SI) microscopy that offers some compromise between the high imaging resolution of 0,15λ and high energy efficiency, which is due to the absence of any subwavelength probe in an optical scheme [2,3]. Recent achievements, challenging problems, and prospects of SI microscopy are overviewed [5–8] with an emphasis on resolving the inverse problem and applications in THz biophotonics [9,10].

[1] Y.-S. Lee, *Principles of Terahertz Science and Technology* (Springer, 2009).
[2] N. V. Chernomyrdin, A. O. Schadko, S. P. Lebedev, V. L. Tolstoguzov, V. N. Kurlov, I. V. Reshetov, I. E. Spektor, M. Skorobogatiy, S. O. Yurchenko, and K. I. Zaytsev, «Solid immersion terahertz imaging with sub-wavelength resolution,» Appl. Phys. Lett. **110**(22), 221109 (2017).
[3] N. V. Chernomyrdin, A. S. Kucheryavenko, G. S. Kolontaeva, G. M. Katyba, I. N. Dolganova, P. A. Karalkin, D. S. Ponomarev, V. N. Kurlov, I. V. Reshetov, M. Skorobogatiy, V. V. Tuchin, and K. I. Zaytsev, «Reflection-mode continuous-wave 0.15λ -resolution terahertz solid immersion microscopy of soft biological tissues,» Appl. Phys. Lett. **113**(11), 111102 (2018).
[4] A. J. L. Adam, «Review of Near-Field Terahertz Measurement Methods and Their Applications,» J. Infrared, Millimeter, Terahertz Waves **32**(8–9), 976–1019 (2011).
[5] V. A. Zhelnov, K. I. Zaytsev, A. S. Kucheryavenko, G. M. Katyba, I. N. Dolganova, D. S. Ponomarev, V. N. Kurlov, M. Skorobogatiy, and N. V. Chernomyrdin, «Object-dependent spatial resolution of the reflection-mode terahertz solid immersion microscopy,» Opt. Express **29**(3), 3553 (2021).
[6] N. V. Chernomyrdin, V. A. Zhelnov, A. S. Kucheryavenko, I. N. Dolganova, G. M. Katyba, V. E. Karasik, I. V. Reshetov, and K. I. Zaytsev, «Numerical analysis and experimental study of terahertz solid immersion microscopy,» Opt. Eng. **59**(6), 061605 (2019).
[7] N. V. Chernomyrdin, M. Skorobogatiy, A. A. Gavdush, G. R. Musina, G. M. Katyba, G. A. Komandin, A. M. Khorokhorov, I. E. Spektor, V. V. Tuchin, and K. I. Zaytsev, «Quantitative super-resolution solid immersion microscopy via refractive index profile reconstruction,» Optica **8**(11), 1471 (2021).
[8] N. V. Chernomyrdin, M. Skorobogatiy, D. S. Ponomarev, V. V. Bukin, V. V. Tuchin, and K. I. Zaytsev, «Terahertz solid immersion microscopy: Recent achievements and challenges,» Appl. Phys. Lett. **120**(11), 110501 (2022).
[9] K. I. Zaytsev, I. N. Dolganova, N. V Chernomyrdin, G. M. Katyba, A. A. Gavdush, O. P. Cherkasova, G. A. Komandin, M. A. Shchedrina, A. N. Khodan, D. S. Ponomarev, I. V. Reshetov, V. E. Karasik, M. Skorobogatiy, V. N. Kurlov, and V. V Tuchin, «The progress and perspectives of terahertz technology for diagnosis of neoplasms: a review,» J. Opt. **22**(1), 013001 (2020).
[10] O. A. Smolyanskaya, N. V. Chernomyrdin, A. A. Konovko, K. I. Zaytsev, I. A. Ozheredov, O. P. Cherkasova, M. M. Nazarov, J.-P. Guillet, S. A. Kozlov, Y. V. Kistenev, J.-L. Coutaz, P. Mounaix, V. L. Vaks, J.-H. Son, H. Cheon, V. P. Wallace, Y. Feldman, I. Popov, A. N. Yaroslavsky, A. P. Shkurinov, and V. V. Tuchin, «Terahertz biophotonics as a tool for studies of dielectric and spectral properties of biological tissues and liquids,» Prog. Quantum Electron. **62**, 1–77 (2018).

DOI: 10.24412/cl-35039-2022-22-66-66

Terahertz and Infrared Spectroscopy of blood plasma for glioblastoma diagnosis

O. Cherkasova[1,2], M. Konnikova[2,3], A. Mankova[3], D. Vrazhnov[4], Yu. Kistenev[5], Y.Peng[6], A. Shkurinov[2,3]

1-Institute of Laser Physics of SB RAS, pr. Lavrentyeva, 15B, 630090 Novosibirsk, Russia
2- Institute on Laser and Information Technologies - Branch of the Federal Scientific Research Centre "Crystallography and Photonics" of RAS, 1 Svyatoozerskaya st., 140700 Shatura, Moscow Region, Russia
3 - Lomonosov Moscow State University, 1 Leninskiye Gory, 119991 Moscow, Russia,
4 - Institute of Atmospheric Optics, Siberian Branch of the RAS, pr. Akademicheskii 1, 634055 Tomsk, Russia
5 - Tomsk State University, 36 Lenin Ave., 634050 Tomsk, Russia
6 - University of Shanghai for Science and Technology, 516 Jungong Rd., 200093 Shanghai, R. P. China
e-mail: o.p.cherkasova@gmail.com

Glioblastoma belongs to deadliest neoplasms. A reason for the glioblastoma poor outcome is a late-stage diagnosis [1]. In this work, we use Terahertz (THz) and Infrared (IR) spectroscopy to study mouse blood plasma in the dynamics of glioblastoma development. IR spectroscopy allows determining concentrations of different compounds present in a biological sample by characteristic frequencies of individual chemical groups [2]. On the other hand, THz spectroscopy is most sensitive to the state of the water, which can be in free and bound states [3]. We compare the capabilities of each method for the early diagnosis of glioma. U87 human glioblastoma in mice of the SCID line was created by the method detailed in [4]. Animals were removed from the experiment on days 7, 14, 21 and 28 after tumor cells inoculation. The THZ and IR spectra analysis was conducted by the Principal Component Analysis, and multidimensional scaling. The prognostic models were developed by the linear kernel Support vector machine, Random forests, and Gradient boosting methods [5, 6].

We have shown a decrease in THz absorption of blood plasma in the dynamics of glioblastoma development. Analysis of the Attenuated Total Reflectance (ATR)–FTIR blood plasma spectra showed an increase in the intensity of the characteristic bands with the glioblastoma development. It was demonstrated that it is possible to use THz and IR spectral data to differentiate glioma stages and to build a predictive model to distinguish between experimental and healthy groups. A machine learning pipeline was proposed to extract the informative features, with good results (sensitivity, specificity, accuracy over 90%). The use of automatic methods to remove outliers in the data improves the robustness of predictive models.

This work was supported by the Russian Foundation for Basic Research (grant # 19-52-55004), the Ministry of Science and Higher Education of the Russian Federation within the State assignment FSRC "Crystallography and Photonics" RAS, by the Interdisciplinary Scientific and Educational School of Moscow University "Photonic and Quantum Technologies. Digital Medicine". The research was carried out with the support of a grant under the Decree of the Government of the Russian Federation No. 220 of 09 April 2010 (Agreement No. 075-15-2021-615 of 04 June 2021).

[1] O. Cherkasova, Y. Peng, M. Konnikova, et al., "Diagnosis of Glioma Molecular Markers by Terahertz Technologies", Photonics, vol. 8(1), pp. 22, (2021).
[2] J. R. Hands, K. M. Dorling, P. Abel, et al., "Attenuated total reflection fourier transform infrared (ATR-FTIR) spectral discrimination of brain tumour severity from serum samples", *J Biophotonics*, vol. 7(3-4), pp. 189-199 (2014).
[3] M. M. Nazarov, O. P. Cherkasova, E. N. Lazareva, et al., "A Complex Study of the Peculiarities of Blood Serum Absorption of Rats with Experimental Liver Cancer", Opt. Spectrosc, vol. 126, pp. 721-729, (2019).
[4] E. L. Zavjalov, I. A. Razumov, L. A. Gerlinskaya, A. V. Romashchenko, "In vivo MRI Visualization of U87 Glioblastoma Development Dynamics in the Model of Orthotopic Xenotransplantation to the SCID Mouse", Russ. J. Genet. Appl. Res., vol. 6 (4), pp. 448–453, (2016).
[5]Kistenev Y.V., Borisov A.V., Kuzmin D.A. et al. J. Biomed. Opt. 22(1), 017002 (2017).
[6] N. Mazumder, G. Gangadharan, Yu. V. Kistenev, Advances in Brain Imaging Techniques (Springer Singapore), pp. 203-230, (2022).

DOI: 10.24412/cl-35039-2022-22-67-67

Study the life activity of regenerative worm *Aeolosoma Viride* using Raman spectroscopy and Two-Photon Fluorescence Lifetime Imaging Microscopy

Pooja Manik Badgujar[1], Jia-Hua Wu[1], Pei-Yang Huang[1], Wrenit Gem Pearl[1], Artashes V. Karmenyan[1], Elena V. Perevedentseva[2], Jiun-Hong Chen[3], Chia-Liang Cheng[1]*

[1]Department of Physics, National Dong Hwa University, Hualien 97401, Taiwan
[2]P. N. Lebedev Physics Institute of Russian Academy of Sciences, Moscow, 119991, Russia
[3]Department of Life Sciences, National Taiwan nNiversity, Taipei, Taiwan
** clcheng@gms.ndhu.edu.tw*

Abstract: Many regenerative studies have been conducted to understand Regeneration's mechanism and which molecular signal is responsible for Regeneration. Freshwater annelid *Aeolosoma Viride* is considered one of the most advanced worms because of its strong regenerative properties, both anterior and posteriorly [1]. Many researchers have been trying to understand the regenerative ability in annelids, but the mechanism is not fully understood. This study investigates the molecular signature present at the sight of regeneration in these annelids using Raman spectroscopy, confocal fluorescence microscopy and FLIM. We observe a strong Raman signal of carotenoids at wound healing, blastema formation, and blastema proliferation of the regenerated worm. This gives a clear understanding that the carotenoid molecule plays the role of a potent antioxidant and is accumulated in the wound healing region. At blastema formation, a strong accumulation of Reactive oxygen species (ROS) is confirmed by observation of strong fluorescence from the DCF dye. At blastema formation, the appearance of carotenoids can be assumed as an antioxidant as a large amount of ROS is generated, Carotenoids act as a scavenger for ROS. Carotenoids on one hand act as potent antioxidant enzymes, however, in other organisms such as invertebrates they are known to promote SOD activity by upregulating the expression of the *ZnCuSOD* gene and invertebrate immunity [2]. Confocal microscopy results clearly display that after carotenoids complete their first role, which is acting as an antioxidant for ROS production, later they play a role of overexpressing the SOD1 gene which plays a major role in worm and invertebrate immunity and in the process of neuronal motor cells. Two-photon imaging of *A. viride* body segments displays a lifetime of 0.65 ns and 2.5 ns. The novelty of this work is we can very clearly observe the participation of carotenoids in cell signaling, proliferation, dedifferentiation, and regeneration using the spectroscopic method.

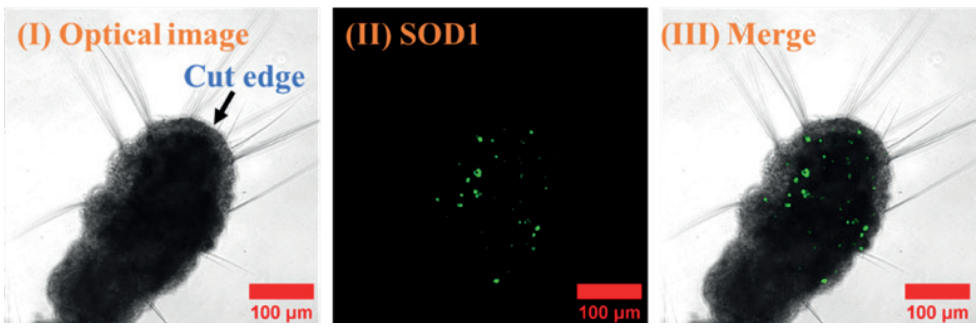

Fig.1. (I) Optical image of anterior regeneration of *A. viride* at 6 hpa (i.e wound healing), (II) antibody tagged SOD1 gene, (III) merged image.

[1] Chen, C-P, Fok, SK-W, Hsieh, Y-W, et al. General characterization of regeneration in *Aeolosoma viride* (Annelida, Aeolosomatidae). *Invertebr Biol*; 139:e12277. 2020.
[2] Tan K, Zhang H, Lim LS, Ma H, Li S, Zheng H. Roles of Carotenoids in Invertebrate Immunology. Front Immunol. 17;10:3041 2020 Jan

DOI: 10.24412/cl-35039-2022-22-68-68

Raman-based liquid biopsy of chronic heart failure patients

L. Bartchenko[1], S. Al-Sammarrae[1], P. Lebedev[2], M. Skuratova[3], I. Bratchenko[1]

1- Samara National Research University, Samara, Russia
2- Samara state medical university, Samara, Russia
3- Samara regional clinical hospital named after VD Seredavin
Main author email address: iabratchenko@gmail.com

Today, one of the most accessible methods of primary assessment of the human body state is a blood test [1]. However, in identifying a specific pathological process in the body, the prognostic significance of a particular biochemical blood index or a set of indices may be insufficient. Improved prognostic significance of a blood test for identifying pathological processes is possible by examining a complex of changes in the blood component composition. Raman spectroscopy is a promising method to reach this goal [2].

In this study, the in vitro analysis of human serum was performed for 205 subjects, including 69 healthy subjects and 61 patients with chronic heart failure (CHF). For surface-enhanced Raman spectroscopy (SERS) analysis, each serum sample was dropped in a volume of 1.5 µl on aluminum foil with a layer of silver structures and dried. The analysis of the serum spectral characteristics was carried out using an experimental stand consisting of a spectrometric system (EnSpectr R785, Spektr-M, Chernogolovka, Russia) and a microscope (ADF U300, ADF, China). Analyzed groups separation based on deep learning was implemented using a separate one-dimensional convolutional neural network (CNN). The choice of the CNN architecture for recognition of the current SERS dataset consisted of several consecutive stages. At the first stage, the verified CNN configurations and advanced deep learning practices based on CNN were examined. Analysis of the work by other research teams has shown that the following CNN configurations are characterized by their possible abilities to recognize Raman spectra: sequential CNNs, CNNs containing the Inception module, CNNs with residual connections, ensemble CNNs, CNNs based on a combination of convolutional layers with recurrent layers [3].

The results of the SERS data for CHF demonstrates that CNN significantly outperforms standard methods of analysis as projection on latent structures and allows for detection of CHF with 95-100% accuracy. By means of multivariate analysis, the informative spectral bands associated with the CHF during disease progression were identified. In addition, the analysis of the correlation between the serum spectral characteristics and urea, creatinine has made it possible to determine the spectral bands correlated with levels of creatinine and urea into the complex spectral characteristics of serum. In general, the reported approach may form the basis for monitoring the health status of CHF patients and find application in studying other pathological conditions of the human body.

[1] J. Watson, I. de Salis, J. Banks, and C. Salisbury, "What do tests do for doctors? A qualitative study of blood testing in UK primary care," Family Practice 34(6), 735–739 (2017).
[2] C. G. Atkins, K. Buckley, M. W. Blades, and R. F.B. Turner, "Raman spectroscopy of blood and blood components," Appl. Spectrosc. 71(5), 767–793 (2017).
[3] P. Wang, L. Guo, Y. Tian, J. Chen, S. Huang, C. Wang, P. Bai, D. Chen, W. Zhu, H. Yang, W. Yao, and J. Gao, "Discrimination of blood species using Raman spectroscopy combined with a recurrent neural network," OSA Continuum 4, 672–687 (2021).

DOI: 10.24412/cl-35039-2022-22-69-69

Laser drug delivery by radiation of Vis and IR lasers: efficacy and spectral study

Belikov Andrey, Fedorova Yulia, Smirnov Sergey, Kozlova Anastasia

ITMO University, 49 Kronverksky Pr., 197101, Saint Petersburg, Russia
Main author email address: avbelikov@gmail.com

Lasers are widely used in modern medicine, including dermatology. The structures of the skin and nails are a serious barrier to most topical medicines. Chemical, physical, and mechanical methods can be used to improve the efficacy of local drug delivery. The use of laser radiation can be an effective and painless physical method for biological tissue microporation and drug delivery. In this case, Vis and IR lasers can be used for microporation, the radiation of which is effectively absorbed by the chromophores of skin and nails (water, proteins, etc.). There are passive and active laser drug delivery. During passive delivery, water-based drugs penetrate into microporated tissue extremely slow due to the high surface tension coefficient [1]. The penetration rate of water-based drugs can be significantly increased with active laser delivery, for example, due to the action of laser-induced hydrodynamic processes occurring in an aqueous solution [2]. One of the most common dermatological problems is a fungal infection. For the treatment of fungal infection, systemic and local drugs are used, including chlorine-containing photodynamic drugs. The combination of laser microporation and the delivery of such photosensitizing drugs with photodynamic action can significantly increase the efficacy of the treatment of fungal diseases. In this case, it should be considered that laser radiation can affect the conformational state of the photodynamic drug during the delivery and change its photodynamic efficacy [3]. In this regard, it is relevant to study the processes of microporation and active delivery of modern chlorine-containing photosensitizing drugs to the skin and under the nail plate, as well as to study the conformational states of these drugs after exposure to Vis and IR laser radiation and photodynamic exposure. In our study we investigate photodynamic drugs «Chloderm 660» and «Chloderm 660 with hyaluronic acid» (Russia).

For in vitro microporation of human nail plates and chicken skin and laser delivery of the drugs, laser radiation with wavelengths of 405 nm (average power up to 1 W, exposure time up to 1 s), 450 nm (average power up to 2 W, exposure time up to 1 s) and 2810 nm (average power up to 0.4 W, pulse duration of 270 μs, exposure time up to 1 s) was used. Optical microscopy was used to study the rate and efficiency of nail plate and skin microporation by laser radiation with and without a layer of the drug of various thicknesses deposited on nail surface. The ablation efficiency increased nonlinearly with an increase in the power of laser radiation with wavelengths of 405 nm, 450 nm and 2810 nm, and decreased with an increase in the exposure duration.

The active delivery of the photosensitizing drugs and their aqueous solutions with different concentrations (0.65 ÷ 90 %) by laser radiation with the same parameters as during microporation was studied. During delivery, various effects were observed in photodynamic preparations as a result of laser exposure, including hydrodynamic processes stimulating active delivery of preparations through a micropore created during laser microporation of a biological tissue. It was established that the rate of active laser delivery of the studied drugs decreases with an increase in the concentration of the drug in water. Extinction spectra of 5 % aqueous solutions the drugs before and after laser exposure to radiation with wavelengths of 405 nm, 450 nm, 2810 nm and photodynamic exposure with a wavelength of 654 ± 10 nm were studied in the spectral range 200÷900 nm. The influence of laser and photodynamic effects on the conformational state of chlorin e6 in the photodynamic drugs was evaluated. The range of radiation parameters of Vis and IR lasers, which leads to a change in the extinction spectra and the conformational state of the studied drugs, was determined.

The research was supported by Russian Science Foundation (project No. 22-25-00468).

[1] A. V. Belikov et al., Er: YLF-laser microperforation of the nail plate for drug delivery, Saratov Fall Meeting 2017: Optical Technologies in Biophysics and Medicine XIX, vol.10716, pp.107160X, (2018).
[2] A.V. Belikov et al., Multi-beam laser-induced hydrodynamic shock waves used for delivery of microparticles and liquids in skin, Lasers in Surgery and Medicine, vol.47, pp.723-736, (2015).
[3] A. V. Belikov, S. N. Smirnov and A. D. Tavalinskaya, Laser Delivery and Spectral Study of a Chlorine-Containing Drug for the Treatment of Onychomycosis at Sequential Laser (λ= 2810 nm) and Photodynamic (λ= 656±10 nm) Impact, Optics and Spectroscopy, pp.1-9, (2021).

DOI: 10.24412/cl-35039-2022-22-70-70

The study of laser-assisted skin optical clearing *in vivo*

E.A. Genina[1,2*], V.D. Genin[1,2], A.B. Bucharskaya[1,3], N.A. Navolokin[1,3], G.S. Terentyuk[1,3], N.G. Khlebtsov[4], V.V. Tuchin[1,2,5]

1 - Saratov State University, 83 Astrakhanskaya str. Saratov, 410012, Russia
2 - Tomsk State University, 36 Lenin's av. Tomsk, 634050, Russia
3 - Saratov State Medical University, 112 Bolshaya Kazachia str., Saratov, 410012, Russia
4 - Institute of Biochemistry and Physiology of Plants and Microorganisms, 13 Prospekt Entuziastov, Saratov, 410049, Russia
5 - Institute of Precision Mechanics and Control RAS, 24 Rabochaya str., Saratov, 410028, Russia
**eagenina@yandex.ru*

Photothermal therapy (PTT), which refers to treatment methods based on photothermal conversion under the action of light radiation, is attracting increasing attention due to its growing potential in oncology [1]. Due to the serious side effects of traditional tumor treatment strategies such as chemotherapy and radiation therapy, PTT may eventually become an alternative. To increase the selectivity of tumor hyperthermia, plasmon resonance nanoparticles can be used, which have a local surface plasmon resonance in a certain spectral range [2].

The use of near-IR radiation falling within the transparency window of biological tissues NIR-I (625–975 nm) [3] for excitation of plasmon resonance provides an advantage over other spectral ranges, since it is less absorbed by the main chromophores: melanin, hemoglobin, and water. However, due to light scattering in skin tissues, the penetration depth of laser radiation decreases. Optical cleaning is an effective means of increasing the effectiveness of PTT. [4].

In this study, the combined use of an immersion agent with low-intensity laser irradiation for optical clearing of the skin before the procedure of plasmon photothermal therapy (PPTT) is suggested. The pilot results of the study of the effect of immersion agents on the optical parameters of the skin, subcutaneous connective tissue and model tumor in rats in vivo with hyperthermia during PPTT are presented. A model of alveolar liver cancer – cholangiocarcinoma transplanted subcutaneously was used as a model tumor. Gold nanorods with an absorption band in the area of diode laser radiation (808 nm) were injected into the tumor. Measurements of the optical parameters of the whole tumor and its layers were carried out using spectrometers in the wavelength range 350-2200 nm. A reduction in thermal damage of the skin was obtained during PPTT with preliminary optical clearing using an immersion agent (a mixture of 70% aqueous glycerol solutions with 5% and 10% DMSO) and low-intensity laser irradiation at a wavelength of 808 nm.

The reported study was funded by the grant of RFBR (#20-52-56005) and the grant under the Degree of the Government of the Russian Federation No. 220 of 09 April 2010 (Agreement No. 075-15-2021-615 of 04 June 2021).

[1] H.S. Jung, P. Verwilst, A. Sharma, J. Shin, J.L. Sessler, J.S. Kim, Organic molecule-based photothermal agents: an expanding photothermal therapy universe, Chem. Soc. Rev., vol. 47, pp. 2280–2297 (2018).
[2] X. Huang, P.K. Jain, I.H. El-Sayed, M.A. El-Sayed, Plasmonic photothermal therapy (PPTT) using gold nanoparticles, Lasers Med. Sci., vol. 23, pp. 217-228 (2008).
[3] A.N. Bashkatov, K.V. Berezin, K.N. Dvoretskiy, M.L. Chernavina, E.A. Genina, V.D. Genin, V.I. Kochubey, E.N. Lazareva, A.B. Pravdin, M.E. Shvachkina, P.A. Timoshina, D.K. Tuchina, D.D. Yakovlev, D.A. Yakovlev, I.Yu. Yanina, O.S. Zhernovaya, V.V. Tuchin, Measurement of tissue optical properties in the context of tissue optical clearing, J. Biomed. Opt., vol. 23, pp. 091416-1 – 091416-31 (2018).
[4] J.-I. Youn, The effect of an optical clearing agent on tissue prior to 1064-nm laser therapy, Med. Laser, vol. 10, pp. 146-152 (2021).

DOI: 10.24412/cl-35039-2022-22-71-71

Laser Speckle Auto-inverse Covariance for Blood Flow Imaging

Jiachi Hong[1], Jinling Lu[1], Pengcheng Li[1,2]

[1]Britton Chance Center for Biomedical Photonics, Wuhan National Laboratory for Optoelectronics, Optics Valley Laboratory-Huazhong University of Science and Technology, Wuhan, 430074, China
[2]School of Biomedical Engineering, Hainan University, Haikou, 570228, China
pengchengli@mail.hust.edu.cn

As a non-contact wide-field imaging technique for measuring the blood flow speed, laser speckle imaging is widely used in clinical diagnosis and therapy. However, several factors affect the accuracy of laser speckle detection of blood flow, such as coherence loss and noise associated with the imaging system, the form of the auto-correlation function of the electric field related to the characteristics of biological tissue, non-ergodic components associated with static scattering, and finite statistical sample size. To realize the quantitative measurement of blood flow speed and improve the robust of the measurement in the practical clinic conditions. The influence of the statistical sample size on the mean of the speckle contrast was deduced by the probabilistic and statistical methods [1]. A method for unbiased estimation of flow velocity in the range of 0.1~30 mm/s was proposed [2]. The influence of the properties of biological tissue and the imaging system on laser speckle auto-inverse covariance was discussed. The quantitative laser speckle auto-inverse covariance model for imaging blood flow velocity was established and validated in phantom and animal experiments [3].

This work was supported by the National Natural Science Foundation of China (Grant No. 61890951, 61890950, 81971659), the National Key Research and Development Program of China (Grant No. 2021YFC2400102), the Innovation Project of Optics Valley Laboratory (Grant No. OVL2021BG012).

[1] Jiachi Hong, Yang Wang, Xiao Chen, Jingling Lu and Pengcheng Li, Fluctuations of temporal contrast in laser speckle imaging of blood flow, Optics Letters, 2018, 43(21): 5214-5217
[2] Jiachi Hong, Liang Shi, Xuan Zhu, Jinling Lu and Pengcheng Li, Laser speckle auto-inverse covariance imaging for mean-invariant estimation of blood flow, Optics Letters, 2019, 44(23):5812-5815
[3] Jiachi Hong , Xuan Zhu, Jinling Lu and Pengcheng Li, Quantitative laser speckle auto-inverse covariance imaging for robust estimation of blood flow, Optics Letters, 2021, 46(10): 2505-2508

DOI: 10.24412/cl-35039-2022-22-72-72

Laser assisted methods in haemorheologic research

Alexander Priezzhev[1], Andrei Lugovtsov[1], Petr Ermolinskiy[1], Alexei Semenov[2], Sergey Nikitin[1], Yuri Gurfinkel[3], Kisung Lee[4]

[1]Department of Physics, Lomonosov Moscow State University, Leninskye Gory, 1-62, Moscow, 119991, Russia;
[2]Department of Biology, Lomonosov Moscow State University, Leninskye Gory, 1-12, Moscow, 119991, Russia;
[3]Medical research and educational center, Lomonosov Moscow State University, Lomonosovskiy ave., 27-10, Moscow, 119234, Russia;
[4]Center for Soft and Living Matter, Institute of Basic Science, Ulsan 44919, Korea;
avp2@mail.ru

Laser technologies (laser tweezers, diffuse light scattering, laser diffractometry and digital capillaroscopy) have shown their high potential in haemorheologic research since several decades ago because of a large variety of the effects of laser light interaction with biological structures constituting blood. Quick development of biophotonics methods of visualization, sensing and measurement based of registration of light scattering and fluorescence have given an impetus to the studies, in particular, of blood composition and rheology and their alteration under pathologies. We describe our more than 20-years long experience in designing and implementing laser technologies for studying blood microrheology and microcirculation. We evaluate the feasibility of these techniques to assess microrheological effects of various molecular mechanisms affecting erythrocyte aggregation and deformability. In particular, we show that laser tweezers and diffuse light scattering allow for assessing the changes in erythrocyte aggregation in whole blood samples and cell suspensions both on the level of single cells and on the level of large ensembles of cells. Application of these methods in vitro enable one to study the mechanisms of erythrocyte aggregation because they are sensitive to changes in the medium surrounding the cells (i.e., blood plasma, serum or model solutions of blood plasma proteins) and to changes in the cellular properties of the erythrocytes (i.e., effects on the cell membrane due to glycoprotein inhibition). Using the laser diffractometry technique we are able to assess the distribution of the erythrocytes in sizes and deformabilities. Using digital capillaroscopy we are able to monitor in vivo the alterations of blood flow parameters on the microcirculatory level where the major exchange of gases between blood and tissues takes place. We have been applying all these techniques to monitor the alterations of blood microrheology and microcirculation in patients suffering from such socially important diseases as arterial hypertention and diabetes mellitus.

This work was supported by the Russian Science Foundation (Grant No. 22-15-00120) and performed according to the Development program of the Interdisciplinary Scientific and Educational School of Lomonosov Moscow State University «Photonic and Quantum technologies. Digital medicine»

DOI: 10.24412/cl-35039-2022-22-73-73

Correlation of red blood cell and platelet aggregation measured in vitro by optical techniques in blood of patients suffering from arterial hypertension

P. Ermolinskiy[1], A. Lugovtsov[1], D. Umerenkov[1], L. Dyachuk[2], A. Priezzhev[1]

1- Physics Department, Lomonosov Moscow State University, Leninskie Gory 1-2, Moscow, 119991, Russia
2- Medical Research and Education Center, Lomonosov Moscow State University,
Lomonosovskii pr-t 27, Moscow, 119192, Russia
ermolinskiy.pb15@physics.msu.ru

The aim of this work was to find correlations between RBC-AG and PLA-AG parameters measured *in vitro* by optical methods in blood of patients suffering from AH.

Red blood cell (RBC) aggregation (RBC-AG) is a reversible process of formation of linear and complex structures, and it strongly influences the blood microcirculation and human health in general [1]. Blood aggregation properties depend on many factors, and significantly change in various diseases, such as arterial hypertension (AH), diabetes mellitus, etc. [1]. On the other hand, blood coagulation, which performs the function of homeostasis, mainly depends on platelet aggregation (PLA-AG). PLA-AG also depends on a variety of factors, and in the case of many diseases can vary significantly.

The study included 48 patients with AH who were treated in the cardiology department of Medical Research and Education Center of Lomonosov Moscow State University. Blood of a patient was taken in the morning on an empty stomach and EDTA and sodium citrate anticoagulants were used to stabilize blood samples.

RBC-AG parameters were measured by laser aggregometry technique implemented in the RheoScan device. Several parameters were measured such as the hydrodynamic strength of RBC aggregates, characteristic time of RBC aggregation, and aggregation index.

Biola as the platelet's laser aggregometer was used to measure PLA-AG parameters [3]. Platelet activation was performed by adding the ADP aggregation inducer at different concentrations. The degree and rate of PLA-AG were measured.

Numerical value of correlations of different parameters between each other was calculated using Pearson's criterion. Several correlations were found between RBC-AG and PLA-AG parameters such as degree of PLA-AG and RBC-AG index (R_{Pirson} = 0.32), degree of PLA-AG and characteristic RBC-AG time (R_{Pirson} = -0.34), maximum PLA-AG rate and RBC-AG index (R_{Pirson} = 0.37) and others. It was observed that the characteristic time and the RBC-AG index correlated best with the PLA-AG parameters, whilst the strength of RBC aggregate did not correlate with PLA-AG parameters.

In summary, RBC-AG parameters such as the RBC-AG index and characteristic RBC-AG time correlate with PLA-AG parameters; the strength of RBC aggregates does not correlate with PLA-AG parameters.

This work was supported by the Russian Science Foundation (Grant No. 22-15-00120) and performed according to the Development program of the Interdisciplinary Scientific and Educational School of Lomonosov Moscow State University «Photonic and Quantum technologies. Digital medicine».

[1] O. Baskurt, B. Neu, and H. Meiselman, Red Blood Cell Aggregation, CRC Press, Boca Raton, United States (2012).
[2] A. Lugovtsov, Y. Gurfinkel, P. Ermolinskiy, A. Maslyanitsina, L. Dyachuk, A. Priezzhev. Optical assessment of alterations of microrheologic and microcirculation parameters in cardiovascular diseases. Biomedical Optics Express, vol. 10, 3974. 10.1364/BOE.10.003974 (2019).
[3] A.A. Filkova, A.A. Martyanov, A.K. Garzon Dasgupta, M.A. Panteleev, A.N. Sveshnikova. Quantitative dynamics of reversible platelet aggregation: mathematical modelling and experiments. Sci Rep, vol. 9, 6217 (2019).

DOI: 10.24412/cl-35039-2022-22-74-74

OCE-assisted monitoring and quantification of osmotically-induced strain in biological tissues

Yu.M. Alexandrovskaya[1], O.I. Baum[1], A.A. Sovetsvky[2], A.L. Matveyev[2], L.A. Matveev[2], V.Y. Zaitsev[2]

[1] Institute of Photon Technologies, Federal Scientific Research Centre 'Crystallography and Photonics' of Russian Academy of Sciences, Troitsk, 108840 Moscow, Russia
[2] Institute of Applied Physics of the Russian Academy of Sciences, 603950 Nizhny Novgorod, Russia
yu.alexandrovskaya@gmail.com

The work shows that diffusion of the non-isotonic solutions through biological tissues is accompanied by non-uniform strain, for which its sign and amplitude depend on the solution type and concentration. Such strain often occurs when various optical clearing and/or contrast agents are applied in order to improve the quality of MRI, CT or optical diagnostics. Osmotic strains may affect the tissue integrity, as well as influence the results of diagnostic procedures. Besides, in some cases it may provide additional diagnostically relevant information concerning the tissue hydration and permeability. In the present work the recently developed technique, optical coherence elastography, is used to enable monitoring of spatial distribution and dynamics of osmotically-induced strain within porous biological tissues [1,2]. The effect of different types and concentrations of optical clearing and osmotically active agents, such as polyhydric alcohols, PEGs, saccharides and polyelectrolytes, on the dynamic of osmotically-induced strain within porous biological tissues is discussed in comparative manner. The general regularities of the tissue response to concentration gradients are revealed and described.

The study was supported by the Russian Science Foundation grant No. 22-12-00295

References

[1] Alexandrovskaya, Y.; Baum, O.; Sovetsky, A.; Matveyev, A.; Matveev, L.; Sobol, E.; Zaitsev, V. Optical Coherence Elastography as a Tool for Studying Deformations in Biomaterials: Spatially-Resolved Osmotic Strain Dynamics in Cartilaginous Samples. Materials 2022, 15, 904. https://doi.org/10.3390/ma15030904

[2] Yu. Alexandrovskaya, O. Baum, V. Zaitsev, A. Sovetsky, A. Matveyev, L. Matveev, K. Larin, E. Sobol, V. Tuchin, Optical and mechanical properties of the cartilage during optical clearing, In book Tissue optical clearing: new prospects in optical imaging, CRC Press (Dan Zhu, Elina Genina, and Valery Tuchin Eds.), 2021, Boca Raton, Florida, United States

DOI: 10.24412/cl-35039-2022-22-75-75

Imaging of Molecular Oxygen Using Time-resolved Phosphorescence

V. Shcheslavskiy[1,2], P. Morozov[3], M. Shirmanova[2], G. Goltzman[3] and W. Becker[1]

1- Becker&Hickl GmbH, Nunsdorder Ring 7-9, 12277 Berlin, Germany
2- Privolzhsky Research Medical University, Minin and Pozharsky Sq. 10/1, 603005 Nizhny Novgorod, Russia
3- Moscow State Pedagogical University, Ul. Malaya Pirogovskaya 1/1, 119435 Moscow, Russia
Main author email address: vis@becker-hickl.de

Oxygen molecules both in the ground state and in the first excited state ($^1O_2$) play an important role in photochemical, photophysical and photobiological processes. [1] For this reason, detection and study of oxygen in solutions, cells and whole living organisms is essential for better understanding of the above processes. This presentation describes the development of the technique that allows to map oxygen both in solutions and in biological samples. The technique is based on time-correlated single photon counting and the detection of the photons during the «on» and «off» phases of the high repetition rate laser operation. This way both fluorescence and phosphorescence may be registered simultaneously from the same pixel of an object. We present the results on using this technique for monitoring oxygen content in cells and tissues. Furthermore, this approach can be effectively used to study also singlet oxygen. The most reliable and informative method for $^1O_2$ investigation is the direct measurement of its phosphorescence with a peak around 1270 nm. [2] Unfortunately, most of the detectors have a low quantum efficiency (typically less than 25%) at these wavelengths. [3] In addition, singlet oxygen phosphorescence is very weak with efficiency less than 10^{-6} in aqueous media and has short lifetimes that can be less than a microsecond due to its high reactivity with biomolecules.[4] Therefore, direct $^1O_2$ detection is not in general a trivial task. We show how to do this using a highly efficient superconducting detector [5] in combination with the technique for simultaneous fluorescence and phosphorescence lifetime imaging. The performance of the developed system is verified by measurement of phosphorescence from singlet oxygen generated by the photosensitizers that are commonly used in photodynamic therapy, methylene blue and chlorin e6.

Acknowledgements: The authors acknowledge the support of the studies related to singlet oxygen detection from the Russian Science Foundation (Grant # 22-69-00034).

[1] A.A. Krasnovsky, "Photodynamic Action and Singlet Oxygen", Biophysics ,49, pp. 305- 321(2004).
[2] S.Y. Egorov, S.V. Zinukov, V.F. Kamalov, N.I. Koroteev, A.A. Krasnovskii, and B. N. Toleutaev, "Measurement of photosensitized luminescence of singlet molecular oxygen with nanosecond resolution", Optics and Spectroscopy, 65, pp. 530-533 (1988).
[3] www.idquantique.com/single-photon-systems/products/id230
[4] M. Niedre, M. Patterson, and B. Wilson, "Direct Near-infrared Luminescence Detection of Singlet Oxygen Generated by Photodynamic Therapy in Cells in Vitro and Tissues In Vivo", Photochem. Photobiol,, 75, pp.382-391 (2002).
[5] G. Gol'tsman, O. Okunev, G. Chulkova, A. Lipatov, A. Semenov, K. Smirnov, B. Voronov, A. Dzardanov, C. Williams, R. Sobolewski, "Picosecond superconducting single-photon optical detector" Appl. Phys. Lett. 79, 705 (2001).

DOI: 10.24412/cl-35039-2022-22-76-76

Gold concentration in colloids from extinction at 400 nm: universality for nanoparticles of various shape, morphology, and nanoparticle clusters

N. Khlebtsov[1,2], B. Khlebtsov[1], S. Zarkov[3]

1- Institute of Biochemistry and Physiology of Plants and Microorganisms, Saratov Scientific Centre of the Russian Academy of Sciences (IBPPM RAS)
2- Saratov State University
3- Institute of Precision Mechanics and Control, Saratov Scientific Centre of the Russian Academy of Sciences
khlebtsov@ibppm.ru

The gold concentration in colloids represents important information for biomedical applications, including bioimaging, photothermal therapy, and nanotoxicology. Similarly, the formation and aggregation studies of gold nanoparticles (GNPs) in colloids need an accurate Au concentration as a crucial input parameter. There are several well-established methods to evaluate the GNP concentration in colloids such as ICP-MS, AAS, OES, SAXS, XANES, XAFS, NAA, and voltammetry. However, an optimal procedure would be that requires only standard laboratory equipment such as common UV-Vis spectrophotometry. In particular, the size and concentration of spherical GNPs can be determined from the extinction and the plasmon resonance (PR) wavelength position or the extinction ratio A_{PR}/A_{450}. As the PR amplitude/position strongly depend on the particle shape/morphology or clustering, the most attractive approach seems to be the measurement of 400-nm extinction (absorption) because it corresponds to the interband transition energies from 5d to 6sp in bulk gold and should not be sensitive to the particle details. Specifically, it has been shown that the 400-nm extinction method is suitable for spherical particles of different size and Au nanorods with aspect ratio 3, 4, and 5. Now a reasonable question arises: how universal the 400-nm extinction method is? In other words, can we use it for particles of any shape/morphology or for clusters made of spherical particles? To the best of our knowledge, this point has not been addressed yet. Here, we present a detailed numerical investigation of the method for several models: (1) gold nanorods and nanodiscs with aspect ratios from 2 to 6; (2) gold nanostars and primitive nanostars such as cone, bicone, bicone on a sphere, etc; (3) 2D nanotriangles and nanoplates; (4) ballistic cluster aggregates made of bare GNPs and two-layered GNPs with a dielectric coating. Our main conclusion is that the 400-nm extinction (absorption) does allow the Au(0) concentration to be determined accurately (Fig. 1), as the extinction cross-section scales as the gold volume with a universal prefactor. Therefore, the extinction A_{400} is proportional to the mass-volume gold concentration regardless of the particle morphology and cluster structure. To validate the method, we have fabricated a representative set of samples to analyze them with AAS and ICP-MS techniques. These experiments are ongoing and preliminary data are encouraging.

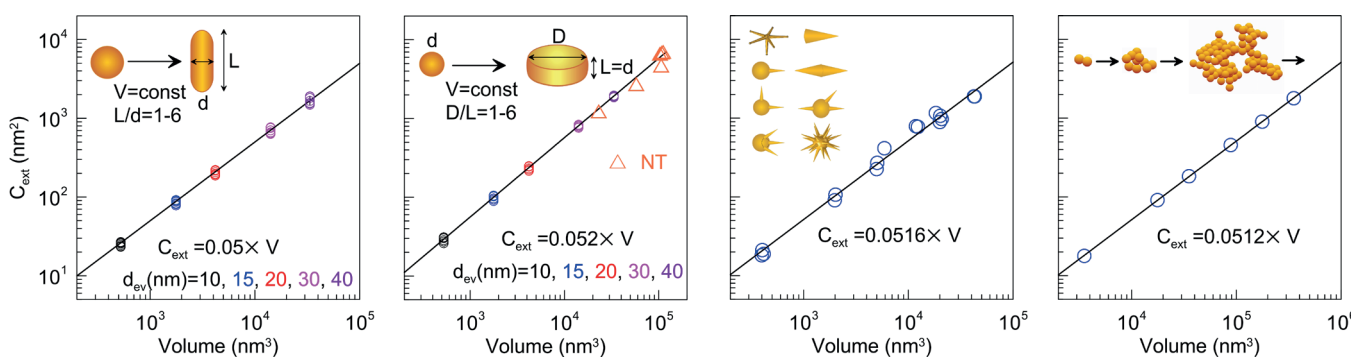

Fig. 1. Evidence for the linear dependence of the extinction cross section of randomly oriented Au nanorods, nanodiscs, nanostars, and clusters on their volume. Simulations were made for 400-nm, the external medium is water. In panels (a) and (b), for each set of 6 points, the aspect ratio varies from 1 to 6 at a constant volume for all 6 aspect ratios. NT stands for nanotriangles (c), different points correspond to models with different volumes; in panel (d), the number of cluster particles varies from 2 to 1000. For all models, the linear fits are very close.

This research was supported by the Russian Scientific Foundation (project no. 18-14-00016-П).

DOI: 10.24412/cl-35039-2022-22-77-77

Microrheologic effects of magnetic nanodiamonds assessed by laser methods

A.E. Lugovtsov[1], P.B. Ermolinskiy[1], E.V. Perevedentseva[2], C.-L. Cheng[3], A.V. Priezzhev[1]

1- Physics Department, Lomonosov Moscow State University, Leninskie Gory 1-2, Moscow, 119991, Russia
2- Lebedev Physical Institute of the Russian Academy of Sciences, Leninskiy ave. 53, Moscow, 119991, Russia
3- National Dong Hwa University, Da Hsueh Rd. 1-2, Hualien, 974301, Taiwan
anlug@biomedphotonics

In the last decade, different types of nanoparticles have been proposed as biocompatible and promising for various applications in many fields of life sciences [1]. In particular, carbon nanoparticles - nanodiamonds (ND) have been proposed for using in theranostic applications – biomedical imaging and photodynamic therapy, direct drug delivery and etc. There are different types of ND that differ in size, surface functionalization, structure, chemistry, physical properties to achieve the desired biophysical properties. For example, it was demonstrated that ND with surface functionalization by carboxylated groups (cND) are more biocompatible and can be used for drug delivery and for contrast visualization of tissues [2]. Another kind of ND – magnetic ND (MND) were proposed and characterized for using as agent for bio-imaging and for magnetic guidance with external magnetic field. Effectiveness of these nanoparticles as anti-cancer drugs for different biological models, such as cancer cell culture (A549 lung carcinoma cell), 3D tissue model (Multi-Cellular Tumor Spheroid on the base of human oral squamous carcinoma cell, SAS) and murine skin tissue was demonstrated [3]. The mehanism of MND action includes their possible interaction with red blood cells (RBCs) in the process of their adsorption on the membranes and penetrations into the cells as well as targeted delivery to the tissues and cancer tumors through the blood flow. It is presumed that in order to reach the target these particles would be intravenously administered into blood. However, so far there is little information on the interaction of MND with blood components. It can be assumed that MNP can affect the RBCs properties such as their ability to reversibly aggregate and deform in shear flow when propagating along blood vessels and capillaries. These alterations can impair blood rheology and, as a result, increase the risk of development of cardiovascular diseases and even mortality during medical application of MND. The aim of our work was to study the *in vitro* effect of MND on blood microrheology – aggregation and deformability properties of RBCs.

Laser diffractometry, diffuse light scattering aggregometry [4] were used to study microrheologic aspects of the interaction of MND with human RBC in vitro. It is expected that the results can provide a basis for determining the cytotoxicity of MND without conducting experiments with animals *in vivo*. When accomplished, this test may significantly reduce the need for experiments with animals when studying the effect of NPs on the human organism. All experimental results were obtained on EDTA stabilized human and rat blood samples incubated with MND in different concentrations.

In vitro effects of MNP on blood microrheology – aggregation and deformability properties of RBC are demonstrated. Incubation of blood with MND at high concentrations of the latter does negatively affect both aggregation and deformability of the cells, the effect being dependent on the particle concentration. Basing on the results one can conclude that the MND can be administered into blood in ambient conditions at low concentrations (30 μg/ml), without significant complication of the blood rheological conditions.

This work was supported by the Russian Scientific Foundation (Grant No. 20-45-08004) and performed according to the Development program of the Interdisciplinary Scientific and Educational School of Lomonosov Moscow State University «Photonic and Quantum technologies. Digital medicine».

[1] M.L. Etheridge et al., The big picture on nanomedicine: the state of investigational and approved nanomedicine products, Nanomedicine: Nanotechnology, Biology, and Medicine, v. 9(1), pp. 1–14, (2013).
[2] Lin-Wei Tsai et al., Nanodiamonds for medical applications: Interaction with blood in vitro and in vivo, *International Journal of Molecular Sciences, v. 17(7), pp. 1111, (2016).*
[3] E. Perevedentseva et al., Multifunctional biomedical applications of magnetic nanodiamond, J. Biomed. Opt., v. 23(9), pp. 091404, (2018).
[4] A. E. Lugovtsov et al., Optical assessment of alterations of microrheologic and microcirculation parameters in cardiovascular diseases, Biomedical Optics Express, v. 10(8), pp. 3974–3986, (2019).

DOI: 10.24412/cl-35039-2022-22-78-78

Silicon Nanoparticles Fabricated by Laser Ablation and Fragmentation: Perspectives in Optical Bioimaging and Photohyperthermia

S. Zabotnov[1], V. Nesterov[1], O. Sokolovskaya[1], D. Shuleiko[1], L. Golovan[1], P. Kashkarov[1], A. Khilov[1,2], D. Kurakina[2], P. Agrba[1,3], E. Sergeeva[1,2], M. Kirillin[2,3]

1- M.V. Lomonosov Moscow State University, Faculty of Physics, 1/2 Leninskie Gory, Moscow, 119991, Russia
2- Institute of Applied Physics RAS, 46 Uljanov St., Nizhny Novgorod, 603950, Russia
3- N.I. Lobachevsky State University of Nizhny Novgorod, 23 Gagarin Ave., Nizhny Novgorod, 603950, Russia
zabotnov@physics.msu.ru

Biodegradability and low toxicity of silicon nanoparticles (Si-NPs) [1,2] allow considering them as diagnostics and therapeutic agents in such optical imaging modalities as fluorescence imaging [1–3] or optical coherence tomography (OCT) [3] as well as in tumor photohyperthermia [4]. To properly address the requirements raised by the biophotonics applications, appropriate nanotechnology approaches are required. Pulsed laser ablation and fragmentation in liquids are powerful tools to control the nanoparticles properties [2,3].

In our work to enhance the efficiency of Si-NPs production, we suggested using preliminary nano- or microstructured silicon instead of usually used bulk crystalline silicon targets: porous silicon films, silicon nanowires arrays and mechanically grinded silicon microparticles (1–8 μm in size) were used as targets at irradiation by picosecond laser pulses (1064 nm, 34 ps, 1–16 mJ). As a result, variation of the silicon-based targets morphology and buffer liquid (water or ethanol) allowed to fabricate Si-NPs with mean sizes from 25 to 200 nm and the high degree of crystallinity [3,5–7]. Additionally, we revealed that at pulsed laser fragmentation of the silicon microparticles in water, the Si-NPs size distributions strongly depend on their initial concentration. An appropriate simulation of propagation of a focused laser beam in a scattering suspension of silicon microparticles was performed for their different mass concentrations and allowed to explain the obtained results [7].

The crystallinity of the Si-NPs ensures fluorescence with a maximum in the red spectral range [3] that indicates the prospects of the fabricated nanoparticles as fluorescence markers in optical bioimaging. Another way to vizualize structural inhomogenities in biological tissuses is using effective Mie scattering in the red and near infrared spectral ranges when the fabricated suspensions may be applied as contrast agents in OCT techique. Experiments with suspensions drops administered on agar gel surfaces confirm such possibility [3].

Using the extracted scattering and absorption parameters of the Si-NPs suspensions, the heating of tumor tissue (basal-cell carcinoma) with embedded nanoparticles was numerically modelled [4]. It was demonstrated that irradiation by a laser beam with the wavelength 633 nm allows to obtain a temperature contrast between tumor and surrounding normal tissues about 5 K, which is suitable for photohyperthermia. Photoinduced heating of agar phantoms with embedded Si-NPs confirmed this tendency.

Thus, the obtained results allow to conclude that the Si-NPs fabricated via laser ablation and fragmentation are promising both optical bioimaging modalities and in photohyperthermia of tumors.

[1] J.-H. Park, L. Gu, G. von Maltzahn, et al., Biodegradable luminescent porous silicon nanoparticles for in vivo applications, Nat. Mater., 8, 331–336, (2009).
[2] M.B. Gongalsky, L.A. Osminkina, A. Pereira, et al., Laser-synthesized oxide- passivated bright Si quantum dots for bioimaging, Sci. Rep., 6, 24732, (2016).
[3] S.V. Zabotnov, A.V. Skobelkina, E.A. Sergeeva, et al., Nanoparticles produced via laser ablation of porous silicon and silicon nanowires for optical bioimaging, Sensors, 20, 4874, (2020).
[4] O.I. Sokolovskaya, E.A. Sergeeva, L.A. Golovan, et al., Numerical simulation of enhancement of superficial tumor laser hyperthermia with silicon nanoparticles, Photonics, 8, 580, (2021).
[5] S.V. Zabotnov, A.V. Skobelkina, F.V. Kashaev, et al., Pulsed laser ablation of silicon nanowires in water and ethanol, Solid State Phenomena, 312, 200–205, (2020).
[6] A.V. Skobelkina, F.V. Kashaev, A.V. Kolchin, et al., Silicon nanoparticles formed via pulsed laser ablation of porous silicon in liquids, Tech. Phys. Lett., 46(7), 687–690, (2020).
[7] V.Yu. Nesterov, O.I. Sokolovskaya, L.A. Golovan, et al., Laser fragmentation of silicon microparticles in liquids for solution of biophotonics problems, Quantum Electron., 52(2), 160–170, (2022).

DOI: 10.24412/cl-35039-2022-22-79-79

Effect of various NP on in vitro development of preimplantation mouse embryos

A. Karmenyan[1], A. Krivokharchenko[2], M. Kormacheva[1], M. Sarmiento[1], E. Barus[1], E. Perevedentseva[3], C.-L. Cheng[1]

1- Department of Physics, National Dong Hwa University, Hualien 97401, Taiwan
2 - N.N. Semenov Institute of Chemical Physics, Moscow 119991, Russia
3- P. N. Lebedev Physics Institute, Moscow, 119991, Russia
artashes@gms.ndhu.edu.tw

Recently, with the tremendous progress in nanotechnologies, the use of various types of nanoparticles (NPs) in mass production and in number of applications has become widespread. Among other applications NPs due to their unique physicochemical properties are promising for biomedical use [1] as a drug carriers, biosensors, coating for medical implants and more. Various surface functionalizations are developed to customize nanomaterials for different application. Despite all the advantages of NPs, there is an enormous variety of cells, the biological effect on which is still insufficiently studied and unpredictable. Thus, development of reproductive technologies (for human and animals) including in-vitro manipulation with early embryos, can lead to increase the interaction probability between NP and the preimplantation embryos.

In this work, we are presenting an express examination of the effect of few different types of NPs on the development of a preimplantation embryo during prolonged incubation (in some cases, during the entire period of development until hatching from the zone pelucida (ZP)), the interaction of NPs with the ZP of oocytes and early mammalian embryos. The assessment of the embryo state included the observation of morphological changes, the period of development, the possibility of passing into the zone, and inside the developing embryo.

The 2-cell stage mice embryos and the oocytes have been used for observation interaction with different kinds of nanodiamonds (ND), titanium dioxide (TiO_2), graphene oxide (GO) particles. The NPs tested were selected due to their wide varied application in many household products, technological and industrial processes and materials; - rapidly growing interest in bio-medical research and applications. They also have previously demonstrated non-toxicity for cellular models and applicability for bioimaging applications and some bio-optical therapies [2,3]. Physical characteristics of used NPs were analyzed (UV-VIS absorption, FTIR and Raman spectra, size distributions, and z-potential were measured). Their interaction with embryos and oocytes was observed using methods of confocal laser microscopy, Raman spectroscopy and fluorescence lifetime imaging with two-photon excitation (TP-FLIM) and analyzed in correspondance with the development observations.

No strong disturbing effect of NPs in applied concentrations neither well-observable penetration of the NDs and TiO_2 into the embryos has been detected. Note that it can opens more opportunities for controllable nanobioapplications of these NPs. Additionally, using TP-FLIM gave the possibilities to detect the penetration of GO NPs through the ZP and to discuss the possible mechanisms of the NP penetration into the ZP and through the ZP into embryos and of relationship between the NPs surface properties, spectral characteristics, and their interaction with the ZP.

Acknowlegement: This work partly was supported by the grant MOST 109-2923-M-259-001-MY3

[1] K. Riehemann, S.W. Schneider, T.A. Luger, B. Godin, M. Ferrari, and H. Fuchs, Nanomedicine—Challenge and Perspectives, Angew. Chem. Int. Ed., 48, pp. 872-897, (2009).
[2] E. Perevedentseva, Y.-C. Lin, Mona Jani, and C.-L. Cheng, Biomedical applications of nanodiamonds in imaging and therapy, Nanomedicine, 8, pp. 2041-2060, (2013).
[3] E. Perevedentseva, D. Peer, V. Uvarov, B. Zousman, and O. Levinson, Nanodiamonds of laser synthesis for biomedical applications, J. Nanoscience & Nanotechnology, 15, pp. 1045-1052, (2015).

DOI: 10.24412/cl-35039-2022-22-80-80

Quantum nano-plasmonics for biosensing and bioimaging on the level of single molecules and virions

P. Melentiev,[1] D. Kudryavtsev,[2] V. Mozhaeva,[2] A. Kalmykov,[1] A. Gritchenko,[1] B. Khlebtsov,[3] R. Kirtaev,[4] D. Negrov,[4] I. Ivanov,[2] A. Siniavin,[2,5] V. Tsetlin,[2] V. Balykin[1]

[1]Institute of Spectroscopy RAS, Moscow 108840, Russia;
[2]Shemyakin-Ovchinnikov Institute of Bioorganic Chemistry of the RAS, Moscow 117997, Russia
[3]Institute of Biochemistry and Physiology of Plants and Microorganisms, Saratov Scientific Centre of the Russian Academy of Sciences, 13 Prospekt Entuziastov, Saratov 410049, Russia
[4]Moscow Institute of Physics and Technology, Dolgoprudniy, Moscow reg., 141700, Russia
[5]N.F. Gamaleya National Research Center for Epidemiology and Microbiology, Ivanovsky Institute of Virology, Ministry of Health of the Russian Federation, Moscow 123098, Russia

The detection and visualization of single atoms and molecules has always been one of the primary tasks of both fundamental scientific and practical importance: the study of the effects of quantum electrodynamics, the development of monatomic/single-molecule devices, the visualization of biological tissues, and much more. Recently, single-molecule detection methods have been used to detect substances at very low concentrations: The molecules of an analyte are detected one by one in a sample, which is known as the single molecule counting method (SMCM).

Recent advances in quantum technology at the nanoscale have enabled the construction of nanoscale mesoscopic systems with quantum emitters, metal and dielectric nanostructures. These systems can exhibit profound quantum electrodynamic properties due to various physical mechanisms such as Foerster energy transfer, plasmonic field enhancement, and strong optical matter-wave coupling. In our study, we demonstrate the realization of ultra-brigh and optically stable plasmonic nano-emitters suitable for the detection and visualization of single biomolecules and virions.

In our study, we consider SMCM in sensing based on the use of ultra-bright and optically-stable plasmonic nano-emitters of light. The approach demonstrates sensitivity at the single molecule level, enabling 5-minute-per-detection of practically important biomarkers of human diseases. As a practical implementation of SMCM, we demonstrate: (i) detection of biomolecules at ultralow concentrations of troponin in human blood - the most important biomarker for human cardiovascular disease - at a level of 10 - 20 fM, (ii) detection of SARS-COV -2 viral particles (human coronavirus). The basic limitations of the sensitivity of such approaches and the issues of their practical implementation will be discussed.

DOI: 10.24412/cl-35039-2022-22-81-81

Unified Monte Carlo platform for light transport in complex geometries

M. Kirillin[1], D. Kurakina[1], I. Fiks[1], A. Getmanskaya[1,2], A. Gorshkov[1,2], A. Khilov[1], V. Perekatova[1], V. Shishkova[1,2], I. Turchin[1], and E. Sergeeva[1]

1 - Institute of Applied Physics RAS, 46 Ulyanov St., Nizhny Novgorod, Russia, 603950
2 - N.I. Lobachevsky State University of Nizhny Novgorod, 23, Gagarin av., Nizhny Novgorod, Russia
Main author email address: mkirillin@yandex.ru

Development of novel optical imaging modalities and interpretation of the optical diagnostic data requires accurate models of light transport in biotissues, in many cases accounting for complex morphology of biological objects. Monte Carlo technique is a recognized gold standard methods for simulation of light transport in tissues benefiting from wide application areas, however, at the expense of computational time. In this paper we report on a unified Monte Carlo platform for simulation of light transport in complex geometries based on triangulation of the morphological structures boundaries. In contrast to traditional voxelization approach, such technique allows to accurately account for refraction of light beams on the boundaries, which is important in the case of low scattering inclusions, such as cerebral spinal fluid in the case of simulation of light transport in brain. The capabilities of the developed platform is demonstrated for murine head geometry (Fig.1a) extracted from the cryo-imaging data and for human skin geometry extracted from in vivo OCT-images. The murine head geometry was employed for simulations of fluorescence probing of a labeled inclusion in brain (Fig.1b-d). The segmentation of the diagnoistic data was performed based on routine machine learning techniques. The platform was also employed to evaluate probing depth in diffuse optical imaging modalities, such as optical diffuse spectroscopy (DOS) and fluorescence imaging (FI). Spectral dependencies of probing depth in DOS were acquired for different source-detector separations in the range of 1-8 mm. Simulations of fluorescence imaging allowed to develop an approach to detection of fluorophore localization based on sevral fluorescence excitation wavelengths.

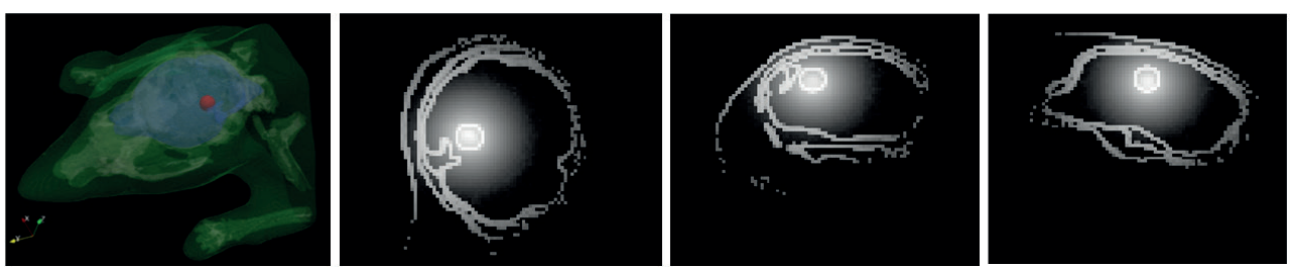

(a) (b) (c) (d)

Fig.1. Complex geometry of murine head extracted from cryo-imaging (a); top (b), frontal (c) and side (d) views of the fluorescence emission from a labeled spherical inclusion in murine head.

The work was supported by Center of Excellence «Center of Photonics» funded by The Ministry of Science and Higher Education of the Russian Federation, contract № 075-15-2020-906.

DOI: 10.24412/cl-35039-2022-22-82-82

Ultrawideband 100 kHz-100kMHz ultrasonic detectors for multiscale optoacoustic angiography

P. Subochev

Institute of Applied Physics, Russian Academy of Sciences,
603950, 46 Ulyanov str., Nizhny Novgorod, Russia
pavel.subochev@gmail.com ; www.photoacoustics.ru;

We report on the development of piezopolymer ultrasound detectors for optoacoustic (OA) angiography with unique characteristics:

- 0.1-100 MHz receiving frequency band;
- <10 Pa noise equivalent pressure;
- 180-degree angular coverage;
- up to ~1 mm^2 apertures.

Using the developed detectors, we demonstrate the true potential of OA technology providing multiscale 30–500 μm angiography of versatile biological objects at depths up to 7 mm.

DOI: 10.24412/cl-35039-2022-22-83-83

Broadband dielectric spectroscopy of astrophysical ice analogues: from the most common molecules toward complex organic compounds

A.A. Gavdush

Prokhorov General Physics Institute of the Russian Academy of Sciences, Russia, 119991 Moscow, Russia
Arsenii.a.gavdush@gmail.com

Estimation of the amount, chemical and physical properties of matter contained in molecular clouds and protoplanetary disks remains a challenging problem of modern astrophysics [1-3]. The interplay between gas phase and icy mantles forming on the surface of dust grains can significantly affect the physical and chemical properties. Molecular freeze-out, found at the center of pre-stellar cores, and expected in the mid-plane of protoplanetary disks implies that the majority of species heavier than He reside on dust grains in these regions. Then the broadband optical properties of astrophysical ice analogues in the infrared (IR) and terahertz (THz) ranges are required for modelling the dust continuum emission and radiative transfer in dense and cold regions. Such data are still missing from the literature, which can be attributed to the lack of appropriate spectroscopic systems and methods for laboratory studies. Moreover, such data are necessary for answering different key questions of astrophysics, including one about the origin and prevalence of organic compounds in space, and therefore about the possible causes of the organic substances appearance.

In the present research the THz time-domain spectroscopy (TDS) and the Fourier-transform IR spectroscopy (FTIR) are combined to study optical and dielectric properties of CO and CO_2 ices in the broad THz–IR spectral range. The measured ices are grown at cryogenic temperatures by gas deposition on a cold silicon window. A method to quantify the broadband THz–IR optical constants of ices is developed. It is based on the direct reconstruction of the complex refractive index of ices in the THz range from the TDS data [4], and the use of the Kramers-Kronig relation in the IR range for the reconstruction from the FTIR data. Uncertainties of the Kramers-Kronig relation are eliminated by merging the THz and IR spectra. The reconstructed THz–IR response is then analyzed using classical models of complex dielectric permittivity.

The complex refractive index of CO and CO_2 ices deposited at the temperature of 28 K is obtained in the range of 0.3–12.0 THz, and fitted using the analytical Lorentz model. Based on the measured dielectric constants, opacities of the astrophysical dust with CO and CO_2 icy mantles are computed. The developed method can be used for a model-independent reconstruction of optical constants of various astrophysical ice analogs in a broad THz–IR range. Such data can provide important benchmarks to interpret the broadband observations from the existing and future ground-based facilities and space telescopes.

[1] A.C.A. Boogert, P. Gerakines, D. Whittet, Observations of the Icy Universe, Annual Review of Astronomy & Astrophysics, 53, pp. 541 (2015).
[2] A. Dutrey et al., CO study of the GM Aurigae Keplerian disk, Astronomy & Astrophysics, 338, pp. L63 (1998).
[3] P. Caselli et al., CO Depletion in the Starless Cloud Core L1544, The Astrophysical Journal, 523, pp. L165 (1999).
[4] B.M. Giuliano et al., Broadband spectroscopy of astrophysical ice analogues: I. Direct measurement of the complex refractive index of CO ice using terahertz time-domain spectroscopy, Astronomy & Astrophysics, 629, pp. A112 (2019).

DOI: 10.24412/cl-35039-2022-22-84-84

Complex of $NaYF_4$:Yb,Er –HSA-MB for cancerous tumour destruction

E. N. Lazareva,[1,2] A. A. Doronkina,[1] D. K. Tuchina,[1,2,3] A. M. Mylnikov,[4] N. A. Navolokin,[4,5,6] V. I. Kochubey,[1,2] I. Yu. Yanina[1,2]

[1]- Saratov State University (National Research University), Institute of Physics, 83 Astrakhanskaya str., Saratov 410012, Russia

[2]- Tomsk State University (National Research University), Laboratory of laser molecular imaging and machine learning, 36 Lenin's av., Tomsk 634050, Russia

[3]- A.N. Bach Institute of Biochemistry, Research Center of Biotechnology of the Russian Academy of Sciences, Moscow, 33Leninsky prospect, building 2 Moscow, 119071, Russia

[4]- Saratov State Medical University, Department of Pathological Anatomy, 112 B Kazachaya str., Saratov 410012, Russia

[5]- Saratov State Medical University, Center for Collective Use of Experimental Oncology, Experimental Department, 112 B Kazachaya str., Saratov 410012, Russia

[6]- State Healthcare Institution «Saratov City Clinical Hospital No. 1 named after Yu.Ya. Gordeev», 19 Kholzunova st., Pathological Department, Saratov 410017, Russia

e-mail: irina-yanina@list.ru

Upconversion nanoparticles (UCNPs) are of interest as novel luminescent probes for numerous applications in biophotonics. In this paper, we present data of the stable surface coating of the UCNPs with human serum albumin (HSA) and methylene blue (MB).

One of the promising materials for the development of biophotonics therapy methods are functionalized UCNPs, which can not only increase the effectiveness of therapy, but also expand the diagnostic tool. Cross-linking of a photosensitizer (PS) with a shell of NPs requires an additional coating of their surface. HSA nanoshells are biocompatible with many cell types over a wide range of concentrations, [1] are easily internalized by cells, [1, 2] are non-immunogenic, and have a long half-life in the circulation [3, 4].

Some PSs, such as MB, spontaneously bind to albumin, which makes it quite easy to cover the surface of NPs with a dye. The choice was based on the overlap of the NP luminescence and PS absorption bands.

Spectral measurements of the optical characteristics of biological tissues were carried out after intravenous administration of the complex of $NaYF_4$:Yb,Er –HSA-MB to laboratory animals. For histological studies, samples of skin, organs and cancer were taken by surgery from rats.

The effect of intravenous injection of the complex of $NaYF_4$:Yb,Er –HSA-MB on the change in the optical characteristics of biological tissues was shown in comparison with the injection of UCNPs.

The results of histological analysis of biopsy of organs and tumors of laboratory animals showed weak complex toxicity. The changes in the liver and lungs were reversible. Myocardial edema developed in the heart. A suggested way of excreting complex of $NaYF_4$:Yb,Er –HSA-MB and the body is through the urine. The accumulation of complex occurs in the spleen, which is consistent with the data of other researchers.

We have proposed a complex promising for photodynamic therapy.

The study was supported by a grant Russian Science Foundation No. 21-72-10057, https://rscf.ru/project/21-72-10057/

[1] K. Michaelis, M. M. Hoffmann, S. Dreis, E. Herbert, R. N. Alyautdin, M. Michaelis, J. Kreuter, K. Langer, Covalent linkage of apolipoprotein e to albumin nanoparticles strongly enhances drug transport into the brain, J. Pharmacol. Exp. Ther., vol. 317, pp. 1246-1253 (2006).

[2] J. M. Irache, M. Merodio, A. Arnedo, M. A. Camapanero, M. Mirshahi, S. Espuelas, Albumin nanoparticles for the intravitreal delivery of anticytomegaloviral drugs, Mini Rev. Med. Chem., vol. 5, pp.293-305 (2005).

[3] A. Loureiro, N. G. Azoia, A. C. Gomes, A. Cavaco-Paulo, Albumin-Based Nanodevices as Drug Carriers, Curr. Pharm. Des., vol. 22, pp. 1371-1390 (2016).

[4] F. F. An, X. H. Zhang, Strategies for Preparing Albumin-based Nanoparticles for Multifunctional Bioimaging and Drug Delivery, Theranostics, vol. 7, pp. 3667-3689 (2017).

DOI: 10.24412/cl-35039-2022-22-85-85

Photoacoustic sensor for the diagnosis of Asthma

Nidheesh V. R[a+], Aswini Kumar Mohapatra[b], Unnikrishnan V. K[a], Vasudevan Baskaran Kartha[a], and Santhosh Chidangil[a*]

a) Centre of Excellence for Biophotonics, Department of Atomic and Molecular Physics, Manipal Academy of Higher Education, Manipal, Karnataka, India;
b) Department of Respiratory and Pulmonary Medicine, KasturbaMedical College, Manipal, Manipal Academy of Higher Education, Manipal, Karnataka, India
**Corresponding author: santhosh.cls@manipal.edu*

Photoacoustic spectroscopy (PAS) can be effectively used to detect volatile organic compounds (VOCs) present in exhaled breath. A PAS setup using laser excitation at 266nm and calibrated with Acetone, was used to record photoacoustic signals from a cohort of normal healthy volunteers and asthma patients. The photoacoustic wave-form signals were Fourier-transformed to frequency domain and subjected to Principal Component Analysis (PCA) for classification. It was shown that the two sets of photoacoustic signal data, could be discriminated from each other by distinct cluster formation in a plot of Factors PC1 and PC2. A Match/No Match analysis, using Mahalanobis Distance and Sum of Squared Differences of simulated and actual signal (Spectral Residual) using a Calibration set of Asthma samples, gave a sensitivity of 89% and specificity of 93%. A comparison of results obtained from present data with the E-nose based VOC screening of the same volunteers confirmed the validity of the PAS technique for the diagnosis of Asthma.

Keywords: Photoacoustic spectroscopy, Volatile organic compounds, Asthma, Noninvasive diagnosis, Breath analysis.

DOI: 10.24412/cl-35039-2022-22-86-86

Refractive index measurement of the mouse skin in the visible wavelength range

M.A. Ansari[1, *], M. Samani[1], S. Ziaee[1], E.A. Lazareva[2], Yu.I. Surkov[2,3], I.A. Serebryakova[2,3], E.A. Genina[2,3], V.V. Tuchin[2,3,4]

1 - Laser and plasma research institute, Shahid Beheshti University, Tehran, Iran. 1983969411.
2 - Saratov State University, Astrakhanskaya str. 83, Saratov, 410012, Russia
3 - Tomsk State University, Lenin's av. 36, Tomsk, 634050, Russia
4 - Institute of Precision Mechanics and Control RAS, Rabochaya str. 24, Saratov, 410028, Russia
e-mail: m_ansari@sbu.ac.ir

The Refractive index is one of the most key factors in finding the different properties of the materials. So, its measurement could have different applications, such as medical applications. For example, it could be used in finding the type of the cancer tissues because of the different amount of their refractive index compared with the normal ones.

To measure the refractive index, different methods have been used, which have their advantages and disadvantages. One of these devices is the abbe refractometer. This device is used for finding the refractive index of the liquids at a single wavelength. The other one is a reflectometer system using a prism. This method is used for finding the refractive index for liquids and solids but at limited number of wavelengths.

The method presented here uses the Kramers-Kronig (KK) relation to find the refractive index. Using diffuse reflectance spectroscopy (DRS), the reflectance of the material could be measured with the use of an optical fiber in a visible wavelength range. The accuracy and precision of the KK method are evaluated using results obtained via commercial multi-wave refractometer (at 450, 480, 486, 546, 589, 644, 656, and 680 nm). The measured reflectance helps to find the refractive index using the KK relation in that range.

The point that makes this method special and better than other ones, is the measurement of the refractive index in the visible wavelength range (not just for a single amount of wavelength) and the useability for liquids and solids. Using this method, the refractive index of distilled water, glycerol, and the skin of the mouse is measured. The refractive index is measured before and during optical clearing of the skin using the immersion method. The optical clearing agent used, is a solution of 10% DMSO, 20% distilled water, and 70% glycerol. The temporal change in the content of water and the optical clearing agent in the skin is evaluated using optical coherence tomography (OCT). The results show that during the optical clearing the refractive index increases for some minutes and then decreases to be optically cleared after about 30 minutes.

This work is based upon research funded by Iran National Science Foundation (INSF) under project number 98029460 and Russian Foundation for Basic Research (RFBR) under project number 20-52-56005.

DOI: 10.24412/cl-35039-2022-22-87-87

Photoacceptors and photochemical processes determining the regulatory effect of visible laser radiation on various cell types

V. Plavskii, T. Ananich, O. Dudinova, J. Kruchenok, I. Leusenko, A. Mikulich, R. Nahorny, L. Plavskaya, A. Tretyakova, A. Sobchuk, S. Yakimchuk

B.I.Stepanov Institute of Physics of the National Academy of Sciences of Belarus, Minsk, Belarus
v.plavskii@ifanbel.bas-net.by

This paper presents the results obtained using various types of cells (eukaryotes, prokaryotes, blood cells (erythrocytes), spermatozoa), indicating that the regulatory effect of low-intensity laser radiation in the visible region of the spectrum is based on a change in the redox state of cells. Spectral-fluorescence methods have been developed, allowing one to detect and identify for the first time the endogenous photosensitizers of the porphyrin and flavin types in all of the listed cell types. Among the tetrapyrrole compounds with sensitizing properties, metal-free porphyrins, such as protoporphyrin IX, coproporphyrin III, uroporphyrin III, and zinc complex of protoporphyrin IX predominate in cells. The concentration of these compounds is extremely low ($C < 10^{-9}$ M); it depends on the type of cells and conditions of their cultivation. It was shown for the first time that at the same concentration of non-transformed and cancer cells in suspension, the concentration of porphyrin photosensitizers in the supernatant of cancer cells is approximately 1.5 times higher.

It has been established that light-induced formation of reactive oxygen species (ROS) in the result of excitation of endogenous sensitizers can influence the course of metabolic processes in the cell. It has been shown for the first time that the main contribution to cell inactivation by blue light is made not by singlet oxygen, but by hydrogen peroxide. At the same time, cancer cells accumulating higher concentrations of endogenous porphyrins are also characterized by greater sensitivity to the action of blue light compared to non-transformed cells. Depending on the concentration of ROS formed (singlet oxygen, hydroperoxide, superoxideanionradical), the exposure of light can lead both to stimulation of cellular processes and their inhibition, as well as to initiation of lethal outcome. As a rule, the dose dependence of such processes is a typical two-phase curve described by well-known Arndt-Schulz law: at low doses, a living organism responds to exposure with stimulation; as the dose increases, the stimulating effect reaches its maximum, then it is replaced by oppression, and with further increase of a dose, death of the organism is observed.

The complex of the performed studies showed the ability of laser radiation in the blue-green region of the spectrum a) to have a bactericidal and bacteriostatic effect on gram-negative and gram-positive bacteria and fungi [1]; b) to influence (both in the direction of stimulation and inactivation) the functional characteristics of spermatozoa of animals (motility, preservation, fertility) [2, 3]; c) to change the metabolic activity of somatic and cancer cells [4]; d) to initiate the release of hemoglobin molecules through the erythrocyte membrane in the absence of exogenous dyes-photosensitizers.

The conducted comparative studies of the biological effects of continuous, quasi-continuous, pulsed radiation of nano- and picosecond durations have shown the opportunity of significant enhancement of the stimulation effects through the use of quasi-continuous radiation. The differences in action of continuous, quasi-continuous and pulsed laser radiation of green spectral region can be explained with photochemical and photothermal effects initiated by a spatially inhomogeneous distribution of temperatures and ROS concentrations in the cell due to the heterogeneity of the absorbed light energy during the pulse in the microregions, adjacent to the localization of molecules-acceptors of radiation, and free of them. The dependence of the biological action on the frequency of radiation modulation has also been established. The conditions under which a clear dependence of the magnitude of photobiological effects on the polarization of radiation is traced have been found.

[1] V. Plavskii, A. Mikulich, A. Tretyakova et al., Porphyrins and flavins as endogenous acceptors of optical radiation of blue spectral region determining photoinactivation of microbial cells, J. Photochem. Photobiol. B., vol. 183, pp. 172–183 (2018).
[2] V. Plavskii, A. Mikulich, N. Barulin et al., Comparative effect of low-intensity laser radiation in green and red spectral regions on functional characteristics of sturgeon sperm, Photochem. Photobiol., vol. 96, pp. 1294–1313 (2020).
[3] V. Plavskii, N. Barulin, A. Mikulich et al., Effect of continuous wave, quasi-continuous wave and pulsed laser radiation on functional characteristics of fish spermatozoa, J. Photochem. Photobiol. B., vol. 216, 112112 (2021).
[4] V. Plavskii, A. Mikulich, N. Barulin et al., Laser Therapies: Types, Uses and Safety (Nova Science Publishers Inc.), Chapter I, (2020).

DOI: 10.24412/cl-35039-2022-22-88-88

Breathomics using laser spectroscopy and machine learning

Yury V. Kistenev[a] , Alexey V. Borisov[a], Viktor E.Skiba[a], Igor K. Lednev[b], Han Jin[c, d]

[a]Tomsk State University, Tomsk 634050, Russian Federation
[b]University at Albany, SUNY, Albany, NY 12222, USA
[c]Institute of Micro-Nano Science and Technology, School of Electronic Information and Electrical Engineering, Shanghai Jiao Tong University, Shanghai 200240, P. R. China
[d]National Engineering Research Center for Nanotechnology, Shanghai, 200241, P. R. China
Yv.kistenev@gmail.com

Analysis of volatile molecular biomarkers in the exhaled air, called breathomics, is suitable for operative non-invasive medical screening tests. The report is devoted to applications of laser spectroscopy and machine learning for evaluation of volatile molecular biomarkers' profile to detect a specific disease. Breath air analysis can be conducted through the chemical-composition-based and pattern-recognition-based approaches. For the former approach implementation, we use deep neural networks [1] and original chemometrics' methods: (a) a combination of the standard addition method with multivariate curve resolution called HAMAND [2]; (b) criterium based on reducing a spectrum complexity (RSC) [3] to provide exhaled air chemical composition. The latter approach is typical for supervised machine learning algorithms. We will compare both approaches.

We also presented results of absorption spectra resolution improving using computer super-resolution (SR) reconstruction, using several machine learning models based on different network architectures, including sequential ensemble architecture.

The research was carried out with the support of a grant under the Decree of the Government of the Russian Federation No. 220 of 09 April 2010 (Agreement No. 075-15-2021-615 of 04 June 2021).

[1] V. V. Prischepa, et al. Proc. SPIE 11582, 2020. P. 115821J; doi:10.1117/12.2581568
[2] M. Ando, I.K. Lednev, and H.-o Hamaguchi. In: Frontiers and Advances in Molecular Spectroscopy. 2018. P.369-378. doi:10.1016/B978-0-12-811220-5.00011-3
[3] A.Borisov, et al. *Journal of Breath Research 2021.* P.027104. doi:10.1088/1752-7163/abebd4

DOI: 10.24412/cl-35039-2022-22-89-89

Lasers in the evolving world of biomedical sensing and diagnosis

Z. Zalevsky

Faculty of Engineering, Bar-Ilan University, Ramat-Gan 52900, Israel
z.zalevsky@gmail.com

I will present a technological platform that can be used for remote sensing of many biomedical parameters simultaneously as well as to use those bio-parameters for performing medical diagnosis. The presented technological platform is based upon illuminating a tissue (e.g. located close to main blood arteries) with a laser and then using an imaging camera to perform temporal and spatial tracking of the back-scattered secondary speckle patterns in order to have nano-metric accurate estimation of the movements/vibrations occurring in the back-reflecting surface. After extracting various bio-parameters a medical diagnosis can be performed by applying machine learning post-processing.

The main feature of this technology is that the same single sensor is used for sensing of many biomedical parameters simultaneously and thus can provide a more comprehensive medical image needed for doing more precise medical diagnosis. The proposed technology was already applied for remote and continuous estimation of (1) vital bio-signs (such as heart beats rate and sound, respiration rate and sound, blood pulse pressure and velocity), (2) for hemodynamic sensing of blood flow characteristics and for (3) molecular and hematology related sensing of concentration of various chemicals in the blood stream (chemicals such as saturation of oxygen, blood coagulation, lactate, alcohol and glucose concentration).

The developed sensor was used for performing medical grade sensing of many bio-medical parameters simultaneously and performing medical diagnosis/diseases monitoring such as measuring intra ocular pressure (for glaucoma), photonic detection of fractures in bones, melanoma, breast cancer, atrial fibrillation (AFib) and congestive heart failure (CHF).

DOI: 10.24412/cl-35039-2022-22-90-90

Non-obvious features of low-coherence interferometry

G.V. Glikonov

Institute of Applied Physics Russian Academy of Sciences
e-mail address: grgel@ipfran.ru

Low-coherence interferometry has occupied a special niche not only in measurements of physical quantities, but also in sensor and diagnostic systems and devices. The most striking example of such an application is Optical Coherence Tomography. Despite its apparent simplicity, the measurement of low-coherence interference is associated with a number of features that significantly affect the result. Often these features are not obvious. We will discuss the issues of the observed optical noise and achieving its minimum values, calculating the dispersion characteristics of an object when direct measurement is impossible, and the influence of the spectrometer resolution on the attenuation of the spectral OCT signal with depth.

Optical noise contains fundamental and technical parts. Technical noise has multiple sources and can be eliminated. Fundamental noises consist of shot and beat noises of the spectral components, due to the incoherent nature of the radiation sources for low-coherence interferometry. In the case of weak reflection or scattering from the observed object, the intensity of the reference radiation in the Michelson interferometer has an optimum, which is achieved by attenuating this radiation in the reference arm while maintaining the division ratio of 50/50. [1, 2]

When using a tandem scheme with a measuring interferometer and an additional interferometer that compensates for the difference in the path of the measuring one, both waves of the compensating interferometer must have the same intensity. In this case, the excess noise cannot be completely subtracted, and its value will differ by times from the original one. [3]

In the case of impossibility of directly measurement the dispersion characteristics of the object of study (for example, when examining the retina), they can be calculated from the registered interference signal. [4]

In spectral optical coherence tomography, the signal decay with depth, in addition to the general scattering and absorption factors, is also determined by the resolution of the measuring spectrometer. An improved model of the spectrometer is presented, which more accurately describes the signal decay with depth. [5]

The work was supported under IAP RAS State financing, project #0030-2021-0013

[1] Feldchtein F., Bush J., Gelikonov G., Gelikonov V., Piyevsky S. Cost effective, all-fiber autocorrelator based 1300 nm OCT system // Progress in Biomedical Optics and Imaging - Proceedings of SPIE. V. 5690. P. 349-355 (2005)

[2] Bush J., Feldchtein F., Gelikonov G., Gelikonov V., Piyevsky S. Cost effective, all-fiber autocorrelator for Optical Coherence Tomography imaging // Proceedings of SPIE - The International Society for Optical Engineering. V. 5855 PART I. P. 254-257 (2005)

[3] Gelikonov V.M., Romashov V.N., Gelikonov G.V. Excess broadband noise at equal intensities in the interferometer arms. // Quantum Electronics. V.51, №.5, P. 377-382.(2021)

[4] Gelikonov G.V., Gelikonov V.M. Measurement and Compensation for the Amplitude and Phase Spectral Distortions of an Interference Signal in Optical Coherence Tomography for the Relative Optical-Spectrum Width Exceeding 10%. // Radiophysics and Quantum Electronics. V.61, №.2, P. 135-145.(2018)

[5] Sherstnev E.P., Shilyagin P.A., Terpelov D.A., Gelikonov V.M., Gelikonov G.V. An Improved Analytical Model of a Spectrometer for Optical Coherence Tomography. // Photonics. V.8, №.12, P. 1-10. (2021)

DOI: 10.24412/cl-35039-2022-22-91-91

Viscoelasticity measurement using laser speckle techniques

Jiachi Hong[1], Xiao Chen[1], Jinling Lu[1], Alexander Priezzhev[3], Andrei E. Lugovtsov[3], Pengcheng Li[1,2]

[1]Britton Chance Center for Biomedical Photonics, Wuhan National Laboratory for Optoelectronics-Huazhong University of Science and Technology, Wuhan, 430074, China
[2]School of Biomedical Engineering, Hainan University, Haikou, 570228, China
[3] Department of Physics, Lomonosov Moscow State University, Leninskye Gory, 1-62, Moscow, 119991, Russia; pengchengli@mail.hust.edu.cn

Viscosity and elasticity are important physiological characteristics of biological tissues. Viscoelastic measurement is of great significance for assessing tissue functions and deciphering pathological mechanisms, especially in blood microcirculation. Magnetic resonance elastography (MRE) and ultrasound elastography (UE) have been widely applied to clinical diagnosis. Compared to MRE and UE, optical elastography methods, such as optical coherence elastography (OCE) and laser speckle elastography (LSE), are getting more and more attention for the advantages of high spatial resolution and motion detection sensitivity. Laser speckle imaging can detect the scattered particles velocity related to the strain by solving the motion-induced decorrelation time with speckle statistical analysis. Although LSE has a wide field and high temporal resolution, there are still some limitations for clinical application scenarios. Therefore, we first estimate the apparent viscosity of blood microcirculation by analyzing the blood flow velocity with laser speckle imaging. Then, we develop a laser speckle elastography method with a low-frame-rate camera by using the aliasing effect. It simplifies the complexity of the elastography system and enhances portability due to the no need for synchronization between excitation and acquisition [1]. Further, as biological tissue is both elastic and viscous, ignoring the viscosity of the tissue can make elastic measurements inaccurate. We accomplish the simultaneous quantitative detection of viscosity and elasticity based on reflective laser speckle contrast imaging [2]. The viscosity and elasticity moduli are obtained by fitting the Rayleigh wave dispersion curves to the Voigt model. Compared with results obtained from a conventional mechanical rheometer, both phantom and biological experiment results support our method for viscoelasticity measurement.

This work was supported by the National Natural Science Foundation of China (61890951, 61890950, 61775071); CAMS Innovation Fund for Medical Sciences (CIFMS, 2019-I2M-5-014); Fundamental Research Funds for the Central Universities, HUST: 2019KFYXMBZ009); Innovation Fund of Wuhan National Laboratory for Optoelectronics (WNLO)

[1] Xiao Chen, Jinling Lu, and Pengcheng Li, "Elastography with low-frame-rate laser speckle contrast imaging using the aliasing effect," Opt. Lett. 43, 2811-2814 (2018)
[2] Xiao Chen, Yang Wang, Jinling Lu, and Pengcheng Li, "Simultaneous viscosity and elasticity measurement using laser speckle contrast imaging," Opt. Lett. 43, 1582-1585 (2018)

DOI: 10.24412/cl-35039-2022-22-92-92

Analytical capabilities of the intrinsic fluorescence of blood plasma proteins for biomedical diagnostics

A. Gayer[1,2], B. Yakimov[1,2], E. Shirshin[1,2]

1- Faculty of Physics, M.V. Lomonosov Moscow State University, 1-2 Leninskie Gory, Moscow, Russia, 119991
2- World-Class Research Center "Digital Biodesign and Personalized Healthcare", Sechenov First Moscow State Medical University, Trubetskaya 8, Moscow, Russia, 119048
Main author email address: shirshin@lid.phys.msu.ru

Since early 1960s, intrinsic fluorescence of proteins has attracted attention of researchers as a versatile diagnostic modality. It was discovered that fluorescence of tryptophan residues (Trp), the main contributor to proteins' emission, is highly sensitive to the parameters of its microenvironment. However, in general, Trp fluorescence of blood plasma exhibits low variability independent on the disease, e.g., cancer or diabetes, and its capabilities in detection of pathologies are limited. Moreover, a detailed analysis of Trp fluorescence variability in blood plasma on a large (>100 samples) dataset is lacking in the literature.

Another important phenomenon in the proteins photophysics is the influence of post-translational modifications, namely, oxidation processes, on the optical properties of the system. Having a low ionization potential, Trp can be easily oxidized, resulting in a decrease of its fluorescence and in the formation of novel fluorescent products. Trp oxidation results in the formation of fluorescence in the visible spectral range, untypical for globular proteins, as well as in an apparent "yellowing" of the sample. Oxidative modifications are accumulated through the whole protein's life span, and their fluorescence may potentially serve as a diagnostic parameter for detection of pathologies.

This work aims at the analysis of variability and analytical capabilities of proteins' intrinsic fluorescence based on the open dataset of excitation-emission matrices (EEMs) measured for 300 patients with suspected colorectal cancer described in and supporting model experiments. For the first time, we demonstrate the dominant role of HSA in the formation of blood plasma fluorescence in the visible range. Using size-exclusion chromatography of blood plasma, fluorescence properties of protein fractions are analysed in detail. We quantify "classical" descriptors such as Trp fluorescence intensity and band shape, Tyr fluorescence and the impact of fluorescent oxidation products, and then use these parameters as features to build a classification model for distinguishing between the control group and cancer patients. The obtained results provide novel information on conformational changes of blood plasma proteins as revealed by fluorescence spectroscopy as well as extend current approaches used for the analysis of blood plasma fluorescence.

DOI: 10.24412/cl-35039-2022-22-93-93

Resolving Ultrafast Fluorescence Decays with Hybrid Detectors

V. Shcheslavskiy[1,2], V. Elagin[2], E. Shirshin[3], M. Shirmanova[2], and W. Becker[1]

1- Becker&Hickl GmbH, Nunsdorder Ring 7-9, 12277 Berlin, Germany
2- Privolzhsky Research Medical University, Minin and Pozharsky Sq. 10/1, 603005 Nizhny Novgorod, Russia
3- Moscow State University, Vorob'evy Gory, 119435 Moscow, Russia
Main author email address: vis@becker-hickl.de

It is commonly believed that autofluorescence lifetimes of biological material are in the range from a few 100 ps to about 5 ns. This is supported by fluorescence-decay data of reduced nicotinamide adenine dinucleotide (phosphate) (NAD(P)H), an endogenous fluorophore that plays a crucial role in redox reactions in living cells and exhibits a lifetime of about 400 ps for the free form and from 2 to 5.7 ns for the protein-bound form, depending on the protein to which the fluorophore is bound. [1] While protein binding to NAD(P)H causes an increase in fluorescence lifetime and quantum yield, protein binding of flavine adenine dinucleotide (FAD) to many protein complexes (stack conformation) will typically cause significant quenching and a decrease in lifetime from 2.3 to 2.9 ns for its free state (open conformation) to 0.1 ns in its stacked conformation. [1] Lifetimes of other endogenous fluorophores are in the same range, with fast decay components down to about 200 ps. The fact that there are no faster decay time known may in part be due to the instruments. Commonly used FLIM systems have instrument response functions with a full width at half-maximum (FWHM) of about 250 ps (when using PMT detectors) and around 120 ps (when using hybrid detectors with GaAsP cathodes) [2]. This is not much faster than the dominating decay time of the unbound NADH and comparable to the fluorescence lifetime of FAD in the stacked conformation, and to melanin [1]. Therefore, one can expect that faster detectors may improve the accuracy of the fluorescence decay analysis of these endogenous fluorophores. However, there is a problem. The GaAsP cathode of the typical high- efficiency FLIM detectors limits the speed to about 120 ps. Faster detectors either have extremely small active areas (SPADS) and are thus not applicable to NDD detection in two-photon microscopes, or they have conventional photocathodes with low quantum efficiency (PMTs). A possible compromise are the new Hamamatsu R10467-06 and -07 hybrid detectors with high-efficiency bi-alkali and multi-alkali cathodes. Although the photocathodes do not reach the quantum efficiency of a GaAsP cathode the hybrid detector principle makes up for a part of the loss: unlike a conventional PMT a hybrid detector has no loss of photoelectrons at the first dynode. Virtually all photoelectrons that leave the photocathode also cause a pulse at the output of the detector. This talk presents the investigation of use of ultrafast hybrid detector based on Hamamatsu R10467-06 and its application to record the decay functions of such endogenous fluorophores as NAD(P)H, FAD, both in solutions and cells, and melanin in melanoma.

Acknowledgements: The authors acknowledge the support of the studies related to singlet oxygen detection from the Russian Science Foundation (Grant # 20-65-46018).

[1] J.R. Lakowicz, Principles of Fluorescence Spectroscopy, Springer New York, 3 ed. (2006).
[2] W. Becker, B. Su and A. Bermann, Better FLIM and FCS data with by GaAsP hybrid detectors, Proc. SPIE 7569, Multiphoton Microscopy in the Biomedical Sciences X, 75690S (26 February 2010)

DOI: 10.24412/cl-35039-2022-22-94-94

Protein-mediated carotenoid delivery into liposomes affects local microviscosity of the membranes as revealed by fluorescence anisotropy

A.N. Semenov[1], D.A. Gvozdev[1], A.R. Hashimova[1], Eu.Yu. Parshina[1], D.V. Zlenko[1], A.A. Bayzhumanov[1], N.Y. Lotosh[2], A.A. Selishcheva[1,2], N.N. Sluchanko[1,3], Eu.G. Maksimov[1,3]

1- M.V. Lomonosov Moscow State University, 1 Leninskie Gory St., Moscow, 119991, Russia
2- National Research Center "Kurchatov Institute", 1 Acad. Kurchatov Sq., Moscow, 123182, Russia
3- Federal Research Center of Biotechnology of the Russian Academy of Sciences, 33 Leninsky prospect, Moscow, 119071, Russia
semenov@physics.msu.ru

Carotenoids are natural substances with a range of biomedical applications due to their profound antioxidant properties. Anti-inflammation and oxidative protection effects of carotenoids significantly improve the efficiency of treatment of neurodegenerative pathologies, cancer, hematologic and cardiovascular deceases. Since carotenoids are not synthesized in human, there should be a constant supply of carotenoid-rich nutrients or specialized supplements and drugs. However, the delivery of carotenoids is limited by their lipophilic properties, which limits their efficiency in water solutions and hence biocompatibility. A possible means to overcome this obstacle is the use of special water-soluble proteins capable of reversibly binding carotenoids and transferring them into the cell membrane. In particular, the AnaCTDH protein based on the water-soluble carotenoprotein isolated from the cyanobacterium *Anabaena* sp. PCC 7120 [1] proved efficient in delivering carotenoid echinenone into membranes of cultured human cells of a different type. The aim of the present work was to study the interactions between AnaCTDH and the membrane of model mono-lamellar liposomes by assessing membrane microviscosity to characterize the efficiency of protein-mediated delivery of carotenoids.

Liposomes were made from soy lipid S75 (phospholipid with 70 % phosphatidylcholine and 20% phosphatidylethanolamine, Lipoid GmbH, Germany) as described earlier [2]. The produced liposomes were homogeneous with a mean diameter of 100 nm. Liposomes were labeled by fluorescent probe 1,3,5,7-tetramethyl-BODIPY which steadily emits fluorescence only being bounded within membrane and its fluorescence intensity and lifetime depend on the local surroundings. After the labeling, the solution of liposomes was supplemented with echinenone-carrying AnaCTDH. The membrane microviscosity was measured by assessing anisotropy of fluorescence of BODIPY in the membrane. The excitation was performed by picosecond optical pulse generator (InTop, Russia) with excitation at 500 nm and detection at 560 nm. Two fluorescence decay curves, corresponding to vertical and horizontal polarization of detected fluorescence, were measured using TCSPC system with hybrid photodetector GaAsP (Becker&Hickl GmbH, Germany). Kinetics were comprised to each other to determine the rotational correlation time (θ) of the BODIPY molecule in the membrane. Since θ is proportional to membrane viscosity η [3], we were able to estimate changes in microviscosity of liposomes membranes after the incubation with AnaCTDH at different concentrations.

Addition of AnaCTDH to liposomes increased θ only in the temperature range 10°-30°C. The effect was concentration-dependent: at 20°C with AnaCTDH concentration 720 nM θ=0.429±0.007 ns, at 1440 nM θ=0.492±0.010 ns (in control intact liposomes θ=0.370±0.013 ns). It means echinenone is delivered into liposomes membrane. At higher temperatures (30°-40°C), the correlation time θ does not change with an addition of AnaCTDH, demonstrating that echinenone does not change microviscosity. It means that at physiological temperatures incorporation of liposomes with echinenone does not erupt viscoelasticity and biomechanics of membrane and does not affect its stability and integrity.

The present work was supported by Russian Scientific Foundation grant № 22-25-00183.

[1] E. G. Maksimov, E. Yu. Parshina, N. N. Sluchanko et al. Soluble cyanobacterial carotenoprotein as a robust antioxidant nanocarrier and delivery module, Antioxidants, Vol. 9(869), PP. 1-23 (2020).
[2] V. A. Shchelkonogov, N.Y. Lotosh, A.A. Selishcheva et al. Lipoic acid nanoforms based on phosphatidylcholine: production and characteristics, European Biophysics Journal, Vol. 49, PP. 95–103 (2020).
[3] J. R. Lakowicz, Principles of Fluorescence Spectroscopy (Springer), Fluorescence Anisotropy (1999).

DOI: 10.24412/cl-35039-2022-22-95-95

Contrast-free FLIM diagnostics of the quality of pancreas islet of Langerhans

A. Kashina[1], P. Ermakova[1], I. Kornilova[1], A. Bogomolova[1], A. Kashirina[1], N. Naraliev[1], D. Kuchin[2], E. Zagaynova [1,3], V. Zagainov [1,4]

1-Privolzhsky Research Medical University, Nizhny Novgorod, Russia
2- Nizhny Novgorod Regional Clinical Hospital named after N.A. Semashko».
3- Lobachevsky State University of Nizhny Novgorod, Russia
4-Nizhny Novgorod Regional Clinical Oncological Dispensary
bardina-polina@mail.ru

Insulin-deficient conditions such as type 1 and type 2 diabetes mellitus, pancreatogenic diabetes are a major global public health problem. β cell stress and dysfunction precede progressive loss of β cell mass in both type 1 diabetes (T1D) and type 2 diabetes (T2D). β cell dysfunction is at least in part due to remodeled glucose metabolism as a component of a conserved pro-survival signaling program. In healthy β cells, as glucose concentrations increase, there is a proportionate increase in adenosine triphosphate (ATP) generation from oxidative phosphorylation (OxPhos) that, in turn, acts on membrane channels, electrically coupling oxidative phosphorylation to insulin secretion. It has been suggested that there is increased glycolysis in stressed β-cells, which is largely unrelated to oxidative phosphorylation in both T1DM and T2DM, consistent with such a high survival-inducing Warburg level characteristic of cancer cells.

Most studies of cell metabolism are based on methods such as PCR, immunocytochemistry, transcriptomic studies, which, on the one hand, do not give a complete picture of the islets in native tissue, and, on the other hand, are quite contradictory. Metabolic FLIM represents a powerful tool that may potentially provide a diagnostic tool for treatment aimed at restoring islet cell function in diabetes. To bring FLIM closer to clinical reality, new FLIM criteria are needed to identify islet quality and metabolism in various insulin-deficient conditions.

In this study based on FLIM and intracellular metabolite NAD(P)H was developed non-invasive and label-free method of the quality assessment of isolated islet cells and pancreatic islets in tissue. For fluorescence lifetimes (t1, t2) and fluorescence lifetimes contributions free and bound forms of NAD(P)H (a1, a2) analysis we used LSM 880 (Carl Zeiss, Germany), equipped with short-pulse femtosecond Ti:Sa laser Mai Tai HP with a pulse repetition rate of 80 MHz, duration of 140±20 fsec (Spectra-Physics, USA) and FLIM system for time resolved microscopy (Becker&Hickle GmbH, Germany).

Using the FLIM approach we checked FLIM opportunity to assess the islet cells quality in the pathological (T1D, T2D/chronic pancreatitis) and normal pancreas. We found that FLIM parameters (a1 and a1/a2) of islet cells in the pathological and normal pancreas were different. In particular, we demonstrated more glycolytic phenotype islet cells in pancreas with T1D and T2D/chronic pancreatitis. Metabolic FLIM imaging was also applied to assess the isolated islet cells metabolism and viability. The isolated islets were characterized by typical for NAD(P)H fluorescence lifetimes which indicates the viability and metabolically active status of the islets after their isolation.

Non-contrast FLIM diagnostics can be used both to obtain new FLIM criteria for the identification of islet cells quality and metabolism and to develop a rapid technique for islets viability analysis in order to help for islets transplantation in clinic.

This work has been financially supported by the Ministry of Health of the Russian Federation (state assignment № AAAA-A20-120022590096-6).

DOI: 10.24412/cl-35039-2022-22-96-96

FLIM imaging of pathological liver during regeneration

I.D. Shchechkin[1,2], S.A. Rodimova[1,2], N.V. Bobrov[1,3], , D.P. Krylov[1,2], D.S. Kozlov[1,2], V.V. Elagin[1], M.M. Karabut[1], A.M. Mozherov[1], V.E. Zagainov[1,3], E.V. Zagaynova[1,2], D.S. Kuznetsova[1,2]

1 - Privolzhsky research medical university, 603005, Nizhny Novgorod, Minin and Pozharsky sq. 10/1
2 - Lobachevsky Nizhny Novgorod National Research State University, 603022, Nizhny Novgorod, Gagarina 23
3 - The Volga District Medical Centre of Federal Medical and Biological Agency, 603000, Nizhny Novgorod, Ilinskaya st. 14
e-mail: daria.s.kuznetsova@gmail.com

Surgical liver resection remains the most effective treatment of liver tumors [1]. However, in the presence of hepatic pathologies, the regenerative potential of the liver is significantly reduced [2]. Standard clinical methods do not allow predicting the function of the liver remnant. Modern label-free methods of multiphoton microscopy with fluorescence lifetime imaging microscopy (FLIM) and second harmonic generation (SHG) expand the possibilities of studying the structural and functional state of liver tissue at the cellular level [3]. Thus, the search for criteria for intraoperative express assessment of the regenerative potential of the liver in the presence of liver pathologies remains an urgent task.

A series of experiments were carried out on Wistar rats. We induced toxic liver fibrosis by CCl4 injections and steatosis by 60% high-fat diet, the regenerative process was induced by 70% partial hepatectomy. Using multiphoton microscopy, we analysed the structure of the liver tissue on 3rd and 7th day after surgery. Using FLIM, we determined the fluorescence lifetime contributions of the free and bound forms of NADH and NADPH. Morphological analysis and a standard biochemical blood test were performed as controls.

As a result, we revealed the features of the structural and functional state at different stages of liver regeneration with steatosis and fibrosis. In case of steatosis, we identified zones with a reduced NADH autofluorescence intensity, corresponding to lipid infiltration or fibrosis. We also showed a decrease in the contributions of the bound form of NADH and NADPH already in the early stages of steatosis. During regeneration with the presence of steatosis, there was no sharp increase in the contributions of the bound form of NADH and NADPH on the 3rd day after hepatectomy, which we previously found during normal regeneration. This may be due to mitochondrial dysfunction of hepatocytes. In case of fibrosis, we also identified zones with a reduced signal of NADH autofluorescence intensity, which corresponded to fibrosis. There was sharp a decrease in the contributions of the bound form of NADH and NADPH in the early stages of pathology, followed by an increase in these parameters in the later stages. Such changes are associated with mitochondrial dysfunction in the early stages and the progression of compensatory processes in the later stages of pathology.

The work was supported by the Grant from the Russian Science Foundation №19-15-00263 (metabolic imaging, analysis of FLIM data), and by the Grant from the Russian Science Foundation №22-25-00098 (morphological analysis).

[1] E. Ramos., J. Torras., L. Lladó. et al., The influence of steatosis on the short-and long-term results of resection of liver metastases from colorectal carcinoma, Hpb, 18(4), 389-396 (2016).
[2] V.E. De Meijer, B.T. Kalish, M., Puder, J.N.M. IJzermans, Systematic review and meta-analysis of steatosis as a risk factor in major hepatic resection, Journal of British Surgery, 97(9), 1331-1339, (2010).
[3] M. S. Roberts, Y. Dancik, T.W. Prow, et al., Non-invasive imaging of skin physiology and percutaneous penetration using fluorescence spectral and lifetime imaging with multiphoton and confocal microscopy, European Journal of Pharmaceutics and Biopharmaceutics, 77(3), 469-488, (2011).

DOI: 10.24412/cl-35039-2022-22-97-97

Berberine mediated gold nanoclusters for optical diagnostics and improved photodynamic effect in 2D and 3D cell model

W. G. Pearl[1], R. Selvam[1], A. V. Karmenyan[1], Y. C. Ko[1], E. V. Perevedentseva[2], C. L. Cheng[1]

1- Department of Physics, National Dong Hwa University, Hualien 97401, Taiwan
2- P. N. Lebedev Physics Institute of Russian Academy of Sciences, Moscow, 119991, Russia
wrenit3@gmail.com

Gold nanoclusters (AuNC) are ultra-small in size that are of significant interest in recent cancer diagnosis and therapeutic advances. Their excellent biocompatibility, good photostability and discrete electronic state makes them a great potential for bioimaging applications [1]. The photosensitive characteristics of AuNCs have the ability to generate reactive oxygen species (ROS) in the presence of oxygen under near infrared (NIR) laser irradiation and can be used as a photosensitizer for deep tissue photodynamic therapy (PDT) [2]. In this study, AuNCs was synthesized surface-decorated on the Berberine (BBR) molecule and used for highly efficient photodynamic treatment. The AuNCs showed good biocompatibility towards human lung cancerous A549 cell line and was analysed using MTT assay. AuNCs prepared in colloidal solution have non-homogenous size (3±2 nm). However, this inherent disadvantage could be considered as an advantage for emission wavelength tunability [3]. The simultaneous red, green and blue fluorescence emission from the nanoclusters offers a great potential for optical imaging without the need of additional dyes. A549 2D and 3D cell cultures treated with AuNC@BBR when irradiated with 808 nm NIR laser exhibited high phototoxicity effect by increasing the reactive oxygen species (ROS) level and further promoting to cell death. The ROS generated intracellularly was estimated via DCFDA assay and the result showed increase in AuNC concentration in AuNC@BBR complex increased the ROS level. Therefore, AuNC@BBR can be suggested as a promising agent for bioimaging and photodynamic therapy.

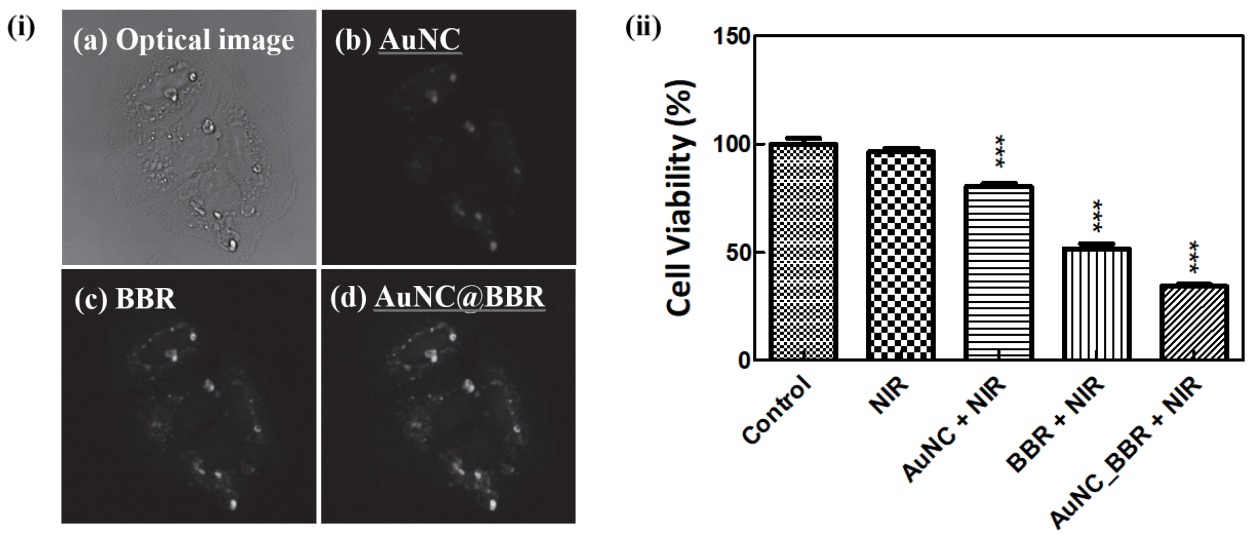

Fig. 1 (i) represent the confocal fluorescence images of A549 cells incorporated with AuNC@BBR complex- (a) optical image; (b) AuNC (Ex/Em : 514/610-660 nm); (c) BBR (Ex/Em : 405/540-565 nm) and (d) merged. (ii) represent the cell viability of A549 cells associated with NIR laser irradiation for 5 minutes (Wavelength : 808 nm; Power density : 70 mW cm^{-2}).

[1] S. M. Van De Looij, E. R. Hebels, M. Viola, M. Hembury, S. Oliveira and T. Vermonden, Gold nanoclusters: imaging, therapy, and theranostic roles in biomedical applications, Bioconjugate Chem., 33, 4-23, (2022).
[2] C. Fan, S. Zhai, W. Hu, S. Chi, D. Song and Z. Liu, Gold nanoclusters as a GSH activated mitochondrial targeting photosensitizer for efficient treatment of malignant tumors, RSC Adv., 11, 21384-21389 (2021).
[3] A. K. Sahoo, S. Banerjee, S. S. Ghosh and A. Chattopadhyay, Simultaneous RGB emitting Au nanoclusters in chitosan nanoparticles for anticancer gene theranostics, ACS Appl. Mater. Interfaces, 6, 712-724, (2014).

DOI: 10.24412/cl-35039-2022-22-98-98

Meet new photo-pharmacological agents – functionalised phosphonates with cholinesterase activity

I. Kolesnikov[1], D. Mamonova[2], D. Pankin[1], A. Pilip[3], A. Egorova[3,4], and A. Manshina[2],*

1 Center for Optical and Laser Materials Research, St. Petersburg State University, St. Petersburg, Russia
2 Institute of Chemistry, St. Petersburg State University, St. Petersburg 198504, Russia
3 St. Petersburg Federal Research Center of the Russian Academy of Sciences (SPC RAS), Scientific Research Centre for Ecological Safety of the Russian Academy of Sciences, St. Petersburg 197110, Russia
4 St. Petersburg State Technological Institute (Technical University), St. Petersburg 190013, Russia
**e-mail: a.manshina@spbu.ru*

Rapid development of pharmacology generated several breakthrough directions one of which is Photopharmacology. Nowadays the main players of photopharmacology are 'photoswitch-pharmacore' couples that change biological activity because of light irradiation. The most widely used photoswitchers are azobenzenes and diarylethenes; as pharmacore various antibiotics, Takrin (treatment of Alzheimer's disease) were demonstrated. However, the main practical problem in current strategy is losing of drugs activity after photoswitch introduction. It requires further optimization of the structure for each 'photoswitch-pharmacore' couple. That is why development of new photopharmacological agents combining both functions – bioactivity and ability to change it under light irradiation – is necessary.

Here, we present phosphorylated arylaminomalonates (Fig 1a) and thiazolotriazole (Fig 1b) that demonstrate laser-induced change of bioactivity (butyrylcholinesterase (BChE) inhibition) due to the formation of conformers associated with the phosphonate group twisting [1,2]. We found that laser-induced 3D geometry reorganization of the presented compounds leads to the fundamental change of the inhibition mechanism and loss of site-specificity due to the change of interaction region. It is important to note that arylaminomalonates and thiazolotriazole demonstrate opposite effect to laser irradiation in terms of sign of BChE inhibition change – thiazolotriazole decrease inhibition, while arylaminomalonates increase inhibition as a result of laser irradiation. The uncovered photosensitivity and bioactivity of new phosphorylated phosphonates makes them promising compounds for clinical therapy as photopharmacological agents.

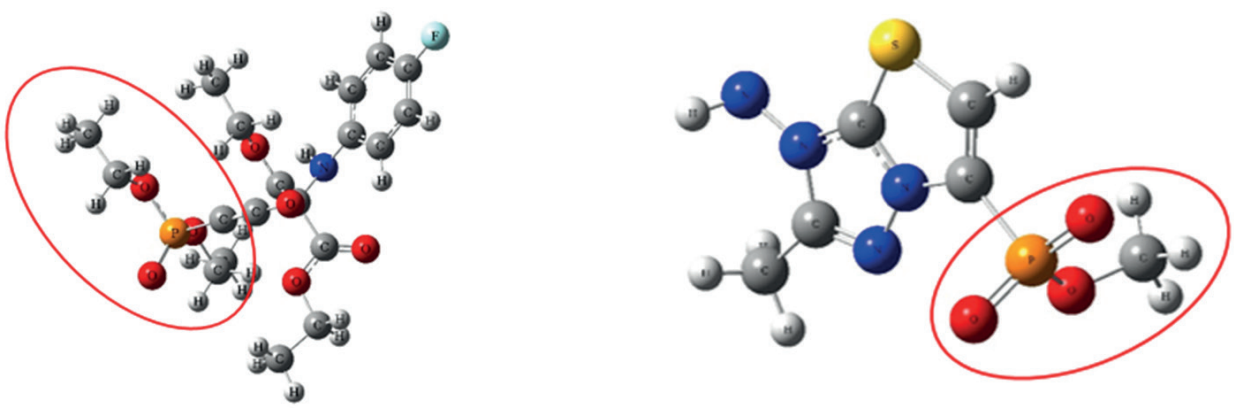

Figure 1. Structures of (a) phosphorylated arylaminomalonates and (b) thiazolotriazole compounds

This work was supported by RSF project 22-13-00082. Authors are grateful to "Centre for Optical and Laser materials research", Research Park of Saint Petersburg State University for technical support.

[1] D. Pankin, A. Khokhlova, I. Kolesnikov, A. Vasileva, A. Pilip, A. Egorova, E.Erkhitueva, V. Zigel, M. Gureev, A. Manshina, Spectrochimica Acta Part A: Molecular and Biomolecular Spectroscopy. 246, 118979(2021).
[2] I. Kolesnikov, A. Khokhlova, D. Pankin, A. Pilip, A. Egorova, V. Zigel, M. Gureev, G. Leuchs, A. Manshina, New J. Chem. 45, 15195–15199(2021).

DOI: 10.24412/cl-35039-2022-22-99-99

NIR responsive Fe doped nanodiamond for Fenton enhanced chemotherapy

R.Selvam[1], W.G.Pearl[1], E.Prevedentseva[1,2], A.Karmenyan[1], C.L Cheng[1*]

[1] Department of Physics, National Dong Hwa University, Hualien 97401, Taiwan
[2] P. N. Lebedev Physics Institute of Russian Academy of Sciences, Moscow, 119991, Russia
Presenting author: 810714313@gms.ndhu.edu.tw; corresponding author: clcheng@gms.ndhu.edu.tw

Chemodynamic therapy (CDT) based on Fenton or Fenton-like reactions is an emerging technique that has made significant progress in cancer treatment by efficiently fighting cancer while reducing negative effects on normal cells and tissues. Cancer cells exhibit elevated levels of hydrogen peroxide [1], which can be utilized to catalyze the Fenton reaction leading to the formation of reactive oxygen species (ROS) leading to cell death or apoptosis. Taking advantage of tumor microenvironment, we used Fe doped nanodiamond (FeND) as a therapeutic agent for cancer by using Fenton reaction. FeND exhibits excellent biocompatibility against A549 cells, however, when exposed to laser light, the nanodiamond exhibits significant toxicity. In the presence of NIR laser light, FeND can undergo a redox reaction with endogenous H_2O_2 in the cells to produce highly toxic hydroxyl radicals (·OH). Upon production of an hydroxyl radical in a cell, it can reacts with biological system components and causes the cell to undergo apoptosis. However, endogenous H_2O_2 is rather insufficient to effectively treat cancer. We have therefore conjugated doxorubicin (DOX), a commercially available anthracycline drug, which can undergo redox reaction to generate excess amounts of H_2O_2 inside the cells [2], which can then be converted into hydroxyl radicals by FeND. The effectiveness of the FeND and FeND-DOX complex have been studied with and without exposure to the NIR laser against A549 cells using MTT assay. Based on our findings, FeND has a potential to be used as a biological probe as well as a carrier for drug, along with it's ability to treat cancer.

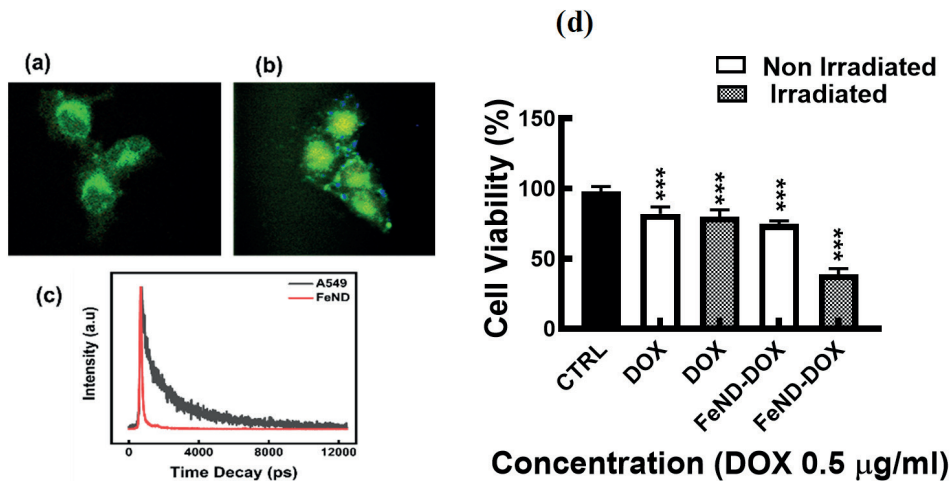

Figure 1. FLIM images of (a) A549 (b) A549 incubated with Fe-ND for 4 hrs. (c) Lifetime decay curves of Fe-ND fluorescence and A549 cancer cells autofluorescence. (d) cytotoxicity of DOX and Fe-ND-DOX complex evaluated in A549 cells with and without exposure irradiation with laser of 808 nm

[1] T.P.Szatrowski, and C.F. Nathan, Production of large amounts of hydrogen peroxide by human tumor cells. Cancer Res, **51**(3): p. 794-8, 1991

[2] H. Mizutani, S.Tada-Oikawa, Y. Hiraku, M.Kojima and S.Kawanishi, Mechanism of apoptosis induced by doxorubicin through the generation of hydrogen peroxide. Life Sci,. **76**(13): p. 1439-53, 2005.

DOI: 10.24412/cl-35039-2022-22-100-100

Non-invasive diagnosis of histopathological patterns in vulvar dermatoses by multimodal optical coherence tomography

A. Potapov[1], M. Sirotkina[1], M. Karabut[1], I. Kuznetsova[2], S. Radenska-Lopovok[3] and N. Gladkova[1]

1- Privolzhsky Research Medical University, 603950, 10/1, Minin and Pozharsky sq., Nizhny Novgorod, Russia;
2- N.A. Semashko Nizhny Novgorod Regional Clinical Hospital,
603126, 190, Rodionova str., Nizhny Novgorod, Russia;
3- I.M. Sechenov First Moscow State Medical University (Sechenov University), 8, Trubetskaya str., Moscow, Russia.
Arseniy1109@gmail.com

Accurate clinical diagnosis of skin inflammatory diseases of the vulvar area today remains a challenge. Caused by nonspecific skin manifestations as well as the warm, moist, frictional environment of the vulva obscures characteristic morphologic hallmarks [1]. This is due to nonspecific skin manifestations, as well as the fact that the warm, humid, frictional environment of the vulva obscures the characteristic morphological features. Histopathological diagnostics, as a reference method, has limitations due to its traumatic nature, a small area of the tissue being examined, and also due to the complexity of such diagnostics in the early stages of diseases. In the absence of a specific histopathological diagnosis, the physician is provided with a description of the histopathological pattern, and the final diagnosis is made clinicopathologically. The pattern approach allows narrowing the range of diagnostic search, as some of the suspicious diagnoses are excluded [1].

In this paper, we propose multimodal optical coherence tomography (MM OCT) as a non-invasive diagnostic technique of histopathological patterns in vulvar dermatoses. The MM OCT provides 3D (3.4×3.4×1.25 mm) real-time visualization of the vulvar skin structure with a spatial resolution of 10-20 microns at a depth of 1-2 mm, as well as label-free visualization of blood and lymphatic vessels. The study involved 16 patients with a clinical diagnosis of vulvar dermatoses and 5 patients without vulvar diseases. Parallel MM OCT and histopathological examination were performed.

The *acanthotic pattern* is characterized by a layered tissue structure with pronounced thickening of the epidermis on the OCT b-scan. In some cases, acanthotic ridges are visualized, but they are usually masked due to the optical homogeneity of the dermal-epidermal junction. OCT angio- and lymphangiography demonstrates good vascularization of the dermis.

The *lichenoid pattern* is characterized by a high signal level in the b-scan OCT co-channel from a band-like inflammatory infiltrate, since numerous cell nuclei act as scatterers. If the inflammatory infiltrate is located under the epidermis, then the layered structure of the tissue is preserved, and the dermal-epidermal junction is emphasized. When the infiltrate penetrates the epidermis, the layered structure of the tissue is disturbed.

The *dermal homogenization pattern* is characterized by the formation of homogeneous masses in the dermis that do not scatter light back, making these areas dark on the OCT b-scan. Homogenization areas have different signal intensity in co- and cross-channels of OCT, it depends on the length and thickness of collagen fibers, the presence of edema and inflammatory cells. OCT angio- and lymphangiography demonstrates impaired tissue vascularization [2].

The *vesiculobullous pattern* is characterized by the formation of fluid-filled cavities in the dermis. Such areas have a zero signal in both co- and cross-channel OCT.

In conclusion, non-invasive MM OCT effectively identifies histopathological patterns, which can be used as basic information for the clinicopathological diagnosis of vulvar dermatoses.

The study was financially supported by Russian Science Foundation project No19-75-10084.

[1] P.J. Lynch, M. Moyal-Barracco, F. Bogliatto, L. Micheletti, J. Scurry, 2006 ISSVD classification of vulvar dermatoses: pathologic subsets and their clinical correlates, The Journal of reproductive medicine, Vol. 52(1), pp. 3–9, (2007).

[2] M. A. Sirotkina, A. L. Potapov, M.M. Karabut, N. N. Vagapova, A. A. Moiseev, S. S. Kuznetsov, S. G. Radenska-Lopovok, I. A. Kuznetsova, and N. D. Gladkova, Multimodal OCT for in-vivo diagnosis of vulvar lichen sclerosus and evaluate the therapy success, Proc. SPIE 11924, Optical Coherence Imaging Techniques and Imaging in Scattering Media IV, 1192419 (2021).

DOI: 10.24412/cl-35039-2022-22-101-101

Assessment of the forces of paired erythrocytes aggregation by the optical tweezers in Type 1 and Type 2 diabetes mellitus

Fabrichnova A.A.[1*], Koshelev V.B.[1], Misnikova I.V.[3], Kovaleva Y.A.[3], Semenov A.N.[4], Lugovtsov A.E.[2], Kadanova I.M.[2], Neznanov A.I.[2], Priezzhev A.V.[2]

[1]Faculty of Fundamental Medicine,
[2]Faculty of Physics and
[4]Faculty of Biology, Lomonosov Moscow State University, Moscow, Russia
[3]Moscow Regional Research Institute of Clinical Institute named M.F. Vladimirsky, Moscow, Russia
**anastasia.fabrichnova@mail.ru*

Biophotonics offers new modalities that can be efficiently implicated into both fundamental medical research and clinical applications. One of such techniques is laser tweezers that were used in this work dedicated to the study of alteration in individual erythrocyte interaction by measuring the forces of their reversible aggregation.

The complex of metabolic alterations in diabetes mellitus usually leads to disturbance of the rheological properties of the blood. Pathological aggregation, unequal distribution of erythrocytes over microvascular networks, leads to a decrease in blood flow velocity, spreads the zones of local hypoxia [1]. Normally, in whole blood, erythrocytes exist in dynamic equilibrium, spontaneously aggregating and disaggregating under the action of shear stresses.

Previous studies of the ability of erythrocytes to aggregate in diabetes mellitus mainly took into account only the average ability of erythrocytes to aggregate and were carried out on large ensembles of cells in whole blood samples [2-4].

The aim of this investigation was to measure and compare the aggregation and disaggregation forces of individual erythrocytes during the formation or breakdown of a paired aggregate in vitro in the blood of patients suffering from type 1 diabetes mellitus (T1DM) and type 2 diabetes mellitus (T2DM) using the optical tweezers method [5].

A total of 50 people were included in the study. Of these, 10 people suffering from T1DM (aged 28 ± 15.8), 26 people with suffering from T2DM (aged 66 ± 13). The control group consisted of 14 apparently healthy volunteers (46 ± 21 years old). Measurements of the forces of interaction of erythrocytes were carried out in vitro by the method of two-channel optical tweezers. The force of aggregation of erythrocytes FA (pN) and the force of disaggregation FD (pN) were measured and their ratio FD / FA was calculated.

The erythrocyte aggregation forces did not differ significantly from the control group in the T1DM group. However, the forces of disaggregation in the T1DM group were significantly lower than in the control group ($p<0,05$). The ratio of the forces of disaggregation to the forces of aggregation was lower in the T1DM group compared to the control group ($p<0.005$). In T2DM group, erythrocyte aggregation forces were higher compared to the control group ($p<0.005$). The erythrocyte disaggregation forces in the T2DM group were also higher ($p=0.05$). The ratios of the forces of disaggregation to the forces of aggregation of erythrocytes in T2DM group were significantly lower than in the control group ($p <0.005$). At the same time, the ratios of the forces of disaggregation to the forces of aggregation in T1DM group and T2DM group did not differ.

Thus, both T1DM group and T2DM group are characterized by hyperaggregation of erythrocytes. However, given the obtained data, it can be assumed that the mechanisms of such hyperaggregation are different.

This work was supported by RSF grant № 22-15-00120.

[1] Young I.Ch. et al., Hemorheological disorders in diabetes mellitus, Journal of Diabetes Science and Technology, 2(6), pp. 24-8 (2006).

[2] Singh M., Shin S., Changes in erythrocyte aggregation and deformability in diabetes mellitus: A brief review, Indian Journal of Experimental Biology, 47(1), pp. 7-15. (2009).

[3] Babu N., Singh M., Influence of hyperglycemia on aggregation, deformability and shape parameters of erythrocytes, Clin Hemorheol Microcirc., 31(4), pp. 273-80, (2004).

[4] Maslianitsyna, A., Ermolinskiy, P., Lugovtsov, A., Pigurenko, A., Sasonko, M., Gurfinkel, Y.,Priezzhev, A. Multimodal Diagnostics of Microrheologic Alterations in Blood of Coronary Heart Disease and Diabetic Patients. *Diagnostics 11*, 76 (2021). https://doi.org/10.3390/diagnostics11010076.

[5] Fabrichnova A.A., Koshelev V.B., Misnikova I.V., Kovaleva Y.A., Semenov A.N., Lugovtsov A.E., Kadanova I.M., Neznanov A.I., Priezzhev A.V. Assessment of the forces of pair interaction of erythrocytes during their aggregation by the optical tweezers in Type 1 and Type 2 diabetes mellitus. *Regional Blood Circulation and Microcirculation* 20(1):77-83 (2021). (In Russ.) https://doi.org/10.24884/1682-6655-2021-20-1-77-83.

DOI: 10.24412/cl-35039-2022-22-102-102

Imaging of plasma membrane microviscosity in cancer cells during chemotherapy using molecular rotor and FLIM

L. Shimolina[1], A. Hlynova[1], I. Druzhkova[1], N. Ignatova[1], M. Kuimova[3], E. Zagaynova[1,2], M. Shirmanova[1]

1- Privolzhsky Research Medical University, 603005 Minin and Pozharsky Sq., 10/1, Nizhny Novgorod, Russia
2- Nizhny Novgorod State University, 603950 Gagarin Av., 23, Nizhny Novgorod, Russia
3- Imperial College London, Faculty of Natural Sciences, Department of Chemistry, SW7 2AZ, London, United Kingdom
shimolina.l.e@gmai.com

The microscopic viscosity plays an essential role in cellular biophysics by controlling the rates of diffusion and bimolecular reactions within the cell interior [1]. Understanding the role of the plasma membrane in the response of cancer cells to chemotherapy is important, since the cell membrane is actively involved in the transport of drugs and the regulation of the unfolding of biological processes [2-3]. Recent studies suggest that tumor response to chemotherapy is determined by not only interaction of the drug with the primary target (e.g. nuclear) but can include multiple physiological and physicochemical changes [4]. The study of the effects of chemotherapeutic drugs on the viscosity of living cells is important for better understanding the mechanisms of the drug action and evaluating the effectiveness of therapy.

The present work is aimed to study of plasma membrane's microviscosity in cancer cells using the fluorescent molecular rotor BODIPY 2 and fluorescence lifetime imaging FLIM microscopy during chemotherapy with platinum drugs.

The study was performed on cultured cancer cells CT26 (mouse colorectal cancer), HCT116 (human colorectal cancer) and oxaliplatin-resistant cell line - HCT116-OXAR. The molecular rotor fluorescence lifetime was recorded using an LSM 880 confocal microscope (Carl Zeiss, Germany) equipped with a TCSPC-based FLIM module (Becker&Hickl Inc., Germany). Microviscosity was measured in individual cell plasma membranes using a BODIPY2 fluorescent molecular rotor (eg 850 nm, em 500–550 nm). The cells were treated with cisplatin (Teva, Israel) at a dose of 2.6 μM (IC50) for CT26, and oxaliplatin (Teva, Israel) at a dose of 2.0 μM (IC50) for HCT116.

We showed a significant increase in membrane viscosity in viable cells CT26 in 24 h after cisplatin treatment from 322 ± 21 cP up to 400 ± 27 cP [2]. Treatment of HCT116 cells with oxaliplatin resulted in an increase in membrane microviscosity from 437 ± 77 cP to 593 ± 139 cP after 24 h of incubation with chemotherapy drug [3]. To validate the obtained effects on membrane viscosity, an analysis was made of the viscosity changes in chemoresistant HCT116-OXAR cells under the action of oxaliplatin. Incubation with oxaliplatin did not affect the membrane microviscosity, the values were ~450 cP. We suggest that the registered increase in membrane microviscosity at late time point of incubation with platinum-containing drugs (24 h) is part of the response of the tumor cell to treatment, and is not associated with direct interaction of the drug with the membrane.

The presented study is important for a deep understanding of the mechanisms platinum drug action and to assess the effectiveness of chemotherapy. This work is supported by the Russian Science Foundation under grant No: 20-14-00111.

[1] L. Shimolina et.al, Imaging tumor microscopic viscosity in vivo using molecular rotors, Scientific Reports, 7, 41097, (2017).
[2] L. Shimolina et.al, Mapping cisplatin-induced viscosity alterations in cancer cells using molecular rotor and fluorescence lifetime imaging microscopy, Journal of biomedical optics, 25(12), 126004, (2020).
[3] L. Shimolina et.al, The Role of Plasma Membrane Viscosity in the Response and Resistance of Cancer Cells to Oxaliplatin, Cancers, 13(24), 6165, (2021).
[4] Rebillard A. et al. Cisplatin-induced apoptosis involves membrane fluidification via inhibition of NHE1 in human colon cancer cells, Cancer Res. , 67, 7865–7874, (2007).

DOI: 10.24412/cl-35039-2022-22-103-103

Decrease Stiffness of Patients' Breast Cancer Tissue During Neoadjuvant Therapy

A.A. Plekhanov[1], E.V. Gubarkova[1], M.A. Sirotkina[1], V.V. Elagin[1], A.A. Sovetsky[2], D.A. Vorontsov[3], A.Y. Bogomolova[1], A.Y. Vorontsov[3], S.V. Gamayunov[3], V.Y. Zaitsev[2], and N.D. Gladkova[1]

1- Privolzhsky Research Medical University, Nizhny Novgorod, Russia
2- Institute of Applied Physics of the Russian Academy of Sciences, Nizhny Novgorod, Russia
3- Nizhny Novgorod Regional Oncologic Hospital, Nizhny Novgorod, Russia
strike_gor@mail.ru

In the presented study, we demonstrate patients' clinical cases with diagnosed breast cancer and prescribed neoadjuvant (preoperative) chemotherapy (NACT). We examined tumor tissues taken by core needle biopsy before and during NACT. The studies were carried out using original home built multimodal optical coherence tomography system (IAP RAS, Nizhny Novgorod) [1] in the elastographic scanning mode – compression optical coherence elastography (OCE), which is described elsewhere [2, 3]. Multiphoton microscopy (MPM, LSM 880, Carl Zeiss, Germany) based on second harmonic generation and two-photon-excited fluorescence was used to assess connective tissue fibers and other breast cancer tissue. To determine the morphological features of the studied tissues, a histological study (with hematoxylin and eosin staining) was used. Previously, we have established the ranges of stiffness values for the morphological structures of breast cancer tissue [4]. Besides, we performed the studies of postoperative tumor samples of patients after treatment [5], where we found both the areas of very low stiffness values (Young's modulus) (less than 100 kPa) and medium stiffness values (~200-400 kPa) corresponding to necrotic tumor cells and connective tissue stromal fibers (that replace dead tumor cells), respectively.

In this study, we compared the elastic properties of tumors before and during NACT. According to the results of OCE studies, a decrease in stiffness values of the residual (saved after therapy) tumor cells was found, compared with stiffness of tumor cells before treatment. Areas of tumor cells with a stiffness of ~500-700 kPa prevailed, whereas before NACT, areas with a stiffness more 700 kPa prevailed. Histological examination of tumor tissue during NACT revealed a large number of dystrophic tumor cells (with destruction of cell nucleus – karyopyknosis or karyorrhexis). The study of tumor tissue with MPM before and during NACT revealed a change in mutual arrangement of tumor cells and connective tissue fibers: a transition from dense clusters of tumor cells lying among thick connective tissue fibers of the stroma to single cells densely surrounded by thin connective tissue fibers. Our further research will focus on the determination of the contribution of tumor cells and stromal fibers to the reduction of tumor stiffness during treatment. In addition, the correlation between tumor stiffness values on OCE and characteristics of connective tissue fibers on MPM will be determined.

The study was funded by the Russian Science Foundation, grant No. 18-75-10068.

[1] V.M. Gelikonov, G.V. Gelikonov, P.A. Shilyagin. Optimization of Fizeau-based optical coherence tomography with a reference Michelson interferometer. Bulletin of the Russian Academy of Sciences: Physics, 72(1), 93-97, (2008).
[2] V.Y. Zaitsev, A.L. Matveyev, L.A. Matveev, G.V. Gelikonov, E.V. Gubarkova, N.D. Gladkova, A. Vitkin. Hybrid method of strain estimation in optical coherence elastography using combined sub-wavelength phase measurements and supra-pixel displacement tracking. Journal of Biophotonics, 9(5), 499–509, (2016).
[3] A.A. Plekhanov, M.A. Sirotkina, A.A. Sovetsky, E.V. Gubarkova, S.S. Kuznetsov, A.L. Matveyev, L.A. Matveev, E.V. Zagaynova, N.D. Gladkova, V.Y. Zaitsev. Histological validation of in vivo assessment of cancer tissue inhomogeneity and automated morphological segmentation enabled by Optical Coherence Elastography. Scientific Reports, 10(1), 11781, (2020).
[4] E.V. Gubarkova, A.A. Sovetsky, V.Y. Zaitsev, A.L. Matveyev, D.A. Vorontsov, M.A. Sirotkina, L.A. Matveev, A.A. Plekhanov, N.P. Pavlova, S.S. Kuznetsov, A.Y. Vorontsov, E.V. Zagaynova, N.D. Gladkova. OCT-elastography-based optical biopsy for breast cancer delineation and express assessment of morphological/molecular subtypes. Biomedical Optics Express, 10(5), 2244–2263, (2019).
[5] A.A. Plekhanov, E.V. Gubarkova, A.A. Sovetsky, M.A. Sirotkina, S.S. Kuznetsov, L.A. Matveev, D.A. Vorontsov, A.L. Matveyev, E.V. Zagaynova, V.Y. Zaitsev, N.D. Gladkova. Improvement of breast cancer histological examination by means of multimodal OCT. Proceedings of SPIE, 11924, 119241H, 1-4, (2021).

DOI: 10.24412/cl-35039-2022-22-104-104

Vacuum atraumatic tissue fixation enables multimodal OCT monitoring of the enterostomy condition

E. Kiseleva[1], M. Ryabkov[1], M. Sizov[1], P. Peretyagin[1], E. Bederina[1], P. Shilyagin[2], N. Gladkova[1]

[1]FSBEI HE PRMU MOH Russia, 603005, Nizhny Novgorod, Minin and Pozharsky Square 10/1
[2]FRC Institute of Applied Physics RAS, 46 Ul'yanova St., Nizhny Novgorod, 603950, Russia
kiseleva84@gmail.com

Enterostomy is a common component of surgical treatments for various gastrointestinal conditions, including acute mesenteric ischemia, Crohn's disease or ulcerative colitis and bowel cancer [1, 2]. An enterostomy is a surgical formation of an opening into the intestine through the abdominal wall and the opening is known as a stoma. The ideal time to close the stoma is about 3 to 12 months after surgery, but there are no well-defined criteria for evaluating it to decide whether it is ready for reconstructive surgery or not [3, 4].

The aim was to *in vivo* assess the microcirculation and microstructure of the enterostomy for different periods after its formation using the multimodal optical coherence tomography (MM OCT) method.

Materials and methods. 10 patients with enterostomies formed in 3-20 days after surgery were enrolled in the study. A high-speed spectral-domain multimodal optical coherence tomograph (IAP RAS, Russia) operating at a wavelength of 1310 nm with a spectral width of 100 μm and a power of 2 mW was used [5]. It allows for real-time observation of tissue microstructure (cross-polarization mode — CP OCT) (fig. 1 e-j) and microcirculation (angiography mode — OCTA) (fig. 1 b-d). A special vacuum cap to be out on the OCT probe (fig. 1a) was used to obtain MM OCT images in a contact mode without motion artifacts.

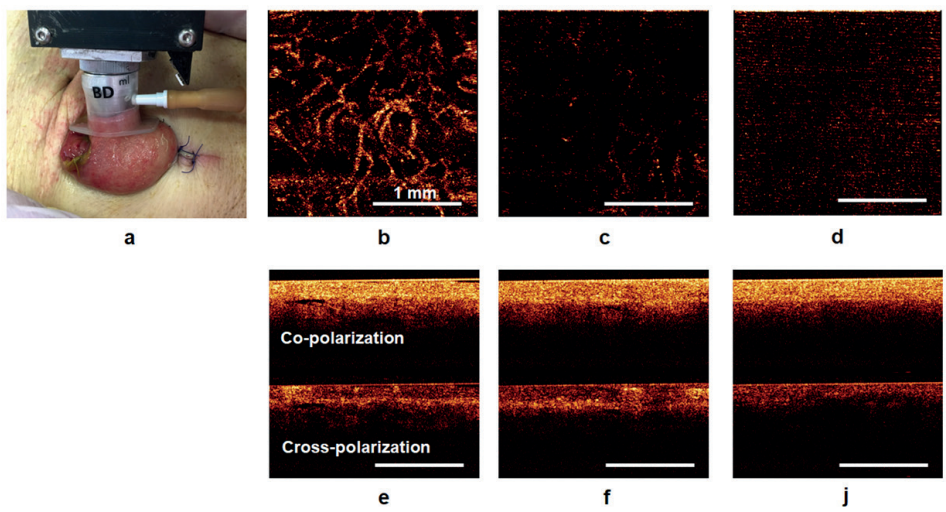

Fig. 1. An example of blood vessels visualization from the surface of the small bowel stoma of patient Ivg (76 years old) using multimodal OCT on the 5th after surgery. a - photo of the stoma with an OCT probe attached to its surface using a vacuum cap. b-d - OCTA images, e-j - structural images in co- and cross-polarizations. 3 regions of interest were studied: b - side where the mesentery was previously located, c - anterior side, c - antimesenteric side.

Results. The use of a vacuum cap (fig. 1a) creates a temporary immobilization of tissues and blood flow becomes visible (fig. 1 b-d) due to the reduction of most of the motion artifacts. It can be seen that the network of blood vessels as well as tissue structure are different on different sides of the stoma. These can be used to assess the quality of the blood supply and the degree of morphological changes in intestine tissues which can help determine the optimal time for closure surgery.

The study was funded by the Russian Science Foundation #19-75-10096.

1. Saunders R.N., Hemingway D. Intestinal stomas. Surgery (Oxford). 2008, 26(8), 347-351.
2. Rajaretnam N., Lieske B. Ileostomy. StatPearls [Internet]. Last Update: July 31, 2021. Avaliable from https://www.ncbi.nlm.nih.gov/books/NBK519003/
3. Sherman KL, Wexner SD. Considerations in Stoma Reversal. Clin. Colon. Rectal Surg. 2017, 30(3), 172-177.
4. Goldwag J.L., Wilson L.R., Ivatury S.J., et al. Stoma closure and reinforcement (SCAR): A study protocol for a pilot trial. Contemp. Clin. Trials Commun. 2020, 19, 100582.
5. Gelikonov V.M., Romashov V.N., Shabanov D.V., et al. Cross-polarization optical coherence tomography with active maintenance of the circular polarization of a sounding wave in a common path system. Radiophys. Quant. El. 2018, 60, 897-911.

DOI: 10.24412/cl-35039-2022-22-105-105

Optical coherence angiography of the ischemic bowel in open and laparoscopic surgery

M. Ryabkov, E. Kiseleva, P. Zarubenko, M. Sizov, M. Bagryantsev, N. Gladkova

FSBEI HE PRMU MOH Russia, 603005, Nizhny Novgorod, Minin and Pozharsky Square 10/1
maxim-ryabkov@yandex.ru

International and Russian guidelines «Management of acute mesenteric ischemia» include open and laparoscopic surgical operations [1]. Optical coherence angiography (OCA) has the potential to be able provide the surgeons with the data of blood circulation in the ischemic intestine [2]. However, to date the problem of high sensitivity of OCA to gastrointestinal peristalsis with OKA-images artifacts is not resolve [3,4]. Laparoscopic operation increasingly makes harder the colon fixation during the research.

The aim is to develop the device with the increasing of quality OCA-images of colon in open and laparoscopic surgery by the decreasing a number of peristalsis artifacts.

Materials and methods. We developed the device - nozzle on the detector of OCA. The device temporarily fixes the colon by the local controlled pressure deficit in open and laparoscopic surgery. The device tested in two series of the experiment with the approval of the Ethics Committee FSBEI HE PRMU MOH Russia. The first series of the experiment (mini-pigs, n=10) was organized in open surgery. We modeled an acute mesenteric ischemia and examined microstructure, microcirculation of the colon wall using an OCA-method. We compared the efficacy of the traditional method of hand colon fixation and the developed device. In the second series of the experiment (chinchilla, n=6) we research OCA of the colon with an acute mesenteric ischemia in laparoscopic surgery (fig. 1).

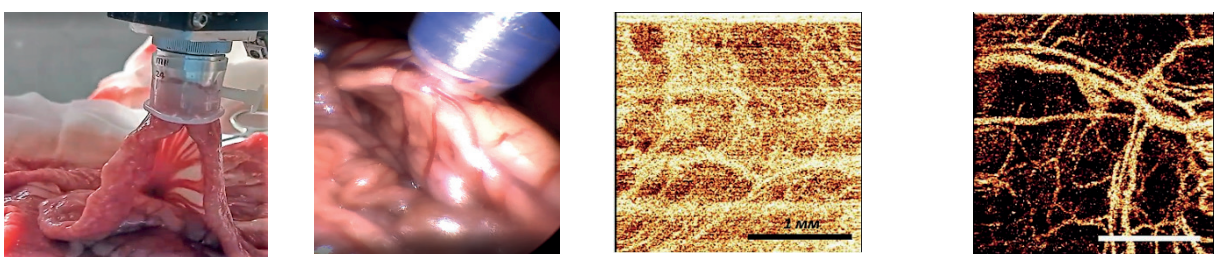

a b c d

Fig. 1: OCA of ischemic colon: a – a detector OCA on the colon, open surgery, b – a detector OCA on the colon, laparoscopic operation, c – traditional fixation of tissue, OCA-image, d – developed device, OCA-image.

Results. In the first series of the experiment the traditional method of the detectors fixation has proved to produce OCA-images without artifacts in 64% cases. It allowed to receive high-quality artefact-free 2D structural and angiographic images of the gastrointestinal tract in minipigs в 92 in 100 cases (p=0.001). In the second series of the experiment we got 24 small intestine OCA-images and 22 colon OCA-images. The number of informative OCA-images without artifacts of movement: 18 for small intestine and 21 for colon. Histological examination in two series confirmed the safety of device: there weren't hematoma or mechanical damage.

Conclusions. The traditional way of getting OCA-images of colon ended with non-artifacts images only in 64 % cases. The device has reduced artifacts of movement in OCA-images and increased informative angiograms before 92 % in open surgery (p=0.001) and before 84,7 % in laparoscopic surgery.

The study was funded by the Russian Science Foundation #19-75-10096.

1. Bala, M.; Kashuk, J.; Moore, et al. Acute mesenteric ischemia: Guidelines of the World Society of Emergency Surgery. World J. Emerg. Surg. 2017, 12, 1–11.
2. Kiseleva E, Ryabkov M, Baleev M, et al. Prospects of Intraoperative Multimodal OCT Application in Patients with Acute Mesenteric Ischemia. Diagnostics. 2021; 11(4):705.
3. Spaide, R.F.; Fujimoto, J.G.; Waheed, N.K. Image artifacts in optical coherence angiography. Retina (Philadelphia, Pa.) 2015, 35, 2163.
4. Kiseleva E, Ryabkov M, Baleev M, et al. "Intestinal optical coherence tomography (angiography) imaging: a comparison between animal models and humans," Proc. SPIE 11949, Advanced Biomedical and Clinical Diagnostic and Surgical Guidance Systems XX, 1194908 (7 March 2022)

DOI: 10.24412/cl-35039-2022-22-106-106

Comparison of the antitumor activity of the photosensitizer based on indotricarbocyanine dye and Photolon

M.P. Samtsov, D.S. Tarasov, A.P. Lugovski

A.N Sevchenko Institute for Applied Physical Problems of BSU, 220045 Minsk, Belarus
tarasovds@bsu.by

Photodynamic therapy (PDT) takes place one of the leading positions among modern methods of treating malignant neoplasms. Further development of the PDT method is associated with the creation of a new generation of photosensitizers (PS), the requirements for which are not limited only by a high therapeutic effect. The scientific community is developing new PSs that are activated by light in the transparency window of biological tissues (700–900 nm). This makes it possible to increase the depth of both damage and diagnosis of neoplasms.

Based on the results of complex studies of the photophysical properties of a number of indotricarbocyanine dyes in model media and tumor models on experimental animals in vivo, a dye with optimal properties for theranostics of malignant neoplasms was selected [1]. At the current stage of development, a synthesis scheme and laboratory procedures for obtaining a new PS have been worked out, a prototype of the drug dosage form based on glucose has been developed, and optimal conditions for a photodynamic therapy session in experiments with transplantable tumors on laboratory animals have been determined. This paper presents the results of a comparison of its therapeutic properties with PS Photolon (RUE Belmedpreparaty, Belarus) approved for use in clinical practice.

The study of the antitumor activity of photosensitizers was carried out on sexually mature inbred female mice of the C57BL/6 line, which were inoculated with Ehrlich ascites carcinoma on the outer surface of the thigh. Studies for both photosensitizers were performed 10 days after tumor inoculation into animals in one experiment. Experimental and control groups were formed from animals with tumors, the volume of which reached 30-40 mm^3 (the linear dimensions of the tumor node were about 4-6 mm).

For both PS, the dose of the drug, the start time of photoexposure, the wavelength of radiation, the energy and power density of irradiation were selected in accordance with the protocol for its use. At the same time, the PDT parameters were identical in terms of the following points: the same tumor model, the method of drug administration, the parameters of the light spot on the surface of the tumor node.

To activate the indotricarbocyanine photosensitizer during PDT, a semiconductor laser light source with a generation wavelength of 750 nm (IAPP, Belarus) was used. PDT with the photosensitizer Photolon was carried out using a therapeutic apparatus "PDT-laser" (B. I. Stepanov Institute of Physics, Belarus) with a laser generation wavelength of 660 nm.

The antitumor activity of photosensitizers was evaluated according to the recommendations of the Pharmaceutical Committee for preclinical studies of drugs [2]. Within 21 days, the condition of the animals and the dynamics of tumor growth in the experimental and control groups were monitored. For both studied PSs, the same dynamics of tumor growth after PDT was observed. After PDT in animals of the test groups [PDT with PS Photolon] and [PDT with indotricarbocyanine PS], burns with the formation of a scab were observed at the site of tumor localization on days 3-5. On days 14 and 21 after PDT, no tumors were detected in any of the test groups. In the control groups, tumor growth continued, on the 21st day the tumor volume increased by 6-8 times.

Thus, under optimal conditions for photodynamic therapy, PS Photolon and the new PS demonstrate the same antitumor activity for the Ehrlich ascites carcinoma.

[1] A.A. Lugovski, M.P. Samtsov, K.N. Kaplevsky, D.S. Tarasau, E.S. Voropay, P.T. Petrov, Y.P. Istomin, Novel indotricarbocyanine dyes covalently bonded to polyethylene glycol for theranostics, Journal of Photochemistry and Photobiology A: Chemistry, vol. 316, pp. 31-36, (2016).
[2] A.N. Mironova (red.) Rukovodstvo po provedeniyu doklinicheskih issledovanij lekarstvennyh sredstv. CHast' pervaya. (M.: Grif i K), Glava 40, (2012).

DOI: 10.24412/cl-35039-2022-22-107-107

Bactericidal and Bacteriostatic Effect of Blue Light: Basic Patterns and Methods for the Efficiency Enhancement

V. Plavskii[1], A. Tretyakova[1], A. Mikulich[1], N. Dudchik[2], O. Emelyanova[2], L. Plavskaya[1], T. Ananich[1], O. Dudinova[1], A. Sobchuk[1], R. Nahorny[1], I. Leusenko[1], S. Yakimchuk[1]

1- Institute of Physics of the NAS of Belarus, 68-2 Nezavisimosti Ave., Minsk, 220072, Republic of Belarus
2- Republican Unitary Enterprise «Scientific Practical Centre of Hygiene», 8 Akademicheskaya str., Minsk, 220012, Republic of Belarus
v.plavskii@ifanbel.bas-net.by

It was believed for a long time, that only radiation of the short-wave ultraviolet range (200-300 nm), corresponding to the absorption spectrum of DNA, has an antimicrobial effect. However, the studies performed during the last decade with the use of the appeared intense light sources (super-bright LEDs, semiconductor lasers) convincingly indicate the ability of blue light to have a bactericidal or bacteriostatic effect without introducing external exogenous dye-photosensitizers to irradiated microorganisms.

Our studies made it possible to find out the main patterns of the antimicrobial effect of blue light and to develop methods for enhancing its bactericidal and bacteriostatic effectiveness:

It has been established that the exposure of laser radiation of violet and blue spectrum regions to suspensions of microbial cells leads to suppression of growth of both gram-positive streptococci *S. aureus* and gram-negative *E. coli,* as well as yeast-like fungi *C. albicans,* having significantly different structure of the cell membrane. No significant difference in photosensitivity of gram-negative and gram-positive bacteria to the action of radiation of the same wavelength has been revealed. At the same time, among various cell phenotypes, the types with high resistance to the blue light have been found.

It has been established that endogenous metal-free porphyrins, as well as zinc complexes of porphyrins and flavin compounds having photosensitizing properties, act as acceptors of optical radiation, which determine the antimicrobial effect of this physical factor. The participation of these compounds in realization of the antimicrobial effect of laser radiation is indicated by the registration of porphyrin and flavin fluorescence in extracts of microbial cells upon excitation by radiation used to inactivate pathogens. The contribution of porphyrin photosensitizers is mostly pronounced at the exposure with 405 nm radiation (maximum of the Soret band of porphyrins), and flavin ones - at the exposure with 445 nm radiation (maximum in the absorption spectrum of flavins and minimum in the absorption spectrum of porphyrins). The ratio between the intensity of the porphyrin and flavin components in the fluorescence spectrum of extracts depends on the type of microbial cells.

A characteristic feature of the effect of the blue light on microbial cells is an increase of the speed of their photoinactivation with an increase in the dose of radiation. In our opinion, this type of dose dependence can be explained by the model of many photoinactivation targets, assuming that each cell contains not one, but several sensitive targets important for cell life, and a certain number of these targets must be hit to inactivate the cell. Indeed, under the blue spectrum region radiation exposure on microbial cells, there is a violation of the integrity and loss of the most important functional characteristics of cell membranes, release of DNA into the extracellular environment, as well as the oxidation of intracellular DNA, depletion of the level of intracellular ATP due to inhibition of ATPhase, photodamage of some enzymes, as well as a range of metabolites. All this supports the model of many targets of cellular photoinactivation. This conclusion is also supported by the formation of complexes of endogenous porphyrins with molecules of some enzymes, as well as DNA, that we have established.

It has been shown that the effectiveness of the method of suppressing the growth of microorganisms by exposure with laser radiation of the blue spectrum region can be significantly enhanced by: a) the use of radiation of two wavelengths addressed to different cellular targets; b) the use of pulsed radiation, characterized by a high amplitude value of the intensity; c) selection of the optimal wavelength corresponding to the effective excitation of various cellular photosensitizers.

DOI: 10.24412/cl-35039-2022-22-108-108

Nanocomposites of graphene-porphyrins for solar cells

G. Gyulkhandanyan[1], V. Tuchin[2], G. Shmavonyan[3]

1-Institute of Biochemistry, NAS of Armenia, 5/1, P. Sevak st., Yerevan 0014, Armenia
2- Science Medical Center, Saratov State University, 83 Astrakhanskaya st., Saratov 410012, Russia
3-National Polytechnic University of Armenia, 105, Teryan st., Yerevan 0009, Armenia
Main author email address: gvg536898@gmail.com

As photosensitizers, porphyrins are widely used in biophotonics, in particular, for photodynamic therapy of tumors, as well as in phototherapy of microorganisms and viruses. Another rapidly developing area is their use as elements of third-generation solar cells. The first and most important nodal element of a solar battery is a nanocomposite consisting of porphyrins/metalloporphyrins (an effective element for absorbing solar energy) and graphene (a binding element and effectively transferring energy without loss to the next nodal element, the semiconductor part of the battery) [1]. The aim of the study is to develop and obtain a new structure of the key and most important element of the third generation solar battery, consisting of a nanocomposite based on new nanostructures of graphene and porphyrins with a high solar energy conversion efficiency. Porphyrins as photosensitizers can convert solar energy according to the first of three processes, namely - (I) light harvesting and exciton diffusion. A simple synthesis pathway, a high molar extinction coefficient, and a lower fabrication cost compared to other photosensitizers give to porphyrin sensitizers a big advantage [2]. Graphene, which has a high conductivity and unique electronic properties, can convert solar energy by the second of three processes - (II) charge separation. These two substances, porphyrin and graphene, forming a nanocomposite, turned out to be extremely promising and effective in terms of converting solar energy into electrical energy without loss of light energy [1,3]. In order to obtain such nanocomposites, we investigated firstly a number of cationic and anionic porphyrins to study the phenomenon of photobleaching, since this phenomenon can lead to a decrease in the efficiency of collecting sunlight by the porphyrin molecule. The study were carried out in aqueous solutions with cationic porphyrins both metal-free and containing a central Zn atom, as well as with an anionic photosensitizer Al-phthalocyanine in a wide range of concentrations from 10^{-6} to 10^{-4} M for 1 to 24 hours. The results showed a significant dependence of photobleaching of all cationic porphyrins on the concentration of the preparation in solution, while Al-phthalocyanine in the whole concentration range from 10^{-6} to 10^{-4} M was subject to photobleaching within 24 hours insignificantly. To achieve a homogeneous (equable) incorporation (interaction) of porphyrin molecules with graphene, we studied the solubility of the studied photosensitizers in various organic solvents, for which the solubility of graphene was previously studied: acetonitrile, dimethyl formamide, and dimethyl sulfoxide. All studied compounds of photosensitizers showed good solubility in these solvents in a wide range of concentrations. Severally, we also studied the production of new graphene nanostructures in the same organic solvents by the previously developed substrates rubbing method [4]. Presented results is of great importance for designing novel effective materials and devices for advanced phototherapy systems [5] and wireless electrical power delivery using light through human skin to supply smart implants [6].

[1] B. Mao, B. Hodges, C. Franklin, D. G. Calatayud, S. I. Pascu, Self-Assembled Materials Incorporating Functional Porphyrins and Carbon Nanoplatforms as Building Blocks for Photovoltaic Energy Applications, Front. Chem., vol. 9, pp. 1-36, paper 727574, (2021). doi: 10.3389/fchem.2021.727574
[2] V. Armel, J. M. Pringle, P. Wagner, M. Forsyth, D. Officer, D. R. MacFarlane, Porphyrin Dye-Sensitised Solar Cells Utilising a Solid-State Electrolyte, Chem. Commun., vol. 47, paper 9327, (2011). doi:10.1039/c1cc13205a
[3] R. Ge, X. Wang, C. Zhang, S.-Z. Kang, L. Qin, G. Li, X. Li, The influence of combination mode on the structure and properties of porphyrin–graphene oxide composites, Colloids Surf. A, vol. 483, pp. 45-52, (2015).
[4] G. Sh. Shmavonyan, C. Vázquez-Vázquez, M. A. López-Quintela, Single-step rubbing method for mass production of large-size and defect-free 2D materials, Trans. Mater. Res., vol. 4(2), paper 025001, (2017). doi: https://doi.org/10.1088/2053-1613/aa783d
[5] J. Seung Lee, J. Kim, Y.-s. Ye, T.-i. Kim, Materials and device design for advanced phototherapy systems, Advanced Drug Delivery Reviews, 186 114339 (2022). https://doi.org/10.1016/j.addr.2022.114339
[6] J. Seo, J. Kim, J. Jeong, D. Jung, H. Ju, T. Lee, H. Park, J. Lee, Wireless Electrical Power Delivery Using Light through Soft Skin Tissues under Misalignment and Deformation, Adv. Mater. Interfaces, 2102586, (2022). https://doi.org/10.1002/admi.202102586

DOI: 10.24412/cl-35039-2022-22-109-110

Проявление гидрофобности молекул воды на реологические свойства исключённой зоны нафиона

Н.Ф. Бункин[1,2], Л.М. Сабиров[3], В.А. Козлов[1,2], Й.Т. Жураев[3], М.Т. Махамадиев[3], М.А.Хасанов[3]

[1]МГТУ им. Н.Э. Баумана, Москва, РФ
[2]Институт общей физики имени А. М. Прохорова РАН, Москва, РФ
[3] СамГУ, Самарканд, Республика Узбекистан
jorayev-1989@inbox.ru

Интерес к этим исследованиям связан с применением Нафиона в низкотемпературных водородных элементах, см. [1, 2]. Нафион представляет собой полимерный (Тефлоновый) каркас с подшитыми концевыми сульфогруппами. Известно, что Тефлон гидрофобен, в то время как сульфогруппы гидрофильны, т.е. набухший в воде Нафион обладает амфифильными свойствами; в мембране Нафиона формируется структура типа цилиндрических мицелл с заполненными водой цилиндрическими каналами с размером 2 – 3 нм. На границе этих каналов происходит диссоциация концевых сульфогрупп по схеме $R—SO_3H + H_2O \Leftrightarrow R—SO_3^- + H_3O^+$, границы заряжены отрицательно и притягивают катионы [3], что используется в установках по водородной энергетике.

На основании полученных спектров можно оценить усредненную по длине кюветы L концентрацию воды $\langle C_w \rangle$. Переписав закон Бугера в виде:

$$I(t) = I_0 \exp\left(-\kappa \int_0^L C_w(t,x)dx\right) \approx I_0 \exp\left(-\kappa \left\langle C_w(t)\right\rangle L\right), \quad (1)$$

получаем $\left\langle C_w \right\rangle = \dfrac{\left|\ln K_{\min}\right|}{\kappa L}$. В этой формуле учтена зависимость $\langle C_w \rangle$ от времени вымачивания t. На Рис. 1 приведены зависимости $\langle C_w \rangle$ от времени вымачивания t для кювет с расстоянием между окнами L = 180, 190, 200, 210 и 220 микрон. Пунктирная линия соответствует концентрации воды в сухом Нафионе $(C_w)_0$ = 0.174 (базовая линия). Рассмотрим зависимость для L = 180 микрон. Видно, что концентрация воды испытывает резкий скачок примерно через 10 минут набухания. Далее, примерно на 90-й минуте набухания происходит еще один скачок, который не связан со схлопыванием полости (выделено контуром синего цвета). Отметим, что такие же скачки, только с меньшей амплитудой, наблюдаются и для расстояний L = 190, 210 и 220 микрон (выделены соответствующими контурами). Мы предположили, что в данном случае мы имеем дело со структурными изменениями в объеме мембраны; параметром порядка для таких изменений является концентрация воды внутри мембраны, см., например, [4]. Поскольку эти скачки возникают на временах t > 100 min, а переход в гидрофильное состояние завершается при 190 < t < 200 min, см. Рис. 1, можно предположить, что эти скачки являются проявлением динамики перехода в гидрофильное состояние.

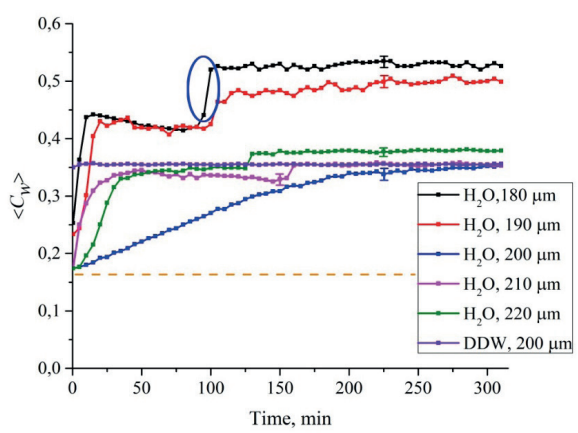

Рис. 1. Зависимость средней концентрации воды $\langle C_w \rangle$ от времени t вымачивания Нафиона при $180 \le L \le 220$ микрон для обычной воды (содержание дейтерия 157 ppm). Также приведен график для вымачивания Нафиона в обедненной по дейтерию воде (содержание дейтерия 1ppm). Штриховая линия соответствует концентрации воды C_{w0}= 0.174 для сухого Нафиона в пустой кювете.

Как уже отмечалось, особенности временной динамики изображенной на рис.1. 3 полости мы связываем с эффектом «прорастания» полимерных волокон в объем воды. Этот вывод основан на отсутствии этой полости для воды, облегченной дейтерием, для которой эффект прорастания отсутствует. Если расстояние L между окнами кюветы меньше размера X_0 области, внутрь которой прорастают полимерные волокна в случае неограниченного размера кюветы (напомним, что этот размер оценивался на основе обработки экспериментальных данных по фотолюминесцентной спектроскопии, см. [5]), то проросшие в объем воды полимерные волокна неизбежно упираются в окна кюветы, что должно привести к возникновению поля механических напряжений и связанных с ними деформаций, т.е. в данном случае проявляются микрореологические свойства набухающей полимерной мембраны (о микрореологических свойствах мягкой материи см., например, монографию [6]). Очень важно, что механические напряжения возникают в системе «скрученных» полимерных волокон, которые исходно обладают существенно гидрофобными свойствами, т.е. положение молекулы воды, оказавшейся в промежутке между двумя такими волокнами, будет неустойчивым.

В экспериментах по Фурье ИК-спектрометрии было показано, что набухание изначально гидрофобной пластинки Нафиона в обычной воде (содержание дейтерия 157 ppm) и в обедненной по дейтерию воде (содержание дейтерия 1 ppm) в кювете ограниченного объема происходит по-разному. Именно, в первом случае проявляются реологические эффекты, которые проявляются в вытеснении воды из области между мембраной и окнами кюветы и формированию полости, свободной от молекул воды, которая с течением времени схлопывается. Обнаружено, что для пластинки Нафиона толщиной 175 микрон схлопывание полости происходит аномально медленно.

ЛИТЕРАТУРА

1. Lunyang Liu,Wenduo Chen,Yunqi Li, An overview of the proton conductivity of nafion membranes through a statistical analysis, Journal of Membrane Science, (2016) **504**, 1–9.
2. Y. Wang, K. S. Chen, J. Mishler, S. Ch. Cho, X. C. Adroher, A review of polymer electrolyte membrane fuel cells: Technology, applications, and needs on fundamental research, Applied Energy, (2011) **88,** 981–1007.
3. K.A. Mauritz, R.B. Moore, State of understanding of Nafion, Chem. Rev., (2004) **104**, 4535-4585.
4. G. Gebel, Structural evolution of water swollen perfluorosulfonated ionomers fromdry membrane to solution, Polymer, (2000),**41** 5829–5838.
5. Bunkin N.F., Shkirin A.V., Kozlov V.A., Ninham B.W., Uspenskaya E.V., Gudkov S.V., Near-surface structure of Nafion in deuterated water, J. Chem. Phys., (2018)**149**, 164901.
6. E. M. Furst and T. M. Squires, *Microrheology*, Oxford University Press, 2017.

DOI: 10.24412/cl-35039-2022-22-111-111

Bimodal Fluorescence Imaging of Bladder Cancer

N. Kalyagina[1,2,*], D. Kustov[1], E. Kozlikina[1,2], A. Borodkin[1,2], M. Loshchenov[2], D. Yagudaev[3]

1- Prokhorov General Physics Institute of the Russian Academy of Sciences, 119991, Moscow, Vavilov Str. 38, Russia
2- National Research Nuclear University MEPhI, 115409, Moscow,Kashirskoe Sh., 31, Russia
3- Central Clinical Hospital, Russian Railways-Medicine, 129128, Moscow, Budayskaya Str. 2, Russia
**Nina.Kalyagina@gmail.com*

Early diagnosis of pathological cancerous micro-areas with their subsequent removal is highly important and can be achieved by the development of new modeling techniques and conducting relevant experiments. In order to study visualization properties at fluorescence endoscopy, bimodal fluorescence imaging was performed. Two-channel video fluorescence system was used as an instrunent to perform the measurements and visualization. Intraoperative images of the bladder wall were obtained in a patient with bladder cancer. A video system was used to reveal and image pathological areas with increased fluorescence intensity. Fluorescence indices in tumor tissue were recorded and corresponded to different concentrations of PpIX photosensitizer. The obtained images and fluorescence intensity measurements showed the ability of the video fluorescence system to register bladder wall structures and accumulated in them photosensitizers in different concentrations. The results of the diagnosic study allowed a doctor to reveal the tumor bodreds and new inconspicuous foci.

DOI: 10.24412/cl-35039-2022-22-112-112

Blood plasma protein constitution and erythrocytes aggregation relationships: study with laser tweezers

K.N. Korneev, P.B. Ermolinsky, A.E. Lugovtsov, A.V. Priezzhev

Faculty of Physics, Lomonosov Moscow State University, Moscow, Russia
korneev.kn19@physics.msu.ru

Erythrocytes aggregation (EA) significantly affects the viscosity of blood which, in turn, influences the process of blood fluidity in the body. The mechanisms of EA phenomenon are not fully investigated so far. However, it is known that the parameters of EA depend on the constitution of the blood plasma and the concentration of the different proteins. At normal conditions, i.e., in healthy individuals, the concentrations of different proteins are different.

As a continuation of our previous work [1], in which the effects of fibrinogen, gamma-globulin on aggregation parameters were measured separately. Earlier, the effects of fibrinogen and albumin on EA were considered in works [2, 3]. In this work, we consider the effects of fibrinogen and gamma-globulin on paired EA after in vitro incubating the erythrocytes suspension with these proteins separately or together.

Laser tweezers is a device for manipulating and trapping a single particle into an optical trap, which is a focused laser beam. The principle of operation of the laser tweezers is based on the use of forces acting on the object from the side of the laser light beam.

Laser tweezers (Nd:YAG laser, wavelength: 1065 nm, power: 100 mW) were used for measuring the aggregation time (AT), aggregation and disaggregation forces (AF, DF) in suspensions of highly diluted erythrocytes on cellular level: AT – time starting from the moment of contact of two erythrocytes and ending with the moment of formation of the aggregate; AF - the minimum value of the optical trapping force that can prevent the aggregation of erythrocytes; DF - the minimum force required to separate the pair aggregate of erythrocytes.

The obtained results show that variation of the amount of gamma-globulin within the range of normal physiological concentrations (6 – 16 mg/ml) does not change the EA parameters. In contrast, the variation of the amount of fibrinogen within the range of normal physiological concentrations (2 – 4 mg/ml) gradually changes the EA parameters. However, with further increase of the concentration of these proteins both of them exhibit the proaggregant action. Comparing their influence on AE, we showed that the effect of fibrinogen up to tested concentration of 10 mg/ml is higher than that of gamma-globulin with corresponding maximum tested concentration 15 mg/ml. Detailed relationship of fibrinogen and gamma-globulin with AE parameters is discussed.

This work was supported by the Russian Science Foundation (Grant No. 22-15-00120) and performed according to the Development program of the Interdisciplinary Scientific and Educational School of Lomonosov Moscow State University «Photonic and Quantum technologies. Digital medicine».

[1] K. Korneev et al., "Comparison of the effect of fibrinogen and gamma globulin on the aggregation of erythrocytes of a healthy donor in vitro by optical techniques". Abstracts of the XXIX International Conference "Lomonosov-2022" (Moscow, Russia, 2022), p. 684.
[2] K. Lee et al., "Optical tweezers study of red blood cell aggregation and disaggregation in plasma and protein solutions ". JBO 21(3), 035001 (2016), DOI: 10.1117/1.JBO.21.3.035001.
[3] A. Semenov et al., "Optical trapping and diffuse light scattering techniques for in vitro assessing the effect of albumin and fibrinogen synergy on red cells aggregation in blood plasma". Abstracts of the 25th International Conference on Advanced Laser Technologies "ALT-17" (Busan, Korea, 2017), p. 174.

DOI: 10.24412/cl-35039-2022-22-113-113

Effect of $CaCO_3$ on Optical Parameters of Biological Tissues in Normal and Cancer

E. N. Lazareva,[1,2*] D. K. Tuchina,[1,2,3] A. A. Doronkina,[1] R. A. Anisimov,[1] M. V. Lomova,[1] A. M. Mylnikov,[4] N. A. Navolokin,[4,5,6] V. I. Kochubey,[1,2] I. Yu. Yanina[1,2]

[1]- Saratov State University (National Research University), Institute of Physics, 83 Astrakhanskaya str., Saratov 410012, Russia

[2]- Tomsk State University (National Research University), Laboratory of laser molecular imaging and machine learning, 36 Lenin's av., Tomsk 634050, Russia

[3]- A.N. Bach Institute of Biochemistry, Research Center of Biotechnology of the Russian Academy of Sciences, Moscow, 33Leninsky prospect, building 2 Moscow, 119071, Russia

[4]- Saratov State Medical University, Department of Pathological Anatomy, 112 B Kazachaya str., Saratov 410012, Russia

[5]- Saratov State Medical University, Center for Collective Use of Experimental Oncology, Experimental Department, 112 B Kazachaya str., Saratov 410012, Russia

[6]- State Healthcare Institution «Saratov City Clinical Hospital No. 1 named after Yu.Ya. Gordeev», 19 Kholzunova st., Pathological Department, Saratov 410017, Russia

**email address: lazarevaen@ list.ru*

Currently, optical therapeutic and diagnostic methods are being actively developed, which are distinguished by their speed, low invasiveness and availability [1, 2]. Nanocontainers for targeted delivery help in the implementation of such methods [3]. In such cases, porous particles of calcium carbonate are used as carriers, which have a slight cytotoxic effect on living cells [4, 5]. For example, nanocontainers with dyes are used in photodynamic therapy to slow down the growth of tumor tissue [6, 7]. However, it is important to know the optical properties of tissues in the area of photodynamic exposure both for containers with dye and without, since this makes it possible to evaluate the effect of nanocontainers on the optical properties of tissues in the area of irradiation, which must be taken into account when calculating the loading of dye into containers.

This study shows the change in optical parameters, such as the absorption coefficient, scattering coefficient, anisotropy factor, of biological tissues before and after the introduction of calcium carbonate particles taken from the area of tumor development. The measurements were performed ex vivo at room and physiological temperatures, which makes it possible to approximate the obtained data to the actual conditions during photodynamic therapy.

The study was supported by RSF grant no. 21-72-10057, https://rscf.ru/project/21-72-10057/.

[1] V.V. Tuchin, J. Popp, V. Zakharov, Multimodal Optical Diagnostics of Cancer (Springer), (2020).

[2] V.V. Tuchin, Tissue Optics: Light Scattering Methods and Instruments for Medical Diagnostics (3rd ed., PM 254, SPIE Press, Bellingham, WA) (2015).

[3] H. Chang, J. Xie, B. Zhao, B. Liu, S. Xu, N. Ren, X. Xie, L. Huang, W. Huang, Rare earth iondoped upconversion nanocrystals: synthesis and surface modification, Nanomaterials, Vol. 5(1), pp.1-25, (2015).

[4] X. Li, Y. Tang, L. Xu, X. Kong, L. Zhang, Y. Chang, H. Zhao, H. Zhang, X. Liu, Dependence between cytotoxicity and dynamic subcellular localization of up-conversion nanoparticles with different surface charges, RSC Adv., vol. 7 (53), pp. 33502–33509 (2017).

[5] C. Wang, M. He, B. Chen, B. Hu, Study on cytotoxicity, cellular uptake and elimination of rare-earth-doped upconversion nanoparticles in human hepatocellular carcinoma cells, Ecotoxicol. Environ. Saf., vol. 203, (110951), pp. 1–10, (2020).

[6] M. H. Abdel-Kader, Photodynamic therapy (Springer-Verlag Berlin An), (2016).

[7] H.S. Qian, H.C. Guo, P.C. Ho, R. Mahendran, Y. Zhang, Mesoporous-Silica-Coated UpConversion Fluorescent Nanoparticles for Photodynamic Therapy, Small, vol. 5 (20), pp. 2285-90, (2009).

DOI: 10.24412/cl-35039-2022-22-114-114

The effect of dextrans as optical clearing agents on microrheologic properties of blood in vitro studied by laser techniques

A.V. Priezzhev[1], A.E. Lugovtsov[1], P.B. Ermolinskiy[1], A.A. Romanova[1], Pengcheng Li[2]

[1]Department of Physics, Lomonosov Moscow State University, Leninskye Gory, 1-62, Moscow, 119991, Russia;
[2] Wuhan National Laboratory for Optoelectronics, Huazhong University of Science and Technology, Wuhan, 430074, P.R.China
avp2@mail.ru

Red blood cell (RBC) aggregability refers to the cells' ability to reversibly form multicellular aggregates in the presence of different plasma proteins or macromolecules. Opposing forces determine the extent of aggregation by the repulsive force between the negatively charged cells, the cell-cell adhesion induced by the macromolecules, and the disaggregating flow-induced shear stress. Kinetic and dynamic features of the cells interaction can characterize the RBC aggregation process [1].

The present study is intended to examine the RBC aggregation in dextran solutions using the diffuse light scattering technique applied to large populations of RBC as well as on the single cell level in a highly diluted suspensions using the optical tweezers [2]. Dextran solutions have higher refractive index relative to blood plasma and are osmotically active that makes them potentially useful for optical clearing of blood. However their effect on blood microrheologic properties has not been studied so far.

Experiments were conducted after 45 minutes long incubation of RBC with dextrans of 500 and 40 kDa molecular weights at the concentration of 50 mg/ml.

Basing on the obtained results, we can conclude that dextran with the molecular weight of 40 kDa is an inhibitor of aggregation, while dextran with the molecular weight of 500 kDa is an RBC aggregation inducer. Optical methods provided handy tools to study the kinetic and dynamic peculiarities of RBC aggregation and disaggregation, which can be extremely useful for controlling and correcting the blood microcirculation alterations especially in cases of hemorheological disorders.

The study was supported by the Russian Science Foundation (grant №22-15-00120) and performed according to the Development program of the Interdisciplinary Scientific and Educational School of Lomonosov Moscow State University «Photonic and Quantum technologies. Digital medicine».

[1] A. Semenov, A. Lugovtsov, S. Shin, G. Barshtein, and A. Priezzhev "Red blood cells interaction mediated by dextran macromolecules: in vitro study using diffuse light scattering technique and optical tweezers", Proc. SPIE 11065, Saratov Fall Meeting 2018: Optical and Nano-Technologies for Biology and Medicine, 110651X (2019) https://doi.org/10.1117/12.2523744.
[2] A. Lugovtsov, Yu. Gurfinkel, P. Ermolinskiy, A. Maslyanitsina, L. Dyachuk, and A. Priezzhev, "Optical assessment of alterations of microrheologic and microcirculation parameters in cardiovascular diseases," Biomed. Opt. Express 10, 3974-3986 (2019).

DOI: 10.24412/cl-35039-2022-22-115-115

Antimicrobial Photoinactivation Using Medicinal Plant Extracts

A. Mikulich[1], A. Tretyakova[1], R. Nahorny[1], T. Ananich[1], N.Dudchik[2], O. Emeliyanova[2], A. Zhabrouskaya[2], A. Sobchuk[1], L. Plavskaya[1], O. Dudinova[1], I. Leusenka[1], S. Yakimchuk[1], V. Plavskii[1], Tran Quoc Tien[3], Quang Cong Tong[3], Thanh Phuong Nguyen[4]

1- State Scientific Institution "B. I. Stepanov Institute of Physics of the National Academy of Sciences of Belarus", 68-2 Nezavisimosti Ave., Minsk, 220072, Republic of Belarus
2- Republican unitary enterprise «Scientific Practical Centre of Hygiene», 8 Akademicheskaya str., Minsk, 220012, Republic of Belarus
3- Institute of Materials Science, Vietnam Academy of Science and Technology, 18 Hoang Quoc Viet, Cau Giay District, Hanoi, Vietnam
4- School of Engineering Physics, Hanoi University of Science and Technology, No.1 Dai Co Viet, Hai Ba Trung, Hanoi, Vietnam
Main author email address: a.mikulich@ifanbel.bas-net.by

Antimicrobial resistance (AMR) is serious public health problem worldwide [1]. Antimicrobial photodynamic therapy (APDT) is efficient technology against various microorganisms based on the interaction of a photosensitizer, molecular oxygen, and an appropriate light source. In this work, we show that photosensitizing effect of medicinal plant extracts can be used to overcome AMR.

The following medicinal plant extracts were used in the studies: extract from a mixture of flowers of *Matricaria chamomilla* and *Calendula officinalis*, *Achilléa millefólium* herb (commercial name "Rotatit"); extract from *Hypéricum perforátum* herb; extract from *Eucalypti viminalis folia*. Absorption and fluorescence spectroscopy were used to investigate the composition of extracts. Photosensitized production of singlet oxygen upon excitation of extracts with light was confirmed by the detection of singlet oxygen luminescence at 1270 nm. Antimicrobial photodynamic effect of extracts was studied towards the Gram-negative (*P. aeruginosa ATCC 15442*) and Gram-positive (*S. aureus ATCC 6538*) bacteria by colony-forming units (CFU) assay. Irradiation was performed with LED sources that emitted light with λ_{max} = 405 nm, λ_{max} = 590 nm and λ_{max} = 660 nm.

Spectral-luminescent analysis shows that all extracts under study are multicomponent and reveals the presence of compounds of chlorophyll ($\lambda_{max, abs}$ = 537; 608; 665 nm) and hypericin ($\lambda_{max, abs}$ = 550; 590 nm) nature in them able to act as photosensitizers. Upon excitation with light (665 nm) the extracts generate singlet oxygen with good quantum yield - 0.64 ("Rotatit"), 0.48 (*Eucalypti viminalis foli*a), 0.40 (*Hypéricum perforátum*).

The extracts showed a strong activity as photosensitizers. Upon exposure to light of λ_{max} = 405 nm at intensity of 100 mW/cm^2 complete inactivation was observed at an irradiation time of 5 min for *P. aeruginosa cells* preliminary incubated with extracts. Among the tested wavelengths, the 405 nm light was the most efficient in killing. In our opinion, upon exposure of blue light, photodynamic effect is due to both excitation of exogenous (extracts) and endogenous photosensitizers [2]. Effective photodynamic inactivation was also achieved for Gram-positive bacteria. In case of extracts, where hypericin component was absent, the light with 660 nm was more efficient in microbial inactivation than 590 nm light and vice versa. In general, photosensitizing effect of extracts was higher in case of Gram-positive bacteria.

We suppose that high quantum yield of singlet oxygen generation by photosensitizers, present in the investigated extracts, contributes to the effective photoinactivation of pathogens, proceeding with the participation mentioned reactive oxygen species.

This work was financially supported by Belarusian Republican Foundation for Fundamental Research, Project Ф21ВТНГ-001 and by the Ministry of Science and Technology of Vietnam, Project Grant Number NĐT/BY/22/03.

[1] E. Polat and K. Kang, Natural Photosensitizers in Antimicrobial Photodynamic Therapy. Biomedicines, 9(6), pp. 584, (2021).
[2] V.Yu Plavskii, A.V. Mikulich, A.I. Tretyakova, I.A. Leusenka, L.G. Plavskaya, O.A. Kazyuchits, I.I. Dobysh, T.P. Krasnenkova,Porphyrins and flavins as endogenous acceptors of optical radiation of blue spectral region determining photoinactivation of microbial cells, Journal of Photochemistry and Photobiology B: Biology, vol. 183, pp. 172-183, (2018).

DOI: 10.24412/cl-35039-2022-22-116-116

Photobleaching of cationic porphyrins and their complexes with folic acid in presence of L-histidine and D-mannitol as quenchers

L. Mkrtchyan[1], A. Zakoyan[1], T. Seferyan[1], G. Gyulkhandanyan[1], V. Tuchin[2]

1- Institute of Biochemistry, NAS of Armenia, 5/1, P. Sevak st., Yerevan 0014, Armenia
2- Saratov State University, Science Medical Center, 83, Astrakhanskaya st., Saratov 410012, Russia
Main author email address:mkrtchyanlusine709@gmail.com

Photodynamic therapy (PDT) is an efficient treatment of tumors, and based on the interaction between suitable wavelength of light and a photosensitizer (PS) with the presence of oxygen to produce toxicity [1].

Compared to healthy cells, multiple kinds of tumor cells express high levels of folate receptors (FRs) on their surface [2]. FRα is overexpressed in a large number of cancers of epithelial origin (e.g. breast, lung, kidney and ovarian cancers). The expression in these carcinomas being 100–300 times higher than on healthy cells and in the order of 1–10 million receptor copies per cell [3]. Therefore, it is a promising strategy to improve the effectiveness of PDT by binding PS's with folic acid (FA).

Photobleaching can be defined as the loss of absorption or emission intensity that is caused by light [1]. It is commonly accepted that more stable PS the better it will perform, mainly because it can endure more cycles of singlet oxygen ($^1O_2$) production [4]. Therefore, in this work we obtain the non-covalent complexes of FA and porphyrins as PS's to improve the targeted nature of PDT. Also, the photobleaching of three cationic porphyrins (TOEt4PyP, Zn-TOEt4PyP and Zn-TBut3PyP) and their complexes with FA was studied. The photobleaching of complexes and their components were performed in presence of two quenchers: L-histidine and D-mannitol. It is known that L-histidine is a singlet oxygen quencher and D-mannitol is a free radicals' quencher (mainly, mannitol combines with •OH radical producing water molecule) [1]. Deferent concentrations of these quenchers were tested and it was shown that the mannitol concentration (0.8 mM) that is needed for effective quenching and for decrease of photobleaching rate after 30 min of illumination by tungsten lamp is 10 times higher than the concentration for histidine (0.08 mM). It is also noted that further increase of quenchers' concentration to 10 mM for mannitol and to 1 mM for histidine has the reverse effect as the photobleaching was more intense. Histidine was more effective quencher for Zn-TBut3PyP and for its complex with FA. Mannitol was shown to be more effective for TOEt4PyP and Zn-TOEt4PyP than histidine. The more effective photoprotection by histidine for Zn-TBut3PyP is correlated with higher singlet oxygen quantum yield of this PS (γ_Δ=0,98) compared with other two PS's (γ_Δ=0,7 for TOEt4PyP and γ_Δ=0,84 for Zn-TBut3PyP). It should be noted that both quenchers has a protective effect, thus indicating that both singlet oxygen and free radicals play a crucial role in the photobleaching mechanism of these cationic porphyrins.

[1]. A. Khaled, O. Khalid, J. Mohamad, Photobleaching of Sn(IV) chlorine e6 dichloride trisodium salt in different environments, African Journal of Biotechnology, Vol. 10 (45), pp. 9137, (2011).
[2]. S. Yan, Q. Huang, J. Chen, X. Song, Z. Chen, M. Huang, P. Xu, J. Zhang, Tumor-targeting photodynamic therapy based on folate-modified polydopamine Nanoparticles, International Journal of Nanomedicine, Vol. 14, pp. 6799-6812, (2019).
[3]. M. Fernandez, F. Javaid, V. Chudasama, Advances in Targeting the Folate Receptor in the Treatment/Imaging of Cancers, Chemical Science, Vol. 9, pp. 1-45, (2017).
[4]. T. Tasso, J. Schlothauer, H. Junqueira, T. Matias, K. Araki, E. Liandra-Salvador, F. Antonio, P. Homem-de-Mello, M. Baptista, Photobleaching efficiency parallels the enhancement of membrane damage for porphyrazine photosensitizers, Journal of the American Chemical Society, Vol. 141 (39), pp. 15547-15556, (2019).

DOI: 10.24412/cl-35039-2022-22-117-117

Enhancing diffuse optical tomography using deep learning

M.A. Ansari, A. Meisamy*
Optical Bio-imaging Lab, Laser and Plasma Research Institute, Shahid Beheshti University, Tehran, Iran
m_ansari@sbu.ac.ir

Diffuse Optical Tomography (DOT) is a non-invasive imaging technique using near-infrared electromagnetic waves to measure the optical properties of biological tissue from boundary measurement. Image reconstruction in this method is an inverse, ill-posed, and nonlinear problem [1]. Traditional optimization methods can't overcome explicitly this problem. Recently, deep neural networks were used in image reconstruction and they have achieved significant improvement [2]. In this research, we used neural network algorithms to reconstruct the absorption coefficient distribution of 3-dimensional phantoms. We demonstrate that deep learning algorithms has a good performance in reconstructing DOT images in comparison to the model-based method.We generate 17000 digital cubic phantoms include inclusions with different size, shape, different places and absorption coefficients. The background absorption and scattering coefficient of the phantoms were assumed 0.01 and 1 mm^{-1}, respectively. An imaging system including 25 sources and detectors with Gaussian profile were considered up and down of tissue. Absorption coefficient of inclusions varied from 0.02 to 0.08 mm^{-1} with 0.02 steps and scattering coefficients were the same with background. For solving continuous wave (CW) forward problem of the diffuse equation, we used Toast++ open-source software based on a finite-element solver [3]. We propose two different neural network architectures: a fully connected layer with 8 hidden layers and a convolutional network with 6 convolutional and pooling layers. The learning rate and epoch were set to 0.0001 and 1000, respectively. For preventing overfitting, we used the earlystopping method. Mean squared error was used as a loss function, ReLU as an activation function, and Adam as an optimizer. The models were implemented in Keras and Input data was separated into 12240 training, 3400 testing, and 1360 validation dataset. The performance of networks was evaluated by four metrics including mean absolute error (MAE), mean squared error (MSE), Peak Signal to Noise Ratio (PSNR), and Structural Similarity Index Metric (SSIM). For comparison with model-based DOT reconstruction methods, we used the conjugate gradient algorithm with Total variation (TV) regularization. Fig.1 shows ground truth and reconstructed distribution of absorption coefficient in z=25. Result shows, by using fully connected layer and convolutional neural network, MAE 76% and 69% and MSE 84% and 62% respectively were reduced and PSNR was doubled in comparison with CG. Accordingly, both neural networks have better performance in DOT image reconstruction than model-based method.

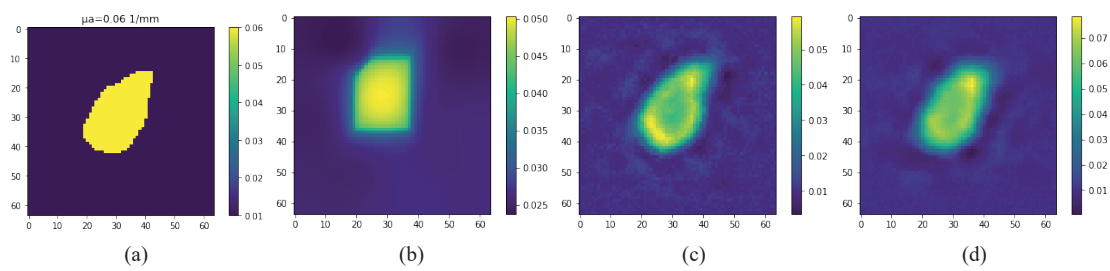

Fig. 1. a) true image in z=25, b) reconstructed image by Conjugate gradient algorithm, c) reconstructed image by fully connected neural network, d) reconstructed image by convolutional neural network.

This work is based upon research funded by Iran national Science Foundation (INSF) under project number 98029460.

[1] Hoshi. Y. and Yamada. Y., Overview of diffuse optical tomography and its clinical applications, Journal of biomedical optics, vol. 21, pp.091312, (2016).
[2] Jalalimanesh. M.H. and Ansari. M.A., Deep learning based image reconstruction for sparse-view diffuse optical tomography, Waves in Random and Complex Media, pp. 1-17, (2021).
[3] Schweiger. M. and Arridge. S. R, The Toast++ software suite for forward and inverse modeling in optical tomography, Journal of biomedical optics, vol. 19, pp. 040801, (2014).

DOI: 10.24412/cl-35039-2022-22-118-118

Raman study of the cyanobacterium *Synechocystis* sp. PCC 6803 mutants deficient in phycobiliproteins

E. Perevedentseva[1], E. Muronets[2], N. Melnik[1], A. Karmenyan[3], I. Elanskaya[2]

1- P.N. Lebedev Physical Institute of Rus. Acad. Sci., Moscow, Russia
2- Biological Dept of Moscow State University, Moscow, Russia
3- Department of Physics, National Dong Hwa University, Hualien, Taiwan
perevedencevaev@lebedev.ru

Cyanobacteria are the model organisms for studying photosynthesis; their applications in ecotoxicological analysis are also suggested. Raman spectroscopy allows analyzing and comparison of chemical composition of the cyanobacteria strains and studying of the state and conformation of the molecules which participate in the living processes of cyanobacteria. In order to collect spectral information about different structural components of cyanobacterial cells, in the present work Raman spectra of the cyanobacterium *Synechocystis* sp. PCC 6803 mutants deficient in phycobiliproteins, which are parts of the light harvesting antenna of cyanobacteria, were measured and analyzed. The wild type of *Synechocystis*, CK mutant, and PAL mutant were grown for 4-5 days in liquid BG-11 medium at 30°C and white light intensity of 40 μmol photons m^{-2} s^{-1}. The suspension of cyanobacteria in growth medium was placed into the quartz cuvette with a thickness 2 mm and the cuvette was positioned on the microscopic stage of InVia Raman spectrometer (Renishaw, GB) equipped with lasers with 785 nm and 1064 nm wavelengths. For the spectra acquisition the laser beam was focused inside the cuvette via objective N Plan 50/0.50 (Leica, Germany) with long working distance.

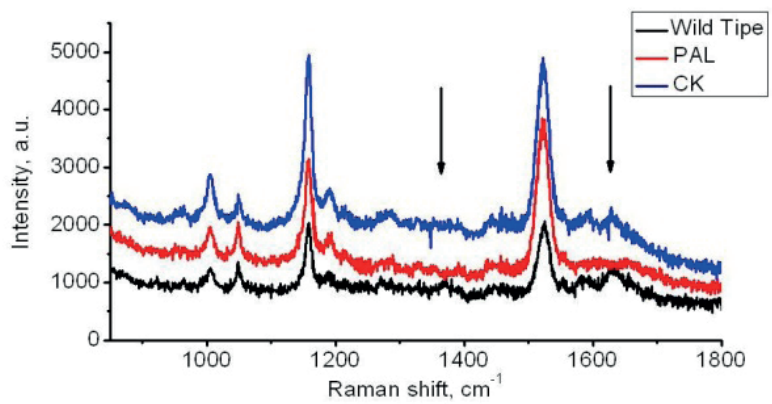

Fig. 1. Raman spectra of cyanobacteria. The most pronounced spectral lines can be attributed to carotenoids (1155 cm^{-1}, 1519 cm^{-1}) and phycobiliproteins (1003, 1110, 1192, 1280, 1370, 1632 cm^{-1}), weaker lines are originated from scytonemin and its derivatives (e.g. near 1450 and 1590 cm^{-1}) and chlorophyll (1328, 1555 cm^{-1}) [1]

Characteristic spectra for 3 samples measured at 1064 nm excitation are shown in Fig. 1. The spectra obtained with excitation 785 nm are comparable. Clear difference in the spectra of studied samples is observed in the areas of peaks 1370 and 1632 cm^{-1} originated from phycobiliproteins. The function of formed by phycobiliproteins antenna complex is to absorb light and to transfer the excitation energy to the photosynthetic reaction centers. Observed results can be brought into line with the data concerning the structure of the antenna complexes of the wild type (contains both phycocyanin and allophycocyanin), CK (contains only allophycocyanin) and PAL (lacking both phycocyanin and allophycocyanin). Thus, Raman spectroscopy with excitation in near IR allows distinguishing different cyanobacterial strains and determining the origin of the difference on the biomolecular level.

[1] P. Vitek, J. Wierzchos. Microbial Ecosystems in Central Andes Extreme Environments: Biofilms, microbial mats, microbialites and endoevaporites, (Springer), Desert biosignatures, (2020).

DOI: 10.24412/cl-35039-2022-22-119-119

Consolidated model for propagation of optical and terahertz radiation through different media in relation to the remote sensing of biological objects

G.S. Rogozhnikov[1], V.V. Kostromykina[1,2], A.A. Skrybykina[1,2]

1- FSUE "Russian Federal Nuclear Center - VNIIEF", Sarov, Russia
2- Lomonosov Moscow State University branch in Sarov, Sarov, Russia
g.s.rogozhnikov@mail.ru

A mathematical model for propagation of visible and infrared optical radiation and submillimeter wavelength terahertz radiation through different media, as well as interaction of the aforementioned types of radiation with matter is proposed. The model is adapted to the problems of remote sensing and imaging of biological objects behind the opaque barriers. Questions concerning the recovery of surface relief and type of the tissue being irradiated are discussed. The model has been verified during the series of experimental research with the use of phantoms (substitutes) of the biological objects. Calculation results can be applied for personal identification by face recognition under the individual means of protection [1] or for inspection of injured tissue under non-metal bandages and dressings.

[1] G.S.Rogozhnikov, V.V.Kostromykina, A.A.Skrybykina Terahertz security vision system in pandemic environment, Proc. of ICLO-2022, St.Petersburg, 2022

DOI: 10.24412/cl-35039-2022-22-120-120

Development of a multimodal approach to the diagnosis of human skin cancer *in vivo*

I. A. Serebryakova[1,2], Yu. I. Surkov[1,2], E. N. Lazareva[1,2], Y. K. Kuzinova[3], O. M. Konopatskova[3], V.V. Tuchin[1,2,4] E. A. Genina[1,2]

1 – Saratov State University, Astrakhanskaya str. 83, Saratov, 410012, Russia
2 – Tomsk State University, Lenin's av. 36, Tomsk, 634050, Russia
3 – Saratov State Medical University, Bolshaya Kazachia str., 112, Saratov, 410012, Russia
4 – Institute of Precision Mechanics and Control RAS, Rabochaya str. 24, Saratov, 410028, Russia
e-mail: s.izabell2014@gmail.com

This work describes a newly developed multimodal method that has the potential to differentiate various skin neoplasms at an early stage of development, allows for postoperative monitoring to detect relapse, and provides additional information useful for selecting treatment tactics. A comprehensive non-invasive method is proposed to search for the specific markers of human skin neoplasms. The method includes: high-frequency ultrasound (US), optical coherence tomography (OCT), backscattering and Raman spectroscopy. In addition, the possibility of increasing the depth of OCT visualization using skin optical clearing was tested.

The study involved 21 volunteers (42 - 80 years old) of both sexes with slightly pigmented skin diagnosed with of basal cell carcinoma (BCC) or benign neoplasm (BN). Areas with neoplasms and nearby healthy and/or symmetrically located skin areas were selected as the object of the study for the subsequent comparison and evaluation of deviations from the norm.

As an optical clearing agent, a aqueous 40% glycerol solution was used, which was applied to the area of interest during 10 minutes.

The sizes of neoplasms were evaluated using US examination. In the OCT images of BCC and BN, in comparison with healthy skin, an inhomogeneous increase of the thickness of the epidermis up to two times was observed, the contrast of the epidermis-dermis border was significantly reduced, in some cases the border between the epidermis and the dermis was indistinguishable. In addition, there was an increase in the number of optical inhomogeneities, some of which can be attributed to blood and lymph microvessels, while others can be attributed to the areas of necrosis and, possibly, local areas of dissociated collagen.

As a result of the analysis of spectral data, one can observe the changes in pigmentation, blood saturation, a decrease in the diffuse scattering coefficient of the skin in the area under study and change in the slope of the spectrum, compared with visually healthy skin. For cancer, a characteristic feature was a low content of lipids and keratin. In the area of benign neoplasms, increased content of proteins, nucleic acids, lipids, and keratin was observed.

Thus, a multimodal approach to the study of skin neoplasms made it possible to obtain comprehensive information on BCC and DN: the boundaries of neoplasm, tissue microarchitecture, effective coefficients of melanin pigmentation and erythema, coefficient of spectral slope k, and coefficient of malignancy R, calculated from backscattering spectra. A multimodal approach to the diagnosis of BCC and DN may have greater sensitivity and specificity than each method to the study of skin neoplasms separately.

The reported study was funded by the grant of RFBR (#20-52-56005) and the grant under the Degree of the Government of the Russian Federation No. 220 of 09 April 2010 (Agreement No. 075-15-2021-615 of 04 June 2021).

DOI: 10.24412/cl-35039-2022-22-121-121

Consolidated model for propagation of optical and terahertz radiation through different media in relation to the remote sensing of biological objects

G.S. Rogozhnikov[1], V.V. Kostromykina[1,2], A.A. Skrybykina[1,2]

1- FSUE "Russian Federal Nuclear Center - VNIIEF", Sarov, Russia
2- Lomonosov Moscow State University branch in Sarov, Sarov, Russia
g.s.rogozhnikov@mail.ru

A mathematical model for propagation of visible and infrared optical radiation and submillimeter wavelength terahertz radiation through different media, as well as interaction of the aforementioned types of radiation with matter is proposed. The model is adapted to the problems of remote sensing and imaging of biological objects behind the opaque barriers. Questions concerning the recovery of surface relief and type of the tissue being irradiated are discussed. The model has been verified during the series of experimental research with the use of phantoms (substitutes) of the biological objects. Calculation results can be applied for personal identification by face recognition under the individual means of protection [1] or for inspection of injured tissue under non-metal bandages and dressings.

[1] G.S.Rogozhnikov, V.V.Kostromykina, A.A.Skrybykina Terahertz security vision system in pandemic environment, Proc. of ICLO-2022, St.Petersburg, 2022

DOI: 10.24412/cl-35039-2022-22-122-122

Nanocomplexes for nanomaterial-based and enzyme-assisted photodynamic therapy

A. Zakoyan[1], L. Mkrtchyan[1], N. Sarkisyan[2], R. Grigoryan[2], V. Tuchin[3], G. Gyulkhandanyan[1]

1-Institute of Biochemistry, NAS of Armenia, 5/1, P. Sevak st., Yerevan 0014, Armenia
2-Institute of Molecular Biology, NAS of Armenia, 7, Hasratyan St., Yerevan 0014, Armenia
3-Science Medical Center, Saratov State University, 83 Astrakhanskaya st., Saratov 410012, Russia
Main author email address: ann.zakoyan@yandex.ru

Photodynamic therapy (PDT) is an effective and minimally invasive therapeutic modality for the treatment of tumors. The efficacy of conventional PDT was usually limited by two factors: photosensitizer (PS) delivery to tumor and hypoxic solid tumor environment. To improve the efficacy of conventional PDT, nanomaterial-based and enzyme-assisted PDT (nano-ezPDT) was developed for enhanced PS delivery and reactive oxygen species (ROS) generation [1]. Smart nanocarriers (endogenous and exogenous enzymes), named enzyme-assisted nanocarriers (EANs), are designed to integrate enzymatic functions with nanomaterials for controlled delivery and enhanced efficacy. PS, oxygen and light are the necessities for a successful nano-ezPDT, which could be improved by an enzyme-mediated PS release, PS accumulation and ROS generation. The delivery of exogenous enzymes is EANs' inner encapsulation or surface anchoring. The PSs are loaded into EANs through either covalent or non-covalent linkages [1]. It is known that the enzyme ceruloplasmin (CP) has an antitumor activity. Under certain conditions, CP is able to enhance free radical oxidation reactions, which leads to the inhibition of tumor cells [2]. This study was designed to evaluate the *in vitro* cytotoxicity and phototoxicity of the novel non-covalent complexes of CP with cationic porphyrins [CP+PS] for nanomaterial-based and enzyme-assisted PDT (nano-ezPDT). We obtained the non-covalent complex of CP and cationic porphyrin Zn-TBut4PyP [CP+Zn-TBut4PyP] with concentrations of CP and Zn-TBut4PyP 1900 μg/ml 6.4 μg/ml, respectively, according to previously described method [3]. The cytotoxic and phototoxic effects of [CP+ Zn-TBut4PyP] complex on human adenocarcinoma HeLa cells (ATCC, US) were assessed using the MTT assay. The results shows that the [CP+Zn-TBut4PyP] complex, its components CP and Zn-TBut4PyP with the same concentrations and Al-phthalocyanine currently used in PDT of tumors are not highly cytotoxic. The content of Al-phthalocyanine and Zn-TBut4PyP in the culture medium under in vitro conditions reduces the survival of the HeLa cell line under illumination with tungsten lamp by 59.8% and 67.9%, respectively. The Illumination of the medium containing the [CP+Zn-TBut4PyP] complex leads to the greatest decrease in the viability of the HeLa cell line relative to the control by 86.2%. The Illumination of the HeLa cell line in the presence of the [CP+Zn-TBut4PyP] complex in the culture medium leads to the formation of reactive oxygen species (including H_2O_2) and conformational changes in the CP. On the other hand, it is known that H_2O_2 in the presence of CP reacts with the DNA and breaks the strands, thus damaging cells *in vitro* [2]. Due to conformational changes in the enzyme component of the [CP+Zn-TBut4PyP] complex, free Cu^{2+} released. The generation of •OH radicals occurs, due to H_2O_2 and free Cu^{2+}. Consequently, free radical oxidation reactions are enhanced which leads to greater inhibition of tumor cells: 1.3 times compared to free porphyrin Zn-TBut4PyP and 1.4 times than compared with Al-phthalocyanine used in PDT. This indicates a high potential of the obtained [CP+Zn-TBut4PyP] complex for nano-ezPDT. This study reveals that the novel complex [CP+Zn-TBut4PyP] on the base of CP and Zn-TBut4PyP cationic porphyrin could be a potential antitumor compound for nano-ezPDT. The obtained [CP+Zn-TBut4PyP] complex can be considered for further cervical cancer preclinical and *in vivo* testing.

[1] B. Du and C-H. Tung, Enzyme-assisted photodynamic therapy based on nanomaterials, ACS Biomater. Sci. Eng., vol. 6, pp. 2506-2517, (2020).
[2] T. P. Vavilova, Yu. N. Gusarova, O. V. Korolyova, A. E. Medvedeva, Role of ceruloplasmin in neoplastic processes development, Biomedicinskaya khimia, vol. 51 (3), pp. 263-275, (2005).
[3] A. A. Zakoyan, Influence of light on optical absorption of photosensitizers and their complexes with human ceruloplasmin, Medical Science of Armenia, vol. 60 (3), pp. 62-70, (2020).

DOI: 10.24412/cl-35039-2022-22-123-123

Monitoring of the ice ball formation during tissue cryosurgery using sapphire shaped crystals

A.K. Zotov[1*], I.N. Dolganova[1,2], K.I. Zaytsev[2,3], I.A. Shikunova[1], L.P. Safonova[2] and V.N. Kurlov[1,2]

1- Institute of Solid State Physics of the Russian Academy of Sciences, Chernogolovka, Russia
2- Bauman Moscow State Technical University, Moscow, Russia
3- Prokhorov General Physics Institute, Moscow, Russia
**E-mail: akzotov@hotmail.com*

Cryoablation is the procedure of living tissue damaging by their freezing. This method has several advantages; among them are relative painlessness, hemostatic effect, minimal damage to healthy tissues, and shorter patient rehabilitation [1]. This method of tissue removal implies special cryoprobes, which must possess a number of features for effective performance, such as biocompatibility, chemical inertness and high thermal conductivity for achieving rather high cooling rate that is essential for tissue cryonecrosis. It is also necessary to be able to control the process of cryodestruction, which may cause risks of damage of surrounding healthy tissues, as well as incomplete cell death. To increase the effectiveness of cryosurgical treatment, it is important to control the tissue freezing depth [1-3].

The sapphire cryoprobes, which are characterized by high transparency in a wide spectral range, chemical resistance and high thermal conductivity at cryogenic temperatures, provide a favorable material platform for cryosurgical instruments [4-8]. To monitor the cryoablation process, the sapphire probe is combined with diffuse reflectance spectroscopy for non-invasive control of tissue freezing [7]. In this work, we demonstrate the developed sapphire cryoprobe and experimentally confirm the possibility to monitoring of the ice ball formation in tissues during their freezing. In addition, we compare the performance of the most commonly used metal probes with the sapphire one. The results reveal the benefits of sapphire for cryosurgical applications.

The work was supported by the Russian Science Foundation Project No. 19-79-10212.

[1] Tumor ablation. Principles and practice. Ed. by E. van Sonnenberg et al. Springer-Verlag New York; (2005).
[2] J. Bischof, K. Christov, B. Rubinsky, "A morphological study of cooling rate response in normal and neoplastic human liver tissue: Cryosurgical implications," Cryobiology 30, 482–492, (1993).
[3] W.B. Bald and J. Fraser, "Cryogenic Surgery," Reports on Progress in Physics, 45, 1381 (1982).
[4]. I. Shikunova et al., "Sapphire capillary interstitial irradiators for laser medicine," Proc. SPIE 10716, 1071605, (2018).
[5] G. Katyba et al., "Sapphire shaped crystals for waveguiding, sensing andexposure applications," Prog. Cryst. Growth Charact. Mater. 64(4), 133–151, (2018).
[6] V.N. Kurlov et al., Crystal Growth Processes Based on Capillarity: Czochralski, Floating Zone, Shaping and Crucible Techniques. Chapter 5. Shaped Crystal Growth (pages 277-354), John Wiley & Sons, United Kingdom, (2010).
[7] E.N. Dubyanskaya, et al. "A concept of cryoapplicator based on sapphire shaped crystal enabling control of the ice ball formation using spatially resolved elastic backscattering of light," Proc. SPIE, 10685, 1068529, (2018)
[8] A.K. Zotov, et al., "In situ terahertz monitoring of an ice ball formation during tissue cryosurgery: a feasibility test, " J. Biomed. Opt. 26(4), 043003, (2021)

ALT'22

LASER SYSTEMS AND MATERIALS

DOI: 10.24412/cl-35039-2022-22-125-125

Multimode and multicore fiber lasers with a cavity based on 3D fs-inscribed refractive-index structures

A.A. Wolf, A.G. Kuznetsov, A.V. Dostovalov, S.A. Babin*

Institute of Automation and Electrometry SB RAS, Novosibirsk 630090, Russia
** babin@iae.nsk.su*

Multimode and multicore fibers (MMF and MCFs) are treated now as an extension to conventional singlemode fibers, which involve transverse modes in optical signal generation, transmission and processing. Developments in this direction resulted in fiber-optic communication systems with increased capacity via spatial division multiplexing [1] and sensing systems with 3D sensitivity to the environmental impact [2]. MMF and MCF lasers are also explored as an alternative to large-mode area singlemode fiber lasers allowing for the power enhancement and/or nonlinear effects suppression [3], but they still have some lacks especially in terms of performance. It may be greatly improved with the use of in-fiber cavity elements analogues to fiber Bragg gratings (FBGs) in singlemode fibers, but conventional UV inscription technique has serious limitations for fabricating structures with necessary spatial resolution, especially in transverse direction. Here we review our recent results on the implementation of femtosecond IR pulses for fabricating 3D refractive-index (RI) structures in active and passive MMF and MCF of different type and development of new laser schemes with them.

First, we describe the femtosecond (fs) inscription technology with an emphasis on possibilities of point-by-point RI modification in MMFs and MCFs with high spatial resolution [4]. With this technology, fs-inscribed FBGs of special transverse structure allowing for the selection of low-order modes (LP_{01} or LP_{11}) in graded-index (GI) MMF have been developed [4] and implemented in MMF Raman laser generating high-power (>50W) high-quality (M^2<2) beam in 950-996 nm spectral band at pumping by highly-multimode (M^2~30) 915-940 nm laser diodes (LDs). In this scheme, brightness enhancement factor ~73 at pump-to-Stokes conversion has been demonstrated [5]. It is also shown with a 2-core fiber as example, a possibility to inscribe FBGs in both cores with a shift in axial direction so that an interference between the reflected signals leads to spectral narrowing (below 0.02 nm) or multiline generation of the 2-core fiber Raman laser, see [4] and citation therein.

Further, FBGs selectively inscribed in side cores of 7-core passive MCF are used as complex reflector of a MCF Raman laser with pumping and output coupling through the central core, which is able to generate singlemode output with narrow spectrum [6]. The narrowing occurs due to the suppression of nonlinear effects in the large effective area of 7-core fiber cavity and due to the interference of signals reflected from FBGs in different cores, which have sufficient optical coupling. Another type of output power concentration in one core is demonstrated for a LD-pumped 4-core Yb-doped fiber with FBGs fs-inscribed in each core, where the core crosstalk is induced via strong bending of the fiber [7]. We also perform similar study of a LD-pumped 7-core Yb-doped fiber with highly-reflective complex mirror consisting of individual FBGs fs-inscribed in each core, where ~35 W output with narrow spectrum (<0.15 nm) is obtained. The role of core coupling and reflected signal interference is studied. We also try to form complex interferometric 3D reflector in GI MMF with random axial and transverse position of individual reflectors and study its effect on spatial and spectral features of output beam in the scheme of LD-pumped MMF Raman laser. The details of the latter studies will be presented at the conference.

This work is supported by Russian Science Foundation (№21-72-30024).

[1] D. J. Richardson, J. M. Fini, & L. Nelson, Space-division multiplexing in optical fibres, Nature Photonics, vol. 7, pp. 354–362 (2013).
[2] K. Bronnikov, A. Wolf, S. Yakushin, A. Dostovalov, O. Egorova, S. Zhuravlev, S. Semjonov, S. Wabnitz, and S. Babin, Durable shape sensor based on FBG array inscribed in polyimide-coated multicore optical fiber, Opt. Express, vol. 27, pp. 38421-38434 (2019).
[3] C. Jaregui, J. Limpert, & A. Tünnermann, High-power fibre lasers, Nature Photonics, vol. 7, pp. 861–867 (2013).
[4] A. V. Dostovalov, A. A. Wolf, M. I. Skvortsov, S. R. Abdullina, A. G. Kuznetsov, S. I. Kablukov, and S. A. Babin, Femtosecond-pulse inscribed FBGs for mode selection in multimode fiber lasers, Opt. Fib. Technol., vol. 52, 101988 (2019).
[5] A. G. Kuznetsov, S. I. Kablukov, E. V. Podivilov, S. A. Babin, Brightness enhancement and beam profiles in an LD-pumped graded-index fiber Raman laser, OSA Continuum, vol. 4, pp. 1034-1040 (2021).
[6] A. Wolf, A. Dostovalov, K. Bronnikov, M. Skvortsov, S. Wabnitz, and S. Babin, Advances in femtosecond direct writing of fiber Bragg gratings in multicore fibers: technology, sensor and laser applications, Opto-Electronic Advances, vol. 5, 210055 (2022).
[7] A. A. Wolf, M. I. Skvortsov, I. A. Lobach, A. V. Dostovalov, and S. A. Babin, Bending induced output power concentration in a core of a 4-core Yb-doped fiber laser, Opt. Exp., vol. 30, pp. 7580-7590 (2022).

DOI: 10.24412/cl-35039-2022-22-126-126

The pulse origin in heavily erbium-doped fiber lasers: experimental evidence and modified theory

O.V. Butov[1,2], A.M. Smirnov[1,2,3], A.V. Dorofeenko[1,2,4,5]

1- Kotelnikov Institute of Radioengineering and Electronics of RAS, Mokhovaya 11-7, Moscow 125009, Russia
2- Moscow Institute of Physics and Technology, 19 Institutskiy pereulok, Dolgoprudny 141700, Russia
3- Faculty of Physics of Lomonosov Moscow State University, Leninskie Gory 1-2, Moscow 119991, Russia
4- Institute for Theoretical and Applied Electromagnetics RAS, 13 Izhorskaya, Moscow 125412, Russia
5- Dukhov Research Institute of Automatics, 22 Suschevskaya, Moscow 127055, Russia
obutov@mail.ru

The comprehensive experimental and theoretical investigation of the heavily doped erbium fiber lasers operation features allowed us to determine the origin of pulse formation. The dependence of the parameters and regimes of lasing on the cavity length, erbium doping level, pump power and external temperature was investigated. Operation regimes in the case of CW pump at a 976 nm and 1490 nm wavelengths have been studied. A new approach to interpretation of self-Q-switched regime provide the explanation of the effect of switching from pulsed to CW operation regime with temperature reduce from room to liquid nitrogen (Fig.1a).

A feature of Erbium-doped fiber lasers is the high probability of stable pulses operation. The parameters of the pulse mode depend both on the composition and concentration of doping in the fiber core, and on external parameters such as pump power and operating temperature.

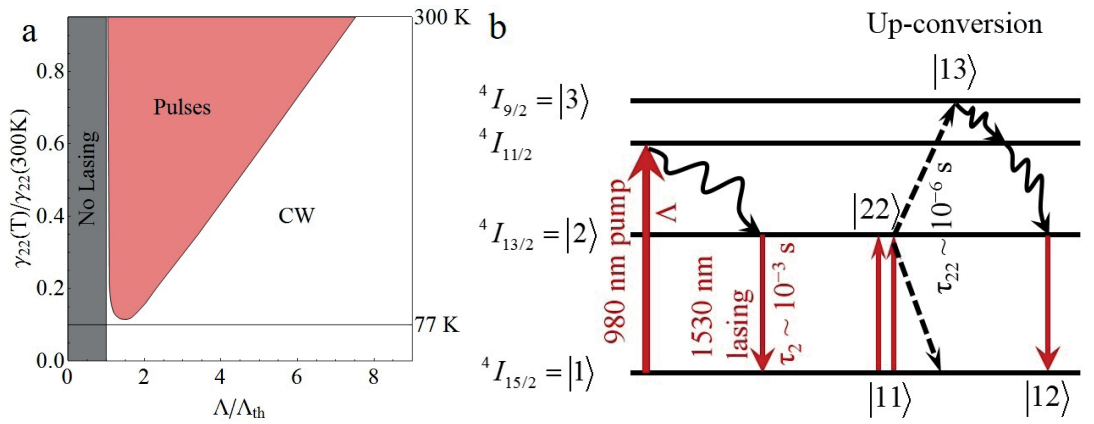

Fig. 1 a) The diagram of laser oscillation regimes in the coordinates of pump intensity (Λ) and up-conversion rate (γ_{22}). b) Energy level structure of a single Er^{3+} ion in silica glass. In the left part of the figure, transitions of the E^{r3+} ion in the lasing process are shown. In the right part of the figure, the up-conversion in ionic pair is shown. The straight and wavy solid lines show radiative and non-radiative relaxation processes, respectively. The dashed line shows a non-radiative energy transfer process between the ions in pair.

It was shown that pulses occur due to the presence of Er^{3+} ion pairs in the glass structure, and a dynamic laser model describing the self-pulsed and CW regimes in the presence of ion pairs in the system was proposed [1,2]. The reason for the pulse formation is the appearance of ion pairs at high concentrations of erbium, which give an absorption effect depending on the populations of levels in the ion pair. Previously this effect was interpreted as saturating absorption. As is known, in classical laser circuits a saturating absorber (passive shutter) leads a passive Q-switched regime and pulse generation. From our point of view, passive Q-switching in heavily doped erbium lasers is realized due to this effect, which is opposite to the saturable absorption. Namely, the absorption increases, rather than saturates, as the intensity of the field increases due to the up-conversion process at the lasing wavelength [3,4] (Fig.1b). For the theoretical description were used the system of rate equations, which takes into account the up-conversion process, appended with a term responsible for the spontaneous emission process.

[1] F. Sanchez, P. Le Boudec, P.-L. François and G. Stephan, Effects of ion pairs on the dynamics of erbium-doped fiber lasers, Phys. Rev. A, vol. 48, pp. 2220-2229 (1993).
[2] F. Sanchez and G. Stephan, General analysis of instabilities in erbium-doped fiber lasers, Phys. Rev. E, vol. 53, pp. 2110-2122 (1996).
[3] A.M. Smirnov, A.P. Bazakutsa, Y.K. Chamorovskiy, I.A. Nechepurenko, A.V. Dorofeenko and O.V. Butov, Thermal Switching of Lasing Regimes in Heavily Doped Er^{3+} Fiber Lasers, ACS Photonics, vol. 5, № 12, pp. 5038-5046 (2018).
[4] A. Smirnov and O. Butov, Pump and thermal impact on heavily erbium-doped fiber laser generation, Optics Letters 46, pp. 86-89 (2021).

DOI: 10.24412/cl-35039-2022-22-127-127

Ultrafast composite fiber-based lasers and amplifiers for the 1.53-1.59 um spectral region

A.D. Zverev[1], V.A. Kamynin[1], B.I. Denker[1], S.E. Sverchkov[1], V.V. Vel'miskin[2], I.S. Panyaev[3], P.A. Itrin[3], D.A. Korobko[3], I.O. Zolotovskii[3], V.B. Tsvetkov[1]

1 - Prokhorov General Physics Institute of Russian Academy of Sciences, Moscow, Russia
2 - Prokhorov General Physics Institute of the Russian Academy of Sciences, Dianov Fiber Optics Research Center, Moscow, Russia
3 - S.P. Kapitsa Scientific Technological Research Institute, Ulyanovsk State University, Ulyanovsk, Russia
Main author email address: kamyninva@gmail.com

Modern photonics devices production requires new robust and technological basic elements. For digital-to-analog-conversion it is laser sources withstable high repetition rate ultrashort pulses (USPs) and for signal transmission it is fiber amplifiers operating in the spectral range of 1.5 μm. Both are in great demand of active media with high gain per unit length coefficient. Thus, the development of such active media is an actual problem. One of the ways to achieve high gain per unit length coefficient is to increase rare-earth elements concentration in fiber core. And it was successfully demonstrated in phosphate fibers: 3 dB/cm gain coefficient [1], and lead realization of tens of GHz repetition rates sources [2]. Despite impressive on-the-table results presented, active fibers have a few serious lacks: degradation in atmospheric moisture and complicated connection to standard optical fibers. In early 2010s FORC RAS and GPI RAS developed composite fiber with a heavily erbium-doped core (3 wt.%) and a silicon cladding that prevents fiber degradation and provides the ability to splice with standard optical components [3]. The fiber combined advantages as phosphate fibers so standard ones.

Now a family of composite Er-, and Er-Yb codoped active fibers were developed. Based on one mentioned media, a passively mode-locked ring laser based on a multicomponent fiber with silica cladding and a 3 wt. % Er-doped phosphate core was realized [4]. The active fiber length was about 19 cm. The laser emitted 570 fs pulses at a repetition rate of 23.9 MHz with an average output power of 1.4 mW. Further active fiber shortening and changing cavity topology to a linear one allowed us to achieve a composite Er-doped fiber laser passively mode-locked by aerosol-synthesized SWCNT film. A stable USPs with a repetition rate of 150 MHz and duration of 973 fs was demonstrated [5].

In the case of USPs amplification, composite active fibers can be promising due to high gain per unit length that lead to decreasing pulses distortion during amplification. It was demonstrated that ultrashort pulses could be amplified in a short composite fiber (20 cm) with a high concentration of Er ions (3 wt.%). Today, we have compared the amplification of ultrashort pulses in amplifiers based on a 31 cm of composite fiberdoped with an Er/Yb complex and standard Er-doped fiber. Analysis of the FROG traces shows that the distortion of the pulse shape in a standard fiber occurs at lower signal gain values.

We believe that composite fiber with high mechanical stability and low air moisture sensitivity supporting splicing with standard silica fibers allows the implementation of a wide range of all-fiber devices and makes it possible to create USPs sources and amplifiers operating at repetition rates between 100 MHz and 10 GHz.

The composite fibers were fabricated within the RFBR project No. 20-02-00425 "Composite optical fibers activated by rare-earth ions".

[1] B. Hwang, S. Jiang, T. Luo, K. Seneschal, G. Sorbello, M. Morrell, F. Smektala,S. Honkanen, J. Lucas, and N. Peyghambarian, Performance of High-Concentration Er3+-DopedPhosphate Fiber Amplifiers, IEEE Photonics Technology Letters, vol. 13(3), (2001).

[2]R. Thapa,, D.Nguyen, J.Zong, A.Chavez-Pirson, All-fiber fundamentally mode-locked 12 GHz laser oscillator based on an Er/Yb-doped phosphate glass fiber, Optics Letters, vol. 39(6), 1418-1421.(2014).

[3] B.I. Denker, B.I. Galagan, V.A. Kamynin, A.S. Kurkov1, Ya.E. Sadovnikova, S. L. Semenov, S. E. Sverchkov, V.V. Velmiskin, E. M. Dianov, "Composite laser fiber with Yb, Er co-doped phosphate glass core and silica cladding, Laser Phys Lett,vol. 10(5), 055109 (2013).

[4] B. I. Denker, B. I. Galagan,.V. A.Kamynin, A. APonosova, S. ESverchkov, S. LSemjonov, V. B. Tsvetkov, Femtosecond laser based on a multicomponent fiber with a 3 wt.% Er-doped phosphate core and silica cladding. Laser Physics Letters, vol. 16(8), 085103,(2019).

[5] A.D. Zverev, V.A. Kamynin, S.A. Filatova, V.G. Voronin, V.B. Tsvetkov, B.I. Galagan, S.E. Sverchkov, B.I. Denker, V.V. Vel'miskin, Y.G. Gladush, E.M. Khabushev, D.V. Krasnikov, A.G. Nasibulin,Passively mode-locked composite erbium fiber laser with a pulse repetition rate of 150 MHz,Optik,vol. 249, (2022).

DOI: 10.24412/cl-35039-2022-22-128-128

Recent Progress in Cladding-Pumped Bismuth-Doped Fiber Lasers and Amplifiers

Sergei V. Firstov*

Prokhorov General Physics Institute of the Russian Academy of Sciences, Dianov Fiber Optics Research Center, 38 Vavilov str., 119333 Moscow, Russia
**E-mail: fir@fo.gpi.ru*

Bismuth-doped fibers exhibit broadband amplification in the near IR range, where efficient active silica-based fibers are not available. Recently, a bismuth-doped laser (BDFL) at a wavelength of 1.46 μm with a slope efficiency of 72% [1], compact [2] and broadband amplifiers (BDFAs) [3] in the O+E+S bands with very promising characteristics interested for telecom industry were developed using new types of bismuth-doped fibers. All the existing Bi-doped fiber devices are core-pumped that notably reduces potential for power scalability.

This report reviews recent progress in cladding-pumped BDFLs and BDFAs. In this regard, the output characteristics of a series of the BDFLs and BDFAs pumped into the active fiber cladding by multimode laser diodes operating at wavelengths of 793 and 808 nm are presented and discussed. The active media for these devices were Bi-doped phospho- and germanosilicate glass core fibers having a circular inner cladding coated by a polymer with low refractive index of 1.396 that allows to provide a light-guiding structure in the inner cladding. Developed BDFLs were assembled in a simple linear scheme consisting of a pump and signal combiner for coupling of pump radiation into the active fiber, a ~100%-reflection fiber Bragg grating and a right-cleaved fiber end as mirrors. A family of BDFAs for the O-, E-, S-telecom bands was implemented using various types of Bi-doped fibers. Length of the active fiber per a device varies in range of 80-200 m.

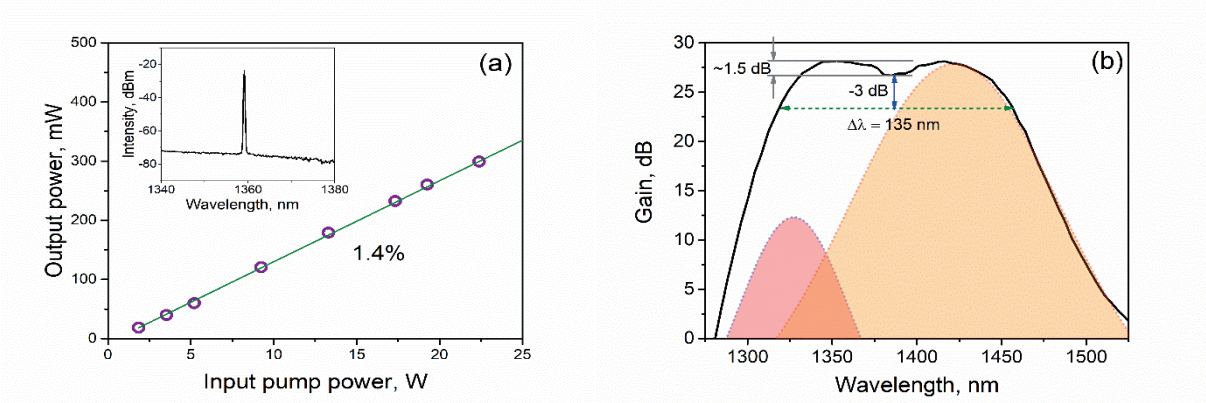

Fig. 1. (a) Output power of the clad-pumped BDFL at ~1360 nm versus the input pump power of 793 nm (inset: output emission spectrum); (b) gain spectrum of BDFA pumped into the cladding by multimode laser diodes at 793 nm with a summarized power of 15 W.

The slope efficiency of the clad-pumped BDFLs operating at a wavelength range of 1.3–1.5 μm was 1–1.5% at a low power threshold of about 1 W. For instance, Fig. 1(a, inset) shows the output power and emission characteristics of the laser operating at ~1360 nm. Figure 1(b) shows the BDFA with a gain spectrum having a width of ~135 nm (at a -3 dB level), a peak gain of 28 dB, a flatness of ~1.5 dB. The minimum noise figure of the BDFA presented was lower than 7 dB.

The progress achieved in this direction opens up previously inaccessible possibilities of devices based on bismuth-doped fibers and their possible practical prospects.

This research was supported by the Russian Science Foundation (22-19-00708).

[1] A. S. Vakhrushev, et al.,W-type and Graded-index bismuth-doped fibers for efficient lasers and amplifiers operating in E-band, Opt. Express 30, pp. 1490-1498 (2022).
[2] S.V. Firstov, et al. Compact and efficient O-band bismuth-doped phosphosilicate fiber amplifier for fiber-optic communications, Sci Rep 10, 11347 (2020).
[3] Y.Wang, et al., Ultra-broadband Bismuth-Doped Fiber Amplifier Covering a 115-nm Bandwidth in the O and E Bands, J. Lightwave Technol., vol.39, pp.795 - 800 (2021).

DOI: 10.24412/cl-35039-2022-22-129-129

Mid-Infrared Ultrashort Pulse Raman Lasers based on Gas-Filled Revolver Silica Fibers

A.V. Gladyshev, A.F. Kosolapov, I.A. Bufetov

Prokhorov General Physics Institute of the Russian Academy of Sciences, Dianov Fiber Optics Research Center, 38 Vavilov st., Moscow, Russia, 119991.
**Corresponding author: alexglad@fo.gpi.ru*

Mid-infrared (mid-IR) ultrashort pulse (USP) lasers are required for a wide range of applications. One of the promising approaches to generate USP in the mid-IR is the concept of gas fiber Raman lasers, which has been successfully used to generate USP at 1.8 and 2.68 μm [1-3]. Here, we extend this approach to longer wavelength and demonstrate efficient USP Raman conversion to wavelength as long as 3.9 μm in a gas-filled hollow-core silica fiber (HCF).

The experimental setup and the HCF properties were reported elsewhere [3]. The HCF was filled by H_2/D_2 gas mixture and pumped by 1.03-μm 250-fs-long pulses that were stretched to 12 ps in duration to promote efficient stimulated Raman scattering (SRS). Total pressure of the mixture was fixed at 30 bar.

At H_2 partial pressure of 25 bar two-cascade SRS based on H_2 and D_2 vibrations was achieved via two complementary schemes 1.03→1.8→3.9 μm and 1.03→1.49→3.9 μm, thus generating a vibrational Stokes component at 3.9 μm. Quantum efficiency about 10 % was demonstrated for 1.03→3.9 μm conversion, and pulse energy as high as 5 μJ was achieved at 3.9 μm.

The results obtained may be used to develop mid-IR laser sources of various types, such as frequency combs, supercontinuum and few-cycle pulse sources, which are promising for a wide range of applications.

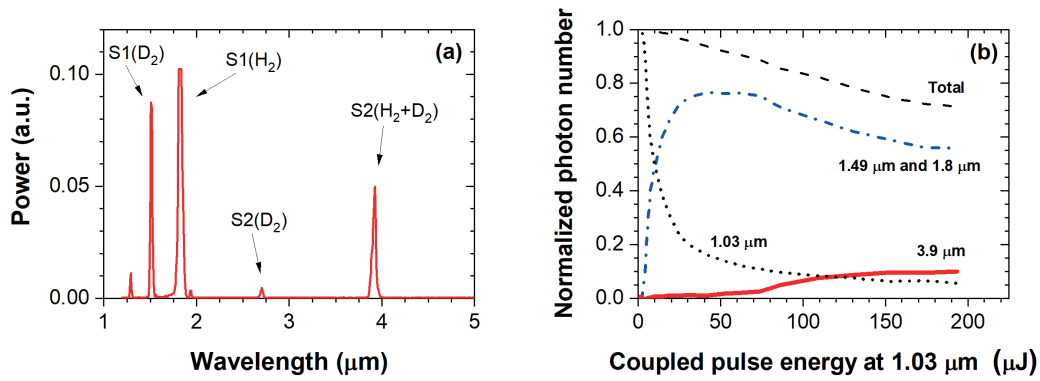

Fig. 1. (a) Spectrum measured at the output of the 2.9-m-long silica HCF that was filled by H_2/D_2 gas mixture and pumped by 80-μJ 12-ps-long pulses at λ=1.03 μm. Partial pressures of H_2 and D_2 were 25 and 5 bar, respectively. The spectrum includes the following vibrational Stokes components: 1st and 2nd Stokes in deuterium ($S1(D_2)$ and $S2(D_2)$), 1st Stokes in hydrogen ($S1(H_2)$) and two-cascade Stokes that involves both deuterium and hydrogen ($S2(H_2+D_2)$). (b) The output number of photons at pump (black dots), 1st Stokes (blue dash-dots) and 2nd Stokes (red solid line) wavelengths as a function of coupled pump pulse energy. The curves are normalized to the number of coupled pump photons. The total photon number is also shown (dashed black line).

This work is supported by Russian Science Foundation (grant №19-12-00361).

[1] S. Loranger et al., "Sub-40 fs pulses at 1.8 μm and MHz repetition rates by chirp-assisted Raman scattering in hydrogen-filled hollow-core fiber," J. Opt. Soc. Am. B, **37**, 3550-3556 (2020).
[2] N. V. Didenko et al., "On the possibility of generation of few-cycle 1.8 μm pulses based on SRS in hydrogen," Laser Phys. Lett., **18**, 125001 (2021).
[3] A. Gladyshev et al., "Mid-infrared 10-μJ-level sub-picosecond pulse generation via stimulated Raman scattering in a gas-filled revolver fiber," Opt. Mater. Express **10**, 3081-3089 (2020).

DOI: 10.24412/cl-35039-2022-22-130-130

High-Power Mid-Infrared Quantum-Cascade Lasers

G.S. Sokolovskii

Ioffe Institute, St.Petersburg, Russia
gs@mail.ioffe.ru

Quantum-cascade lasers (QCL) attract great attention of the research community since the first publication by Kazarinov and Suris proposing the principle in 1971 [1], and especially since the first realization in 1994 by Faist et al. [2]. The main QCL feature distinguishing them from the conventional semiconductor lasers is their unipolarity resulting in the photon emission in the transition of an electron in the conduction band from one quantum level to another instead of recombination of an electron-hole pair. Unfortunately, QCL structures are extremely complicated for practical implementation. The complication comes both from the number of layers that is two orders of magnitude larger than that in a "conventional" semiconductor laser (so-called laser diode) and from the need to maintain the layer homogeneity (i.e., identity of quantum cascades) during long-time epitaxial growth. However, thanks to over quarter of a century efforts of the international research community and over 10 thousand Scopus-indexed publications, QCLs became probably the most efficient sources of coherent radiation in the mid-infrared range, which is well-known for wide atmospheric transparency windows, as well as intense absorption lines of many molecules. Nowadays, mid-infrared QCLs find numerous applications in wireless optical communication, gas analysis, and biomedical research. This report will review the state of the art in mid-infrared QCLs and some practical applications as well as some new results in development of high-power QCLs in this spectral range. Among these results, one should note demonstration of the pulsed output laser power of ~14 W at a wavelength in 4.5 μm region [3], as well as a record-high output power exceeding 16 W achieved in the QCL of the spectral range of 8 μm [4]. In addition, we will discuss very unconventional turn-on dynamics recently revealed in mid-infrared QCLs [5].

This research is supported by the Russian Science Foundation (grant No. 21-72-30020)

[1] R. F. Kazarinov and R.A. Suris, Semiconductors 5, 797 (1971).
[2] J. Faist, et al., Science 264, 553 (1994).
[3] V.V. Dudelev et al., International Conference Laser Optics, St.Petersburg, Russia (2022).
[4] V.V. Dudelev et al., Advanced Photonics Congress, Maastricht, Netherlands (2022).
[5] E.D. Cherotchenko et al., Journal of Lightwave Technology 40(7), 2104–2110 (2022).

DOI: 10.24412/cl-35039-2022-22-131-131

Lasing properties of chalcogenide glasses in the 5÷6 μm spectral range

B.I. Denker[1], B.I. Galagan[1], M.P. Frolov[2], V.V. Koltashev[2], V.G. Plotnichenko[2], G.E. Snopatin[3], M.V. Sukhanov[3], S.E. Sverchkov[1], A.P. Velmuzhov[3]

1 – Prokhorov General Physics Institute of RAS, Vavilov str. 38, Moscow, Russia
2 – Lebedev Physical Institute of RAS, Leninsky prosp. 53, Moscow, Russia
3 – Prokhorov General Physics Institute of RAS, Dianov Fiber Optics Research Center, Vavilov str. 38, Moscow, Russia
4 – Devyatykh Institute of Chemistry of High-Purity Substances of RAS, Tropinin str. 49, Nizhny Novgorod, Russia
glasser@lst.gpi.ru

The wavelengths range >4μm is just beginning to be filled with solid-state lasers. The list of potential low-phonon-energy laser hosts siutable for this range includes chalcogenide (sulfide, selenide and telluride) glasses. The principal advantage of glasses over crystals is the possibility to draw optical fibers of them. Despite many efforts, no laser action in rare-earth doped chalcogenide glasses has been demonstrated in mid-infrared until recently. Now it is clear, that the reason was the insufficient purity of the glasses. S-H, Se-H and Ge-H groups (the main technological impurities in chalcogenide glasses) cause absorption losses at 4÷6 μm and quench the mid-infrared luminescence of rare earth ions. Only recently the progress in rare-earth doped chalcogenide glass technology has made it possible to fabricate high-purity glasses and optical fibers with optical losses as low as ~0.5÷1 dB/m in the mid-infrared.

At present investigation stage we have limited ourselves with selenide glasses and the trivalent rare earth ions (Ce^{3+}, Pr^{3+}, Tb^{3+}) having luminescent transitions at 5÷6 μm, all of them ending at the ground level. Selenide glasses are transparent in approx. 1÷15 μm range and the mentioned rare earth transitions have high quantum yeild in them. The Ge-Ga-Se glass system was chosen for its high solubility of lanthanide ions.

Ce^{3+} ions have no absorption bands in the near infrared and have to be pumped resonantly into the metastable level at ~4 μm. In contrast, Pr^{3+} and Tb^{3+} ions have a whole number of near-infrared absorption bands and can be pumped by several common laser sources. In our experiments [1-4] the highest output energy (34 mJ at ~5.2 μm) was obtained with Ce^{3+} doped bulk glass pumped by pulsed 4.1 μm Fe^{2+}:ZnSe laser (Fig.1). Wavelength tuning in the range of 4.5-5.6 μm and passive Q-switching were also demonstrated. The highest CW output power (35 mW at ~5.2μm) was obtained with Tb^{3+} doped composite sulfo-selenide glass fiber pumped by ~2 μm Tm^{3+} fiber laser (Fig. 2). The longest lasing wavelength (5.9 μm) was observed with bulk Pr^{3+} doped glass.

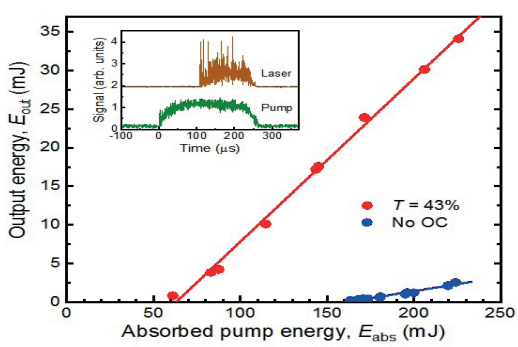

Fig.1. Ce^{3+}:glass laser output under pulsed Fe^{2+}: ZnSe laser pumping at 4.1 μm.

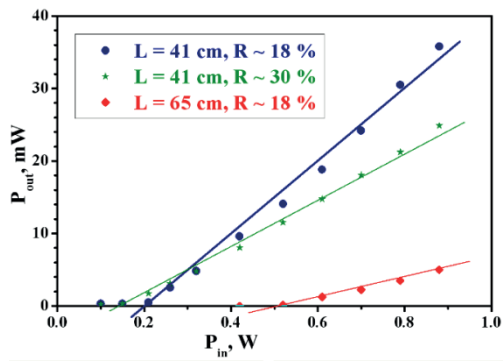

Fig.2. Tb^{3+}:glass fiber laser output under CW Tm^{3+}: fiber laser pumping at 2 μm.

Thus room-temperature 4.5-5.9 μm bulk and fiber glass lasers became reality. The investigations have been supported by RFBR grants 8-29-20079 mk, 20-02-00425 and by RSF grant 22-22-00742.

[1] M.F.Churbanov et al, First demonstration of ~5μm laser action in terbium doped selenide glass, Appl. Phys. B, **126**, 117-119(2020)
[2] M.F.Churbanov et al, Laser potential of Pr doped chalcogenide glass at 5-6 μm spectral range, J. of Non-Cryst. Solids, **559**, 120592(2021).
[3] P. Fjodorov et al, Mid-infrared laser performance of Ce-doped selenide glass. Optics express, **29,** #17, 27674 (2021).
[4] B.I. Denker et al, Continuous Tb-doped fiber laser emitting at ~5.25 μm, J. of Optics and Laser Technology, **154**, 108355(2022).

DOI: 10.24412/cl-35039-2022-22-132-132

Development of mid-IR lasers based on transition metal doped chalcogenide crystals in Lebedev Physical Institute

V.I. Kozlovsky, M.P. Frolov, Yu. V. Korostelin, S. O. Leonov, Ya. K. Skasyrsky

P.N. Lebedev Physical Institute of the Russian Academy of Sciences, 53 Leninsky pr., 119991 Moscow, Russia

For the first time, a laser on transition metal ions in II-VI compound crystals was launched on crystal Cr:ZnSe in 1996 by a scientific group from Lawrence Livermore National Laboratory [1]. High efficiency, wide absorption and emission lines in the mid-IR range and other advantages make these materials attractive for middle infrared (MIR) laser applications. Therefore, many scientific groups around the world have joined the development of these lasers. Our group was the first in Russia who also started developing these lasers in 2003.

The key point of this technology, as well as any other laser technology, is the production of high-quality crystals. By that time, the technology of growing high-quality single crystals of II-VI compounds, including their solid solutions, was developed in P.N. Lebedev Physical Institute for laser cathode ray tubes. Soon it was adapted to produce II-VI compound crystals doped with transition metal ions [2].

The essence of the technology is the physical or chemical transport of vapors of binary polycrystalline sources in a helium or hydrogen gas medium to a single crystal seed. The concentration of the impurity depends on the ratio of the fluxes of the starting substances, which is determined by the design features of the growth ampoule and its equipment (Fig. 1). The report will discuss the advantages of this technology in comparison with alternative technologies used by other scientific groups.

Our main efforts were aimed at launching lasers on new crystals. As a result, we were able to launch lasers on crystals such as Cr:CdS, Cr:CdSe, Fe:ZnS, Fe:CdSe, Fe:ZnTe, Fe:CdTe for the first time. The Fe:ZnSe laser was first realized in CW mode. Also the record pulse energy of 10.6 J was achieved with the Fe:ZnSe laser. Based on our crystals, we managed to cover the spectral region from 2.2 μm to a record 6.8 μm (Fig. 2).

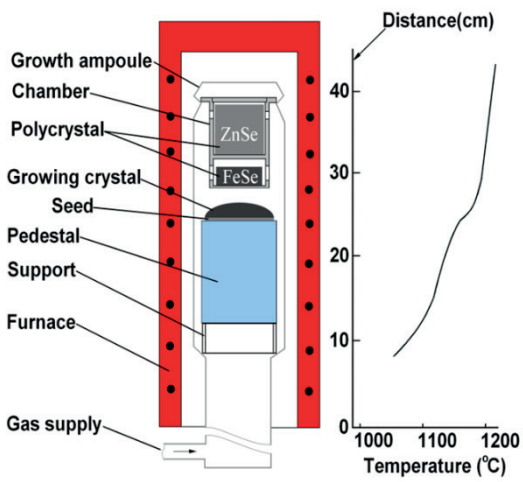

Fig. 1. Scheme of crystal growing.

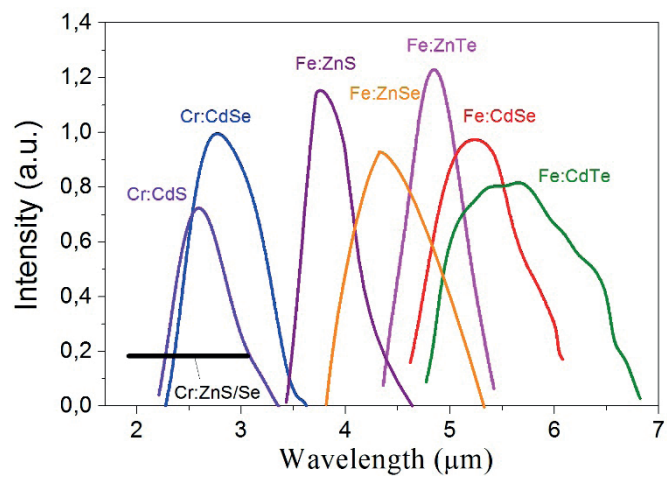

Fig. 2. Tuning curves of lasers based on our grown crystals

[1] L. D. DeLoach, R. H. Page, G. D. Wilke, S. A. Payne, and W. F. Krupke, "Transition metal-doped zinc chalcogenides: spectroscopy and laser demonstration of a new of gain media," IEEE J. Quantum Electron., vol. 32, no. 6, pp. 885–895 (1996.).
[2] V. I. Kozlovsky V. A. Akimov, M. P. Frolov, Yu. V. Korostelin, A. I. Landman, V. P. Martovitsky, V. V. Mislavskii1, Yu. P. Podmar'kov, Ya. K. Skasyrsky, A. A. Voronov, "Room-temperature tunable mid-infrared lasers on transition-metal doped II–VI compound crystals grown from vapor phase," Phys. Status Solidi B, vol. 247, no. 6, pp. 1553–1556 (2010).

DOI: 10.24412/cl-35039-2022-22-133-133

Новые антистоксовые люминофоры и лазерные среды на основе широкозонных халькогенидных полупроводников типа II-III_2-VI_4, легированных редкоземельными элементами

О. Б. Тагиев[1,2], М. С. Леоненя[3], Е. В. Луценко[3], Г. П. Яблонский[3]

[1]Институт физики НАН Азербайджана, Баку
[2]Филиал МГУ им. М.В.Ломоносова, Баку
[3]Институт физики НАН Беларуси, Минск
e-mail: oktay58@mail.ru

Целью работы является получение высокоэффективных лазерных материалов со случайной генерацией на основе кристаллов, нано- и микропорошков широкозонных полупроводников типа $A^{II}B^{VI}$, халькогенидных полупроводников, активированных редкоземельными элементами; установление механизмов поглощения, переноса энергии и усиления, условий и режимов получения случайной генерации в видимой области спектра на одной или на ряде длин волн в микроструктурах полупроводников и халькогенидов с редкими землями при оптической и электронной накачке; выяснение возможности применения указанных материалов для лазерных источников излучения.

Методы работы – экспериментальные. В процессе работы проводились измерения: спектров фотолюминесценции в зависимости от температуры и уровня возбуждения, спектров возбуждения фотолюминесценции, разрешенных во времени спектров фотолюминесценции, спектров антистоковой люминесценции и случайной генерации.

Изучены спектры фотолюминесценции и возбуждения фотолюминесценции, кинетики затухания фотолюминесценции порошков халькогенидных полупроводников $Ca_xBa_{1-x}Ga_2S_4:Eu^{2+}$, $CaGa_2S_4:Er^{3+}$, $CaGa_2S_4:Pr^{3+}$, $EuGa_2S_4:Er^{3+}$,$BaGa_2S_4:Er^{3+}$,Yb^{3+} и $CaGa_4O_7:Eu^{3+}$. Установлено, что изменение состава твердых растворов $Ca_xBa_{1-x}Ga_2S_4:Eu^{2+}$ в пределах параметра *x* от 0.1 до 0.9 приводит к смещению максимума спектра ФЛ в диапазоне от 506 до 555 нм с минимальными потерями в интегральной интенсивности излучения. Показано, что активация халькогенидных полупроводников трехвалентными ионами европия, эрбия и празеодима приводит к наличию структуры линий в видимом диапазоне спектра ФЛ. Определен наиболее эффективный диапазон длин волн возбуждения (от УФ до фиолетово-синей области) ФЛ халькогенидных полупроводников $Ca_xBa_{1-x}Ga_2S_4:Eu^{2+}$, $CaGa_2S_4:Er^{3+}$, $CaGa_2S_4:Pr^{3+}$, $EuGa_2S_4:Er^{3+}$ и $CaGa_4O_7:Eu^{3+}$. **Установлено, что насыщение эффективности излучательной рекомбинации в твердых растворах** $Ca_xBa_{1-x}Ga_2S_4:Eu^{2+}$, соединениях $CaGa_2S_4:Pr^{3+}$ и $CaGa_4O_7:Eu^{3+}$ заметно лишь при уровнях возбуждения выше $2\cdot10^4$ Вт/см^2, 10^5 Вт/см^2 и $2\cdot10^7$ Вт/см^2, соответственно. Установлено, что для получения усиления и случайной генерации в $CaGa_2S_4:Pr^{3+}$ и $CaGa_4O_7:Eu^{3+}$ необходимо использовать излучение накачки с длительностью импульсов порядка времени затухания фотолюминесценции.

Область применения результатов – лазерная физика, полупроводниковая оптоэлектроника, спектроскопия. Актуальность результатов заключается в возможности разработки новых высокоэффективных люминесцентных и лазерных материалов в видимой области спектра и светоизлучающих приборов на их основе.

DOI: 10.24412/cl-35039-2022-22-134-134

Spectral-luminescent and laser characteristics of Y_2O_3 ceramics doped with rare-earth ions (Ho^{3+}, Tm^{3+}, Yb^{3+})

P.A. Ryabochkina[1], S.A. Artemov[1], V.V. Balashov[2], T.V. Volkova[1], A.A. Lyapin[1], I.A. Yurlov[1], S.A. Khrushchalina[1]

1- National Research Mordovia State University, Bol'shevistskaya 68, 430005 Saransk, Russia
2-Fryazino branch of the V.A. Kotelnikov Institute of Radio Engineering and Electronics, RAS , Vvedensky Sq. 1, Fryazino Moscow region, 141120, Russia
Main author email address: ryabochkina@freemal.mrsu.ru

The features of the rare-earth ion energy terms splitting into Stark sublevels in the crystal field of ligands in sesquioxides Ln_2O_3 (Ln – Y, Lu, Sc, Gd) and the high thermal conductivity of these materials provide considerable interest for their use as active media of solid-state lasers with a high output power radiation [1-3]. Growing sesquioxides (Ln – Y, Lu, Sc, Gd) Ln_2O_3 from melt is difficult due to their high melting point (>2400°C)]. Therefore, technologies for obtaining laser ceramics of sesquioxides doped with various rare earth (RE) ions are currently being actively developed, which ensure their production at lower temperatures. Of considerable scientific and practical interest are Ln_2O_3 (Ln – Y, Lu, Sc) crystals and ceramics doped with Tm^{3+} and Ho^{3+} ions for their use as active media of solid-state lasers generating radiation in the two-micron spectral region.

The report presents the results of a study of the spectral-luminescent and laser characteristics of domestic Y_2O_3:Yb, Tm and Y_2O_3:Ho ceramics obtained by solid-phase sintering. Previously, we obtained for the first time continuous-wave lasing at the $^3F_4 \rightarrow {}^3H_6$ transition of Tm^{3+} ions (λ_{gen}= 1.95 μm, λ_{gen}= 2.05 μm) pumped to the $^3H_4$ level by a semiconductor laser diode (λ_{pump}~800 nm) on Y_2O_3:Tm ceramics (C_{Tm}=1.7 at .%) [4]. With this method of pumping, the population of the upper laser level $^3F_4$ of Tm^{3+} ions occurs as a result of radiative and nonradiative processes from the $^3H_4$ level, as well as cross-relaxation of Tm^{3+} ions ($^3H_4 \rightarrow {}^3F_4$, $^3H_6 \rightarrow {}^3F_4$), which is an important channel for the population of the $^3F_4$ level of Tm^{3+} ions when creating population inversion at the $^3F_4 \rightarrow {}^3H_6$ transition. An alternative way to obtain two-micron lasing on the $^3F_4 \rightarrow {}^3H_6$ transition of Tm^{3+} ions is the use of active laser media based on a crystalline matrix co-doped with Tm^{3+} and Yb^{3+} ions [5]. When Yb^{3+} ions are pumped to the $^2F_{5/2}$ level the $^3H_5$ level of Tm^{3+} ions is populated according to the scheme Yb^{3+} ($^2F_{7/2} \rightarrow {}^2F_{5/2}$) → Tm^{3+} ($^3H_6 \rightarrow {}^3H_5$) as a result of nonradiative energy transfer from Yb^{3+} ions to Tm^{3+} ions. Further, the excitation nonradiatively relaxes from this level to the upper $^3F_4$ laser level of these ions.

In the course of this study of the concentration series of Y_2O_3:Yb, Tm (C_{Yb} = 6, 10, 15 at.%, C_{Tm} = 1 at.%), Y_2O_3:Yb, Tm (C_{Yb} = 6, 10, 15 at.%, C_{Tm} = 3 at.%) ceramics, we revealed an effective nonradiative energy transfer from Yb^{3+} ions to Tm^{3+} ions, as well as the interaction between Tm^{3+} ions. We have analyzed the luminescence spectra due to the $^1G_4 \rightarrow {}^3H_6$, $^1G_4 \rightarrow {}^3F_4$, $^3F_3 \rightarrow {}^3H_6$, $^3H_4 \rightarrow {}^3H_6$, transitions and the luminescence decay curves from the $^1G_4$, $^3F_3$, $^3H_4$, $^3F_4$ levels, Tm^{3+} ions, recorded upon excitation of the $^2F_{5/2}$ level of Yb^{3+} ions for concentration series of ceramics Y_2O_3:Yb, Tm, and proposed mechanisms for populating and unloading the energy levels of Tm^{3+} and Yb^{3+} ions.

Also, for the first time, we obtained lasing at the $^5I_7 \rightarrow {}^5I_8$ transition of Ho^{3+} ions in domestic Y_2O_3:Ho ceramics (C_{Ho} = 0.5 at.%) pumped by a thulium fiber laser (λ_{gen}=2117 nm, differential lasing efficiency 33%, P_{out}= 2.4 W).

[1] K. Petermann, G. Huber, L. Fornasiero, S. Kuch, E. Mix, V. Peters, S.A. Basun, Rare-earth-doped sesquioxide, Journal of Luminescence, 87-89, 973-975, (2000).
[2] K. Petermann, L. Fornasiero, E. Mix, V. Peters, High melting sesquioxides: crystal growth, spectroscopy, and laser experiments. Optical Materials, 19, 67-71, (2002).
[3] C. Kränkel, Rare-earth-doped sesquioxides for diode-pumped high-power lasers in the 1-, 2-, and 3-μm spectral range, IEEE Journal of Selected Topics in Quantum Electronics, 21, 1602013, (2015).
[4] P.A. Ryabochkina, A.N. Chabushkin, Yu.L. Kopylov, V.V. Balashov, K.V. Lopukhin, Two-micron lasing on diode-pumped Y_2O_3:Tm ceramics, Quantum Electronics, 46, 597-600, (2016).
[5] P.A. Loiko, J.M. Serres, X. Mateos, M.P. Demesh, A.S. Yasukevich, K.V. Yumashev, V. Petrov, U. Griebner, M. Aguiló, F. Díaz, Spectroscopic and laser characterization of Yb,Tm:$KLu(WO_4)_2$ crystal, Optical Materials, 51, 223-231, (2016).

DOI: 10.24412/cl-35039-2022-22-135-135

Influence of $Ca_3(VO_4)_2$ crystal structural transformations on spectroscopic properties of transition metal ions

L.I.Ivleva[1], G.M.Kuzmicheva[2], M.E.Doroshenko[1]

1-Prokhorov General Physics Institute, RAS, 38 Vavilova str., Moscow 119991, Russia
2-MIREA – Russian Technological University, 78 Vernadsky ave., Moscow 119454, Russia.

Calcium orthovanadate $Ca_3(VO_4)_2$ (CVO) is a multifunctional optical material whose multifunctionality is primarily caused by the disordered whitlockite-like structure without an inversion center. Being well-known ferroelectric material CVO has also received special attention due to its potential use as a host medium for diode-pumped and tunable lasers. The most simple and effective tool to modify functional properties of the material is introduction of dopants or impurities into the crystalline matrix. In present work we consider the spectroscopic properties of CVO crystals doped with TM metals (Mn,Co) in their relation to structural transformations connected to introduction impurities into the matrix.

The main research method for statistical structure was X-ray structural analysis with using diffractometers and synchrotron; and X-ray absorption spectroscopy (synchrotron) was used for determination of local structure. Dopant ions were added into the melt (Czochralski method) over CVO stoichiometry and introduced into the crystalline plates by high-temperature diffusion doping. The full composition for CVO unit cell can be written as [Ca1(18)Ca2(18) Ca3(18)Ca4(6)Ca5(2.65)Ca5*A(*0.35)][(V1(18)V2(18)V3(6)]O168. It was found that Mn ions in green CVO:Mn crystal(as-grown) occupy the Ca3, Ca4, Ca5, Ca5*A* crystallographic sites, (CN Mn3+ = 6 and CN V5+ = 4);Mn ions in yellow-orange CVO:Mn crystal (after air annealing) promote the appearance of Mn4+ and Mn(3+ δ)+ ions having octahedral coordination in the Ca3 and Ca5 sites in the structures, respectively; Mn ions in blue-green CVO:Mn crystal (after high-temperature diffusion annealing) demonstrate the number of sites (Ca2, Ca3, Ca4) occupied by a greater number of Mn(2+δ)+ ions with variable formal charge and tetrahedral local environment. Thus, according to the structural studies, in the CVO:Mn structure,manganese ions $Mn^{(2+\delta)+}$ with a mixed FC can be located in all calcium sites except for Ca1. Co ions in violet CVO:Co3O4 (after high-temperature diffusion annealing) demonstrate the appearance of Co2+ ions, which partially replace the Ca2+ ions in the Ca2, Ca3, Ca4, Ca5, and Ca5*A* crystallographic sites. According to single-crystal-X-ray diffraction, single-crystal synchrotron X-ray diffraction, and powder synchrotron X-ray diffraction methods, a gradual decrease in cell parameters can be observed for Mn and Co doped CVO crystals with increasing of dopant concentration (rCa> rV> rCo> rMn; r, Å are ionic radii).

The measured absorption spectrum of doped materials is characterized by an absorption bands specific for each dopant or their combination which intensity was observed to increase linearly with doping ions concentration. Quite complex absorption spectra of CVO crystals doped with Mn were measured at room temperature within a broad wavelength range (350–1200 nm). The absorption band peaking at 460 nm was assigned to the absorption of Mn2+ ions; absorption about 600 nm is most likely associated with Mn3+ ions while the broad band with maximum at 750 nm and a weak band at 1160 nm can be assigned to Mn5+ ions. Low-temperature site-selective spectroscopy also allowed to confirm the presence of manganese ions in Mn2+and Mn3+ states, which, in general, does not contradict the structural studies. Though, specific lines in low-temperature fluorescence and excitation spectra which are attributed in literature to Mn5+ state (not detected in structural studies) were also observed.

Absorption spectrum of CVO:Co corresponded well to Co2+ ions in tetrahedral sites with absorption band maximum 640 nm. Measured fluorescence spectrum under excitation at 640 nm was broad with maximum about 850 nm. Decay curve is seen to be double exponential with decay times of 8.5 and 30 μs. At least two positions of Co2+ ions with sufficiently different environment (intermediate between tetrahedral and octahedral) can be observed in the crystal. A fundamentally different structural behavior of dopant ions (concentration, formal charge, and coordination environment) in the CVO was defined depending on doping method and special conditions.

DOI: 10.24412/cl-35039-2022-22-136-136

Disk lasers with off-axis beam paths in degenerated type cavities

V.B. Tsvetkov, D.A. Nikolaev

Prokhorov General Physics Institute of the Russian Academy of Sciences, 119991, Vavilov str., 38, Moscow, Russia
e-mail: tsvetkov@lsk.gpi.ru

The wide use of thin disk laser concept occurs due to their excellent property of a significant reduction of the thermal effects in the active medium. Moreover, its outstanding features give rise to new applications with the multipoint pumping. In this case all the intracavity beams become off-axis beams with a closed loop trajectory and the resonator possesses the property of degenerated laser cavity.

At this way we may use two different concepts. The first is the use of the common degenerate cavity configuration with a consequent cavity round trips of a single laser beam through all the pumping points. In this case we may easily realize single frequency or double frequency lasers. The second way consists in the realization of phase synchronization of several laser channels. In this case the super mode with TEM_{00} intensity profile and the sizes corresponding to the whole pumping area is obtained.

Experimental data concerning methods of multi-beam pumping and degenerated cavity realization enable to discuss the possibility of application.

DOI: 10.24412/cl-35039-2022-22-137-138

Радиационная стойкость лазерных кристаллов: вчера, сегодня, завтра

М.Х. Ашуров[1], И.А. Щербаков[2], Б.Л. Оксенгендлер[3]

Институт ядерной физики АНРУз, пос. Улугбек, 100214, Ташкент, Узбекистан
ФИЦ «ИОФ РАН им. А.М. Прохорова», ул. Вавилова 38, 119991, Москва, Россия
ИИПиЛТ им. У.А. Арифова, ул. Дурмон йули 33, 100125, Ташкент, Узбекистан

К настоящему времени сложились устойчивые представления, что лазер является одним из наиболее интересных устройств, органически сочетающих такие глубокие представления как корпускулярно-волновой дуализм, кооперативные квантовые явления и т.д. Этим обусловлено его широчайшее применение фундаментальной и прикладной науках. В самом общем плане можно считать, что базовыми компонентами лазеров всех типов являются активная среда и резонаторы. История лазерной науки и техники вполне естественно развивается на последовательной стадии: создание фундаментальных представлений о квантовых особенностях света; реализация этих идей путем вариации активных сред и типов резонаторов; максимально возможное расширение диапазонов электромагнитных излучений, выдаваемых лазерными устройствами (непрерывного и импульсного типов). Вместе с тем, вовсе времена стояла крайне важная проблема радиационной стойкости лазерных материалов и устройств с их использованием. Чрезвычайно широко и остро этот вопрос проявился в твердотельных лазерах различных типов.

Этот вопрос стал еще более актуальным в связи с широким применением твердотельных лазеров с диодной накачкой на основе полупроводниковых приборов.

Если взглянуть в историю, КПД лазеров при ламповых накачках находились на уровне 1-2%, что было связано с плохим согласованием узких полос поглощения, например, ионов Nd^{3+} с широкими спектрами излучения импульсных ламп накачки. В начале 80-х годов прошлого столетия, в ИОФ РАНе, был найден способ повышения КПД импульсных неодимовых лазеров путем сенсибилизации люминесценции рабочих частиц ионами Cr^{3+}, которые обладали интенсивным широкополосным спектром поглощения, хорошо согласующимися со спектрами излучения импульсных ламп накачки, а также быстро и эффективно передавать поглощенную энергию на верхний лазерный уровень рабочих частиц, которые в свою очередь, должны излучать в заданном спектральном интервале с высоким квантовым выходом [1].

Помимо этого, было показано, что ионы Cr^{3+} препятствуют и образованию центров окраски в результате γ - облучения при комнатной и более высоких температурах в области длин волн более 300 нм во всех исследуемых кристаллов со структурой граната, т.е., выявленное нами свойство ионов Cr^{3+} повышать радиационную стойкость лазерных кристаллов являлось общим [2].

Таким образом, было показано, что ионы Cr^{3+} в данных кристаллах совмещают две важные функции: выступают в качестве эффективных доноров энергии и реализуют высокую радиационную стойкость активных элементов.

На основе этих выводов в конце XX-века были получены рекордные для твердотельных лазеров КПД и были созданы новые приборы и устройства, в том числе, радиационно-стойкие на их основах.

Исследование радиационной стойкости кристаллов Nd^{3+}- $GdVO_4$, одного из наиболее эффективных лазерных кристаллов с диодной накачкой показали, что при γ -облучении кристалл 0,5% Nd-$GdVO_4$ дополнительное радиационно-индуцированное поглощение при длинах волн 808 нм и 1063 нм составляет примерно 0,05 $см^{-1}$, т.е. выдержанный после облучения этот кристалл визуально не окрашен и, при этом, лазер демонстрирует эффективную генерацию на длине волны 1,063 мкм с дифференциальным КПД до 30% с мощностью до 800 мВт при накачке 4 Вт. [3].

Так, путем исследования спектров пропускания лазерного кристалла Nd-$GdVO_4$ и неактивированного кристалла $GdVO_4$ до и после γ-облучения источником ^{60}Co с поглощенными дозами до 10 МР установили, что для кристалла $GdVO_4$ его спектр пропускания в ИК области после облучения в течение нескольких минут релаксирует к спектру поглощения необлученного кристалла. В случае активированного кристалла его спектр пропускания в ИК области после облучения сохраняет остаточное индуцированное поглощение на уровне 0,05 $см^{-1}$, что не значительно сказывается на генерационных свойствах данного кристалла.

Тем самым, эти лазерные эксперименты показывают высокую лазерную эффективность кристалла Nd-$GdVO_4$ несмотря на наличие относительно слабого окрашивания кристалла при интенсивном радиационном облучении. Это означает, данный кристалл можно считать радиационно-стойким при уровнях поглощенной дозы до 10 МР, при последующей выдержке более 1 суток.

Аналогичные результаты были получены и для лазеров на основе ванадата Nd-YVO_4 и кристалла Yb-$LuYSiO_5$ с диодной накачкой [4-5].

Если подытожить исследования проблем радиационной стойкости лазеров за начальный период времени, то можно сказать, что понимание процессов радиационной стойкости происходило в рамках понятии физико-химии материалов (валентность, ионные радиусы, простейший электронный спектр и т.д.). Такой подход в принципе был популярен в качестве объектов исследования в начальный и средний периоды развития идей радиационной физики твердого тела.

Вместе с тем, радиационная физика конденсированного состояния XXI века, следуя общим тенденциям эволюции представлений о науке конденсированных сред вообще, все более стала углубляться в идеи комбинированной нелинейности объектов облучения и использования режима сильной неравновесности, созданной радиационным воздействием.

По началу эта идеология ограничивалась рамками радиационной синергетики [6], однако примерно последние 10 лет произошло углубление идеи радиационной физики конденсированных сред, что получило название «COMPLEXITY» («СЛОЖНОСТЬ») [7].

Теперь исследователей интересовали больше структурные свойства материалов («нано», «фрактальность», «малая размерность», «хиральная симметрия», «иерархичность») попадавших в условия сильно неравновесных облучении. Это немедленно привело к совершенно новым результатам (в частности, даже элементарные атомные перестройки оказывались комбинированными и уже нелинейными; другая частность – существования иерархичности сложных сред давала возможность единовременно реализоваться радиационным эффектам на разных уровнях иерархии материала, а критерием устойчивости материала к облучению стало передача правильно сжатой информации с нижнего иерархического уровня на верхний).

Таким образом, радиационная физика конденсированного состояния резко усложнилась, но это позволило находить новые пути в различных аспектах воздействия радиации на вещество и в том числе, в проблемах радиационной стойкости весьма сложных твердотельных электронных приборов.

Все это позволяет сделать вывод-предположение, что «ЗАВТРА» и для вопросов радиационной стойкости твердотельных лазеров надо будет подходить уже с идеологией «COMPLEXITY» [7].

[1]. Е.В. Жариков, В.В.Осико, А.М.Прохоров, И.А.Щербаков «Кристаллы редкоземельных галлиевых гранатов с хромом как активные среды твердотельных лазеров», Изв. АН СССР Сер.физ. 1984. Т.438, №7. С.1330-1342.
[2]. М.Х.Ашуров, Е.В.Жариков, В.В.Лаптев и др., «Влияние ионов хрома на образование центров окраски в криаталлах со структурой граната», Доклады АН СССР, 1985, Т. 282, №5, С.1104-1106.
[3]. M.Kh.Ashurov, Yu. D. Zavartsev, A. I. Zagumennyi, Sh. Kh. Ismoilov, Yu. L. Kalachev, S. A. Kutovoi, V. A. Mikhailov, I. Nuritdinov, and I. A. Shcherbakov « Radiation Hardness of Nd:$GdVO_4$ Laser Crystal under γ-Ray Irradiation» Physics of Wave Phenomena, 2019, V. 27, No. 4, pp. 271–274.
[4]. S.V. Kaczmarek et.al. «Radiation and structural defects in YVO_4 Laser crystals» / Biuletyn WAT Rok XLV, 2000, N 3, P.115-126.
[5].V.I.Vlasov et.al, «Radiation Resistance of Yb:$LaSc_3(BO_3)_4$ and Yb:$LuYSiO_5$ Laser Crystals», Wave Phenomena, 2018. Vol.26, N4. P.1-5.
[6]. B.L. Oksengendler, et al., «The features of Auger destruction in quasi-one-dimensional objects of inorganic and organic nature»,/Nuclear Inst. and Methods in Physics Research, B. 2022. V.512, P.66-75. https://doi.org/10.1016/j.nimb.2021.12.009.
[7]. Б.Л.Оксенгендлер и др. «Концепция «СЛОЖНОСТИ» в радиационной физике», Журнал «Поверхность», 2022, № 6, с. 1–11, DOI: 10.31857/S1028096022060139

DOI: 10.24412/cl-35039-2022-22-139-139

Light Frequency Converters and Tunable Diffractive Elements Based on Periodically Poled Ferroelectric Crystals and Thin Films

V. Shur[1], A. Akhmatkhanov[1], A. Esin[1], M. Chuvakova[1], B. Slautin[1], V. Pavelyev[2], D. Kolker[3], A. Boyko[3]

1- Institute of Natural Sciences and Mathematics, Ural Federal University, Ekaterinburg, Russia
2- Image Processing Systems Institute of the Russian Academy of Science, Samara, Russia
3- Novosibirsk State University, Novosibirsk, Russia
E-mail: vladimir.shur@urfu.ru

We present the achievements in creation of the periodical domain structures in single crystals of lithium niobate (LN), lithium tantalate (LT) and potassium titanyl phosphate (KTP) families and thin films of LN on isolator (LNOI) for realization of the second harmonic generation (SHG) and optical parametric oscillation (OPO) with record efficiency based on quasi-phase-matching. Various types of LN based tunable diffraction optical elements (DOE) with tailored stable domain structure have been created. The complex study of the domain structure evolution using complementary high-resolution domain imaging methods allows to improve essentially the periodical poling technique.

The detail study of the domain structure evolution and periodical poling have been carried out in thin single-crystalline ion sliced films of LN on SiO_2 isolation layer (LNOI) by conductive tip of the scanning probe microscope [1,2]. The stable domain structures with period less than 200 nm have been created [3,4].

The creation of tunable mid-infrared pulsed optical parametric amplifier (OPA) based on periodically poled LN with fan-out domain structure pumped by 1.053 μm laser and tunable continuous-wave injection seeding have been demonstrated [5]. It was shown that injection seeding leads to four times decrease of the linewidth of output signal wave. The fan-out periodical domain structures allowed to obtain wide OPA tuning range from 2.5 to 4.5 μm [5]. The periodical domain structure in 1-mm-thick KTP single crystals with period 37.97 μm allowed to obtain OPO generation at wavelength 2.4 μm with average power 25 mW for 1300 mW pump.

The opposite values of the linear electrooptic effect for neighboring ferroelectric domains allows to create in ferroelectrics the electrical field controlled DOEs [7]. By creation of tailored stable domain structures in LN single crystals we have created DOEs allowing to obtain Hermite–Gaussian mode (1,0) [7] and mode with orbital angular momentum from Gaussian beam. The possibility of continuous tuning of diffraction efficiency has been demonstrated. It was shown that response time of tunable DOE is less than 200 ns.

The reported study was funded by RFBR and Government of Sverdlovsk region, project № 20-42-660025.

[1] B.N. Slautin, A.P. Turygin, E.A. Pashnina, A.S. Slautina, D.S. Chezganov, and V.Ya. Shur, Evolution of nanodomains and formation of self-organized structures during local switching in X-cut LNOI, Crystals, **12**, 659 (2022).
[2] B.N. Slautin, A.P. Turygin, E.D. Greshnyakov, A.R. Akhmatkhanov, H. Zhu, and V.Ya. Shur, Domain structure formation by local switching in the ion sliced lithium niobate thin films, Appl. Phys. Lett., **116**, 152904 (2020).
[3] B.N. Slautin, H. Zhu, and V.Ya. Shur, Submicron periodical poling in Z-cut lithium niobate thin films, Ferroelectrics, **576**, 119-128 (2021).
[4] B.N. Slautin, H. Zhu, and V.Ya. Shur, Submicron periodical poling by local switching in the ion sliced lithium niobate thin films with dielectric layer, Ceramics International, **47**, 32900-32904 (2021).
[5] E. Erushin, B. Nyushkov, A. Ivanenko, A. Akhmathanov, V. Shur, A. Boyko, N. Kostyukova, and D. Kolker, Tunable injection-seeded fan-out-PPLN optical parametric oscillator for high-sensitivity gas detection, Laser Phys. Lett. **18**, 116201 (2021).
[6] O.L. Antipov, D.B. Kolker, A.A. Dobrynin, Yu.A. Getmanovskiy, V.V. Sharkov, M.A. Chuvakova, A.R. Akhmathanov, V.Ya. Shur, I.A. Shestakova, and S.V. Larin, Mid-infrared optical parametric oscillation and second harmonic generation of repetitively-pulsed radiation of a fiber-laser pumped Tm^{3+}:YAP laser in a fan-out periodically poled MgO:$LiNbO_3$ crystal, Quantum Electronics, **52**, 254-261 (2022).
[7] A.A. Esin, A.R. Akhmatkhanov, V.S. Pavelyev, and V.Y. Shur. Tunable $LiNbO_3$-based diffraction optical element for the control of transverse modes of the laser beam. Computer Optics, **45**, 222-226 (2021).

DOI: 10.24412/cl-35039-2022-22-140-140

Pulses features of the self-Q-switched erbium fiber lasers

A.M.Smirnov[1,2,3], A.V.Dorofeenko[1,3,4,5], A.A. Rybaltovsky[1], O.V.Butov[1]

1- Kotelnikov Institute of Radioengineering and Electronics of RAS, Mokhovaya 11-7, Moscow 125009, Russia
2- Faculty of Physics of Lomonosov Moscow State University, Leninskie Gory 1-2, Moscow 119991, Russia
3- Moscow Institute of Physics and Technology, 19 Institutskiy pereulok, Dolgoprudny 141700, Russia
4- Institute for Theoretical and Applied Electromagnetics RAS, 13 Izhorskaya, Moscow 125412, Russia
5- Dukhov Research Institute of Automatics, 22 Suschevskaya, Moscow 127055, Russia
alsmir1988@mail.ru

The universal dependence of the pulse frequency and duration on the operation power in heavily doped erbium passive Q-switch fiber lasers has been experimentally discovered and theoretically confirmed. It was found that the frequency and duration of pulses are determined by the laser output power and coincides for 1490 nm and 976 nm wavelength pumping regardless of the operation wavelength, fiber core doping level, temperature and cavity length. The frequency and duration of pulses dependencies on lasing power are characterized by equal slopes on a double logarithmic scale in the measured pump power range [1] (Fig.1). The pulses formation is caused by the lasing process itself and the pulse parameters primarily depend on the lasing power. A doping growth leads to the erbium clusterization increase with up-conversion increasing at the lasing wavelength. As a consequence, the pulse duration reduces and the pulses frequency increases, other input conditions being equal.

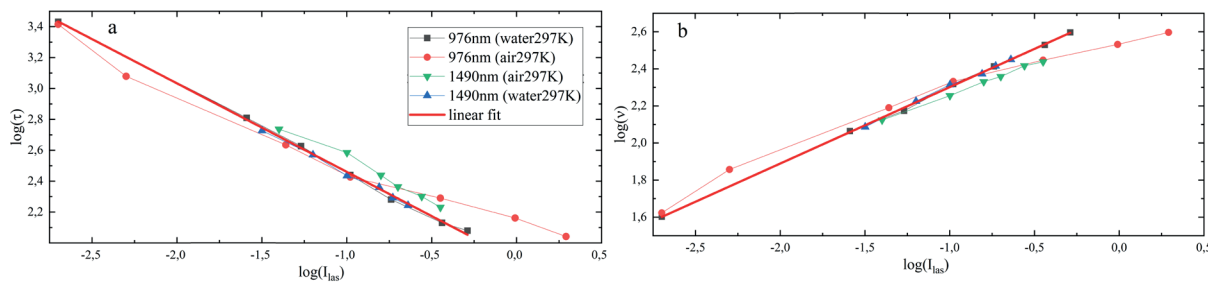

Fig. 1 Dependence of the frequency (a) and pulse duration (b) for 976 nm and 1490 nm wavelength pumping on on the lasing power.

An optical fiber preform was synthesized using both the modified chemical vapor phase deposition (MCVD) and surface plasma chemical vapor deposition (SPCVD) technologies. To achieve a high concentration of erbium oxide in glass (at the level of 0.3 mol.% Er_2O_3) with a minimum level of gray losses SPCVD technology was used. The absorption level at the 1528-1535 nm wavelength of erbium doped fibers varied from 5.3 dBm to 183 dBm. The fiber laser cavity was based on the classical Fabry–Perot scheme. Fiber Bragg gratings (FBGs) inscribed directly in the active fiber core were used as cavity mirrors.

A comparative analysis of the Q-switched lasers operation with different erbium doping level for 1490 nm and 976 nm wavelengths pumping was performed. Resonant excitation at a wavelength of 1490 nm leads to a sharp increase in the pulse frequency and duration reduction compared to 976 nm wavelength excitation. Considering the model presented in Ref. [2], it was assumed that the duration and repetition frequency of pulses are determined by the rate of up-conversion at the lasing wavelength. The occurrence of pulses happens due to the lasing process itself. Taking into account the difference between the lasing efficiency when pumped at 976 nm and 1490 nm wavelengths, the heating caused by the up-conversion at the lasing wavelength can be the primary one.

We acknowledge the support by the Russian Science Foundation Project 20-72-10057.

[1] A.M. Smirnov and O.V. Butov, Pump and thermal impact on heavily erbium-doped fiber laser generation, Optics Letters, vol. 46, pp. 86-89 (2021).
[2] A.M. Smirnov, A.P. Bazakutsa, Y.K. Chamorovskiy, I.A. Nechepurenko, A.V. Dorofeenko, and O.V. Butov, Thermal Switching of Lasing Regimes in Heavily Doped Er^{3+} Fiber Lasers, ACS Photonics, vol. 5, № 12, pp. 5038-5046 (2018).

DOI: 10.24412/cl-35039-2022-22-141-141

Optical pulse compressor using Bayfol based holographic gratings

I. Zhluktova, V. Kamynin, R. Okun, V. Tsvetkov

Prokhorov General Physics Institute of the Russian Academy of Sciences, 38 Vavilov St., Moscow 119991, Russia
Main author email address: romanokun@yandex.ru

Laser sources of highly-chirped subnanosecond pulses are perspective for further amplification to mJ-level energies. Application of such sources reduces high peak power intensity and prevents nonlinear broadening and optical elements damage. One of the main points in such solutions is to compress amplified pulses to spectral limited durations. To solve this problem, usually, pulse compressors are used. The key elements of which are often diffraction gratings [1]. Among the materials that allow creating low-selective and high efficiency diffraction gratings, the most common and commercially successful is Bayfol HX 200 holographic photopolymer. Thus, the main interest of this work refers to the calculation and development of ultrashort pulse compressor based on holographic diffraction gratings recorded in the Bayfol HX 200 photopolymer.

In this work, we used an all-fiber ytterbium laser operating in the passive mode-locking regime as the master oscillator (MO). The fundamental pulse repletion rate is 1 MHz with a pulse duration of 120 ps. At the output of the MO, we have chirped dissipative solitons with the maximum intensity of the spectrum close to the wavelength of 1063 nm [2].

The first issue studied in our work is related to the possibility of application of holographic optical elements recorded in Bayfol HX 200 photopolymer in the near infrared (IR) range, since at the moment the vast majority of applications of the material are limited to the visible range of wavelengths. The paper shows that the refractive index modulation of holograms recorded in Bayfol HX 200 does not significantly decrease in the near IR range compared to the visible range of the spectrum. Thus, Bayfol HX 200 with a thickness of 16 microns allows to obtain holograms with the diffraction efficiency up to 100% in the near IR range. This allows it to be used as a material for diffraction gratings in the laser operating spectral range.

The second question is the calculation of the compressor parameters and simulation of pulse compression. The characteristics of diffraction elements, dimensions, efficiency and dispersion of compressor are calculated. The layout of the proposed compressor is shown in fig. 1(a). Finally we realized and discussed pulse compression in the proposed compressor. As a result, we obtained an oscillogram of the compressed pulse MO up to 27.5 ps, which is a hardware function of the registering pair photodetector-oscilloscope (Thorlabs DX25CF & Tektronix DPO75002SX) (fig. 1(b)). Thus, for the first time, as far as we know, an ultrashort pulse compressor using holographic gratings on the Bayfol HX 200 holographic polymer has been demonstrated.

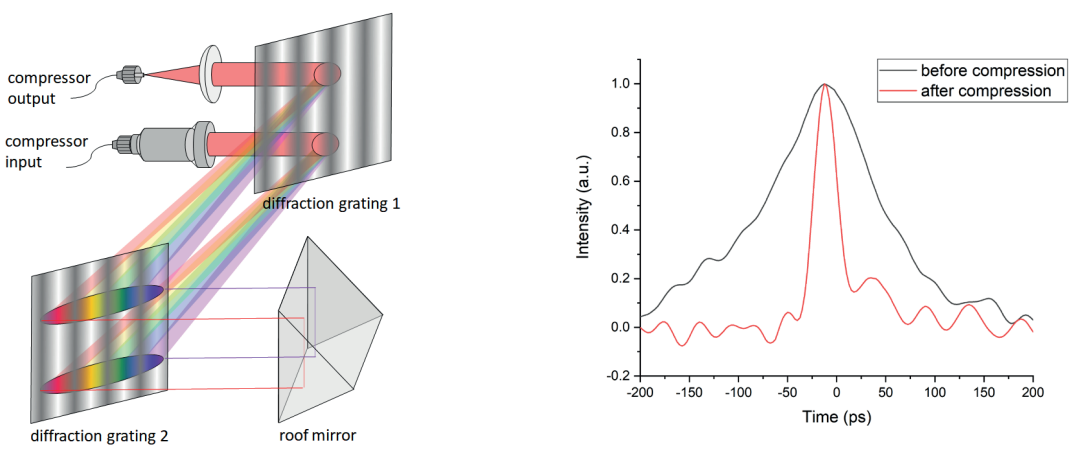

a b

Fig. 1. Compressor layout (a), pulse oscillogram (b)

[1] J. Liu, X. Shen, S. Du and R. Li, Multistep pulse compressor for 10s to 100s PW lasers, Optics Express, 29(11), 17140-17158, (2021).
[2] I. Zhluktova, S. Filatova, A. Trikshev, V. Kamynin, and V. Tsvetkov, All-fiber 1125 nm spectrally selected subnanosecond source, Applied Optics, 59(29), 9081-9086, (2020).

DOI: 10.24412/cl-35039-2022-22-142-142

Physical properties' temperature dynamics of GeTe, $Ge_2Sb_2Te_5$, and $Ge_2Sb_2Se_4Te_1$ materials

A.A. Burtsev, V.V. Ionin, A.V. Kiselev, N.N. Eliseev, V.A. Mikhalevsky, V.V. Grebenev, D.N. Karimov and A.A. Lotin

ILIT RAS — Branch of FSRC "Crystallography and Photonics" RAS, 1, Svyatoozerskaya Str., 140700, Shatura, Moscow Region, Russia
Main author email address: tonyiplit@gmail.com

Phase change materials (PCMs) are compounds with several stable phase states (amorphous and one or more crystalline) with very different properties. For applied application, the high contrast of the optical and electrical properties of PCMs between their amorphous and crystalline states is of great interest. This contrast is primarily due to a significant difference in the structural order, the concentration of charge carriers, and the mechanisms of chemical bonding [1, 2]. Among materials for optical data storage and electric non-volatile memory devices, chalcogenide alloys based on germanium telluride (GeTe, $Ge_2Sb_2Te_5$) are the most mature and widely used in photonic and optoelectronic devices [2]. These alloys have very high amorphization and crystallization rates in the order of nanoseconds, which combined with large cyclability and a pronounced property contrast between the crystalline and amorphous phases [3, 4]. In [5] it was shown that doping of GST with selenium leads to a significant change in its refractive index, almost without changing the extinction coefficient, providing a high optical figure of merit. The presenting results include the results of comprehensive studies of the electrical resistivity and optical transmission coefficient temperature dynamics, phase transition heats, the phase composition, and Raman spectra of GeTe, $Ge_2Sb_2Te_5$, and $Ge_2Sb_2Se_4Te_1$ samples obtained by vacuum thermal deposition. It offers a more holistic view to understand crystallization process in different PCMs and select material for optoelectronic and memristive applications [6].

[1] A.V. Kolobov, J. Tominaga. Chalcogenides: Metastability and Phase Change Phenomena (Springer), ch. 1 (2012).
[2] S. Raoux, M. Wutting (ed.). Phase Change Materials. Science and Applications (Springer), ch. 5 (2009).
[3] N. Yamada, E. Ohno, K. Nishiuchi, N. Akahira, M. Takao. Rapid-phase transitions of GeTe-Sb_2Te_3 pseudobinary amorphous thin films for an optical disk memory. Journal of Applied Physics, 69, pp. 2849-2856 (1991).
[4] K.-Y. Yang, S.-H. Hong, D. Kim, B. Cheong, H. Lee. Patterning of $Ge_2Sb_2Te_5$ phase change material using UV nano-imprint lithography. Microelectronic engineering, 84, pp. 21-24 (2007).
[5] Y. Zhang, J.B. Chou, J. Li, H. Li, Q. Du, A. Yadav, S. Zhou, M.Y. Shalaginov, Zh. Fang, et al. Broadband transparent optical phase change materials for high-performance nonvolatile photonics. Nature communications, 10, pp. 1-9 (2019).
[6] T. Cao and M. Cen. Fundamentals and Applications of Chalcogenide Phase-Change Material Photonics. Advanced Theory and Simulations, 1900094 (2019)

DOI: 10.24412/cl-35039-2022-22-143-143

Thin Film Chalcogenide Materials for Photonic Applications

A.V. Kiselev, A.A. Burtsev, V.V. Ionin, N.N. Eliseev, A.A. Nevxorov, V.A. Mikhalevsky, A.A. Lotin

ILIT RAS — Branch of FSRC "Crystallography and Photonics" RAS,
1, Svyatoozerskaya Str., 140700, Shatura, Moscow Region, Russia
Main author email address: lotin_82@mail.ru

Non-volatile all-photonic memory and neuro-inspired computing are promising technologies for increasing data storage and processing [1]. Photonic memory devices combine the high operation speed and non-volatility. Neuro-inspired computing unifies processing with storage in a single cell. Among materials for optical data storage and electric non-volatile memory devices, chalcogenide alloys based on germanium telluride (GeTe, $Ge_2Sb_2Te_5$) are the most mature and widely used in photonic and optoelectronic devices [2]. These alloys have very high amorphization and crystallization rates in the order of nanoseconds which, combined with large cyclability and a pronounced property contrast between the crystalline and amorphous phases [3, 4]. The presenting results include stable multilevel reversible phase transitions in thin films chalcogenide (GeTe, $Ge_2Sb_2Te_5$) and optical synapse prototype based on planar waveguide with chalcogenide cell. Thin films were deposited by vacuum thermal sputtering. Phase transitions in thin films were induced by nanosecond pulsed laser radiation with «top hat» intensity distribution and different fluence [5]. Structural information was characterized in situ optical parameters measurement, electron microscopy and X-ray diffractometry. Multi-bit devices provide a pathway towards eliminating the von Neumann bottleneck and discover a new applications in all-photonic data storage and computing [6, 7].

[1] W. Zhang, R. Mazzarello, M. Wuttig and E. Ma. Designing crystallization in phase-change materials for universal memory and neuro-inspired computing. Nature Reviews Materials, 4, pp. 150–168 (2019).
[2] K.V. Sreekanth, M. ElKabbash, V. Caligiuri, R. Singh, A. De Luca, G. Strangi. New Directions in Thin Film Nanophotonics, ch. 3 (2019).
[3] P. Guo, A. M. Sarangan and I. Agha. A Review of Germanium-Antimony-Telluride Phase Change Materials for Non-Volatile Memories and Optical Modulators. Applied Sciences. 9, 3, 530 (2019).
[4] N.N. Eliseev, A.V. Kiselev, V.V. Ionin, V.A. Mikhalevsky, A.A. Burtsev, M.A. Pankov, D.N. Karimov, A.A. Lotin. Wide range optical and electrical contrast modulation by laser-induced phase transitions in GeTe thin films. Results in Physics, 19, 10346 (2020).
[5] V. V. Ionin, A. V. Kiselev, N. N. Eliseev, V. A. Mikhalevsky, M. A. Pankov, A. A. Lotin, Multi-level reversible laser-induced phase transitions in GeTe thin films. Applied Physics Letters, 117, 011901 (2020).
[6] C. Ríos, M. Stegmaier, P. Hosseini, D. Wang, T. Scherer, C.D. Wright, H. Bhaskaran and W.H.P. Pernice. Integrated all-photonic non-volatile multi-level memory. Nature Photonics, 9, 725 (2015).
[7] T. Cao and M. Cen. Fundamentals and Applications of Chalcogenide Phase-Change Material Photonics. Advanced Theory and Simulations, 1900094 (2019)

DOI: 10.24412/cl-35039-2022-22-144-144

Spin-coating of deep eutectic solvent for film formation for fabrication of copper patterns using picosecond laser irradiation

L. Logunov[1], D. Shestakov[2]

- School of Physics and Engineering, ITMO University, Lomonosova, 9, Saint-Petersburg, 191002, Russia
Department of Physical Electronics and Technology, Saint Petersburg Electrotechnical University "LETI", 197376 Saint Petersburg, Russia
Main author email address: lev.logunov@metalab.ifmo.ru

Local metallization of dielectrics is an important practical task; inkjet and laser sintering have been developed in industry today. However, each of them has its drawbacks, for Inkjet - the cost of ink, the limitation on the thickness and width of the print area; for laser sintering - the cost of nanoparticles for sintering, damage of the substrate, restrictions on the materials used, and a complex procedure for removing unreacted material [1].

We investigate laser induced chemical deposition method, it is a promising way to template-free metallization methods. The method makes it possible to create metal structures locally on the surface in the zone of laser radiation focus. The advantages of the method include simplicity, low consumption of reagents, the ability to control the shape and size of structures by an optical scheme, low cost of reagents, and environmental friendliness. In addition, the method makes it possible to obtain various metals and their compounds by simply selecting the solution components [2]. Previously, it was possible to obtain conductive metal structures at a scanning rate of 50 um/s using deep eutectic solutions and CW laser radiation [3].

In this work, it was possible to increase the rate of obtaining current-conducting structures on the glass surface by more than an order of magnitude. The maximum scanning speed was 10 mm/s with a resistivity 0.13 Ω mm2/m. We have developed a new method for obtaining thin films of DEC, which made it possible to achieve such results. The process of applying DES films includes several stages and is shown in Figure 1. The first step is to prepare the substrates by the standard cleaning method, then the DES sample is diluted with H2O in a ratio of 3:1 by weight, after solution is spin-coated on the glass surface, samples are dried for 15 minutes on a hot plate at 90C. Then we used galvo scanner with picosecond laser (7pc,1064 nm, 80 mHz) for pattern creation, the unreacted solution is washed off with hot water.

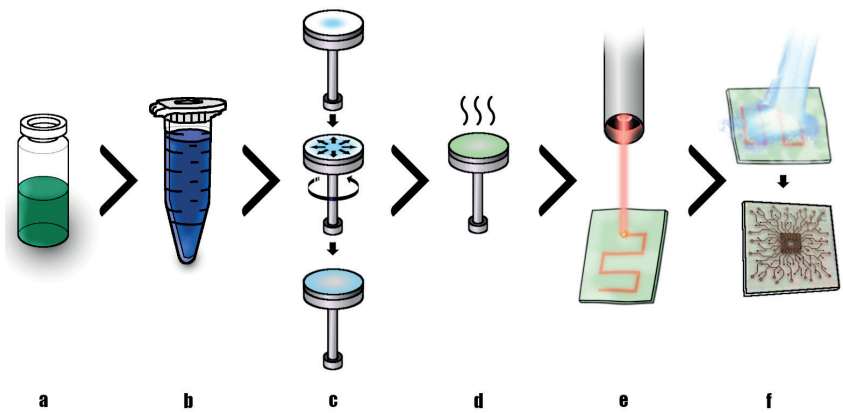

Fig 1. a- initial DES, b - DES with adds of water, b-wet film of DES solution applied by spin-coating, d-dried film of DES solution, e-laser patterning, f-washed sample.

[1] Naghdi, S.; Rhee, K. Y.; Hui, D.; Park, S. J. A Review of Conductive Metal Nanomaterials as Conductive, Transparent, and Flexible Coatings, Thin Films, and Conductive Fillers: Different Deposition Methods and Applications. Coatings, 8 (278), 1–27 (2018).
[2] Logunov, L. S.; Panov, M. S.; Myund, L. A.; Tumkin, I. I.; Khairullina, E. M.; Ryazantsev, M. N.; Balova, I. A.; Kochemirovsky, V. A. Influence of the Ligand Nature on the in Situ Laser-Induced Synthesis of the Electrocatalytically Active Copper Microstructures. Arab. J. Chem. 11 (5), 624–634 (2018).
[3] Shishov, A.; Gordeychuk, D.; Logunov, L.; Tumkin, I. High Rate Laser Deposition of Conductive Copper Microstructures from Deep Eutectic Solvents. Chem. Commun. 55 (2019).

DOI: 10.24412/cl-35039-2022-22-145-145

Formation of Microporous Diamond Films by Microwave Plasma CVD from a Diamond-Germanium Composite

V. Sedov, A. Martyanov, I. Tiazhelov

Prokhorov General Physics Institute of the Russian Academy of Sciences, Moscow
Main author email address: sedovvadim@yandex.ru

Microporous diamond films are a new type of material for applications where a high surface area to volume ratio is required: electrochemistry, electronics, high performance liquid chromatography, in the manufacture of 3D ionizing radiation detectors and mechanically strong filters [1–2]. Porosity can also be used as an antireflection layer in diamond optics. In this work, we propose a new method for the formation of microporous diamond films by growing diamond-germanium composite materials with subsequent selective etching of the germanium component (Fig. 1).

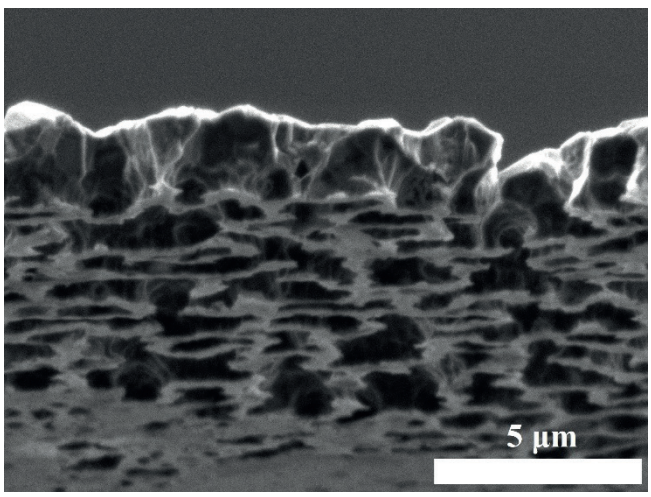

Fig. 1. SEM images of a diamond film after etching of germanium crystallites.

Polished single-crystal silicon wafers used as substrates were seeded with detonation nanodiamonds with an average particle size of 5 nm from an aqueous suspension. Then, a primary microcrystalline diamond film was grown by chemical deposition from methane-hydrogen microwave plasma in an ARDIS 100 reactor (2.45 GHz). At the same time, GeH_4 germanium was injected into the chamber, which led to nucleation and growth of crystalline germanium grains simultaneously with diamond.

The formation of Ge grains in a diamond matrix occurs at relatively low temperatures of 750 – 800°C, while at higher temperatures of 850 – 950°C the diamond phase dominates the growth and blocks the development of Ge grains due to a higher rate. Using selective etching of the germanium component in a mixture of hydrofluoric and nitric acids, samples of microporous poly- and single-crystal diamond were obtained.

The work was supported by the Russian Science Foundation, Grant No. 21-72-10153.

[1] T. Pikuz. et. al., 3D visualization of XFEL beam focusing properties using LiF crystal X-ray detector, Scientific Reports, vol. 5, pp. 1-10, (2015).
[2] V. Ralchenko, et. al., Diamond-germanium composite films grown by microwave plasma CVD, Carbon, vol. 190, pp. 10-21, (2022).

DOI: 10.24412/cl-35039-2022-22-146-146

Two-mode lasing in disk laser with degenerated configuration cavity.

D. Guryev, D. Nikolaev, V. Tsvetkov

Prokhorov General Physics Institute of the Russian Academy of Sciences
e-mail address: guryevden@gmail.ru

The development of stable dual-frequency lasers with narrow linewidths with a sub-gigahertz difference frequency is required for a number of applications. These include, for example, the tasks of radiophotonics [1], interferometry [2], laser spectroscopy and metrology [3]. Usually such lasers operate on two close longitudinal [3] or transverse modes [4]. Usually, cavities with wavelength selectors or spatial selectors of transverse modes are used to obtain two-mode regime.

In this work, the two-mode lasing was obtained in a two mirror Nd:YVO_4 disk laser with a degenerate M-type cavity (Fig. 1). This regime was obtained due to intrinsic wavelength-selective properties of the resonator. No additional wavelength and spatial selectors were used.

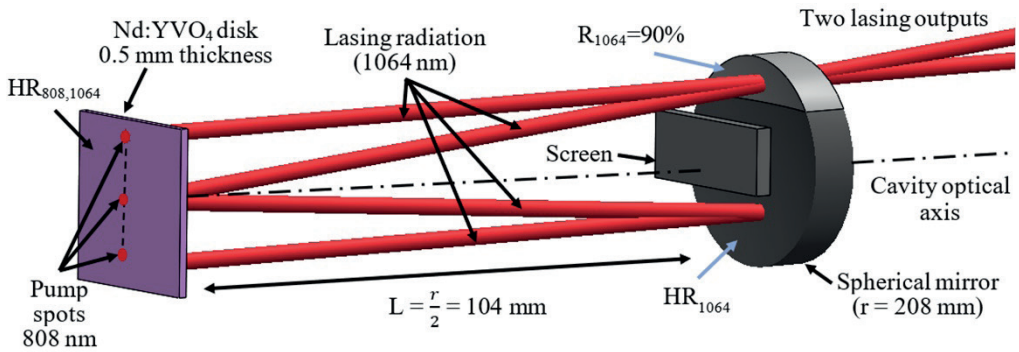

Fig. 1. Scheme of the laser cavity.

Laser was operating in the two-mode beating regime. The frequency separation between two modes was 360 MHz (Fig. 2 (a,b)). At the same time, the linewidth of each mode did not exceed 3 kHz. It was shown that this regime corresponds to two adjacent transverse modes beating (TEM_{00} and TEM_{10}). Laser had two output beams with identical characteristics. The maximum output power from two output beams was 0.32 W at 5.6 W of absorbed pump power.

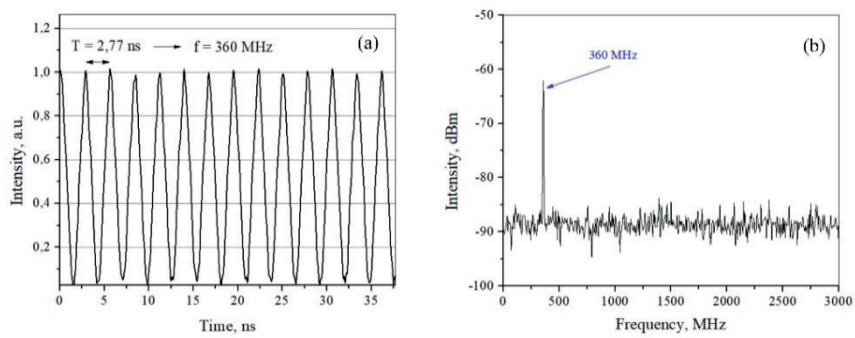

Fig.2. (a) Oscillogram of frequency beating (b) radio-frequency spectrum of lasing radiation.

Acknowledgments: The reported study was funded by RFBR, project number 19-32-90248.

[1] D. Marpaung, J. Yao, J. Capmany, Integrated Microwave Photonics, Nature Photon., vol. 13, pp. 80-90, (2019)
[2] R. Dändliker, R. Thalmann, D. Prongué, Two-wavelength laser interferometry using superheterodyne detection, Opt. Lett, vol. 13 (5), pp. 339-341, (1988).
[3] N.G. Basov, M.A. Gubin, V.V. Nikitin, E.D. Protsenko, Two-mode gas lasers and their applications in spectroscopy and optical frequency standards, Soviet Journal of Quantum Electronics, vol. 14 (6), pp. 731, (1984)
[4] Auston D.H, Transverse mode locking, IEEE J. Quantum Electron, vol. 4 (6), pp. 420-422, (1968).

DOI: 10.24412/cl-35039-2022-22-147-147

Radiation characteristics of crystals and nanoceramics based on CaF_2:SrF_2:YbF_3

M.Kh. Ashurov[1], S.T. Boyboboeva[1,2], I. Nuritdinov[1], P.P. Fedorov[3]

[1]Institute of Nuclear Physics of the Academy of Sciences of the Republic of Uzbekistan,
[2]TRChSPI, st. Amir Temur, 104, Chirchik, 111700, Uzbekistan 111700
[3]FRC "GIP RAS named after by A.M. Prokhorov" st. Vavilova 3, 119991 Moscow, Russia
(ashurov49@mail.ru; izzatilloh@yahoo.com; sohibaboyboboeva@gmail.com)

The interest of researchers in studying the properties of single-crystal and nanoceramic CaF_2:SrF_2:YbF_3 compounds is due to their special position as promising laser materials pumped by laser diodes, as well as the possibility of obtaining tunable laser radiation based on them [1-3]. It was shown in [4] that such a ternary system has the so-called saddle point in which the compositions of the melt and crystal are the same, i.e. congruent melting takes place. As a result, the stability of synthesis in the concentration vicinity of this point is considerably higher, which makes it possible to obtain high-quality single crystals of solid solutions without cells at molar concentrations of Yb^{3+} ions equal to 3–10 %. The synthesizing process of single crystals of solid solutions CaF_2:SrF_2:YbF_3, which provides a lower lasing threshold and higher efficiency (total efficiency is 53%, differential efficiency is 83%) of lasers, based on them, is simpler than the synthesis of single crystals of the MeF_2:YbF_3 (Me=Ca, Sr) [3]. In this work, comparative studies of the effect of gamma radiation in single crystals and nanoceramics of CaF_2:SrF_2:YbF_3 solid solutions were carried out.

The optical absorption spectra of the initial crystal and ceramic samples on the basis of $65CaF_2$:$30SrF_2$:$5YbF_3$ had identical optical absorption spectra, which contained bands in the UV- region with maxima at 227, 261, 273, 300, and 361 nm, as well as a group of lines in the wavelength range of 860-1060 nm, with maxima at 922, 930, 966, 975, 1010 nm in the IR-region. Under excitation gamma irradiation at room temperature in the doses range of 10^5-10^8 rad, the intensities of all bands of Yb^{2+} ions in the wavelength range of 200-400 nm increase, the intensities of the line groups of Yb^{3+} ions in the range 860-1060 nm decrease slightly in both types of samples, which indicates a valence $Yb^{3+}\rightarrow Yb^{2+}$ transition on impurity ions. The valence change of Yb^{3+} ions under irradiation is more pronounced in single crystals. Analysis and comparison of the optical absorption spectra of the initial, irradiated, and samples kept after irradiation at room temperature show that, in the samples under γ -irradiation and holding after-irradiation, in addition to $Yb^{3+}\rightarrow Yb^{2+}$ transitions, complex $Yb^{3+}\rightarrow Yb^{3+}$ transformations occur within the Yb^{3+} - states themselves.

The surface state analysis of the single crystals and nanoceramics of solid mixtures CaF_2:SrF_2:YbF_3, carried out using a scanning probe microscope, showed that the average height of roughness on the ceramic surface decreases from Ra=74,18 nm (initial) to Ra=55,94 nm (irradiated to 10^7 rad), but on the surface of the crystal it increases from Ra=5,86 nm (initial) to Ra=41,06 nm (irradiated to 10^7 rad). The ratio of the average height of the roughness tubercle on the surface of the irradiated and unirradiated samples shows that many defects appear in the crystal under the influence of γ-irradiation, which corresponds to a stronger $Yb^{3+}\rightarrow Yb^{2+}$ valence transition associated with the loss of interstitial fluorine. It is assumed that in nanoceramics, in contrast to single crystals, there are interfaces between "grains" and "voids" strongly developed, which impede the movement of fluorine ions and the repeated reduction of the initial Yb^{3+} state.

1. AkchurinM.Sh., Basiev T.T., Demidenko A.A. et al. CaF_2:Yb lazer ceramics. Opt. Mater. 2013. V. 35. P. 444−450.
2. Sulc, H. Jelınkova, M. E. Doroshenko et al. Tunability of lasers based on Yb^{3+} doped fluorides SrF_2, SrF_2-CaF_2, SrF_2-BaF_2 and YLF. Conference Paper, February 2009. 2009 OSA / ASSP 2009
3. T.T.Basiev, M.E. Doroshenko, P.P. Fedorov,. Efficient laser based on CaF_2-SrF_2-YbF_3 nanoceramics // Optics Letters. 2008. V. 33(5). P. 521-523.
4. Stasyuk V.A. abstract. kand. dis. (M., MIXT im. M.V. Lomonosova, 1998)

DOI: 10.24412/cl-35039-2022-22-148-148

All-glass single-mode microstructured optical fibers with a large mode area and low bending losses

A. Denisov[1], S. Semjonov[1], M. Likhachev[1], V. Velmiskin[1], A. Kosolapov[1], O. Egorova[2], S. Zhuravlev[1]

1- Prokhorov General Physics Institute of the Russian Academy of Sciences, Dianov Fiber Optics Research Center, Vavilov Str., 38, 119333, Moscow, Russia
2- Prokhorov General Physics Institute of the Russian Academy of Sciences, Vavilov Str., 38, 119991, Moscow, Russia
denisov@fo.gpi.ru

Currently, there is a continuing interest in continuous fiber lasers with a power of several kW [1,2]. This is due to the expanding fields of practical applications of lasers of this power range, including fundamental sciences, industrial materials processing, and medicine. At the same time, research is ongoing in the field of single-mode optical fibers with a large mode area, both active ones, which are the basis for high-power fiber lasers, and passive ones, necessary for transmitting laser radiation with the required beam parameters [2]. Various types of microstructured optical fibers (MOFs) can be used for these tasks, including fibers with a photonic band gap, Bragg fibers and leakage channel fibers (LCF). An important feature of MOF with leakage channels is the relative simplicity of their geometric structure, which allows the selection of its parameters quite easily to achieve single-mode guidence with a large mode area and at the same time provide low bending losses. At the same time, for use in high-power continuous fiber lasers, only all-glass MOFs can be used, the cladding of which is formed by elements from fluorine-doped silica glass with a reduced refractive index [3].

In the present work, the results of experimental studies of all-glass microstructured fibers containing two layers of elements from fluorine-doped silica glass with a reduced refractive index, different diameters and different distances between themselves are presented [4,5]. SEM image of the fabricated MOF is presented in Fig.1. Such a structure of the MOF provides ample opportunity to vary its various parameters in order to optimize the characteristics of the MOF, in particular, leakage losses for fundamental and higher order modes in both straight and bending states. Tests have shown that this MOF with a length of more than 5 m are single-mode. The measured loss of MOF with a 22.5 μm core for a bending radius of 0.1 m was less than 0.1 dB/m in the spectral range from 0.9 μm to 1.5 μm, while in the wavelength range from 1.0 μm to 1.1 μm these losses smoothly vary from 0.025 dB/m to 0.015 dB/m.

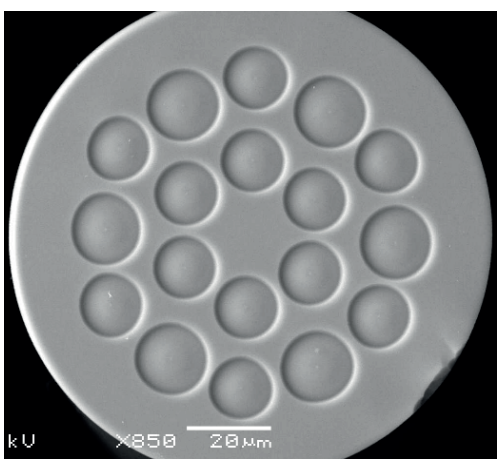

Fig.1. SEM image of the fabricated MOF.

This MOF may be of interest for applications such as the transmission of high-power laser radiation and for use in high-power fiber lasers and amplifiers.

This work was supported by the Ministry of Science and Higher Education of the Russian Federation (Grant No. 075-15-2020-912 for creation and development of the World-Class Research Center "Photonics Center").

[1] B. Pulford, R. Holten, T. Matniyaz, M.T. Kalichevsky-Dong, T.W. Hawkins, L. Dong, "kW-level monolithic single-mode narrow-linewidth all-solid photonic bandgap fiber amplifier", Opt. Lett. **46**, 4458–4461 (2021).
[2] J.W. Nicholson, A. DeSantolo, R.S. Windeler, E. Monberg, V. Lukonin, J. Pincha, A. Hariharan, X. Xu, G. Williams, Z. Goldberg, A. Rosales-Garcia, P. Kristensen, D. Knight, D.J. DiGiovanni, "Next generation Yb-doped fibers for high-power, narrow-linewidth lasers", Proc. SPIE **11981**, 119810R (2022).
[3] K. Saitoh, Y. Tsuchida, L. Rosa, M. Koshiba, F. Poli, A. Cucinotta, S. Selleri, M. Pal, M. Paul, D. Ghosh, S. Bhadra, "Design of all-solid leakage channel fibers with large mode area and low bending loss", Opt. Express **17**, 4913–4919 (2009).
[4] A.N. Denisov, S.L. Semjonov, "All-Glass Single-Mode Microstructured Fibers with a Large Mode Area", Dokl. Phys. **66**, 64–66 (2021).
[5] A.N. Denisov, S.L. Semjonov, "All-glass single-mode microstructured optical fibres with a large-diameter core and low bending losses", Quantum Electron. **51**, 1081–1089 (2021).

DOI: 10.24412/cl-35039-2022-22-149-149

Comparison of pulsed generation parameters in dumbbell-shaped and ring cavities of the Holmium-doped fiber laser

S.A. Filatova[1,*], V.A. Kamynin[1], Y.G. Gladush[2], E.M. Khabushev[2], D.V. Krasnikov[2], A.G. Nasibulin[2,3], V.B. Tsvetkov[1]

1 - Prokhorov General Physics Institute of the Russian Academy of Sciences, 38 Vavilov Str., 119991 Moscow, Russia
2 - Skolkovo Institute of Science and Technology, Nobel Str. 3, Moscow, 121205, Russia
3 - Aalto University, P.O. Box 16100, Aalto, FI-00076, Finland
**email address: filatova@kapella.gpi.ru*

Particular interest is observed in ultrashort pulsed lasers operating in the spectral range of 2 – 3.5 μm due to their many possible applications in spectroscopy, gas sensing, materials processing, laser surgery, biodiagnostics, and etc [1]. One of the promising active medium for such sources are Holmium-doped (Ho) fibers due to their broad gain spectrum of 2–2.2 μm. So in recent years, mode-locked Ho-doped fiber lasers have been intensively studied [2,3].

Most cavities of mode-locked fiber lasers contain expensive or complicated elements such as isolators, polarizers, beam splitters, circulators, etc. However for the further use of ultrashort pulsed lasers as a seed source or in complex hybrid systems, the laser scheme should be simplified and free of elements that can affect laser generation. Therefore, it is of interest to study a fiber laser with a simple dumbbell-shaped cavity [4,5]. This work is focused on comparison of the parameters and efficiency of ultrashort pulse generation in different types of cavities (dumbbell-shaped and ring) and on simplifying of Ho-doped fiber laser scheme.

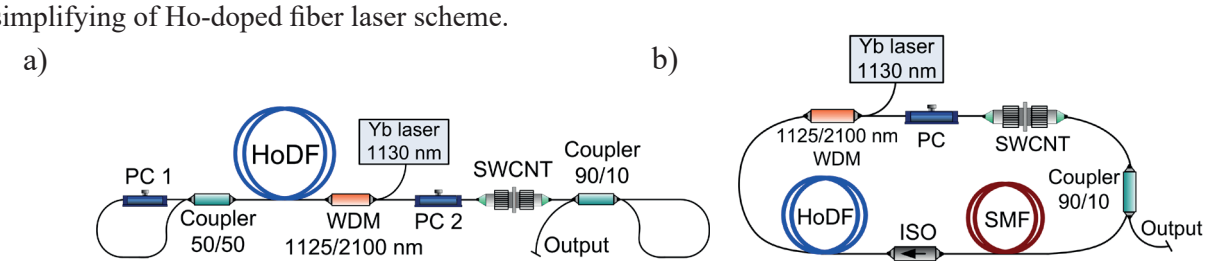

Fig. 1. Experimental setup of the mode-locked Ho-doped fiber laser with dumbbell-shaped cavity (a) and ring cavity (b).

The experimental setups of Ho-doped fiber laser with different cavities types are shown in Fig. 1. The laser cavities consist of a 2 m of Ho-doped fiber with counter-propagating pumping by a continuous-wave Yb-doped fiber laser at 1130 nm through a 1125/2100 nm wavelength division multiplexer (WDM), fiber couplers, polarization controllers (PC), FC/APC connectors with saturable absorber, single mode fiber (SMF), and isolator in the case of ring cavity. We have used single-walled carbon nanotubes (SWCNT) as saturable absorber for mode-locking implementation. The length of the dumbbell-shaped cavity was about 8.6 m what corresponded to the pulse repetition rate of about 12 MHz, and the length of the ring cavity was compensated by SMF to obtain the same repetition rate and was about 17.3 m.

The dumbbell-shaped cavity configuration, proposed in this work, allowed us to decrease the lasing threshold and increase the generation efficiency relative to the ring cavity of Ho-doped fiber laser. Besides simplifying the laser scheme, we achieved stability and repeatability of laser parameters (λc = 2076 nm, Pavg = 7 mW, τ = 1.3 ps, E = 0.6 nJ).

This work was carried out with the support of a grant from the President of the Russian Federation for young scientists-candidates of science MK-3465.2022.1.2.

[1] D.C. Kirsch, S. Chen, R. Sidharthan, Y. Chen, S. Yoo, M. Chernysheva, Short-wave IR ultrafast fiber laser systems: Current challenges and prospective applications, *Journal of Applied Physics*, **128(18)**, 180906 (2020).
[2] M. Pawliszewska, A. Dużyńska, M. Zdrojek, and J. Sotor, Metallic carbon nanotube-based saturable absorbers for holmium-doped fiber lasers, *Opt. exp.* **27(8)**, 11361-11369 (2019).
[3] S.A. Filatova, V.A. Kamynin, N.R. Arutyunyan, A.S. Pozharov, E.D. Obraztsova, P.A. Itrin, V.B. Tsvetkov, Comparison of mode-locking regimes in a holmium fibre laser, *Quantum Electronics*, ***48*(12)**, 1113 (2018).
[4] H. Chen, S.P. Chen, Z.F. Jiang, and J. Hou, 80 nJ ultrafast dissipative soliton generation in dumbbell-shaped mode-locked fiber laser, *Opt. Lett.* **41(18)**, 4210-4213 (2016).
[5] D. Majumder, S.D. Chowdhury, M. Pal, A. Dhar, and A. Pal, Passive Q-switch and Rectangular Mode-locked Pulses from a Dumbbell Shaped Holmium Fiber Laser, In The European Conference on Lasers and Electro-Optics (p. cj_p_11), (2019, June).

DOI: 10.24412/cl-35039-2022-22-150-150

New $Ca_3(VO_4)_2$:Cr crystal: synthesis, doping technique, optical properties

I.S. Voronina, E.E. Dunaeva, M.E. Doroshenko, L.I. Ivleva

Prokhorov General Physics Institute, RAS, 38 Vavilova str., Moscow 119991, Russia
ivleva@lst.gpi.ru

The calcium orthovanadate Ca3(VO4)2 (CVO) single crystals are considered as a laser host material with high optical damage threshold and nonlinear optical coefficients compared with KDP. They can be potentially useful for frequency conversion of tunable laser sources. In periodic scientific literature many papers are devoted to growth and investigations of CVO single crystals doped with RE and TM metal ions. CVO is multifunctional material whose properties are defined by disordered whitlokite-like acentric crystal structure. At present work CVO crystals doped with chromium ions were obtained for the first time and their spectroscopic parameters depending on crystallization conditions and doping technique were studied.

CVO crystals doped with chromium ions were obtained by two different doping techniques: growth from the melt by Czohralski method and high temperature diffusion technique. Cz-crystals were grown from the melt with adding Cr2O3 in concentration from 0.01 to 0.1 wt.% over stoichiometry, along [100] crystallographic direction, pulling rate was 6mm/h, rotation velocity - 30 rpm. CVO:Cr crystals (20x70mm) of optical quality suitable for preparing active elements were obtained.

Another CVO samples doped with chromium ions were fabricated by high-temperature diffusion doping. Nominally pure CVO plates prepared from the Cz-grown single crystal were used as an effective matrix for impurity ions diffusion from solid phase (Cr2O3 powder) to solid phase (CVO single crystal). The high-temperature diffusion conditions were optimized (temperature 1300 C, time 24 h) to obtain the doped crystals of optical quality using special annealing zone. In diffusion doped CVO crystals estimated Cr ions concentration of 0.12 at.% was 3.5 times higher in comparison with optically homogeneous Cz-CVO:Cr (0.035 at.% Cr, $2.5*10^{19}$ cm^{-3}). Some of Cz-grown CVO:Cr samples were annealed in the air at 1000 C during 6 h. In this case typical green coloration of Cr-doped crystals was varied to yellow one.

Green and yellow CVO:Cr samples were investigated by the methods of optical spectroscopy. In CVO:Cr crystals the presence of Cr^{3+}, Cr^{4+} and Cr^{5+} ions was detected. The position of absorption and fluorescence lines for chromium ions in all valence states seems not to differ much from that observed previously in forsterite crystal. At the same time lifetimes for chromium ions in all valence states (1.3 ms, 0.3 ms, 9 ms) were measured to be several times shorter than that in forsterite. Annealing of the $Ca_3(VO_4)_2$:Cr crystal in the air was observed to result in increase of chromium ions in 4+ valence state. Some Cr^{5+} to Cr^{3+} ions charge exchange process ($Cr^{5+}\rightarrow Cr^{4+}+e^-$; $Cr^{3+}+e^-\rightarrow Cr^{4+}$) resulting in formation of two Cr^{4+} ions is suggested to explain the decrease of both Cr^{5+} and Cr^{3+} ions concentration while annealing.

DOI: 10.24412/cl-35039-2022-22-151-151

Effect of isomorphic substitution in the cationic sublattice of langasite family crystals on their optical and electrophysical properties

N. Kozlova[1], E. Zabelina[1], O. Buzanov[2]

1 - National University of Science and Technology MISiS, Moscow, Russia
2 - FOMOS-Materials, Moscow, Russia
Kozlova_nina@mail.ru

Langasite family crystals are a group of crystals with a calcium-gallium germanate $Ca_3Ga_2Ge_4O_{14}$ structure, symmetry point group 32, first of all - lanthanum gallium silicate (langasite, LGS, $La_3Ga_5SiO_{14}$) and lanthanum gallium tantalate (langatate, LGT, $La_3Ga_{5,5}Ta_{0,5}O_{14}$). $Ca_3Ga_2Ge_4O_{14}$ structural type was first synthesized in the USSR in the 80th of XX century [1] during the scientific experimental search for new laser media. This structure type allows a wide isomorphic substitution of cations, which allows to be modify the properties of crystals for specific applications.

Langasite family crystals are grown by the Czochralski method from the Ir crucibles mostly in the atmosphere of Ar with addition of oxygen to suppress gallium oxide evaporation [3, 4]. Gallium oxide evaporation leads to the appearance of significant concentrations of gallium and oxygen vacancies, and contributes to the defect formation, especially to F-centers formation, which are observed in these crystals on spectral dependencies of transmission in the form of absorption bands in the region of ~ (480-490) nm, and results in yellow color [5]. The nature of the defect centers in langasite crystals has not yet been definitively determined. Defects in crystals influence electric conductivity and may be observed on the transmission spectra in the form of absorption bands.

Here we present the results of our research of the optical and electrophysical properties of the langasite family crystals with isomorphic substitution in the cationic sublattice.

Crystals with compositions $La_3Ga_{5,5}Ta_{0,5}O_{14}$; $La_3Ga_{5,5}Ta_{0,5}O_{14}$ doped with Ga_2O_3 in 2 different concentrations; $La_3Ga_{5,5}Ta_{0,5}O_{14}$ dopped with Al; crystals of intermediate composition $La_3Ga_5SiO_{14}$ -$La_3Ga_{5,5}Ta_{0,5}O_{14}$; $La_3Ga_5SiO_{14}$ were grown and samples were prepared at FOMOS-Materials.

Optical and electrophysical parameters of crystals were studied in the accredited testing laboratory «Single crystals and Stocke on their base» of NUST MISIS. Spectral dependences of the transmission of samples were obtained at t = 300 K on the UV-Vis-NIR spectrophotometer Cary-5000 (Agilent Technologies) in the wavelength range (200 – 800) nm. Temperature dependences of specific electrical conductivity (electrical resistance) were measured with an electrometer Keithley Instruments model 6517A.

[1] B.V. Mill, A.V. Butashin, G.G. Khodzhabagyan, E.A. Belokoneva, N.V. Belov, Modified rare-earth gallates with the structure $Ca_3Ga_2Ge_4O_{14}$, Reports of the Academy of Sciences of the USSR, 264 (1982) 1385 - 1389.
[2] B.V. Mill', Z.A. Kazei, D.M. Tsymbarenko Formation of Phases with the $Ca_3Ga_2Ge_4O_{14}$ Structure in Ln_2O_3–M_2O_3–GeO_2–BeO (Ln = La–Gd, M = Ga, Al, Fe, Cr) Systems, Russian Journal of Inorganic Chemistry, 63 (2018) 1283–1290
[3] O.A. Buzanov, A.V. Naumov, V.V. Nechaev, S.N. Knyazev 54 A new approach to the growth of langasite crystals, Proc. 1996 IEEE Int. Freq. Control Symp, (1996) 131-136.
[4] S. Uda, S.Q. Wang, N. Konishi, H. Inaba, J. Harada Growth habits of 3 and 4-inch langasite single crystals, Journal of Crystal Growth, 237-239 (2002) 707-713.
[5] E. Zabelina thesis «Inhomogeneities in lanthanum-gallium tantalate crystals and their influence on optical properties» (date of defense 31.05.2018, date of approval 12.12.2018), supervisor: Ph.D., senior researcher Kozlova N.S.

DOI: 10.24412/cl-35039-2022-22-152-152

Sensitivity limit of a chemical sensor based on porous silicon microresonator

V.I. Krasovskii, L.A. Apresyan, T.V. Vlasova, S.I. Rasmagin

Prokhorov General Physics Institute of the Russian Academy of Sciences,
38 Vavilova str., Moscow 119991, Russia
E-mail: krasovskii@inbox.ru

The use of porous silicon as an inorganic matrix for embedding organic materials combines the potential of organic and nanoelectronic devices with traditional silicon technology. Porous silicon is produced by electrochemical etching. The electrolyte composition and etching current determine the average pore size and morphology, degree of porosity, and pore surface condition.

Porous silicon has high specific surface area (~ 200 m2/cm3 or 500-800 m2/g) and can be used for chemical and biochemical sensors. A promising direction to create sensors of nitroaromatic compounds, acting on the principle of quenching the fluorescence of certain polymers embedded in a multilayered structure with a microcavity should be highlighted. These sensors use sorption of the analyte in the pores and have been shown to have a high sensitivity of 10^{-15} [1].

In this work, a microcavity structure similar to [1] was used, the starting material for the microresonators were p-type boron-doped silicon wafers with an orientation (100) with a conductivity of 0.01 Ohm cm in a 15% HF solution in ethanol. Low and high porosity layers were formed at current densities of 6 and 50 mA/cm^2 , respectively. The structure contained a layer of porous silicon with high porosity of optical thickness $\lambda/2$, located between two Bragg mirrors formed by a sequence of alternating layers of high and low porosity. The first Bragg mirror consisted of 5 periods, and the second one consisted of 20 periods; each period contained two layers of optical thickness $\lambda/4$, with high and low porosity. By selecting the appropriate layer thicknesses, the resonance in the reflection spectrum was tuned to the desired wavelength.

The transfer matrix formalism was used to calculate the structure [2]. The wavelength was varied between 300 and 900 nm. The parameter values were obtained from the results of electron microscopic studies and were close to the real ones.

The signal of the chemical sensor was determined in two ways: as a diffrent reflectance spectrum or as a ratio of the reflectance spectra before or after exposure to the analyte. The sensitivity of the chemical sensor was calculated numerically and analytically using the effective medium approximation [3] to account for the volume fraction of the sensitive component in the microcavity structure, taking into account technological limitations. Calculations were performed using phthalocyanine and phthalocyanine-gold complexes as an sensitive media [4]. It was shown that the sensitivity growth can reach several orders of magnitude compared to film-based sensors.

[1]. I.Levitsky, Fluorescent polymer-porous silicon microcavity devices for explosive detection Appl. Phys. Lett. 90, 041904, (2007);
[2]. McLeod, Thin film optical filters, Adam Hilger Ltd., Bristol.
[3].L.Apresyan, T.V. Vlasova., V.I. Krasovskii et al., Effective medium approximations for the description of multicomponent composites, Technical Physics. 65 (7), 1130-1138, (2020).
[4].D.MKrichevsky, A.Tolbin, T.Dubinina et al., Resonant plasmon-enhanced absorption of charge transfer complexes in a metal–organic monolayer, Advanced Optical Materials, 9 (1), 2100065, (2021).

DOI: 10.24412/cl-35039-2022-22-153-153

Er:Y_2O_3 optical ceramics as a gain medium for in-band pumped 1.6 μm lasers: synthesis and spectroscopic properties

K.N. Gorbachenya[1], A.S. Yasukevich[1], V.E. Kisel[1], A.I. Lazarchuk[1], A.A. Tarachenko[1], K.V. Lopuhin[2], V.V. Balashov[2], A.V. Fedin[3], M.N. Gerke[3], E.A. Volkova[4], V.O. Yapaskurt[4], N.N. Kuzmin[4,5,6], D.A. Ksenofontov[4], D.V. Korost[4], N.V. Kuleshov[1]

1- Center for optical materials and technologies, Belarusian National Technical University, Belarus, Minsk, Nezalezhnasti ave., 65;
2- Fryazino branch of the Institution of Science V.A. Kotelnikov Institute of Radio Engineering and Electronics Russian Academy of Sciences, Vvedenskogo ave. 1, Fryazino, Russia;
3- Vladimir State University named after Alexander and Nikolay Stoletov; Gorky str. 87, Vladimir, Russia;
4- Department of Crystallography and Crystal Chemistry, Moscow State University, Moscow, Russia;
5- Institute of Spectroscopy, RAS, 108840, Fizicheskaya Str. 5 Troitsk, Moscow, Russia; kolyanfclm@gmail.com
6- Moscow Institute of Physics and Technology, 9 Institutskiy per., Dolgoprudny, Moscow Region, Russia
nkuleshov@bntu.by

In-band pumping at near 1.5 μm (direct excitation of the Er^{3+} ions to the upper laser energy level $^4I_{13/2}$) is a promising means of developing erbium lasers emitting at neat 1.6 μm. Recenly Er:Re_2O_3 (Re=Y, Sc, Lu) sesquioxide crystals have been considered as promising gain media for in-band-pumped erbium lasers [1]. However, the growth complexity is a major limitation for the application of sesqui-oxide crystals. One solution is to use optical ceramics based on these crystals. Here we present the details of Er:Y_2O_3 optical ceramics synthesis and investigation of structural and spectral-luminescent properties.

Er (0.25 mol.%):Y_2O_3 samples of transparent ceramics with a high optical quality (transmission coefficient more than 99% at 600 nm), diameter > 20 mm, and thickness >3 mm were produced (Figure 1). The microstructure and elemental analysis were performed by the analytical scanning electron microscopy (SEM) technique. Phase purity and structure were confirmed using XRD method. XRCT scanning demonstrates that synthesized ceramics specimens are characterized by homogeneous microstructure without any associated phases. The absorption and emission cross-section spectra of the Er^{3+}:Y_2O_3 optical ceramics in the spectral range 1420–1700 nm are presented in Figure 2. The maximal absorption cross-section of 1.28×10^{-20} cm^2 is observed at 1536 nm. The highest magnitude of the stimulated emission cross-section of 1.16×10^{-20} cm^2 is located at 1535 nm. The decay curve of 1.6 μm emission was single exponential and the luminescence decay time of the $^4I_{13/2}$ level was measured to be 7.5 +/- 0.5 ms. In the frame of the conventional Judd-Ofelt theory the emission properties of the $^4I_{13/2}$ and $^4I_{11/2}$ energy levels of Er^{3+} were calculated. The gain coefficient curves are demonstated in the Figure 3.

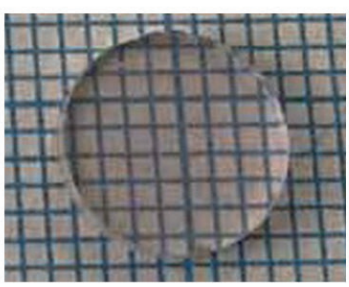

Fig. 1. Er^{3+}:Y_2O_3 optical ceramics

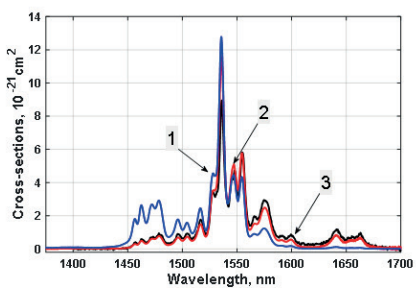

Fig. 2. Absorption (1) and emission (2, 3) cross-section spectra: 2 — IRM; 3 — FLE.

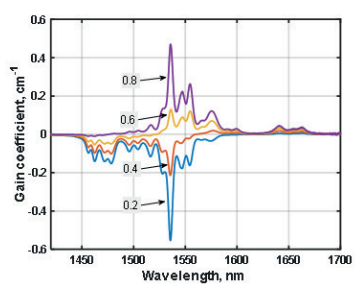

Fig. 3. Gain spectra for inversion parameters β=0.2-0.8

The Er:Y_2O_3 ceramics with high optical quality was fabricated. The obtained spectroscopic characteristics indicate the promise of the use of Er:Y_2O_3 optical ceramics as an active medium for eye-safe in-band-pumped lasers emitting near 1.6 μm.

[1] Merkle, L.D.; Ter-Gabrielyan, N.; Kacik, N.J.; Sanamyan, T.; Zhang, H.; Y, H.; Wang, J.; Dubinskii, M. Er:Lu2O3—laser-related spectroscopy. Opt. Mater. Express 2013, 3, 1992–2002.

DOI: 10.24412/cl-35039-2022-22-154-154

Magneto-optical and structural properties of ultrafine-grained Tb_2O_3 transparent ceramics

R.N. Maksimov[1,2,*], V.V. Osipov[1], G.R. Karagedov[3], V.V. Platonov[1], A.N. Orlov[1], A.V. Spirina[1], A.S. Yurovskikh[2], V.A. Shitov[1]

[1]Institute of Electrophysics UrB RAS, 106 Amundsen St., Ekaterinburg 620016, Russia
[2]Ural Federal University named after the first President of Russia B.N. Yeltsin, 19 Mira St., Ekaterinburg 620002, Russia
[3]Institute of Solid State Chemistry and Mechanochemistry SB RAS, 18 Kutateladze St., Novosibirsk 630128, Russia
**email: romanmaksimov@e1.ru*

Recently, ceramic materials based on terbium sesquioxide (Tb_2O_3) have attracted considerable interest as promising magnetically active media for Faraday isolators used in high-power solid-state lasers owing to their extremely high Verdet constant (up to 154 rad·T^{-1}·m^{-1} at 1064 nm) [1,2]. Transparent polycrystalline Tb_2O_3 ceramics offer several important advantages over their single-crystalline counterparts including enhanced optical quality and feasibility for large aperture samples [3].

Manufacturing of high performance ceramic elements is complicated by the reversible phase transformation of Tb_2O_3 from the cubic to the monoclinic structure above 1500°C causing fracture of sintered material. Consequently, special additives such as Y_2O_3 stabilizing the cubic modification and/or grain growth inhibitor (ZrO_2) are used to prevent phase conversion and for achieving a pore-free microstructure. However, the thermal conductivity and Verdet constant of $(Tb_xY_{1-x})_2O_3$ solid solutions are inferior to those of "pure" Tb_2O_3 [3]. Tetravalent Zr doping could lead to unwanted absorption near 1 μm and thus one of the current trends in the manufacture of sesquioxide ceramics for advanced laser applications is avoiding any kind of foreign impurities [4,5].

In this work, Tb_2O_3 nanoparticles with an average size of 13 nm produced by laser ablation of solid target in air flow were used to fabricate transparent ceramics without sintering additives by a combination of pressureless densification and hot isostatic press (HIP) treatment. The as-synthesized nanopowder was uniaxially dry-pressed at 50 MPa into cylindrical compacts of 14 mm diameter and then subjected to vacuum sintering for 1–2 h at 1300–1450°C followed by HIPing for 2 h at 1450°C under an Ar gas pressure of 200 MPa. The crystal structure of the obtained Tb_2O_3 ceramics was studied using XRD and lattice vibrational modes were analyzed by Raman and FTIR reflection spectroscopy to confirm the phase purity. According to SEM observations, the samples exhibited an ultrafine-grained and dense microstructure consisting of polyhedral-shaped crystallites of less than 1 μm in size. The distribution of scattering centers throughout the depth of the samples was obtained using an optical microscope and its correlation with transmission spectra registered over the wavelength range 200–1100 nm was investigated. The Verdet constant of the fabricated Tb_2O_3 ceramics was measured at 632.8 nm and 1064 nm using He–Ne and Nd:YAG lasers, respectively. For instance, the Verdet constant at 632.8 nm was evaluated to be at least 478 rad·T^{-1}·m^{-1}, which is comparable to that of high purity Tb_2O_3 single-crystal grown by the flux method (476 rad·T^{-1}·m^{-1}) [6]. Thus, the highly sinterable nanopowders produced by laser ablation could be promising for the fabrication of transparent Tb_2O_3 ceramics without sintering additives.

The reported study was carried out with the use of grant № 22-23-00658 of the Russian Science Foundation, https://rscf.ru/en/project/22-23-00658/

[1] J. Dai and J. Li, Promising magneto-optical ceramics for high power Faraday isolators, Scripta Materialia, vol. 155, pp. 78–84, (2018).
[2] D. Vojna, O. Slezak, A. Lucianetti, T. Mocek, Constant of magneto-active materials developed for high-power Faraday devices, Applied Sciences, vol. 9, p. 3160, (2019).
[3] A. Ikesue, Y.L. Aung, S. Makikawa, A. Yahagi, Total performance of magneto-optical ceramics with a bixbyite structure, Materials, vol. 12, p. 421, (2019).
[4] D. Yin, J. Ma, P. Liu, B. Yao, J. Wang, Z. Dong, L.B. Kong, D. Tang, Submicron-grained Yb:Lu_2O_3 transparent ceramics with lasing quality, Journal of the American Ceramic Society, vol. 102, pp. 2587–2592, (2019).
[5] Q. Li, J. Wang, J. Ma, M. Ni, F. Yang, P. Liu, K.Y. Lee, H.-I. Hsiang, D. Shen, D. Tang, Fabrication of high-efficiency Yb:Y_2O_3 laser ceramics without photodarkening, Journal of the American Ceramic Society, vol. 105, pp. 3375–3381, (2022).
[6] P. Veber, M. Velazquez, G. Gadret, D. Rytz, M. Peltzc, R. Decourta, Flux growth at 1230 °C of cubic Tb_2O_3 single crystals and characterization of their optical and magnetic properties, CrystEngComm, vol. 17, pp. 492–497, (2014).

DOI: 10.24412/cl-35039-2022-22-155-155

Promising materials for optoelectronics - $CdGa_2Se_4$: Theoretical calculations and experimental studies of electronic properties

I.A. Mamedova[1], Z.A. Jahangirli[1,2], E.H. Alizade[1], T.G. Kerimova[1], T.G. Mammadov[1], N.A. Abdullayev[1,2]*

1-Institute of Physics of NAS of Azerbaijan, ave.H.Javid, 131, AZ1143, Baku, Azerbaijan
2-Baku State University, st.Z. Khalilov, 33, AZ-1148, Baku, Azerbaijan
e-mail address: abnadir@mail.ru

$CdGa_2Se_4$ single crystals crystallize in a tetragonal structure in space symmetry group $I\bar{4}$. These compounds are characterized by birefringence, significant values of the coefficient of nonlinear susceptibility, and bright photoluminescence, which puts these compounds forward among the promising materials for optoelectronics.

The electronic band structure and projected onto atoms partial densities of states (PDOS) are theoretically calculated from first principles using density functional theory (DFT). An analysis of the partial density of states shows that the group of valence bands in the energy range from approximately –6.5 eV to 0 eV originates from the s states of Ga1 and Ga2, as well as the p states of the chalcogen Se atoms. It also follows from the partial density of states that the bottom of the conduction band is formed mainly from the s states of the Ga1 and Ga2 atoms with some addition of the p states of the Se atom. According to the calculated electronic band structure, the top of the valence band and the absolute minimum of the conduction band are at the Γ point of the Brillouin zone and, accordingly, according to our calculations, $CdGa_2Se_4$ is a direct-gap semiconductor with a band gap of ~ 2.5 eV.

Since spectral ellipsometry is one of the accurate methods for determining the optical characteristics of crystals, we carried out spectral ellipsometric studies of $CdGa_2Se_4$ single crystals. These measurements are based on determining the change of polarization state of light as a result of its interaction with the surface of crystals upon reflection. The measurements were carried out on an optical range ellipsometer M-2000 DI (J.A. Woollam Co, Inc.). The spectral dependence of the ellipsometric parameters Δ and Ψ was measured in the photon energy range of 0.7–6.5 eV with a step of 50 meV at radiation incidence angles in the range of 60°–75° with a step of 5°.

A comparison is made between the ab initio calculations in the 0–14 eV spectral range and the experimentally measured the real and imaginary parts of the dielectric function, coefficients of refraction, extinction, and absorption of $CdGa_2Se_4$ for different polarizations of the incident light (along and perpendicular to the tetragonal c axis). A good agreement is observed between the characteristic critical points at energies of approximately 2.4 and 4 eV.

It was found that the spectral dependence of the absorption coefficient α is well approximated by the dependence $\alpha h\nu \sim (Eg-h\nu)^{1/2}$, for direct allowed optical transitions. This is also evidenced by the high values of the absorption coefficient α (10^4-10^5 cm^{-1}), its sharp increase in the energy range of 2-3.5 eV.

The work was supported financially by the Science Development Foundation under the President of the Republic of Azerbaijan (grant no. EIF-BGM-3-BRFTF-2+/2017-15/02/1).

DOI: 10.24412/cl-35039-2022-22-156-156

Growth of nanocrystalline CVD diamond films doped with germanium

A. Martyanov, V. Sedov, I. Tiazhelov

Prokhorov General Physics Institute of the Russian Academy of Sciences, Moscow
Main author email address: art.martyanov@gmail.com

Color centers in diamond have unique spectral characteristics: high brightness and stability at room temperature, quantum efficiency, short photoluminescence (PL) decay times, and narrow PL lines, which are which are in demand for nanophotonics and quantum optics [1]. Nitrogen-vacancy (NV) and silicon-vacancy (SiV) color centers are the most actively studied. Germanium-vacancy (GeV) color centers in diamond (discovered in 2015) are less studied. They have a narrow zero-phonon line in the photoluminescence spectra at $\lambda = 602$ nm [2].

In this work, polycrystalline diamond films were doped with nitrogen and germanium at the same time. Diamond films were deposited in the microwave plasma CVD system ARDIS-100 (2.45 GHz). Polished single-crystal silicon wafers were seeded in a water-based slurry of detonation nanodiamond with an average particle size of 5 nm. Diamond was deposited under the following parameters: gas mixture pressure 100 Torr, microwave power 5 kW, substrate temperature 850°C. The film thickness was controlled *in-situ* with a laser interferometer technique. For correct comparison of the films obtained at different process parameters, their thickness was kept always the same 2 μm.

Even small additions of nitrogen to the reactor during CVD diamond synthesis stimulate the secondary nucleation of diamond and lead to the formation of nanocrystalline films (NCD) instead of standard microcrystalline (MCD) (fig.1). Therefore, an alternative method of stimulating secondary nucleation was also used: increasing the methane concentration (up to 20%) [3].

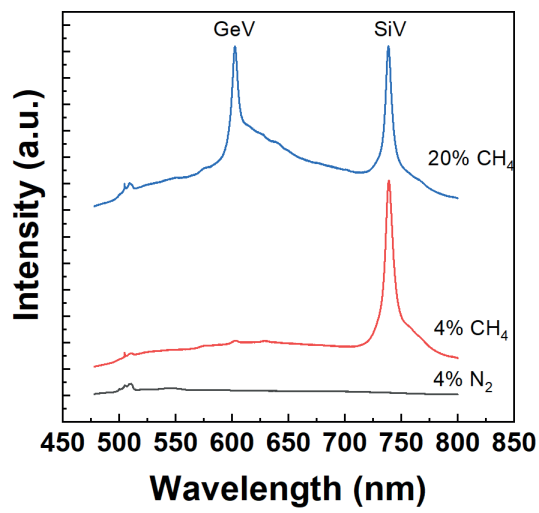

Fig. 1. Photoluminescence spectra of polycrystalline diamond films doped with germanium: MCD at 4% CH_4; NCD with nitrogen addition or with increased methane concentration up to 20%.

It was found that a change in the structure of diamond with an increase in methane concentration leads to a 50-fold increase in the intensity of GeV centers. At the same time, a change in the structure of diamond with the addition of nitrogen or air completely quenches the photoluminescence of GeV and SiV.

The work was supported by the Russian Science Foundation, Grant No. 21-72-10153.

[1] I. Aharonovich. E. Neu, Diamond nanophotonics, Advanced Optical Materials, vol. 2, pp. 911-928, (2014).
[2] V. Sedov, et. al., Growth of polycrystalline and single-crystal CVD diamonds with bright photoluminescence of Ge-V color centers using germane GeH_4 as the dopant source, Diamond and Related Materials, vol. 90, pp. 47-53, (2018).
[3] V. Sedov, et. al., Deposition of diamond films on Si by microwave plasma CVD in varied CH_4-H_2 mixtures: Reverse nanocrystalline-to-microcrystalline structure transition at very high methane concentrations, Diamond and Related Materials, vol. 109, p. 108072, (2020).

DOI: 10.24412/cl-35039-2022-22-157-157

Photoluminescence of SrF_2:Eu powders after annealing in CH_4/H_2 microwave plasma

I. Tiazhelov[1], A. Martyanov[1], V. Sedov[1], K. Boldyrev[2], A. Drobysheva[1], Yu. Ermakova[1], A. Alexandrov[1], V. Voronov[1], S. Kuznetsov[1]

1- Prokhorov General Physics Institute of the Russian Academy of Sciences, Moscow
2- Institute of Spectroscopy of the Russian Academy of Sciences, Troitsk, Moscow
Main author email address: tiazhelov@rambler.ru

In the last decade, high-power X-ray sources have been developed: synchrotrons and XFEL-lasers [1]. Materials used for visualization of intense radiation (for example, LiF) degrade rapidly due to the low thermal conductivity (~4 W/(m*K) at ambient conditions), weak heat dissipation and sharp local heating occur [2].

Radiation-resistant materials for use in X-ray imaging devices must have (i) high thermal conductivity, (ii) intense X-ray luminescence, (iii) chemical stability. Diamond has record-breaking physical and chemical properties such as the highest thermal conductivity among bulk materials (~2100 W/(m*K) at ambient conditions), transparent in wide spectral range, X-ray resistant, and chemically inert. Europium ions embedded in the crystal lattice of some compounds are capable of causing intense luminescence, and the wavelength of the emitted light depends on the degree of oxidation of the europium ions and symmetry of optical center. Previously, in our paper [3], it was shown that diamond-matrix composites with embedded rare-earth particles can exhibit bright X-ray luminescence in the visible range.

In this work, we studied the impact effect of microwave plasma on the optical properties of SrF_2:Eu powders. SrF_2:Eu nanopowders were obtained by precipitation from aqueous solutions followed by heat treatment at a temperature of 600°C. A series of powder on substrates (100) of oriented single-crystal silicon was annealing in methane-hydrogen plasma at a temperature of 880°C for 2, 6, 10, and 30 min and in pure hydrogen plasma at a temperature of 840°C for 10 min. Exposure to any plasma for even 2 minutes changes the photoluminescence spectrum of the samples (Fig. 1).

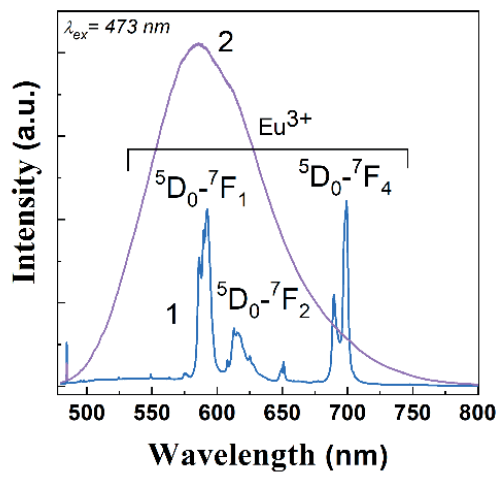

Fig. 1. Typical photoluminescence spectra before (1) and after (2) annealing of samples in plasma upon excitation at a wavelength of 473 nm.

As a result, it was found that the action of methane-hydrogen plasma on SrF_2:Eu powders leads to a radically change in the photoluminescence spectrum: instead of a set of narrow lines, broadband photoluminescence is observed in the range of 480–750 nm with a maximum at about 580 nm. A change in the luminescence spectrum may arise from set of reasons such as partially reduction of Eu^{3+} to Eu^{2+} or occurrence of defects on the particles surface.

The work was supported by the Russian Science Foundation, Grant No. 22-13-00401.

[1] T. Pikuz. et. al., 3D visualization of XFEL beam focusing properties using LiF crystal X-ray detector, Scientific Reports, vol. 5, pp. 1-10, (2015).
[2] T. Kurobori, et. al., A comparative study of optical and radiative characteristics of X-ray-induced luminescent defects in Ag-doped glass and LiF thin films and their applications in 2-D imaging, Nuclear Instruments and Methods in Physics Research, vol. 326, pp. 76-80, (2014).
[3] S. Kuznetsov, et. al., Cerium-doped gadolinium-scandium-aluminum garnet powders: Synthesis and use in X-ray luminescent diamond composites, Ceramics International, vol. 48, pp. 12962-12970, (2022).

DOI: 10.24412/cl-35039-2022-22-158-158

Influence of Sc on luminescence properties of GAGG:Ce scintillator

D. Spassky[1], O. Buzanov[2], N. Kozlova[3], V. Kasimova[3], E. Zabelina[3]

1 - Skobeltsyn Institute of Nuclear Physics, Moscow State University, Moscow, Russia
2 - FOMOS-Materials, Moscow, Russia
3 - National University of Science and Technology MISiS, Moscow, Russia
zabelina.ev@misis.ru

$Gd_3Al_2Ga_3O_{12}:Ce^{3+}$ (CAGG:Ce) is a high-density and chemically stable compound with scintillation yield up to 60000 ph/MeV, which is promising for application as a scintillator in medicine (SPECT, PET) and high-energy physics [1]. The main disadvantage of this crystal is the presence of slow decay components. Along with the typical for the 5d-4d Ce^{3+} emission decay component ~60 ns additional slow components with $\tau > 200$ ns appear in the scintillation response, which deteriorate the scintillation performance [2]. The presence of slow decay components is related to the energy migration via the Gd sublattice as well as to intermediate localization of charge carriers at traps.

The method of bandgap engineering allows fine tailoring of physical properties by gradual change of crystal composition [3]. Previously it was shown by us that partial substitution of Al and Ga cations by Sc in GAGG:Ce crystals considerably change the conduction band structure in garnets due to the contributions of the electronic states of Sc [4]. For that reason, the modification of cation composition by partial substitution of the Al and Ga cations with Sc is expected to influence the relaxation of high-energy excitations and energy transfer to Ce^{3+} emission centers in GAGG:Ce crystals. Here we present the study of the influence of Sc on luminescence properties of GAGG:Ce. The modification of luminescence decay curves will be in the focus of the study.

The influence of Sc on the electronic band structure of GAGG:Ce and the energy of the 4f and 5d Ce^{3+} levels is shown. It is shown that the modification of the band structure induced by the Sc electronic states results in the suppression of Gd emission and enhancement of Ce^{3+} emission at low temperatures. The influence of Sc incorporation into GAGG:Ce crystal on decay kinetics of Ce^{3+} emission was studied under excitation in the region of intranceter Ce^{3+} and Gd^{3+} excitation as well as in the region of direct exciton formation, Sc – related excitation band and at high-energy excitation. It is shown that Sc accelerates energy transfer to Ce^{3+} emission centers. The origin of the observed effects is discussed in the presentation.

Financial support from the grant RFBR 20-02-00688 is gratefully acknowledged.

[1] P. Lecoq, Development of new scintillators for medical applications, Nucl. Instrum. Meth. A, 809 (2016) 130–139.
[2] K. Kamada, M. Nikl, Sh. Kurosawa, A. Beitlerova, A. Nagura, Y. Shoji, J. Pejchal, Y. Ohashi, Y. Yokota, A. Yoshikawa, Alkali earth co-doping effects on luminescence and scintillation properties of Ce doped $Gd_3Al_2Ga_3O_{12}$ scintillator, Opt. Mater., 41 (2015) 63-66.
[3] M. Nikl and A. Yoshikawa, Recent R&D Trends in Inorganic Single-Crystal Scintillator Materials for Radiation Detection, Adv. Opt. Mater., 3 (2015) 463–481.
[4] D. Spassky, N. Kozlova, E. Zabelina, V. Kasimova, N. Krutyak, A. Ukhanova, V.A. Morozov, A. V. Morozov, O. Buzanov, K. Chernenko, S. Omelkov, V. Nagirnyi, Influence of Sc cation substituent on structural properties and energy transfer processes in GAGG:Ce crystals, CrystEngComm 22, 2621 – 2631 (2020).

DOI: 10.24412/cl-35039-2022-22-159-159

Chalcogenide Film Electrical and Optical Properties Modification by 1064 nm Laser Irradiation

A.A. Olhova, A.A. Patrikeeva, I.G. Zaytsev, M.M. Sergeev

ITMO University, St. Petersburg, 197101, Russian Federation
Main author email address: lazareva.a.a@mail.ru

The pulsed laser influence on the optical properties and PbSe films structure modification was investigated.

In recent years, the issue of preserving the environment from harmful emissions into the atmosphere from the production of the oil and gas, coal and chemical industries has been increasingly raised. For effective space sensing and environmental protection, various gas analyzers and sensors capable of capturing the content of harmful substances in the air are in demand. Chalcogenide films are excellent gas detectors because they have high absorption in the IR range, where gas molecules have absorption peaks. There are many ways to increase the photosensitivity of such films: heat treatment, alloying, etc., however, one of the affordable and low-cost methods is laser modification of their structure.

The result of laser influence on PbSe films at a moving spot of pulsed radiation with a 1064 nm wavelength was studied. The laser processing of these films in the scanning regime led to the formation of a track in the case of structure photodarkening and photobleaching (Fig. 1). The spectral reflection in these regimes differ insignificantly from each other and tend to black body, however, they have a strong difference from the original PbSe film and are close in position to the film after heat treatment.

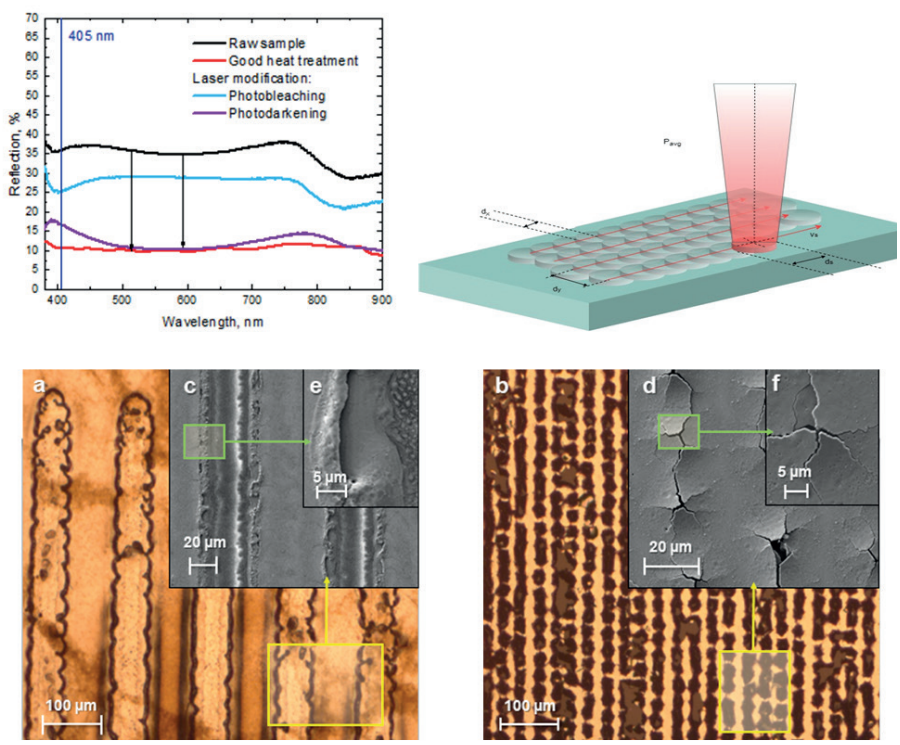

Fig. 1. Reflectance spectra and SEM images obtained from samples subjected to various treatments

Thus, the possibility of controlling the optical and structural characteristics of lead selenide films by means of pulsed laser radiation was demonstrated. Laser processing of this material can be used in the application of gas analysis, since chalcogenide films have a high absorption capacity in the mid-IR range (1–4 μm), as well as in the creation of substrates for microanalytical studies of various liquids.

DOI: 10.24412/cl-35039-2022-22-160-160

Quasi-CW lasing performance of Yb:YSAG ceramics

V. Zhmykhov[1], D. Guryev[1], V.S. Tsvetkov[1], E. Dobretsova[1], S. Kuznetsov[1], M. Nikova[2], I. Chikulina[2], D. Vakalov[2], V. Tarala[2] and V.B. Tsvetkov[1]

1- Prokhorov General Physics Institute of the Russian Academy of Sciences
2-North Caucasus Federal University, Scientific and Laboratory Complex Clean Room, Stavropol, Russia
Vadimzhmykhov56@gmail.com

Optical transparent ceramics have been widely considered as promising substitute for single crystal laser gain media of the next generation [1]. This substitution becomes possible due to their remarkable advantages, such as high doping concentration, low cost [2], high-dopant homogeneity, easy fabrication of large sample, and realizability of multilayer structure [3]. As one of potential candidates for high-power laser materials, Yb:YSAG ceramics have always gained much attention because of the superior physical properties of Yb ions, e.g. the broad absorption and emission bands, long lifetime, low defect density, no excited state absorption or up-conversion loss and wide range of tunability [4-7].

In this work we demonstrate quasi-CW lasing performance of 10 at. % Yb:YSAG ceramics. The ceramic sample had a thickness of 1 mm and no antireflective coatings. We used a cavity with a length of 2 cm formed by two spherical mirrors. Such cavity provided optimal overlap of the pumping and lasing areas. The ceramics were pumped at a wavelength of 938 nm. The size of the pump spot in the active element was approximately 100 μm. Laser operation was obtained with the quasi-CW pump. The laser performance was studied with different output couplers (Fig. 1 (a)). The maximum output power was 1 W at absorbed pump power of 2.4 W. Laser was operating in TEM_{00} transverse mode. The best slope efficiency was 49.7% with an output mirror transmittance of 14.5%.

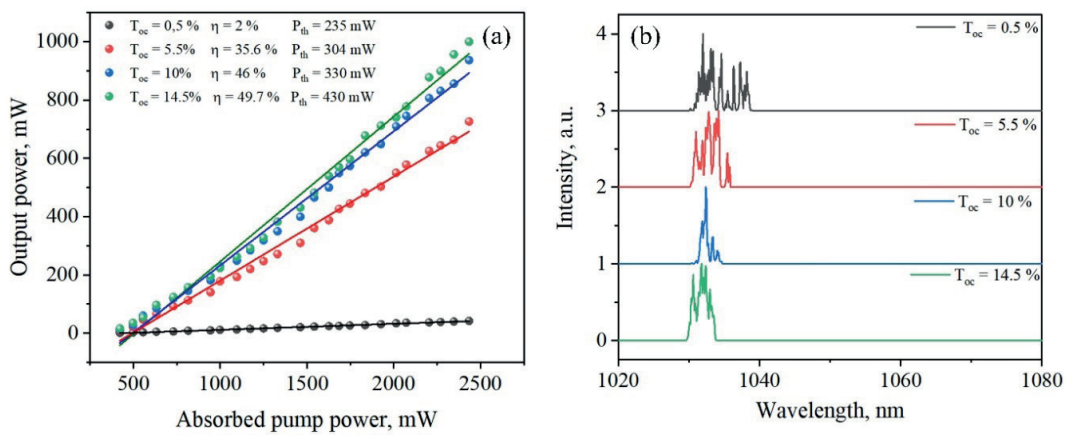

Fig. 1. (a) Quasi-CW performance of the Yb:YSAG laser; (b) typical laser emission spectra measured at absorbed pump power of 2.4 W.

The spectral characteristics of laser radiation were also studied at different output couplers (Fig. 1 (b)). The lasing spectrum depends on the output mirror type insignificantly. Also, to obtain the best result, it is possible to use antireflection coatings on the sample on both sides. In future investigations we will assess the impact of the composition (in particular the ratio between Al and Sc) on the spectroscopic properties of the Yb^{3+} and on the overall laser performance of this material, in order to get additional improvements and information.

This work was supported by the Grant of the President of the Russian Federation, grant №MK-72.2022.1.2

[1] D. Kracht, M. Frede, R. Wilhelm, and C. Fallnich, "Comparison of Crystalline and Ceramic Composite Nd:YAG for High Power Diode End-Pumping," Opt. Express, 13., 6212–6216 (2005).
[2] A. Ikesue, T. Kinoshita, K. Kamata, and K. Yoshida, "Fabrication and Optical Properties of High-Performance Polycrystalline Nd:YAG Ceramics for Solid-State Lasers," J. Am. Ceram. Soc., 78., 1033–1040 (1995).
[3] J. Lu, M. Prabhu, J. Song, C. Li, J. Xu, K. Ueda, A. A. Kaminskii, H. Yagi, and T. Yanagitani, "Optical Properties and Highly Efficient Laser Oscil- lation of Nd:YAG Ceramics," Appl. Phys. B, 71., 469–473 (2000).
[4] F. Tang, Y.G. Cao, J.Q. Huang, H.G. Liu, W. Guo and W.C. Wang, "Comparative investigation on Yb:YAG and Yb:LuAG transparent laser ceramics" J. Am. Ceram. Soc. 95., 56–59 (2012).
[5] F. Tang, Y.G. Cao, J.Q. Huang, W. Guo, H.G. Liu, Q.F. Huang, W.C. Wang, "Diode-pumped tape casting planar waveguide YAG/Nd:YAG/YAG ceramic laser" J. Eur.Ceram. Soc. 32., 3995–4002, (2012).
[6] H. Chu, S.Z. Zhao, K.J. Yang, Y.F. Li, D.C. Li, G.Q. Li, J. Zhao, W.C. Qiao, X.D. Xu, J.Q. Di, L.H. Zheng and J. Xu, "Composite Yb:YAG/Cr^{4+}:YAG/YAG crystal passively Q-switched lasers at 1030 nm" Opt. Laser Tech. 56., 398–403 (2014).

ALT'22

LASER DIAGNOSTICS AND SPECTROSCOPY

DOI: 10.24412/cl-35039-2022-22-162-162

Time-Resolved Electron Diffraction Studies of Laser-Induced Processes in Thin Films

S.A. Aseyev[1], A.A. Ischenko[2], I.V. Kochikov[3], B.N. Mironov[1], E.A. Ryabov[1]

1- Institute of Spectroscopy, Russian Academy of Sciences, Fizicheskaya st. 5, 108840 Moscow, Troitsk, Russia
2- RTU-MIREA - Russian Technological University, M. V. Lomonosov Institute of Fine Chemical Technologies Vernadskii av. 86, 119571 Moscow, Russia
3- Faculty of Physics, Moscow State University, 119234, Moscow, Russia
e-mail: Aseyev<isanfemto@yandex.ru>, Ryabov <ryabov@isan.troitsk.ru>

Using a compact diffractometer that was equipped with a pulsed electron source synchronized with a femtosecond laser, a series of studies of laser-stimulated processes in thin-film samples has been performed. It has been revealed that graphene on a copper grid placed in vacuum and exposed to the action of powerful laser radiation experiences an irreversible structural modification, which is accompanied by the breaking of carbon bonds and formation of new products. Reversible processes of the optical excitation of the crystal lattice in antimony and bismuth thin films have been investigated by ultrafast electron diffraction with a femtosecond time resolution. In a strong laser field, the generaton of coherent optical phonons has been found and their spectra has been measured.

The work is supported in part by RFBR grant № 20-02-00146a

DOI: 10.24412/cl-35039-2022-22-163-163

Nonlinear Polarization Rotation of Laser Radiation in Isotropic Media

S. Bakhramov, A. Kokhkharov, U. Makhmanov

Institute of Ion-Plasma and Laser Technologies named after U.A. Arifov,
Uzbekistan Academy Sciences, Tashkent, Uzbekistan
Main author email address: bahramov@mail.ru

This work discusses the nonlinear rotation of the polarization of laser radiation during propagation in atomic (alkali metal vapors - potassium, rubidium) and molecular (solutions of C_{70} fullerene) media. The observed self-induced optical anisotropy in atomic media is associated with the resonant nature of the nonlinear susceptibility and the finite degree of ellipticity of real laser radiation. The maximum values in the frequency dependence of the nonlinear rotation of the polarization of laser radiation were observed in the vicinity of resonant transitions.

Correlations between the processes of nonlinear rotation of the polarization ellipse of laser radiation passing through a solution of fullerenes and the synthesis of C_{70} fullerene nanoclusters are experimentally established. The experimental setup, the registration system, and the technique for measuring the nonlinear rotation of the polarization of laser radiation are given in [1].

Using the dynamic light scattering method on a ZetasizerNano ZEN3600 (Malvern Instruments Ltd.), the distribution of C_{70} fullerene nanoclusters over the hydrodynamic diameter and the formation of large stable nanoclusters were determined. It was found that a slight increase in the concentration of a fullerene solution is accompanied by an increase in the average diameter and the number of synthesized fullerene nanoclusters in solutions. For direct structural and dimensional studies of the kinetics of the formation of nuclei of C_{70} clusters in solutions, a transmission electron microscope (TEM microscope) with an ultrahigh resolution (~0.2nm) was used. The interaction of intense (I=0.52 MW/cm^2) elliptically polarized laser radiation with a fullerene solution causes the appearance of a nonlinear effect in the solution. The dependence of the specific polarization rotation ($\alpha_{sp.}$) on the degree of radiation ellipticity (θ) in a solution of C_{70} at two different concentrations in xylene was studied (Fig. 1). At a fixed intensity and degree of ellipticity of laser radiation, a gradual increase in the concentration of C_{70} in solution is accompanied by a decrease in the specific polarization rotation. The latter is associated with the tendency of C_{70} fullerene molecules to synthesize nanoclusters of various shapes and sizes in solution.

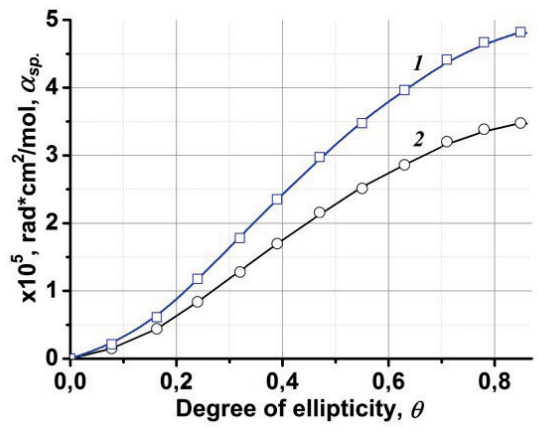

Fig. 1.The dependence of the specific rotation of the elliptical polarization $\alpha_{sp.}$ vs. the degree of ellipticityθ of laser radiation in solutions of C_{70} in xylene at fullerene concentrations of ~0.8 mg/mL (curve 1) and ~1.2 mg/mL (curve 2).The peak intensity of laser pulses was ~0.52 MW/cm^2 at the wavelength of ~532 nm.

Thus, a correlation has been found between the processes of formation of fullerene clusters in solutions and the value of the angles of the nonlinear rotation of the polarization ellipse of radiation passing through the solution. Using the obtained experimental data were determined the nonlinear addition to the refractive index in the studied media.

[1] Kokhkharov A.M., Zakhidov E.A., GofurovSh.P., Bakhramov S.A., Makhmanov U.K.,Clusterization of fullerene C_{70} molecules in solutions and its influence to optical and nonlinear optical properties of solutions, International Journal of Nanoscience, Vol. 12, pp.1350027 (2013).

DOI: 10.24412/cl-35039-2022-22-164-164

Promising schemes of heralded single-photon qubit sources

A. A. Kalachev

Kazan Scientific Center of Russian Academy of Sciences, Russia, 420111, Kazan, Lobachevsky str., 2/31
a.a.kalachev@mail.ru

In this presentation, I would like to discuss some efficient schemes of heralded sources of single photons with controlled parameters based on spontaneous four-wave mixing and spontaneous parametric down-conversion. In particular, a scheme for heralded generation of frequency-bin photonic qubits in a system of coupled microring resonators (a photonic molecule) [1] and quantum hashing via generation of single-photon states with controlled orbital angular momentum [2] are considered.

[1] I.N. Chuprina, A.A. Kalachev, Generating frequency-bin qubits via spontaneous four-wave mixing in a photonic molecule, Phys. Rev. A, **100**, 043843(1-7) (2019).
[2] D. A. Turaykhanov, D. O. Akat'ev, A. V. Vasiliev, F. M. Ablayev, A. A. Kalachev, Quantum hashing via single-photon states with orbital angular momentum, Physical Review A, **104**, 052606(1-8) (2021).

DOI: 10.24412/cl-35039-2022-22-165-165

Near-field Optical and IR Spectroscopies of Semiconductor Nanostructures

A.G. Milekhin[1], I.A. Milekhin[2], N.N. Kurus[1], L.S. Basalaeva[1], R.B.Vasiliev[3], K.V. Anikin[1], V.G. Mansurov[1], K.S. Zhuravlev[1], A.V. Latyshev[1,4], D.R.T. Zahn[2]

[1] A.V. Rzhanov Institute of Semiconductor Physics, 630090, Novosibirsk, Lavrentjev av. 13, Russia
[2] Semiconductor Physics, Chemnitz University of Technology, D-09107 Chemnitz, Germany
[3] Department of Material Science, Moscow State University, Moscow, Russia
[4] Novosibirsk State University, Novosibirsk, 630090, Pirogov str., 1, Russia
milekhin@isp.nsc.ru

Tip-Enhanced Raman scattering, photoluminescence, and nano-InfraRed (TERS, TEPL, and nano-IR) spectroscopies were successfully applied to study the phonon and electron spectra of 2D and 1D single nanostructures with the spatial resolution much below diffraction limit.

TERS imaging by optical phonons in single 2D nanostructures including graphene, colloidal core/shell CdSe/CdS nanoplatelets, and MoS_2 monolayers placed in the gap between the TERS tip apex and plasmonic substrate, which allows determination of nanostructure size and shape, structural defects, mechanical strain, and local electromagnetic field enhancement, is demonstrated. Near-field photoluminescence or TEPL from MoS_2 and WS_2 monolayer islands grown on a Si substrate reveals local variation of exciton PL energy and intensity depending on the number of monolayers and the presence of structural defects.

TERS by surface optical (SO) phonons in AlN nanoclusters grown by molecular beam epitaxy of a Si substrate and nanocolumns placed on an Au surface was observed. The TERS image of a single wurtzite AlN nanocluster with a size of about 300 nm shows its hexagonal shape. TERS taken from AlN nanocolumns with a diameter and height of about 200 and 50 nm, respectively, with different light polarizations with respect to the nanocolumn axes demonstrates different images. The origin of the changes in TERS images upon the light polarization is discussed.

We also present the comparative results of Raman data with the hyperspectral infrared nanoimages of AlN nanostructures based on Fourier transform nano-IR spectroscopy. IR nanospectroscopy allows the studying the spatial localization of surface optical phonon modes originated from optical phonon localized near the edges of hexagonal AlN nanoclusters with different symmetries.

This work was supported by the Russian Science Foundation (project 22-12-00302).

DOI: 10.24412/cl-35039-2022-22-166-166

Atomically thin nanosheets of zinc and cadmium chalcogenides: colloidal growth, ligand exchange, and control of exciton properties

D.A. Kurtina, V.P. Grafova, A.V. Knot'ko, A.V. Garshev, R.B. Vasiliev,

Lomonosov Moscow State University, 119991, Moscow, Russia
romvas@inorg.chem.msu.ru

Two-dimensional (2D) semiconductors have unique electronic properties due to their atomically thin thickness and two-dimensional electronic structure [1]. In this repot, we consider a new class of 2D semiconductors - atomically thin nanosheets of cadmium and zinc chalcogenides with a thickness of less than 1 nanometer (about 2-3 monolayers), synthesized in colloidal solutions.

A growth method was developed for the synthesis of atomically thin nanosheets of cadmium and zinc chalcogenides in a colloidal system of cadmium (zinc) acetate/octadecene/oleic acid/oleylamine in the temperature range of 110–250°C [2]. The choice of conditions made it possible to grow nanostructures with given composition, crystal structure, and a precise (with an accuracy of 1 monolayer) thickness in the range of 0.6–1.2 nm. A growth technique has been developed to increase the lateral sizes of nanosheets up to 700 nm with an anisotropy factor up to 1500. A detailed study using HRTEM, HAADF-STEM, SAED, XRD methods showed a perfect crystal structure of nanosheets, allowing us to consider thees nanostructures as atomically thin crystals. It was found zinc blende structure for CdTe and CdSe and wurtzite structure for ZnSe. Using a set of methods, it was established that the composition of nanosheets follows the ratio $[Cd_{n+1}E_nL_2]$ (E - chalcogen, L - organic ligand, n - number of atomic planes) with integer coefficients.

Correlations between the size, composition, crystal structure of atomically thin nanosheets and their optical properties are established. The two-dimensional nature of the electronic structure and record-breaking narrow exciton bands with a width of about 40 meV at room temperature are shown [3]. The obtained materials with the spectral position of exciton bands specified with an accuracy of 1 nm are of interest for creating light-emitting devices and phosphors.

Approaches to ligand exchange were developed to obtain nanosheets with a variable composition of ligands $[Cd_{n+1}E_nL_2]$, where E = Se or Te, for L = hexadecanethiol, thioglycolic acid, or acetylcysteine in the form of thiolates. The nature of the modification of the optical properties depending on the type of ligand, which consists in a bathochromic shift of all exciton bands, has been established, with the maximum shift up to 200 meV found for the thinnest populations.Chiral nanostructures with a chiral ligand acetyl-L- or -D-cysteine, with pronounced exciton bands of circular dichroism with a record dissymmetry factor of $9 \cdot 10^{-3}$ achieved for a thickness of 0.6 nm, have been synthesized.

A new effect of spontaneous folding of atomically thin nanostructures of cadmium chalcogenides has been discovered. A model is proposed for spontaneous folding due to compressive or tensile deformation at the semiconductor/ligand interface, caused by a mismatch between the available space on the basal cation-terminated (001) plane and the size of the seat of the carboxylate and thiolate ligands. The effect of spontaneous folding on the exciton properties of nanosheets has been revealed

This work was supported by the Russian Science Foundation (grant № 22-13-00101).

[1] Guillemeney, L. et al. Curvature and self-assembly of semi-conducting nanoplatelets. Commun Chem 5, 7 (2022).
[2] D.A. Kurtina et.al., Atomically Thin Population of Colloidal CdSe Nanoplatelets: Growth of Rolled-up Nanosheets and Strong Circular Dichroism Induced by Ligand Exchange, Chem. Mater., 31, 9652–9663, (2019).
[3] R.B. Vasiliev et.al., High-energy exciton transitions in quasi-two-dimensional cadmium chalcogenide nanoplatelets. Phys. Rev. B, 95, 165414, (2017).
[4] R.B. Vasiliev et.al., Spontaneous Folding of CdTe Nanosheets Induced by Ligand Exchange, Chem. Mater., 30, 1710–1717, (2018).

DOI: 10.24412/cl-35039-2022-22-167-167

Photomodification of Silver Nanocubes for Patch Plasmonic Nanoantennas by Visible Laser Light

S.G. Lukishova

Rochester, NY, USA
lukishova@hotmail.com

From all types of plasmonic nanoantennas, the highest Purcell factor with increasing emitter radiative decay rate was obtained with metal plasmonic patch (gap) nanoantennas (a dielectric nanogap with emitters between a metal nanoparticle of a given shape (cube, triangle, etc.) and a metal film [1]. Silver nanoparticles, for instance, nanocubes [2-7] or their arrays [6] are used in patch nanoantennas for emitter fluorescence enhancement in visible spectral range [2-6] as well as for increasing stability and brightness of organic light emitting devices (OLEDs) [7]. We observed spontaneous intensity spikes up to ~400–900 kcounts/s, as well as a step-wise several times, increase in photoluminescence from silver nanocubes. Cw, 532 or 633 nm laser excitation was used (~100 μW incident power with a 1.30 numerical aperture, oil immersion objective). These spontaneous spikes may influence the purity of single-photon emission from single emitters and even prevent photon antibunching. We investigated 100-nm silver nanocubes from nanoComposix protected by a few nanometer layers of polyvinylpyrrolidone (PVP), typically used in patch nanoantennas. Such spontaneous appearance of bright photoluminescence can be a result of photomodification of nanocube surface with formation over time of bright, few nanometer silver nanoclusters [8-10] on an oxidized surface of nanocubes. Confocal fluorescence microscopy micrographs showed appearance in time bright features with single-molecule behavior (stripes and semicircles in raster scans). These effects should be considered working with silver plasmonic nanostructures, especially under cw laser irradiation, see also [11,12].

[1] S.G. Lukishova and L.J. Bissell, "Nanophotonic advances for room-temperature single-photon sources", pp.103-178, in Quantum Photonics: Pioneering Advances and Emerging Applications, R.W. Boyd, S.G. Lukishova, V.N. Zadkov (Eds.), Springer (2019).
[2] T.B. Hoang et al., "Ultrafast spontaneous emission source using plasmonic nanoantennas", Nat. Commun. 6, art. number 7788 (2015).
[3] G.M. Akselrod et al.,"Probing the mechanisms of large Purcell enhancement in plasmonic nanoantennas", Nat. Photonics 8, 835 (2014).
[4] S.I. Bogdanov et al., "Ultrabright room-temperature sub-nanosecond emission from single nitrogen-vacancy centers coupled to nanopatch antennas", Nano Lett. 18, 4837–4844 (2018).
[5] S.I. Bogdanov et al., "Ultrafast quantum photonics enabled by coupling plasmonic nanocavities to strongly radiative antennas", Optica 7 (5), 463-469 (2020).
[6] A.V. Gritsienko et al., "Optical properties of new hybrid nanoantenna in submicron cavity", J. Physics: Conf. Series 2015, 012052 (2021).
[7] M.A. Fusella et al., "Plasmonic enhancement of stability and brightness in organic light-emitting devices", Nature 585, 37 (2020).
[8] LA. Peyser et al.,"Photoactivated fluorescence from individual silver nanoclusters", Science 291, 5501, 103 (2001).
[9] L.A. Peyser et al.,"Mechanism of Agn nanocluster photoproduction from silver oxide films", J. Phys. Chem. B 106, 7725-7728 (2002).
[10] C.D. Geddes et al., "Luminescent blinking from silver nanostructures", J. Phys. Chem. B 107, 9589 (2003).
[11] S.G. Lukishova, J. Brone, Z. Li, L. Young, "Photomodification of silver nanocubes for patch plasmonic nanoantennas by visible laser light", Book of Abstracts, the 51st Winter Colloquium on Physics of Quant. Electron., p. 154 (Snowbird, Utah, January 2022).
[12] S.G. Lukishova, J. Brone, D. Khan and Z. Li, "Ultrabright photoluminescence spikes and stepwise photoluminescence increase from colloidal silver nanoparticles for patch nanoantennas", J. Physics: Conf. Series. 2249, 012002 (2022).

DOI: 10.24412/cl-35039-2022-22-168-168

Novel physical method for 2-D chiral metasurfaces formation

D.R. Dadadzhanov[1], I.A. Gladskikh[1], R.A. Zakoldaev[1], N.A. Toropov[1,2], A.A. Starovoytov[1] and T.A. Vartanyan[1]

1 – School of Physics and Engineering, ITMO University, St. Petersburg, Russia
2 – Living Systems Institute, University of Exeter, Exeter EX4 4QD, United Kingdom
e-mail: daler.dadadzhanov@gmail.com

The ongoing drive in nanophotonics towards the search of new nanomaterials to manipulate the polarization properties of light is an urgent task. Of particular interest are chiral plasmonic nanostructures that support the collective oscillation of free electron in the response of incident electromagnetic wave. Chirality in plasmonic nanostructures originates from a unique natural effect in chiral molecules when the mirror images of which cannot be superimposed on each other. From a physical point of view, chirality in plasmonic nanostructures can be described based on coupling between electric and magnetic dipole moments, which specifically interact with left-/right-handed circularly polarized light unlike achiral nanostructures. This allows the use of chiral nanoparticles as optical light modulators, sensors, and even novel lasing sources. Recent studies, including "bottom-up" and "top-down" approaches, show diversity of the chiral plasmonic nanostructures such as metasurface of nanohelices or nanocrescent, helicoides synthesized by combination achiral nanoparticles and chiral precursors molecules, chiral gold nanostructures prepared by asymmetric photocatalytic metal deposition [1, 2]. However, existing methods are very costly as in case of electron beam and focused ion beam lithography or required sophisticated multistep synthesis procedure. Thus, the searching of alternative strategies for fabrication of chiral plasmonic nanostructures are high demand. We propose a more promising strategy to increase the chiroptical properties of 2D plasmonic nanostructures by applying the spectral hole burning method [3-5] of plasmonic nanostructures with the broadband extinction spectra by pulse laser with circular polarization of radiation. The influence of high-power circular polarized laser irradiation on the optical properties of metasurfaces with self-organized silver nanoparticles obtained using the physical vapor deposition technique was studied. Optimal irradiation parameters at which there is no ablation of silver nanoparticles were established. The results obtained demonstrate strong sign-alternating circular dichroism in the spectral region of the incident radiation wavelength (532 nm) for annealed plasmonic nanostructures, as well as for broadband unannealed metasurface.

This work was supported by the Russian Science Foundation (Project 21-72-10098).

[1] Kong X.T., Besteiro L.V., Wang Z., Govorov A.O. Plasmonic chirality and circular dichroism in bioassembled and nonbiological systems: theoretical background and recent progress //Advanced Materials. – 2020, Vol. 32, No 41, pp. 1801790.
[2] Wu, Wenbing, and Matthias Pauly. "Chiral plasmonic nanostructures: recent advances in their synthesis and applications." Materials Advances (2022).
[3] F. Stietz, J. Bosbach, T. Wenzel, T. Vartanyan, A. Goldmann, F. Träger. Phys. Rev. Lett.,v. 84, Iss. 24, pp. 5644-5647 (2000)
[4] Toropov N.A., Gladskikh I.A., Parfenov P.S., Vartanyan T.A. Fabrication and laser-assisted modification of the Ag particles ensembles supporting quadrupole plasmon oscillations // Optical and Quantum Electronics - 2017, Vol. 49, No. 4, pp. 154
[5] Bosbach, J., et al. "Spectral hole burning in absorption profiles of metal nanoparticles prepared by laser assisted growth." The European Physical Journal D-Atomic, Molecular, Optical and Plasma Physics 16.1 (2001): 213-217.

DOI: 10.24412/cl-35039-2022-22-169-169

Optically tunable nanophotonic structures with Mie-type resonances

A.S. Shorokhov[1]

Faculty of Physics, Lomonosov Moscow State University, Moscow 119991, Russia
shorokhov@nanolab.phys.msu.ru

Mie-resonant nanophotonic structures made of dielectric and semiconductor materials with high refractive indices are considered as a promising platform for novel functional optical devices [1–2]. To make such structures active different mechanisms have been proposed recently [3–4]. All-optical switching based on photo-induced carrier generation manifests itself as one of the most promising techniques owing to the intrinsic ultrafast speed of this process [5]. However, most experimental demonstrations to date are limited by transmittance or reflection changes missing active beam profile control by such nanophotonic structures.

In this work three different examples of the spatial light control with optically tunable nanophotonic structures are presented. First, GaAs metasurface composed of asymmetric nanoparticle trimers is considered. It is shown that such structure can redistribute light energy between different diffraction orders under low-power laser pumping. Experimentally we demonstrate up to 16% modulation at the pump fluence as low as several μJ/cm^2 with the characteristic switching time of 1.2 ps. This effect is caused by the non-uniform absorption of the elements forming the metasurface and by consequent change of their resonant properties due to the free-carrier injection mechanism. Second, we consider asymmetric dimer composed of two GaAs nanoparticles combined with integrated waveguide on the dielectric substrate. It is shown than by optical pumping one can control light coupling efficiency to the waveguide through the modification of the nanoantenna scattering profile. Finally, we investigate gradient GaAs metasurface for the ultrafast image processing using Fourier filtering approach. Achieved results can be used for development of ultrafast optical devices capable of the effective low-power spatial light control.

[1] A. I. Kuznetsov et al., "Optically resonant dielectric nanostructures," Science, 354, aaf2472 (2016).
[2] M. Decker, I. Staude, "Resonant dielectric nanostructures: a low-loss platform for functional nanophotonics," J. Opt., 18, 103001 (2016).
[3] R. Paniagua-Dominguez et al., "Active and tunable nanophotonics with dielectric nanoantennas", Proc. IEEE, 749 – 771 (2020).
[4] T. Badloe et al., "Tunable Metasurfaces: The Path to Fully Active Nanophotonics", Adv. Photonics Res., 2, 2000205 (2021).
[5] R. Shcherbakov et al., "Ultrafast all-optical switching with magnetic resonances in nonlinear dielectric nanostructures," Nano Lett., 15, 6985–6990 (2015).

DOI: 10.24412/cl-35039-2022-22-170-170

Single-layer atom chip for quantum metrology

A. Afanasiev[1], P. Skakunenko [1,2], D. Bykova[1,3], A. Kalmykov [1], R. Kirtaev [2], D. Negrov[2], V. Balykin[1]

1- Institute of Spectroscopy Russian Academy of Sciences, Fizicheskaya Str., 5, Moscow, Troitsk, 108840, Russia
2- Moscow Institute of Physics and Technology, 9 Institutskiy per., Dolgoprudny, Moscow Reg., 141700, Russia
3- National Research University Higher School of Economics, Myasnitskaya str., 20, Moscow, 101000, Russia
afanasiev@isan.troitsk.ru

Atom interferometry is considered as a new platform for high precision fundamental experiments and for solving numerous applied problems. Among the fundamental problems are the following: the detection of gravitational waves, the search for dark matter, tests of dark energy theories, tests of the equivalence principle and validity of quantum mechanics at macroscopic scale. Among the applied problems, the most important, are the study of the Earth's gravitational field and applications to navigation. Obviously, the development of an atom interferometry approaches gives us the new stage of quantum metrology.

One of the most important approaches in the implementation of atomic interferometry is the using of atom chip technology [1]. Atom chip is the combination of advanced industrial microelectronics technology and atom optical techniques to generate and control ultracold atomic ensembles. An atom chip can provide the ability to trap and manipulate atoms. The atom chip also enables Bose-Einstein condensation (BEC) of atoms.

The First Russian atom chip is depicted on the figure 1. The main advantage of such chip is the possibility of continuous loading of magneto-optical trap near the surface using single-layer configuration. It's shown [2] that near the atom chip was trapped about $N \approx 3 \cdot 10^5$ atoms with concentration of $n \approx 10^{10}$ cm^{-3}. The temperature of the atoms in the trap was about 200 μK.

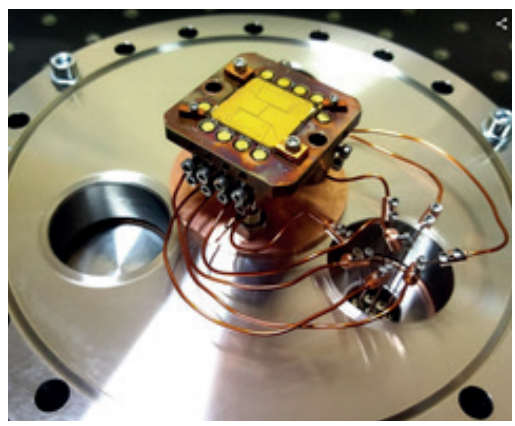

Fig. 1. The First Russian atom chip

Such a chip can be used as source of cold atoms for atom interferometry experiments. For this purpose, atoms will recapture with magnetic trap with additional cooling. As the first quantum sensors, atom clock and gravimeter will be demonstrated.

[1] M. Keil, et. al, "Fifteen years of cold matter on the atom chip: promise, realizations, and prospects", Journal of Modern Optics, 63, 1840, (2016).
[2] A.E. Afanasiev, et al., "Single-layer atom chip for continuous operation: Design, fabrication and performance", Optics & Laser Technology, 148, 107698 (2022).

DOI: 10.24412/cl-35039-2022-22-171-171

Nonlinear optical dynamics of gigawatt single-cycle phase-stable pulses generated in hollow-core photonic-crystal fiber

I.V. Savitsky[1], E.A. Stepanov[1,2], A.A. Voronin[1,2] A.A. Lanin[1,2], A.B. Fedotov[1,2], A.M. Zheltikov[1,2,3]

1 - Physics Department, M.V. Lomonosov State University, Moscow, Russia
2 - Russian Quantum Center, Skolkovo, Moscow Region, Russia
3 - Department of Physics and Astronomy, Texas A&M University, College Station, USA
a.b.fedotov@physics.msu.ru

High-peak power mid-infrared (mid-IR) and short-wavelength-infrared (SWIR) pulses with a pulse width τ_0 close to the carrier field cycle T_0 provide a powerful resource for ultrafast optical science and advanced photonic technologies [1]. Because the photon energy $\hbar\omega_0$ of such T_0-nigh SWIR/mid-IR pulses is below the band gap E_g of most of the technologically relevant solid-state semiconductor materials, these pulses, unlike their near-infrared counterparts, can drive and probe ultrafast electron dynamics not only near the surface, but also deep inside solid-state semiconductors, serving to set an unprecedentedly precise control over the fastest physical processes in solids [2] and helping induce and gate ultrafast electric-current transients in solids as a route toward petahertz optoelectronics [3].

In this work we have shown that soliton self-compression in a suitably designed gas-filled AR-guiding hollow-core fiber provides a source of ultrashort near-to-mid-IR field waveforms with a pulse energy up to 28 μJ, peak power up to 4 GW, and a pulse width smoothly tunable, via gas-pressure adjustment inside the gas-filled hollow fiber, all the way down to a single field cycle at ≤ 6.6 fs. With an active carrier–envelope phase (CEP) stabilization extended to its entire multioctave bandwidth, the single-cycle near-to-mid-IR fiber output is CEP-stable within 140 mrad and can be finely tailored toward a desired CEP profile. High-order harmonics generated by such field waveforms in solids exhibit clear signatures of a strong-field, nonperturbative impulsive response to a single-cycle optical driver.

This research was supported by RSF Grants # 20-12-00088, # 22-12-00149 and RFBR Grant # 20-21-00131.

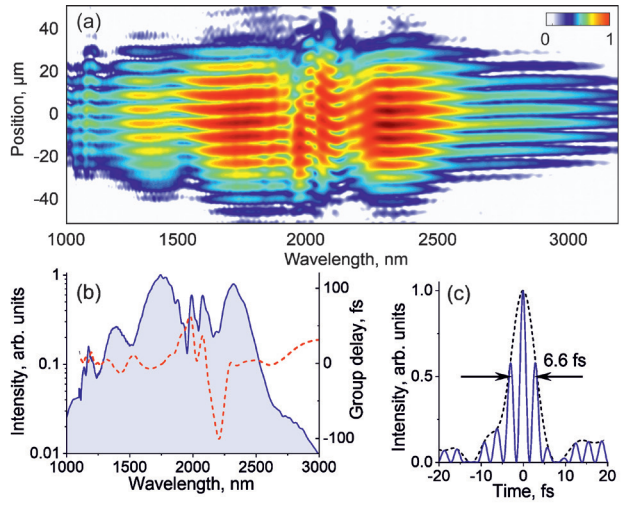

a) X-SEA-F-SPIDER interferogram of the near-to-mid-IR supercontinuum output of the hollow AR fiber. (b) Spectral intensity retrieved from X-SEA-SPIDER measurements along with the spectral phase and (c) the field waveform along with its pulse envelope at the output of the hollow AR fiber.

[1] Balciunas, T.; Fourcade-Dutin, C.; Fan, G.; Witting, T.; Voronin, A. A.; Zheltikov, A. M.; Gerome, F.; Paulus, G. G.; Baltuska, A.; Benabid, F. A strong-field driver in the single-cycle regime based on self-compression in a kagome fibre. Nat. Commun. , 6, No. 6117, (2015).

[2] Ghimire, S.; DiChiara, A. D.; Sistrunk, E.; Agostini, P.; DiMauro, L. F.; Reis, D. A. Observation of high-order harmonic generation in a bulk crystal. Nat. Phys. , 7, 138−141, (2011).

[3] JSchiffrin, A.; Paasch-Colberg, T.; Karpowicz, N.; Apalkov, V.; Gerster, D.; Mühlbrandt, S.; Korbman, M.; Reichert, J.; Schultze, M.; Holzner, S.; Barth, J. V.; Kienberger, R.; Ernstorfer, R.; Yakovlev, V. S.; Stockman, M. I.; Krausz, F. Optical-field-induced current in dielectrics. Nature, 493, 70−74, (2013).

DOI: 10.24412/cl-35039-2022-22-172-172

Low energy nuclear photonics

A. Savel'ev

Lomonosov Moscow State Universiry, Moscow, Russia
abst@physics.msu.ru

Powerful femtosecond lasers could provide for relativistic electrons, high energy protons and heavier ions as well as high fluences of X-rays and gammas. All these high energy particles are very useful for the new emerging field – nuclear photonics. Here we focused at the recent theoretical and experimental advances and perspectives of nuclear photonics with table top femtosecond lasers. Namely we touch isomeric nuclear state excitation, neutron production, nuclear excitation below GDR, etc. Experimental schemes for efficient production of well collimated relativistic electron beams are also presented.

DOI: 10.24412/cl-35039-2022-22-173-173

Control of Femtosecond Filamentation by NIR- and SWIR-Laser-induced Rotational Quantum Wakes in Nitrogen

S.V. Chekalin, V.O. Kompanets, A.A. Melnikov

Institute of Spectroscopy, Russian Academy of Sciences, ul. Fizicheskaya 5, Troitsk, 108840 Moscow, Russia
schekalin@yandex.ru

The possibility of single and multiple filamentation control by field-free revivals of molecular alignment induced by 1400 nm and 800 nm femtosecond laser pulses was demonstrated in molecular nitrogen at typical gas pressure of about 3 bar. The time dependent change of the molecular refractive index seen by the probe pulse is modulated both spatially and temporally depending on the pump-probe delay. Due to molecular alignment dramatic effect on the propagation of an intense probe pulse filament it is possible to control its filamentation by changing the delay time between pump and probe pulses. Under excitation of molecular nitrogen at 1400 nm and probing at 800 nm we observed upshifted or down shifted by several tens of nm spectral and pulse duration change around the half-revival time of the molecular alignment quantum wake following a pump pulse filamenting in nitrogen. It was revealed that spectral shift of the probe pulse following the wake of the molecular alignment is proportional to the slope of the refractive index profile. At multiple filamentation we observed stable and reproducing selective amplification of energy transfer (up to 4%) to distinct daughter filaments accompanied by a spectral broadening up to more than octave at subdifraction divergence. This effect was observed in the divergent beam in the range of the cross-defocusing from the perpendicularly prealigned molecules and can be explained by a decrease of interaction between daughter filaments.

Under excitation at 800 nm a strong plasma lens seen by the probe pulse arised. In this case due to a strong wavelength dependence of plasma refractive index the revival signal was observed mainly in visual spectral parts of the probe radiation (third harmonic and supercontinuum) in the range of the cross-focusing from the parallel orientated prealigned molecules.

DOI: 10.24412/cl-35039-2022-22-174-174

Laser spectroscopy of interactions at the carbon nanoparticle-medium interface

T. Dolenko[1], S. Burikov[1], A. Vervald[1], K. Laptinskiy[2]

1- Department of Physics, Lomonosov Moscow State University, Leninskie Gory 1/2, 119991 Moscow, Russia
2- Skobeltsyn Institute of Nuclear Physics, Lomonosov Moscow State University, Leninsky Gory 1/2, 119991 Moscow, Russia
tdolenko@mail.ru

The unique combination of properties of such carbon nanoparticles (CNPs) as carbon dots (CDs) and nanodiamonds (NDs) make them promising for applications in biomedicine and in technological processes. These nanoparticles have stable and intense luminescence and multifunctional surface, they are non-toxic and biocompatible. Therefore, CNPs can be used as luminescent markers and nanosensors, adsorbents and drug carriers. However, for effective applications it is necessary to understand the mechanisms of formation of CNPs surface luminescence, to know the influence of environment on colloidal, luminescent, adsorption properties of NDs and CDs in various solvents and biological tissues. In biomedicine, it is necessary to make sure that nanoparticles are safe for surrounding molecules. Therefore, the study of interactions at the carbon nanoparticle-medium interface is an actual problem [1].

The report presents the results of the research of the NDs and CDs interactions with the surrounding molecules in normal and heavy water, protonic and aprotonic solvents, solutions of salts and surfactants, proteins and DNA and of the effects of these interactions on the pointed CNPs properties. It was found that the intensity of CNPs photoluminescence increases primarily with an increase in the amount of sp^2-/amorphously hybridized carbon on their surface, and secondarily with an increase in the number of surface oxygen-containing groups. The photoluminescence of oxidized CNPs depends on the value of the environment pH [2]. The mechanism of pH influence on the CNPs photoluminescence is due to (de)protonation of carboxyl and hydroxyl groups on their surface. This conclusion is confirmed by quantum calculations of diamond core structures with surface groups.

Using Raman laser spectroscopy, a general tendency has been established for all investigated CNPs to weaken hydrogen bonds in proton solvents. At the same time, the properties of the CNP themselves depend on the strength of the hydrogen bonds in the suspensions. The significant influence of CNPs on the strength of the hydrogen bonds, on the one hand, and the influence of the hydrogen bonds of environment on the CNPs properties, on the other hand, was found for the first time. The dependence between the efficiency of DNA, proteins and salt ions interactions with the NDs surface groups and the changes of NDs luminescence was found. A significant effect of NDs on the micelle formation of surfactants in water has been discovered and explained [3]. The dependence of this effect on the ratio of hydrophilic and hydrophobic groups on the CNPs surface and in the environment is established. NDs have no effect on the formed micelles, which proves the safety for biotissues.

As a result of the study of the interactions of CDs with metal ions, including heavy metal cations, the selectivity of the CDs luminescence sensitivity to certain ions was discovered and confirmed by calculations of molecular dynamics. The discovered effects provide prospects for the use of CDs as nanosensors of heavy metal cations.

The results were obtained using Raman laser spectroscopy, photoluminescent spectroscopy, Coherent Anti-Stokes Raman scattering, laser correlation spectroscopy, IR absorption spectroscopy.

The research was carried out at the expense of the grant of the Russian Science Foundation No. 22-12-00138, https://rscf.ru/project/22-12-00138/

[1] T. Dolenko, S. Burikov, K. Laptinskiy, J. Rosenholm, O. Shenderova, I. Vlasov, Evidence of carbon nanoparticle – solvent molecule interactions in Raman and fluorescence spectra, Physica Status Solidi A, vol.212(11), pp. 2512-2518, (2015).
[2] A. Vervald, A. Lachko, O. Kudryavtsev, O. Shenderova, S. Kuznetsov, I. Vlasov, T. Dolenko, The Effect of Environment pH on Surface Photoluminescence of Oxidized Nanodiamonds, J. Phys. Chem. C, vol.125(33), pp. 18247-18258, (2021).
[3] A. Vervald, S. Burikov, K. Laptinskiy, T. Laptinskaya, I. Vlasov, O. Shenderova, T. Dolenko, Nanodiamonds and surfactant in water: hydrophobic and hydrophilic interactions, J. of Colloid and Interface Science, vol.547, pp. 206-216, (2019).

DOI: 10.24412/cl-35039-2022-22-175-175

Broadband two-dimensional spectrochronography with ultrashort pulses in the mid-infrared

E.A. Stepanov, A.N. Zhdanov, I.V. Savitskii, G.D. Ivanov, A.A. Lanin, A.B. Fedotov, A.M. Zheltikov

Lomonosov Moscow State University, Leninskie Gory 1, stroenie 2, 119991 Moscow, Russia;
e-mail: a.b.fedotov@physics.msu.ru, zheltikov@physics.msu.ru

The methods of 2D Fourier-transform infrared (2D-FTIR) spectroscopy are most widely used to analyze the dynamics of complex organic compounds, in particular, new types of molecular markers used in the analysis of biological complexes [1 – 6]. Two-dimensional IR spectroscopy makes it possible to obtain information about the environment of proteins reflected in a two-dimensional line shape, to measure the characteristic times of excitation transfer from one vibrational mode to another, to distinguish between solvent affected and disordered proteins, and to increase the spectral resolution due to the so-called off-diagonal peaks. For example, using 2D-FTIR spectroscopy, new features of the relationship between the vibrational degrees of freedom in nucleic acids were discovered [7 – 9]. The high temporal resolution of the technique allows analyzing the dynamics of peptide folding and protein oligomerization [8 – 11], including the technique of labelling cells with the carbon-13 isotope [11].

In this work, we present a universal laser platform for broadband 2D spectroscopy using ultrashort mid-IR pulses. The laser system developed for 2D spectroscopy generates radiation pulses with a duration of less than 70 fs and a wavelength tunable in the range of 2.6 – 10 mm. Broadband excitation and probing by pulses with such parameters, in combination with the heterodyne detection technique implemented in the mid-IR range, open up possibilities for studying ultrafast dynamics of molecular coherence, as well as ultrafast population kinetics and energy exchange between different degrees of freedom in a wide class of complex molecular systems (fig. 1).

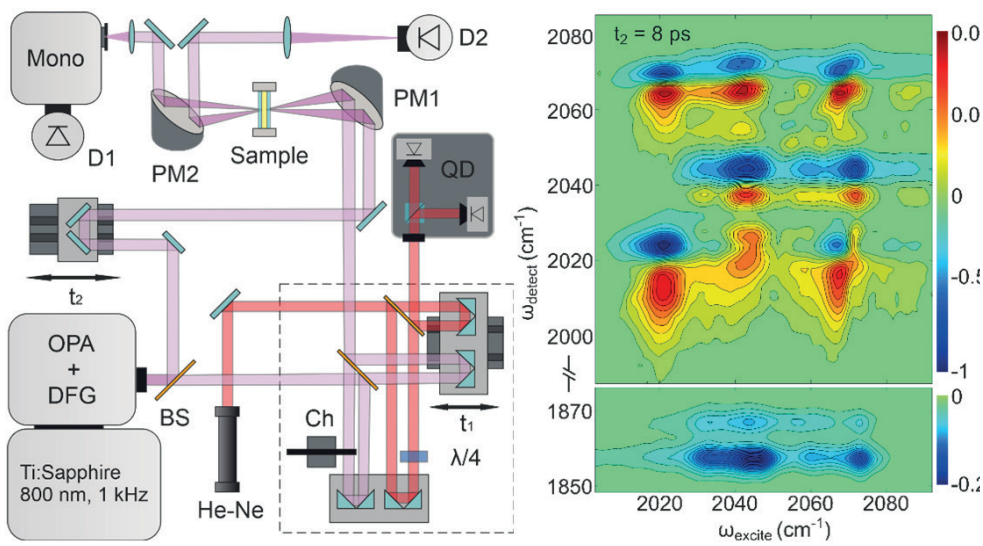

Figure 1. (Left) Schematic of a two-dimensional IR spectrometer; (right) two-dimensional IR spectrum of dicobalt octacarbonyl measured for a delay t_2 = 8 ps.

[1] Park K.-H., Choi S.R., Choi J.-H., Park S., Cho M., *Chem. Phys. Chem.*, **11**, 3632 (2010).
[2] Brookes J.F., Slenkamp K.M., Lynch M.S., Khalil M., *J. Phys. Chem. A*, **117**, 6234 (2013).
[3] Simpson N., Shaw D.J., Frederix P.W., Gillies A.H., Adamczyk K., Greetham G.M., Towrie M., Parker A.W., Hoskisson P.A., Hunt N.T., *J. Phys. Chem. B*, **117**, 16468 (2013).
[4] Dutta S., Li Y.-L., Rock W., Houtman J.C.D., Kohen A., Cheatum C.M., *J. Phys. Chem. B*, **116**, 542 (2012).
[5] Tucker M.J., Gai X.S., Fenlon E.E., Brewer S.H., Hochstrasser R.M., *Phys. Chem. Chem. Phys.*, **13**, 2237 (2011).
[6] Kim H., Cho M., *Chem. Rev.*, **113**, 5817 (2013).
[7] Tucker M.J., Abdo M., Courter J.R., Chen J., Brown S.P., Smith A.B., Hochstrasser R.M., *Proc. Nat. Acad. Sci.*, **110**, 17314 (2013).
[8] Ganim Z., Jones K.C., Tokmakoff A., *Phys. Chem. Chem. Phys.*, **12**, 3579 (2010).
[9] Maekawa H., De Poli M., Toniolo C., Ge N.-H., *J. Am. Chem. Soc.*, **131**, 2042 (2009).
[10] Jones K.C., Peng C.S., Tokmakoff A., *Proc. Nat. Acad. Sci.*, **110**, 2828 (2013).
[11] Moran S.D., Zhang T.O., Zanni M.T., *Protein Sci.*, **23**, 321 (2014).

DOI: 10.24412/cl-35039-2022-22-176-176

High-resolution modulation spectroscopy: opportunities and prospects.

K. Boldyrev

Institute of Spectroscopy of the Russian Academy of Sciences,
Fizicheskaya Str., 5, Troitsk, Moscow, 108840, Russia
kn.boldyrev@gmail.com

The report will present the results of the application of high-resolution modulation spectroscopy in the study of various problems of materials science. External electric and magnetic fields, mechanical stresses, intense light laser beams, X-rays are used as a modulating perturbation. Such techniques allow obtaining completely new information about the materials under study.

DOI: 10.24412/cl-35039-2022-22-177-177

Quasi-equilibrium saturated states of fluorescence emission by laser-pumped fluorescent random media: the fundamental role of characteristic scales of radiative transfer

D.A. Zimnyakov[1,2], S.S. Volchkov[1], L.A. Kochkurov[1], A.F. Dorogov[1]

1- Yury Gagarin State Technical University of Saratov, 77 Polytechnicheskaya St., Saratov, 410054, Russia
2- Institute for Precision Mechanics and Control Problems of the Russian Academy of Sciences, 24 Rabochaya St., Saratov, 410028, Russia
zimnykov@mail.ru

High-intensity laser pumping of fluorescent random media leads to a significant narrowing of the fluorescence spectrum, which is usually interpreted as a manifestation of random lasing in the pumped medium. Typically, the pump intensity at which the fluorescence spectrum narrows by a factor of two compared to the spontaneous fluorescence spectrum is taken as the threshold for random lasing. A characteristic feature of the random lasing mode at pump intensities substantially exceeding the threshold value is the almost constant half-width of the fluorescence spectrum, which is independent of the pump intensity. The spectral quality improvement factor $Q_{sp} = \Delta\lambda_{I\to 0}/\Delta\lambda_{I\to\infty}$ under these overpumping conditions, as a rule, does not exceed 8 – 10 (here $\Delta\lambda_{I\to 0}$ is the halfwidth of the emission spectrum in the spontaneous emission mode and $\Delta\lambda_{I\to\infty}$ is the similar value at large pump intensities). Moreover, various pumped systems with significantly different optical transport parameters of scattering matrices and emission characteristics of fluorophores exhibit close Q_{sp} values at high pump levels. Despite the abundance of theoretical and experimental works on various aspects of random lasing, such an effect of saturation of the spectral quality of fluorescence above the threshold has not yet been considered in detail.

Previously, it was found [1] that speckle modulation of pump radiation in a fluorescent medium has a significant effect on the formation of the fluorescence response. The light emitting system can be considered as a stochastic ensemble of uncorrelated micro-emitters of fluorescence associated with pump field speckles. One of the key parameters controlling the efficiency of pump conversion into a fluorescence response is the cross section of radiation losses of local emitters averaged over the ensemble. Further consideration of the saturation criterion for the excited state of fluorophore molecules and the probabilistic model of fluorescence enhancement in the pumped volume made it possible to determine the extreme value of the characteristic scale of fluorescence amplification in the medium at high pump intensities. It was established that this extreme amplification length does not depend on the emission properties of the fluorophore and the optical transport properties of the scattering matrix, but is determined only by the characteristic size of local fluorescence emitters and the factor of radiation exchange between them. Comparison of theoretical results with experimental data for R6G- and DCM-saturated layers of close-packed anatase particles pumped by pulse-periodic laser radiation at 532 nm showed good agreement between these datasets. The results obtained are of interest for the further development of fluorescent diagnostics of randomly inhomogeneous media and composite materials.

This work is supported by the Russian Science Foundation (the project № 22-29-00612).

[1] D.A. Zimnyakov, S.S. Volchkov, L.A. Kochkurov, V.I. Kochubey, A.G. Melnikov, G.V. Melnikov, Speckle patterning of a pumping laser light as a limiting factor for stimulated fluorescence emission in dense random media, Optics Express, vol. 29, pp.2309-2331 (2021).

DOI: 10.24412/cl-35039-2022-22-178-178

Elastic scattering controls Raman scattering efficiency in suspension

L.A. Golovan[1], O.I. Sokolovskaya[1], V.V. Yakovlev[2]

1- Lomonosov Moscow State University, Faculty of Physics, Moscow 119991, Russia
2- Texas A&M University, College Station, Texas 77843, USA
E-mail: golovan@physics.msu.ru

Elastic light scattering is a well-studied phenomenon intrinsic to random media, which often gives them completely new properties. In random media this phenomenon can lead to increase in the volume of light-matter interaction in comparison with homogeneous medium, which can result in variation of efficiency of different optical processes, e.g., Raman scattering. The question is whether it is possible to increase spontaneous Raman scattering efficiency by utilizing only scattering properties of medium itself or by adding scatterers in a controlled manner?

In this paper, effect of elastic light scattering on dwell time and efficiency of spontaneous Raman scattering in dimethyl sulphoxide (DMSO) was studied for powders of rutile and gallium phosphide with micrometer-sized particles suspended in DMSO both in experiment and by means of Monte Carlo simulation.

The employed medium consisted of spherical particles of rutile (diameter 0.5 μm) and of gallium phosphide (diameter 3 μm) suspended in DMSO. Mean photon dwell time in suspensions was meausred by means of optical heterodyning with the help of 80 fs pulses at wavelength of 1250 nm, repetition rate 80 MHz. Raman measurements were carried out with excitation by cw radiation and picosecond pulses at wavelengths of 1064 and 532 nm, correspondingly.

Both in experiment and in simulation we revealed effect of light elastic scattering on efficiency of Raman scattering in studied suspensions. Applicability the Monte Carlo simulation for description of the light propagation in the suspensions is supported by good agreement of its results and photon femtosecond backscattering dynamics measured in the experiment. In particular, both in experiment and in simulations it was found that increase of the total reflection with rising scatterer volume fraction is corresponded to fall of the photon dwell time. Combination of both these factors results in nonmonotonic dependence of the mean photon pathlength and Raman scattering efficiency on the scatterer volume fraction. Numerical simulations predicted maximal increase of the Raman signal in rutile suspension in DMSO in backscattered geometry up to 5 to 7 times depending on wavelength, whereas experiments demonstrated increase in 3 to 4 times in comparison to pure DMSO. The dependences of the Raman signal on the scatterer volume fraction obtained both in simulations and in experiment are in reasonable agreement. However, despite strong light scattering in gallium phosphide powder suspension weak light absorption in it prevents the Raman signal from its significant enhancement.

Thus, we demonstrated possibility to increase Raman scattering efficiency due to multiple scattering in suspension of transparent microparticles and necessary conditions of this effect.

DOI: 10.24412/cl-35039-2022-22-179-179

Synthesis of monolithic ultraporous 3D nanostructures and nanocomposites with desired optical properties

A. Khodan[1, 2], A. Konovko[3]

1- Frumkin Institute of Physical Chemistry and Electrochemistry Russian Academy of Sciences, Moscow, Russia.
2- Semenov Federal Research Center for Chemical Physics, Russian Academy of Sciences, Moscow, Russia.
3- Lomonosov Moscow State University, Faculty of Physics, Moscow, Russia.

Bulk nanostructures with the open porosity open up exciting prospects for creating new functional materials for various applications in photonics, IR-THz optics, metamaterials, heterogeneous photocatalysis, monitoring of environment and detoxification of harmful impurities. However, availability of 3D nanomaterials is limited by the complexity of controlling the process of synthesis of the nanostructures with desired physicochemical and functional properties. The goals of our research are: I. Development of the methods for growing bulk nanostructures of aluminum oxyhydroxides using oxidation in humid air or inert gas environment of the liquid metal alloys surfaces - Me(Al), where Me = Hg, Ga, In, Sn, Bi and Pb [1, 2]; II. Studies of the 3D structure evolution and nanoparticles morphology, chemical composition and phase transformations during heat treatment at the temperatures from 20 to 1700 °C; III. Development of the methods for chemical surface modification and filling free space in porous 3D nanostructures with nanoparticles of metals, oxides, and organometallic compounds.

The structure of raw nanomaterials grown at 25 °C has a density of 0.018 ± 0.005 g·cm^{-3} and consisting of aluminum oxyhydroxide nanofibrils 3D network with a diameter of ~ 5 – 9 nm and an average length a_0 ~ 100 – 300 nm [2, 3], Fig. 1. The use of an annealing up to 1700 °C causes an isotropic decrease of the sample's linear dimensions, the volume density increasing ~ 160 times up to 2.9 ± 0.1 g cm^{-3} and the open porosity decreasing from 99% to ~ 25%. This is very important technological possibilities allowing to control the physical parameters of 3D structure in a wide range, Fig. 2.

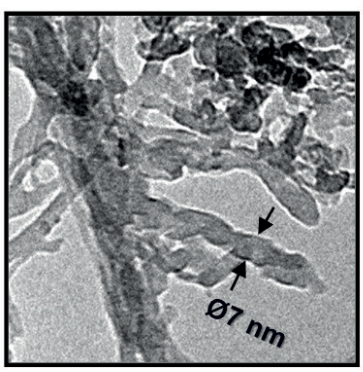

Fig.1. Nanofibrils of raw 3D structure.

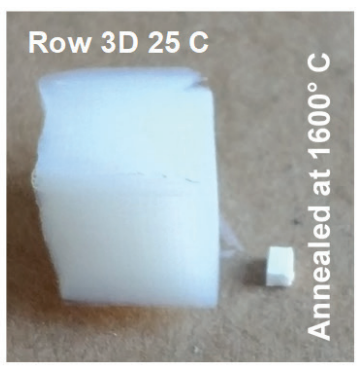

Fig.2. The annealing effect on the samples size.

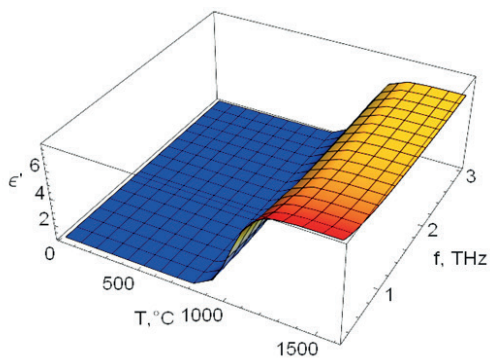

Fig.3. Effect of annealing on refractive index changing: ε'= f(*T*). Calculated values at 1 THz.

3D nanostructure parameters evolution during annealing were interpreted using a physical model that takes into account surface and volume mass transport and the kinetics of nanofibrils sintering,

Using the Bruggemann equation and the Maxwell-Garnett approximation, we developed a model of an effective medium, which makes it possible to take into account the effect of depolarization due to the nanofibrils elongated elliptical shape [4]. Modeling and estimations for the dielectric constant and refractive index carried out taking into account the structural-phase changes in the 3D nanomaterials after annealing at the temperatures up to 1700 °C, Fig. 3. Also were studied the 3D nanocomposites impregnated with oxide nanoparticles: TiO_2, ZrO_2, CeO_2 and with metallic nanoparticles: Ni ad Au.

[1] R. Sh. Askhadullin, A. A. Osipov, D. A. Skobeev, Liquid metal technology of synthesis of AlOOH anisotropic nanostructured aerogel. Nucl Energy Technol 3, 43-48, 2017.
[2] A. Khodan, T. H. N. Nguyen, M. Esaulkov, et al., Porous monoliths consisting of aluminum oxyhydroxide nanofibrils: 3D structure, chemical composition, and phase transformations in the temperature range 25 – 1700 °C. J Nanopart Res., 20, 194-204, 2018.
[3] A. N. Khodan, G. P. Kopitsa, Kh. E. Yorov et al., Structural Analysis of Aluminum Oxyhydroxide Aerogel by Small Angle X-Ray Scattering. J Synch Investig, 12, 296–305, 2018.
[4] E.A. Kekkonen, A.A. Konovko, E.S. Lee et al., Assessment of the degree of hydration of ocular surface tissues using THz reflectometry. Quantum Electronics, 50(1), 61-68, 2020.

DOI: 10.24412/cl-35039-2022-22-180-180

Fluorescence lifetime imaging of porous silicon nanoparticles in heart muscle cells

M.B. Gongalsky[1], D. Akimov[2], E. Tolstik[3], V. Sivakov[2], L.A. Osminkina[1]

1- Lomonosov Moscow State University, Faculty of Physics, Leninskie Gory 1, 119991 Moscow, Russia
2- Leibniz Institute of Photonic Technology, Albert-Einstein-Straße 9, 07745 Jena, Germany
3- Leibniz-Institut für Analytische Wissenschaften – ISAS – e.V.,
Bunsen-Kirchhoff-Straße 11, 44139 Dortmund, Germany
Email: mgongalsky@gmail.com

Porous silicon nanoparticles (pSiNPs) are promising biocompatible and biodegradable agents for various diagnostics and therapy including anticancer treatments [1]. In aqueous media pSiNPs demonstrate a variety of remarkable fluorescent properties attributed to recombination in Si or SiO_x phases [2]. Simple models are based on quantum confinement effect of charge carriers in Si/SiO_2 core/shell structures. That provides relatively long fluorescence decay times in the range of 1-100 μs due to indirect band gap of Si. However, under strong excitation very fast recombination (1-10 ps) may occur in the same core/shell structures [3]. Differences of the decay time allow to discriminate objects in fluorescence lifetime imaging technique (FLIM). This work is aimed to demonstrate capabilities of advanced time-resolved bioimaging of pSiNPs in biological systems. Previously it was shown that time-gated approach for imaging of pSiNPs can increase signal-to-noise ratio about 1000 times [4]. But it has never been tested in non-linear regime.

In present study we used mesoporous silicon nanoparticles, obtained by consequent electrochemical etching of Si wafers (orientation - (100), specific resistivity 1-10 mΩ*cm) in HF solution and grinding in a planetary ball mill (balls and glasses - ZnO_2). As a result 200-nm pSiNPs with porosity about 50-70%, pores and nanocrystals sizes about 10 nm are formed. However, during the formation, storage in aqueous solutions and incubation in cell cultures pSiNPs were additionally oxidized and core/shell structure with reduced 3-6 nm Si core were formed. PSiNPs were incubated with cardiac myoblast cells (H9c2) for 24 hours. The bioimaging of pSiNPs inside H9c2 cells is important, because they can potentially induce cardiotoxicity by themselves or by a drug loaded into their pores.

Images of pSiNPs in H9c2 were obtained by an inverted microscope at wavelength of 746 nm, which approximately corresponds to maximum of PL emission spectrum of pSiNPs. Fluorescence was excited by two photons with wavelength of 833 nm generated by a femtosecond Ti:sapphire laser. PSiNPs were distinguished on FLIM images by their ultrafast and slow fluorescence times. Ultrafast decay times was less than 100 ps, which was much faster than typical decay times of biological compounds (1-5 ns). Slow decay times were longer than 100 ns and appeared as visually constant component. Therefore, they were attributed to microsecond-scale recombination of excitons confined in Si/SiO_2 quantum dots.

Thus, we demonstrated for the first time, that FLIM can be used for imaging of porous silicon nanoparticles inside human cells. They can be distinguished with very high signal-to-noise ratio by their specific lifetimes, which are much shorter or much longer than typical autofluorescence lifetime. The proposed approach is promising for monitoring of silicon nanoparticles as containers for drug delivery or sono/photosensitizers in anticancer treatments.

This work was supported by the Russian Science Foundation (Grant № 22-75-10107).

[1] L. A. Osminkina *et al.*, "Microporous and Mesoporous Materials Porous silicon nanoparticles as ef fi cient sensitizers for sonodynamic therapy of cancer," *Microporous Mesoporous Mater.*, vol. 210, pp. 169–175, 2015.
[2] L. Canham, "Introductory lecture: origins and applications of efficient visible photoluminescence from silicon-based nanostructures," *Faraday Discuss.*, vol. 222, pp. 10–81, 2020.
[3] F. Trojánek, K. Neudert, P. Malý, K. Dohnalová, and I. Pelant, "Ultrafast photoluminescence in silicon nanocrystals studied by femtosecond up-conversion technique," *J. Appl. Phys.*, vol. 99, no. 11, p. 116108, Jun. 2006.
[4] L. Gu *et al.*, "In vivo time-gated fluorescence imaging with biodegradable luminescent porous silicon nanoparticles.," *Nat. Commun.*, vol. 4, p. 2326, 2013.

DOI: 10.24412/cl-35039-2022-22-181-181

Study of the molecular composition of cancer cells immobilized on SERS-active composite plasmonic nanostructures

L.A. Osminkina[1,2]

1- Lomonosov Moscow State University, Physics Department, Leninskie Gory 1, 119991 Moscow, Russian Federation
2- Institute for Biological Instrumentation of Russian Academy of Sciences, 142290 Pushchino, Moscow Region, Russian Federation
Main author email address: osminkina@physics.msu.ru

Surface-enhanced Raman spectroscopy (SERS) is a promising technique for label-free detection and analysis of different molecules, which highly sensitive detection is possible due to the enhancement of electromagnetic fields created by the excitation of localized surface plasmons [1]. Such plasmons can be excited by the interaction of incident light with a metallic rough surface or nanoparticles. As a result, a significant increase in Raman scattering (usually by 10^4-10^8) is observed when the analyzed object is on the nanostructured surface of plasmonic metals [2]. Currently, the SERS method has high sensitivity, excellent selectivity and non-destructive nature, so it is widely used for rapid detection of various chemicals, biomolecules and even living cancer cells [3-6].

In the present work, silicon nanowires (SiNWs) were obtained by electron beam lithography. The surface of the nanowires was decorated with gold nanoparticles (Au@SiNWs) to give them SERS-active properties. The structural properties of Au@SiNWs were examined using scanning (CarlZeiss SUPRA 40 FE-SEM) electron microscopy. MDA 231 human breast cancer cells were incubated on SiNWs and Au@SiNWs substrates for 24 hours and then fixed. To obtain microphotographs of cells on a fluorescence confocal microscope (laser excitation 405 nm), cell cytoplasm was stained with acridine orange (cytoplasm luminescence 520 nm), nuclei were stained with Hoechst 33341 (nuclear luminescence 460 nm), AuSiNWs were luminesced in the red spectral region at 630 nm. The molecular composition of cells immobilized on the obtained substrates was analyzed by Raman light scattering using a Confotec MR350 spectrometer.

According to the data obtained, there is a significant enhancement of the Raman signal from DNA, RNA, lipids, and proteins inside cells cultured on Au@SiNWs substrates compared to cells on SiNWs. Moreover, we have demonstrated that the position of the Au@SiNWs in the cell nucleus or cytoplasm can be clearly determined by measured SERS spectra. The nanowires literally pierce the cells, depending on scanning and fluorescence confocal microscopy. At the same time, the obtained Au@SiNWs are not toxic to the cells up to 4 days of incubation.

The substrates developed will help to approximate the understanding of bioprocesses and cellular functions on a molecular level, which could be crucial for progress in molecular cell biology, oncology, and pathology.

This work was supported by the Russian Science Foundation (Grant No. 20-12-00297).

[1] B. Sharma, R.R. Frontiera, A.I. Henry, E. Ringe, R.P. van Duyne. Materials today, 15(1-2), p. 16 (2012).
[2] P.L. Stiles, J.A. Dieringer, N.C. Shah, R.P. van Duyne. Annu. Rev. Anal. Chem., 1, p. 601 (2008).
[3] A. D. Kartashova, K. A. Gonchar, D. A. Chermoshentsev, E. A. Alekseeva, M. B. Gongalsky, I. V. Bozhev, A. A. Eliseev, S. A. Dyakov, J. V. Samsonova, L. A. Osminkina, Surface-Enhanced Raman Scattering-Active Gold-Decorated Silicon Nanowire Substrates for Label-Free Detection of Bilirubin. ACS Biomaterials Science & Engineering (2021).
[4] K. Kneipp, H. Kneipp, I. Itzkan, R.R. Dasari, M.S. Feld. Journal of Physics: Condensed Matter, 14(18), R597 (2002).
[5] S. N. Agafilushkina, O. Žukovskaja, S. A. Dyakov, K. Weber, V. Sivakov, J. Popp, D. Cialla-May, L.A. Osminkina Raman Signal Enhancement Tunable by Gold-Covered Porous Silicon Films with Different Morphology. Sensors, 20(19), 5634, (2020).
[6] D. Cialla-May, X.S. Zheng, K. Weber, J. Popp. Chemical Society Reviews, 46(13), p. 3945 (2017).

DOI: 10.24412/cl-35039-2022-22-182-182

Hybrid metal-semiconductor nanoparticles produced by laser ablation in liquid for optical nano-sensing, anti-counterfeiting and photothermal conversion

A. Kuchmizhak[3], S. Gurbatov[1,2], V. Puzikov[2],

1- Far Eastern Federal University, Vladivostok 690061, Russia
2- Institute of Automation and Control Processes, Far Eastern Branch of RAS, Vladivostok 690061, Russia
alex.iacp.dvo@mail.ru

Recent progress in hybrid nanomaterials composed of dissimilar constituents permitted to improve performance and functionality of novel devices developed for optoelectronics, catalysis, medical diagnostic and sensing. However, the rational combination of such contrasting materials as noble metals and semiconductors within individual hybrid nanostructures by a ready-to-use and lithography-free fabrication approach is still a standing challenge.

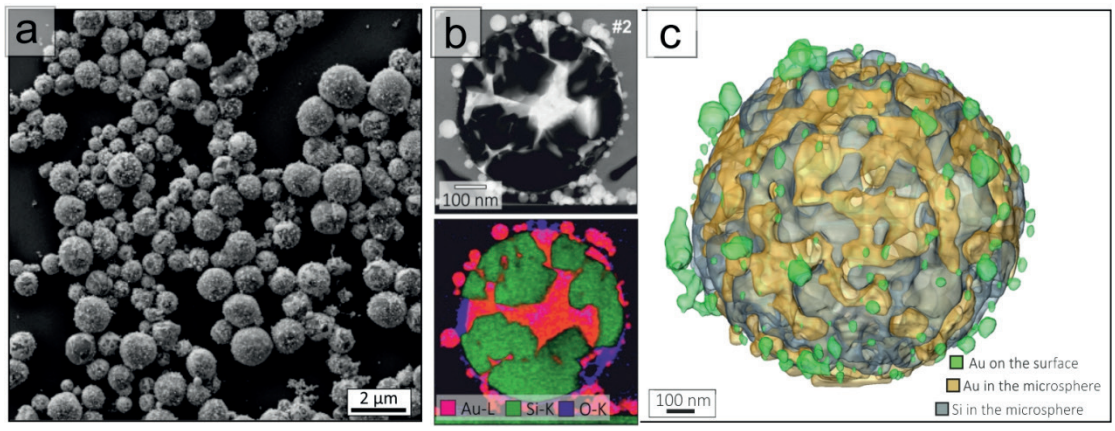

Fig. 1. (a) SEM image of the LAL-synthesized Au@Si nanoparticles. (b) TEM image and EDX elemental mapping of the isolated Au@Si nanoparticle. (c) 3D model of an isolated Au-Si MS reconstructed from a series of 50 cross-sectional focused ion-beam cuts. Several representative cuts are shown as insets. Au nanoparticles on the surface o a Au-Si MS are highlighted by green color to distinguish them from Au material (orange) mixed with Si within the particle.

In our recent works, we used nanosecond-laser ablation of the semiconductor nanoparticle suspensions and bulk targets in functionalizing solutions containing precursor noble metal salts for generation of novel metal-semiconductor (Au@Si, Ag@Si, Au@TiO_2) nanoparticles exhibiting unique morphology and optical properties. Generated nanomaterials were proved their usefulness for realization of SERS-based optical nanosensors for identification of molecular species at trace concentrations, anti-counterfeit labels based on physically unclonable function approach as well as solar steam generator that permits to increase the water evaporation rate by 2.5 times compared with that of pure water under identical 1 sun irradiation conditions [1-3].

[1] S. Gurbatov, V. Puzikov, A. Cherepakhin, E. Mitsai, N. Tarasenka, A. Shevlyagin, A. Sergeev, S.A. Kulinich, A. A Kuchmizhak, Hybrid Au@ Si microspheres produced via laser irradiation in liquid for nonlinear photonics, Optics & Laser Technology 147, 107666 (2022)
[2] S. Gurbatov, V. Puzikov, D. Storozhenko, E. Modin, E. Mitsai, A. Cherepakhin, A. Shevlyagin, A.V. Gerasimenko, S.A. Kulinich, A. Kuchmizhak, Hybrid Au-Si microspheres produced by laser ablation in liquid (LAL) for temperature-feedback optical nano-sensing and anti-counterfeit labeling, ACS Applied Materials & Interfaces (under review) arXiv preprint arXiv:2204.05124.
[3] S.O. Gurbatov, E. Modin, V. Puzikov, P. Tonkaev, D. Storozhenko, A. Sergeev, N. Mintcheva, S. Yamaguchi, N.N. Tarasenka, A. Chuvilin, S. Makarov, S.A. Kulinich, A. A Kuchmizhak, Black Au-Decorated TiO2 Produced via Laser Ablation in Liquid, ACS Applied Materials & Interfaces, vol. 13, 6522-6531, (2021).

DOI: 10.24412/cl-35039-2022-22-183-183

Electron-phonon coupling in the ensemble of colloidal quantum dots: combined study by spectral and time-resolved methods

A. I. Arzhanov[1,2,3], K. R. Karimullin[1,2,3], I. Yu. Eremchev[1,2,3], N. V. Surovtsev[4], A. V. Naumov[1,2,3]

1- Moscow Pedagogical State University, 29 Malaya Pirogovskaya str., 119992 Moscow, Russia
2- Lebedev Physical Institute, Russian Academy of Sciences, Branch in Troitsk, 11 Fizicheskaya str., 142190 Moscow, Troitsk, Russia
3-Institute for Spectroscopy, Russian Academy of Science, 5 Fizicheskaya str., 142190 Moscow, Troitsk, Russia
4-Institute of Automation and Electrometry, Siberian Branch Russian Academy of Sciences,1 acad. Koptyuga str., 630090 Novosibirsk, Russia
arzhanov.artyom@gmail.com

Semiconductor quantum dots (QD) are interesting objects due to their unique features [1,2]. In particular, the quantum size effect is observed in colloidal quantum dots. This effect makes it possible to obtain nanocrystals at the stage of synthesis different sizes and spectral properties. Such properties include variation in the position of the luminescence maximum, high photostability, and a wide absorption contour. Based on these properties, QDs are already used as phosphors for LEDs. They can also be used for medicine (as markers) and in photovoltaics. QDs can be embedded into various amorphous media as probes. Due to local field effects, single QDs are a very sensitive instrument to environmental parameters. The creation of various materials, such as QD-based composites, is of great importance in materials science, because such nanocomposites can have both optical and mechanical properties.

In this paper, we present combined methods for spectral diagnostics of local parameters of nanocomposites based on QD [3]. The parameters of the electron-phonon coupling were studied by measuring the temperature dependences of the exciton luminescence spectra for colloidal CdSe/CdS/ZnS quantum dots on a glass substrate and composites based on QD. Using the Varshni equation [4] for the temperature dependences of the band gap in bulk semiconductors, one can obtain a limited number of internal parameters. Using O'Donnell and Chen equation [5], it was possible to obtain the band gap parameters at zero temperature, Huang-Rhys factor and average phonon energy (E_{LO} = 21.4 meV). The last parameter correlates with direct Raman scattering measurements (E_{LO} = 25 meV) and also with photon echo experiments, where phase relaxation times were observed [6].

The work was carried out within the framework of the State Assignment of the Moscow Pedagogical State University (MPGU) "Physics of Nanostructured Materials: Fundamental Research and Applications in Materials Science, Nanotechnology and Photonics" with the support of the Ministry of Education of the Russian Federation (AAAA-A20-120061890084-9) together with the Centre for Collective Use "Structural Diagnostics of Materials" of the Federal Research Centre of the Russian Academy of Sciences "Crystallography and Photonics". The authors are members of the Leading Scientific School of the Russian Federation (grant of the President of the Russian Federation NSh-776.2022.1.2

[1] B.O. Dabbousi, J. Rodriguez Viejo, F.V. Mikulec, J.R. Heine, H. Mattoussi, R. Ober, K. F. Jensen and M. G. Bawendi, J. Phys. Chem. B 101 9463, (1997).
[2] S.B. Brichkin and V.F. Razumov Russ. Chem. Rev. 85 1297, (2016).
[3] K R Karimullin, A I Arzhanov, I Yu Eremchev, B A Kulnitskiy, N V Surovtsev and A V Naumov, Combined photon-echo, luminescence and Raman spectroscopies of layered ensembles of colloidal quantum dots, Laser Physics, 12, 29, p. 124009, (2019).
[4] Y. P. Varshni, Physica 34 149, (1967).
[5] K.P. Odonnell and X. Chen, Appl. Phys. Lett. 58 2924, (1991).
[6] K.R. Karimullin, M.V. Knyazev, A.I. Arzhanov, L.A. Nurtdinova and A.V. Naumov, J. Phys. Conf. Ser. 859 012010, (2017).

DOI: 10.24412/cl-35039-2022-22-184-184

Testing different models of fluorescence blinking in submicron perovskite crystals by studying photon statistics

A. Tarasevich[1,2,3], J. Li[4], A. Naumov[1,2], I. Eremchev[1,2], I. Sheblykin[4]

1 - Institute of spectroscopy RAS, Fizicheskaya 5, Troitsk, Moscow 108840, Russia
2 - Moscow pedagogical state university, Malaya Pirogovskaya Str. 1/1, Moscow 119991, Russia
3 - Higher school of economics, Pokrovsky bulvar 11, Moscow 109028, Russia
4 - Lund university, Box 124, Lund SE-22100, Sweden
Main author email address: ao.tarasevich@gmail.com

Perovskite crystals are of great interest to science and industry due to their high performance in photovoltaics [1]. At the same time, there is still no consensus on the nature of some phenomena, such as the fluorescence blinking in perovskites of submicron and even micron sizes. There are at least two models describing this phenomenon: the emitting site model and the super-trap model [2]. Both models equally well explain most of the effects in the luminescence of submicron perovskite crystals. The first implies that excitons are captured by one or several low-energy stable radiative recombination centers, each of which is a single photon source [3]. In this case, these centers can switch between two states (with a minimum and maximum quantum yield). The random switching of these centers explains the fluorescence blinking. The super-trap model postulates the existence of metastable high-efficient nonradiative recombination centers capable of capturing excitons, thereby quenching the fluorescence intensity of the whole crystal. Fluorescence flickering in this model is explained by the random appearance and disappearance of such traps [4].

The first model (in contrast to the second) implies the presence of at least partial antibunching of fluorescence photons. The main analyzed parameter was the value of second order cross-correlation functions of fluorescence photons around zero delays. An analysis of the measured functions showed the absence of photon antibunching effect both for the entire set of photons and for photons belonging to certain intensity levels. Received data let to make critical analysis of two models which are good in explanation of perovskites fluorescence blinking effect. [5].

This work was carried out with the financial support of the Russian Science Foundation (grant no. 20-12-00202).

[1] Stranks, S. D., & Snaith, H. J., Metal-halide perovskites for photovoltaic and light-emitting devices, Nature nanotechnology, 10(5), 391-402, (2015).
[2] Tian, Y., Merdasa, A., Peter, M., Abdellah, M., Zheng, K., Ponseca Jr, C. S., ... & Scheblykin, I. G., Giant photoluminescence blinking of perovskite nanocrystals reveals single-trap control of luminescence, Nano Letters, 15(3), 1603-1608, (2015).
[3] Yu, J., Hu, D., & Barbara, P. F., Unmasking electronic energy transfer of conjugated polymers by suppression of O2 quenching, Science, 289(5483), 1327-1330, (2000).
[4] Merdasa, A., Tian, Y., Camacho, R., Dobrovolsky, A., Debroye, E., Unger, E. L., ... & Scheblykin, I. G., "Supertrap" at work: extremely efficient nonradiative recombination channels in MAPbI3 perovskites revealed by luminescence super-resolution imaging and spectroscopy, ACS nano, 11(6), 5391-5404, (2017).
[5] Eremchev, I. Y., Tarasevich, A. O., Li, J., Naumov, A. V., & Scheblykin, I. G., Lack of Photon Antibunching Supports Supertrap Model of Photoluminescence Blinking in Perovskite Sub-Micrometer Crystals, Advanced Optical Materials, 9(3), 2001596, (2021).

DOI: 10.24412/cl-35039-2022-22-185-185

SERS-spectroscopy on microcrakes of metal coating of track-etched membranes

N. Kovalets[1], E. Kozhina[2], S. Bedin[1,2,3], I. Razumovskaya[1], A. Naumov[1, 2]

1- Moscow State Pedagogical University, Moscow, Russia
2- Lebedev Physical Institute RAS, Moscow, Russia
3- Center of Crystallography and Photonics of RAS, Moscow, Russia
bserg5@gmail.com

There are various methods for synthesizing SERS-active metasurfaces that allow achieving high enhancement and detecting ultra-low concentrations of various substances. One of the options for metasurfaces are substrates with nanostructures of a given geometry made of plasmonic metals, adjusted to the required resonant spectral range of the excited radiation source [1]. Another option for substrates is porous templates, for example, polymer track membranes (TM) chemically or physically coated with a plasmonic metal. Interest in the latter is largely related to the possibility of their application as flow systems for SERS spectroscopy of low concentrations of substances under study.

TM are a film with a system of calibrated pores. The pore diameter can vary from several tens of nanometers to several micrometers. If the surface of such a membrane is coated with a thin layer of plasmonic metal by vacuum deposition, then due to the presence of calibrated holes on the surface, a noticeable increase in the Raman signal from the detected compounds can be observed.

In this work, it was found that during uniaxial tension of a metallized track membrane in a metallized layer, a system of small pores arises on the surface, propagating between the pores. At small deformations, the distance between the crack edges is a few nanometers, which corresponds to the conditions for the formation of a gap hot spot between sharp crack edges.

In this work, commercial polymeric membranes were used (Dubna, Russia) made of polyethylene terephthalate (PET) with a thickness of 10 μm with a system of intersecting pores directed at an angle of about 43° to the membrane surface was chosen to create SERS-active metasurfaces 39. A pore diameter was 70 nm, and its surface density was $1{,}2 \cdot 10^9$ см$^{-2}$. A layer of silver or gold with a thickness of about 50 and 25 nm, respectively, was applied to one of the TM surfaces by thermal sputtering in a vacuum. For the uniformity of sputtering, TMs were placed on a rotating holder at an angle of 45 degrees to the sputtering source.

Samples of metalized TMs with a working part of 5x40 mm were cut using a REY RAN (Great Britain) manual cutting press. For uniaxial tension of the metallized TM, a manual tensile machine was used, which makes it possible to observe the deformation process on an optical microscope.

It was shown that the intensity of the Raman scattering signal of the characteristic malachite green peaks increases with increasing strain up to 15%. (Fig. 1) This effect seems to be associated with an increase in the number of small cracks. More surprising is the increase in signal intensity upon removal of deformation and relaxation of the metallized track membrane. In this case, the deformed polymer tends to return to its original size and tightens the edges of the cracks, pinching the malachite green molecules in the area of hot spots.

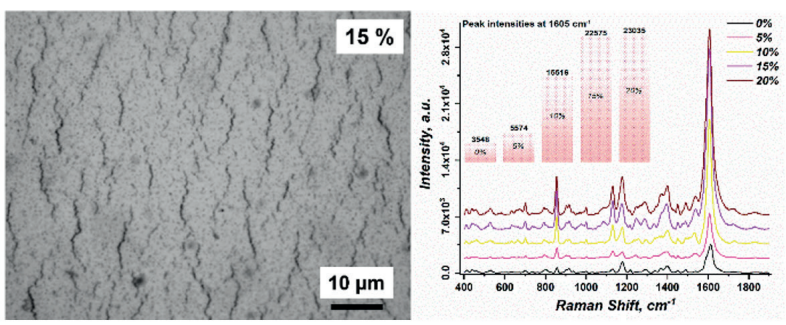

Рис. 1. Image of silver-metallized TM at 15% deformation and SERS spectra of malachite green adsorbed on the surface of TM at different deformations.

[1] E. Kozhina S. Bedin A., N. Nechaeva, S. Podoynitsyn, V. Tarakanov, S. Andreev, Y. Grigoriev, A. Naumov. Ag-Nanowire Bundles with Gap Hot Spots Synthesized in Track-Etched Membranes as Effective SERS-Substrates, Applied Sciences. Vol.11, pp. 1375, (2021)

DOI: 10.24412/cl-35039-2022-22-186-186

Ultrasensitive SERS active sensors based on leaning silver NWs bundles

E. Kozhina[1,2], S. Bedin[1,2], S. Andreev[1], A. Naumov[1,2,3]

1- Lebedev Physical Institute RAS, 119991 Moscow, Russia
2- Moscow Pedagogical State University (MPGU), 119991 Moscow, Russia
3- Institute for Spectroscopy RAS, 108840 Moscow Troitsk, Russia
Liza.kozhina.99@mail.ru

One of the most powerful techniques in analytical science is a Raman scattering. This method allows identifying the unique "fingerprints" of ultra-low analyte concentration, even to detect the infinitesimal angle deformation or elongation of the atomic bonds in the molecule. In addition, compared with the IR absorption spectroscopy the presence of water is not hindering its applicability. Within the years, Raman scattering was improved by developing the various plasmonic surfaces that allowed increasing the analyte signal intensity, leading to the formation of new spectroscopic methods such as the surface enhanced Raman scattering (SERS) and tip enhanced Raman scattering (TERS).

We offer a completely new approach to synthesis SERS-active substrates using track-etched membranes (TM) as a template. Due to significantly low pore density of TMs, we succeeded in achieving a NWs point contact and this is the key to a drastic increase in the SERS signal intensity/substrate sensitivity. Thanks to the variability of the surface pore density of the TM (may be varied from 10^5 to 10^9 cm^{-2}), the spacing between the tips of the individual NWs in the array is also can be varied [1]. That makes possible optimization of NWs density on the surface of the substrate for the gap hot spots formation.

Our substrates with the leaning neighboring silver (may be a different galvanically deposited material as well) nanowires (Ag-NWs) amplify the signal due to the presence of a gap hot spot and the NWs leaning feature may be observed in the real-time mode even in the optical microscope.

Furthermore, it is possible to increase the impact of the NWs agglomeration into the SERS signal enhancement upon synthesis the layered magneto-plasmonic NWs with a ferromagnetic nickel layer in the middle of NWs length [2]. In that case applying the magnet to the substrate before SERS spectra measurements because of the nickel layer there will be a narrow point contact between leaning NWs tips where the local electric fields will be highly concentrated. That may give us an increase in SERS spectra intensity which is an order of magnitude higher comparing with SERS spectra without magnet application (Fig. 1).

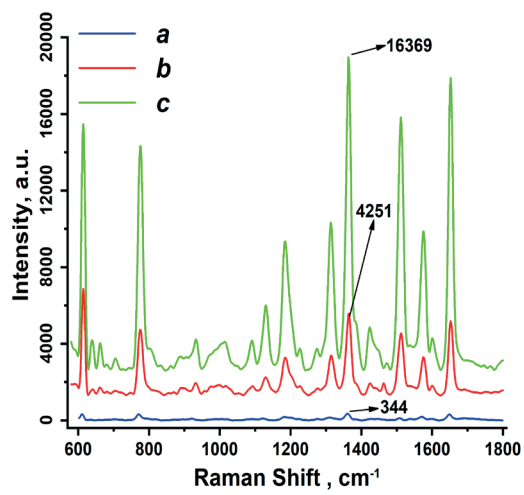

Fig. 1 (a) 10^{-3} mol R6G SERS spectra with magnet application to the substrate before spectra recording; (b) 10^{-3} mol R6G SERS spectra without magnet application; (c) 10^{-3} mol R6G adsorbed on glass Raman spectra.

[1] E. Kozhina S. Bedin A., N. Nechaeva, S. Podoynitsyn, V. Tarakanov, S. Andreev, Y. Grigoriev, A. Naumov. Ag-Nanowire Bundles with Gap Hot Spots Synthesized in Track-Etched Membranes as Effective SERS-Substrates, Applied Sciences. Vol.11, pp. 1375, (2021)

[2] E. Kozhina, E. Kulesh, S. Bedin, I. Doludenko, A. Piryazev, I. Korolkov, A. Kozlovskiy, M. Zdorovets, A. Rogachev, A. Shumskaya One-Dimensional Magneto-Optical Nanostructures: Template Synthesis, Structure, Properties, and Application in Spectroscopy Based on Plasmon Resonance, IEEE Magnetics Letters. Vol. 13. pp. 1-5 (2022)

DOI: 10.24412/cl-35039-2022-22-187-187

Quantum physics of nano-confined water

V.Uskov[1], M. A. Belyanchikov[1], M. Savinov[2], V. A. Abalmasov[3], E. S. Zhukova[1], V. G. Thomas[4] , B.Gorshunov[1]

1- Moscow Institute of Physics and Technology (National Research University), Moscow, Russia
2- Institute of Physics, Czech Academy of Sciences, Prague, Czech Republic
3- Institute of Automation and Electrometry SB RAS, Novosibirsk, Russia
4-Institute of Geology and Mineralogy, Russian Academy of Sciences, Novosibirsk, Russia; Novosibirsk State University, Novosibirsk, Russia
vladimir-ouskov@yandex.ru

Since separate water molecules possess large electric dipole moment (1.85 Debye) their mutual ferroelectric/antiferroelectric ordering mediated by dipole-dipole coupling can be expected. In liquid water or water ice such ordering does not happen due to intermolecular hydrogen bonds that overwhelm dipolar interaction. The existence of a so-called "water ferroelectricity" has been the subject of debate for decades. It is believed that water ferroelectricity can play crucial role in a variety of phenomena and areas of natural sciences, e.g., geology, mineralogy, meteorology, soil chemistry, biology, pharmaceutics, food industry and materials science, as well as in the living organisms (water in cells and membrane channels, and proteins hydration shells) and even in the universe (formation of planets or of prebiotic compounds). It turned out, however, that a detailed study of the phenomenon is hampered by the difficulties of its implementation in laboratory conditions. Since years, corresponding experimental results remained controversial, so that the community had to be "satisfied" with theoretical considerations and computer simulations of possible ordering of H_2O molecular dipoles.

We found an ideal workbench for studying single-particle and collective effects, including ferroelectricity, in ensembles of dipole–dipole coupled water molecules. It is provided by hydrated dielectric crystals of the beryl family. The crystals contain just separate H_2O molecules isolated within nanosized voids formed by the lattice ions. Being only weakly linked to the ions and separated by 5–10 Å, the water molecules do not experience H-bonding (interaction length 1–2 Å); nevertheless, they interact via longer-range dipole–dipole coupling (interaction length 10–100 Å). This kind of network is of broad interest and fundamental importance providing the opportunity to study not only the famous "water ferroelectricity", but also diverse quantum physics of electric-dipolar systems whose properties should be qualitatively different from those occurring in well studied systems with magnetic moments.

We have discovered quantum paraelectricity [1,2] and fingerprints of quantum critical behavior [3], below 20-30 K, of a network of H_2O molecules hosted by the hexagonal matrix of beryl crystal lattice. Below T=0.5 K, we discover an ordered state of water molecules, with the phase transition of yet unknown nature. In orthorhombic matrix of a relative crystal, cordierite, we have observed an order-disorder type ferroelectric phase transition [4], at around 3 K, into a complex ferroelectrically/antiferroelectrically ordered state of polar H_2O molecules. In addition to collective phenomena, we studied single-particle excitation of translational and librational types of separate nano-confined H_2O/D_2O molecules [5,6].

The research was supported by the Russian Science Foundation, Grant 22-22-00091.

[1] Gorshunov et al. Quantum Behavior of Water Molecules Confined to Nanocavities in Gemstones. J. Physical Chemistry Letters, **4** 2015 (2013)
[2] Gorshunov, et al. Incipient ferroelectricity of water molecules confined to nano-channels of beryl. Nature Communications 7, 12842 (2016).
[3] Belyanchikov et al. Fingerprints of critical phenomena in a quantum paraelectric ensemble of nanoconfined water molecules. Nano Letters (2022) https://doi.org/10.1021/acs.nanolett.2c00638
[4] Belyanchikov et al. Dielectric ordering in dipolar lattice of water in cordierite. Nature Communications. **11,** 3927 (2020)
[5] Belyanchikov et al. Vibrational states of nano-confined water molecules in beryl investigated by first principles calculations and optical experiments. Physical Chemistry Chemical Physics, **19**, 30740 (2017)
[6] Belyanchikov et al. Single-particle and collective excitations of polar water molecules confined in nano-pores within cordierite crystal lattice. Physical Chemistry Chemical Physics. **24**, 6890-6904 (2022)

DOI: 10.24412/cl-35039-2022-22-188-188

Raman scattering spectra in zinc oxide microstructures placed in photon traps

I.A.Rakhmatullaev[1], N.V.Tcherniega[2], M.Kh.Davronov[1], O.M.Tursunkulov[1]

[1]Center for Advanced Technologies under the Ministry of Innovative Development of the Republic of Uzbekistan, 3a, Talabalar shaharchasi str., 100174, Tashkent
[2]P.N. Lebedev Physical Institute of the Russian Academy of Sciences, Leninskii prospect, 53, 119991, Moscow
e-mail: ilyoss@rambler.ru

In recent years, interest in studying the structures of zinc oxide (ZnO) has increased significantly due to the high demand for this material [1,2]. In this work, the synthesis of ZnO microstructures was carried out by the method of microwave decomposition: 2 g of ZnO powder (Aldrich, 99% purity) and 1 ml of ethylene glycol solution were mixed and ground in an agate mortar for 20 min. Then, 2 g of the mixed powder was loaded into an alumina crucible and placed in the center of a microwave oven for 15 min at 180°C. As a result, samples in the form of extended rods were obtained. The surface morphology of ZnO microstructures was studied using a SEM-EVO MA10 scanning electron microscope (Carl Zeiss, Germany). The analysis showed (Fig. 1) that the samples are formations in the form of randomly oriented agglomerates with transverse dimensions up to 8 μm. Raman spectra (RS) were recorded using a technique described in detail in [3,4]. RS were excited by the green line of a copper vapor laser (λ=510.6 nm) [3,4].

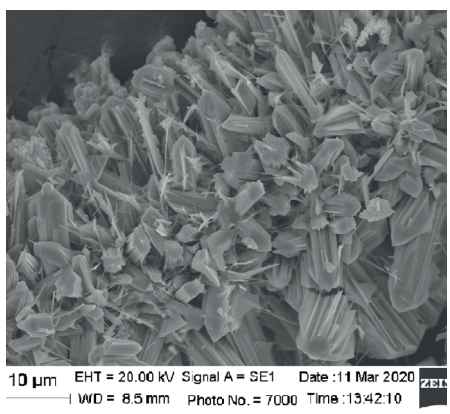

"**Fig. 1.** SEM image of ZnO microstructures"

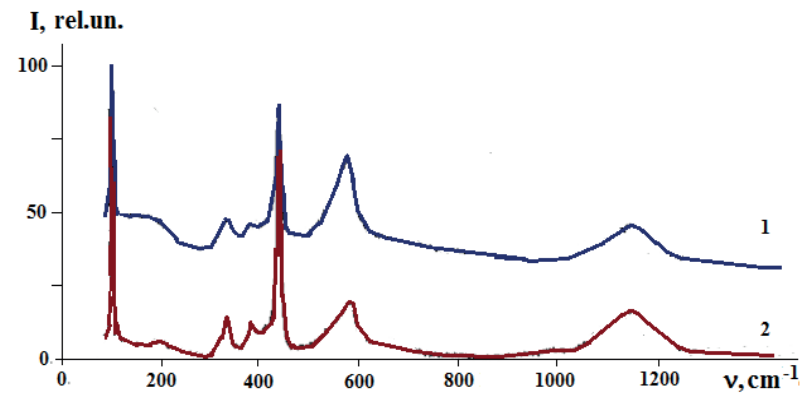

"**Fig. 2.** Raman spectra of ZnO microstructures of various sizes when they are excited by the green line of a copper vapor laser (λ_{ex}=510.6 nm): 1 - d_{av}=3 μm; 2 - d_{av} =7 μm (I_{exc}~ 10^5 W/cm^2)"

The main spectral change observed in the RS of the samples with different average dimension under study (Fig. 2) consists in a monotonic increase in the intensity of the $E_1(LO)$ mode (580 cm^{-1}) and the appearance of a shoulder in the region of 100–200 cm^{-1}, similarly to the results obtained in [2]: the following modes were identified in the RS of ZnO powders: 1) the mode with a frequency of ~100 cm^{-1}; 2) the mode at ~ 340 cm^{-1}, which is attributed to the difference phonon $\mathring{A}_2^{high} - \mathring{A}_1^{low}$; 3) at ~ 435 cm^{-1}; 4) $E_1(LO)$ at ~580 cm^{-1}; 5) a wide band between 1060 and 1190 cm^{-1}, which can be assigned to a combination of the A_1 and E_2 modes. It was found that with a decrease in the size of the microstructures of the sample, an increase in the intensity of the RS signal is due to the fact that pores are formed between the faces of large particles, which contribute more to the scattered light than to the effective absorption of exciting radiation. This is also explained by the fact that when excitation radiation with a wavelength smaller than the size of microparticles enters such structures, radiation can be trapped as a result of multiple reflections from the walls of microresonator cuvettes (photon traps).

[1] B.O. Chin, Y.N. Law, W.M. Abdul. A review of ZnO nanoparticles as solar photocatalysts: synthesis, mechanisms and applications, Renewable and Sustainable Energy Review. vol.81, pp. 536-551 (2018).
[2] I.A. Averin, I.A. Pronin, N.D. Yakushova et al. Analiz strukturnoy evolyutsi poroshkov oksida tsinka, poluchennix metodom mexaicheskogo visokoenergeticheskogo razmola, J.Tex.fiz. vol.89, No. 9, pp.1406-1411 (2019).
[3] V.S. Gorelik, I.A. Rakhmatullaev. Excitation of Raman optical processes in an ultradispersed medium by radiation from a pulsed-periodic laser, Technical Physics, vol. 50, No. 1, pp. 61-64 (2005).
[4] I.A. Rakhmatullaev, V.S. Gorelik, R.A. Muminov et al. Photoluminescence and Raman spectra of diamond micropowders placed in photon traps, Scientific-technical journal, vol. 4, No. 1, 46-53 (2021).

DOI: 10.24412/cl-35039-2022-22-189-189

Laser-induced deposition of topologically controlled nanometal surfaces for sensing and electrochemistry

Anna Vasileva[1], Gulia Bikbaeva[1], Daria Mamonova[1], Ilya Kolesnikov[2], Dmitry Pankin[2], and Alina Manshina[1],*

[1] Institute of Chemistry, St. Petersburg State University, St. Petersburg 198504, Russia
[2] Center for Optical and Laser Materials Research, St. Petersburg State University, St. Petersburg, Russia
**e-mail: a.manshina@spbu.ru*

We found that synthesis in laser light (or laser-induced deposition LID) is efficient and easy-to-realize approach allowing creation of nanostructures with controlled chemical composition, morphology and spatial distribution [1,2,3]. The peculiarity of the LID process is the formation of metal nanophase directly on the substrate thus allowing combining synthesis of nanoparticles (NPs) and their immobilization on the surface in a single-step procedure. The significant advantage of LID is connected with the following features (i) spatial localization of the process in the laser-affected area; (ii) no destructive effects of mild laser irradiation, as a result no decomposition of deposits or substrate; (iii) precise control of composition, structure, and morphology of nanostructures that all together provides fine-tuning of deposits functionality; and (iv) process's sensitivity to laser intensity that allows deposition of topologically controlled NPs in structured laser beams. As a bright demonstration of LID potency, we present 3D electrodes that are nanoporous anodic aluminum oxide (AAO) with mono- and multimetallic nanoparticles deposited inside of the nanoscale pores with high aspect ratio (Figure 1). The obtained 3D electrodes were found to be efficient in electrochemical reactions of glucose oxidation and as glucose sensors (mouse blood plasma as analyte). Another example of LID capacity is creation of periodic arrays of plasmonic nanoparticles with high SERS efficiency and ultralow detection limit of 10^{-11}M.

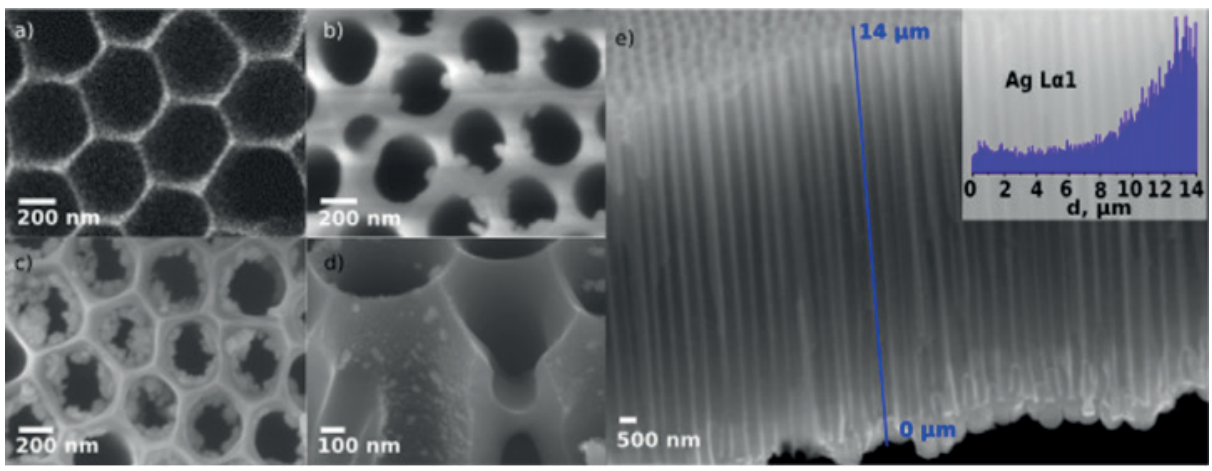

Figure 1. Laser-induced deposition on 3D templates: (a) pure AAO template; (b) PtAg@C NPs on AAO; (c) PtAg@C NPs on AAO modified with silanization; (d) PtAg@C NPs on AAO modified with silanization — cross-section view; (e) silver distribution on sample, inset — EDX data across the line.

This work was supported by RFBR project 20-58-12015. Authors are grateful to "Centre for Optical and Laser materials research", "Centre for X-ray Diffraction Studies" and "Interdisciplinary Resource Centre for Nanotechnology" Research Park of Saint Petersburg State University for technical support.

[1] A. Vasileva, S. Haschke, V. Mikhailovskii A. Gitlina, J. Bachmann, A. Manshina Nano-Structures & Nano-Objects 24, 100547 (2020).
[2]. D. V. Mamonova, A. A. Vasileva, Y. V. Petrov, A. V. Koroleva, D. V. Danilov, I. E. Kolesnikov, G. I. Bikbaeva,, J. Bachmann, and A. A. Manshina, Nanomaterials 12(1), (2022)
[3] D.V Mamonova, A.A.Vasileva, Y.V.Petrov, ... J.Bachmann, A.A.Manshina, Materials, 14(1), p. 1–14, (2021)

DOI: 10.24412/cl-35039-2022-22-190-190

Spectral variables selection in multivariate calibration of concentrations of C, Mn, Si, Cr, Ni, AND Cu in low-alloy steels by LIBS method

M. Belkov, D. Borisevich, K. Catsalap, M. Khodasevich

B.I.Stepanov Institute of Physics, National Academy of Sciences of Belarus, Minsk, Nezavisimosti Ave., 68-2
email address: m.khodasevich@ifanbel.bas-net.by

The advantages of the laser induced breakdown spectroscopy (LIBS) for determining the composition of steels are express multi-element analysis in the open air and the relatively low cost of instrument implementation. The main drawback of LIBS is the lack of accuracy in quantitative measurements [1]. Spectrometers with low spectral resolution are used usually in portable and mobile LIBS devices. Due to the strong overlap of the analytical lines in this case, the classical univariate calibration is inapplicable and multivariate models considering a large number of spectral variables are widely used [2]. Earlier the wideband low-resolution emission spectra (190-440 nm, resolution 0,4 nm, step 0,1 nm) of low-alloy standard steels were recorded in experimental conditions described in [3]. For training dataset selection the Kennard-Stone algorithm is applied to 31 to 39 standard steels. Multivariate models for calibration of C, Mn, Si, Cr, Ni and Cu concentrations without spectral variables selection were developed with root-mean-square error (RMSE) of prediction 0,06 % for C, 0,12 % for Mn, 0,09 % for Si, 0,13 % for Cr, 0,07 % for Ni and 0,08 % for Cu. Here three methods of spectral variables selection are used for improving the calibration accuracy: method of ranking spectral variables by their correlation coefficient with the value of the calibrated parameter [4], a successive projection algorithm [5] and an original modification of the method of searching combination moving windows for partial least squares model (scmwiPLS) [6]. The last model is the best and quantitative for C (RMSE = 0,004 %, the residual prediction deviation (RPD) in the test dataset is 23,4 in the concentration range from 0,13 to 0,43 %), for Mn (0,04 % and 5,2 in the range of 0,47–1,15 %), for Si (0,003 % and 20,7 in the range of 0,15–0,33%), for Cr (0,04 % and 3,1 in the range of 0,09–0,43 %) and for Ni (0,01 % and 4,8 in the range of 0,05–0,25 %). Calibration model is considered quantitative if RPD exceeds 3. For Cu in the concentration range of 0,06–0,26 %, scmwiPLS model is qualitative only (RMSE = 0,04 % and RPD = 1,4). Figure 1 shows the predicted vs measured values of C concentration for wideband PLS model and for scmwiPLS model. One can see a significant improvement in calibration accuracy.

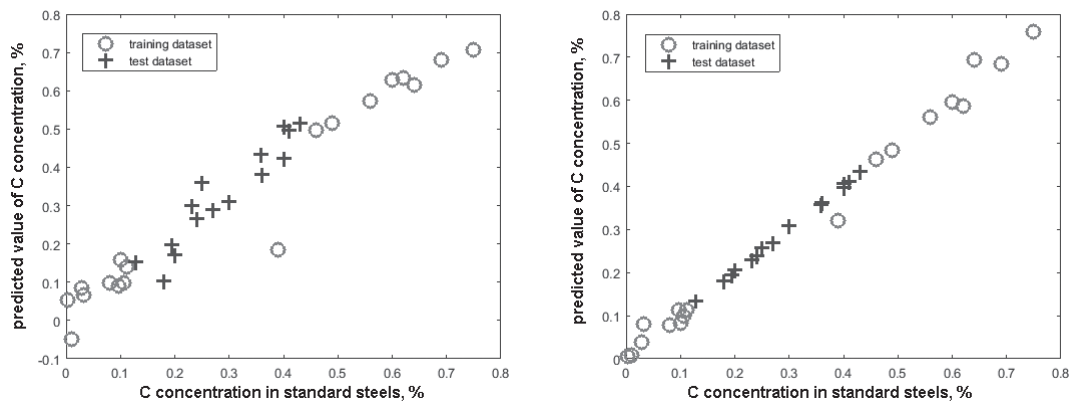

Fig. 1. Predicted vs measured values of C concentration for wideband PLS (left) and for scmwiPLS (right) models.

[1] D. Syvilay [et al.], Guideline for increasing the analysis quality in laser-induced breakdown spectroscopy, Spectrochimica Acta Part B: Atomic Spectroscopy, vol.. 161, pp. 1–34 (2019).
[2] Z. Wang [et al.], Recent advances in laser-induced breakdown spectroscopy quantification: From fundamental understanding to data processing, TrAC Trends in Analytical Chemistry. Vol. 143, pp.116385-1–21 (2021).
[3] M. Belkov [et al], Multivariate Calibration of Concentrations of C, Mn, Si, Cr, Ni, and Cu in Low-Alloy Steels from Raw Low-Resolution Spectra Obtained By Laser-Induced Breakdown Spectroscopy, Journal of Applied Spectroscopy, vol. 88, pp.970-974 (2021).
[4] Z. Xiaobo [et al.], Variables selection methods in near-infrared spectroscopy, Analytica Chimica Acta, vol. 667, pp. 14–32 (2010).
[5] S.F.C. Soares [et al.], The successive projections algorithm, Trends in Analytical Chemistry, vol. 42, pp. 84–98 (2013).
[6] M. Khodasevich, V. Aseev, Selection of Spectral Variables and Improvement of the Accuracy of Calibration of Temperature by Projection onto Latent Structures Using the Fluorescence Spectra of Yb^{3+}:CaF_2, Optics and Spectroscopy, vol. 124, pp. 748–752 (2018).

DOI: 10.24412/cl-35039-2022-22-191-191

Dielectric, infrared and Raman spectroscopy of $BiScO_3$

A. Bush[1,2], V. Kozlov[2], V. Trotsenko[1], E. Zhukova[1], A. Serovaiskii[3], V. Kutcherov[3]

1 - Moscow Institute of Physics and Technology (National Research University), Moscow, Russia
2 - MIREA − Russian Technological University (RTU MIREA), Moscow, Russia
3 - Gubkin Russian State University of Oil and Gas (National Research University), Moscow, Russia
Main author email address: kozlov380@yandex.ru

Bismuth ferrite $BiFeO_3$ is a unique ferromagnet that combines ferroelectric and ferrimagnetic properties. Unlike other known ferromagnetic materials, the ferroelectric Curie temperature (T_C = 840 °C) and the ferrimagnetic Neel temperature (T_N = 340 °C) of the compound significantly exceed the room temperature, which makes $BiFeO_3$ promising for applications in electronic engineering [1–2]. It is considered [1] that other members of the family of the $BiMO_3$ perovskite phases (M = Sc, Y, Cr, Mn, Fe, Co, Ni) can also exhibit ferromagnetic properties similar to those of $BiFeO_3$. Among the series, only $BiFeO_3$ can be formed at atmospheric pressure, while other members of the family are formed only at high pressures (6–10 GPa) [1, 3]. Due to the complexity of the synthesis of these compounds, their properties remain poorly understood. In this report, we describe the conditions for the synthesis of samples of the $BiScO_3$ phase with a perovskite structure under thermobaric conditions, and present the results of studies of their dielectric properties, infrared and Raman spectra. Single-phase samples of the $BiScO_3$ phase with a perovskite structure were obtained at temperatures T = 1000 – 1200 °C and pressures p = 6.0 – 7.5 GPa using a high pressure-high temperature unit URS-2 (Technological Institute of Superhard and New Carbon Materials - TISNUM, Troitsk). Detailed studies of temperature (T = 10 – 350 K) and frequency (f = 25 Hz – 1 MHz) dependences of permittivity dielectric ε'(T) and dielectric loss tangent tgδ(T) did not reveal any pronounced features characteristic of phase transitions. For the first time, the infrared (frequencies 30 – 15600 cm^{-1}) and Raman (frequencies 90 – 2000 cm^{-1}) spectra of the perovskite phase of $BiScO_3$ were studied. Quantitative information was obtained on the parameters of infrared and Raman phonon resonances (frequency positions, dielectric contributions and damping constants). It is found that the number (48) of observed infrared modes is significantly larger than the number (27) predicted by factor group analysis performed for the noncentrosymmetric space group C2, while the number (up to 26) of observed Raman resonances corresponds to a situation with 30 active modes of the centrosymmetric group C2/c. Based on a detailed analysis of infrared and Raman spectra, it was concluded that the crystal structure of the synthesized $BiScO_3$ phase is centrosymmetric. The additional resonances are observed in the infrared and Raman spectra and explained by the violation of the selection rules due to crystal structure distortions and/or the presence of strong local distortions of the crystal structure caused by the Bi^{3+} lone pair of electrons.

The research was supported by the Russian Science Foundation (grant 21-12-00358, study of dielectric properties in the low-frequency range, measurements of infrared and Raman spectra) and the Russian Foundation for Basic Research (grant 20-02-00915, part of the work on thermobaric synthesis of samples).

[1]. Venevtsev Yu.N., Gagulin V.V., Lyubimov V.N. Seignetomagnetics. Moscow: Nauka 1982.
[2]. Catalan G., Scott J.F. Advanced Materials. 2009. V. 21. P. 2463.
[3]. Belik A.A., Iikubo S., Kodama K. et. al. J. Am. Chem. Soc. 2006. V. 122. P. 706.

DOI: 10.24412/cl-35039-2022-22-192-192

Determination of particle concentrations from absorption spectra with fast frequency tuning

V. Lagunov[1], V.Ochkin[1], A.Volkova[1,2]

1- P N Lebedev Physics Institute, Russian Academy of Sciences, Moscow, Russian Federation
2 - Department of Physics, M.V. Lomonosov Moscow State University, Russian Federation
lagunoww@yandex.ru

When the frequency of probing lasers is rapidly tuned, distortions can appear in the absorption spectra, the nature of which depends on the measurement scheme. For single-pass schemes, the effect was observed in [1] and is associated with the interference of the incident radiation and the coherent radiation of the medium induced by the incident radiation. Later, it was repeatedly studied, especially with the development of quantum-cascade laser technology (eg, [2-4]). Features of the spectrum dynamics in measurements with long optical paths inside multi-pass resonators were recently noted in [5]. The question of the possibility of determining particle concentrations from such contours remained open. It is especially relevant for measurements at low particle density, because with its increase the coherence of the interaction of light with particles disappears. In this paper, this issue is investigated for both schemes.

It is shown that in single-pass measurements errors arise due to not taking into account the saturation of the optical transition when interpreting the spectra. Figure 1 shows distortions of the contour of the absorption line of ethylene (a) and the results of measurements of the concentration of these particles (b). Accounting for saturation leads to results close to true concentrations not only at high but also at low pressures of the buffer gas.

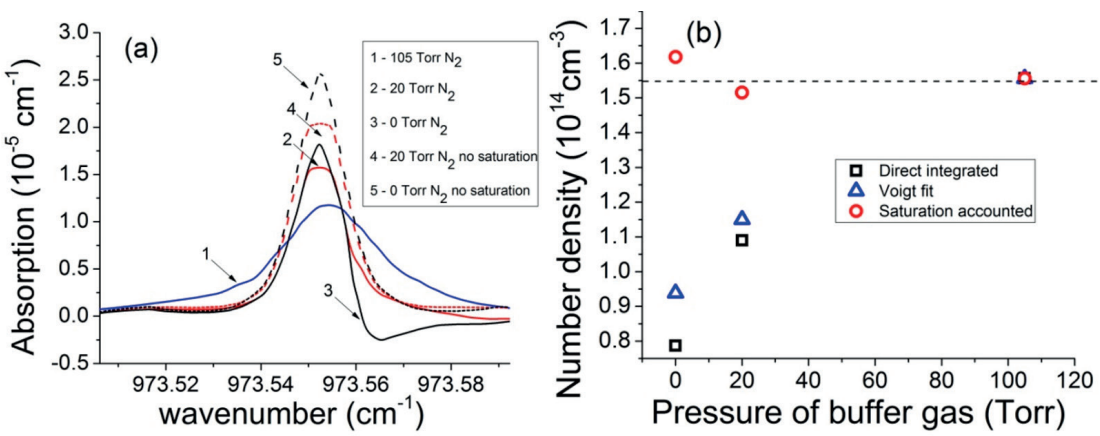

Fig.1. (a) Ethylene absorption contours at a density of $1.55 \cdot 10^{14}$ cm^{-3} with various additions of nitrogen, scanning speed 300 MHz/ns. The solid lines are the measurements from [4], the dashed lines are the correction taking into account saturation. (b) Ethylene concentration measurements with and without nitrogen additions. The dashed line is the true concentration. Squares are direct integration of experimental contours, triangles are Voigt contour approximation, circles are integration of contours corrected for saturation.

For a laser system with an external multi-pass resonator, dynamic distortions already occur at frequency tuning rates approximately two orders of magnitude lower than for measurements on relatively short paths in open space. This is because, at a high quality factor of the resonator, the length of the optical path can exceed the coherence length of the laser source. In this case, the deformations of the contour are of a different nature, not demonstrating areas of negative absorption (Fig. 1a), and the classical Beer-Bouguer-Lambert law is satisfied for the integral absorption. This work was supported by a grant from the Russian Science Foundation (project No.19-12-00310).

[1] S. N. Andreev, et al., Coherent spectroscopy with fast frequency swept lasers, Optics and Spectroscopy, 119.3, 385-391, (2015).
[2] J. H. Van Helden, S. J. Horrocks, G. A. D. Ritchie, Application of quantum cascade lasers in studies of low-pressure plasmas: Characterization of rapid passage effects on density and temperature measurements, Applied Physics Letters, 92(8), 081506, (2008).
[3] G. Duxbury, et al., Rapid passage induced population transfer and coherences in the 8 micron spectrum of nitrous oxide, Molecular Physics, 105.5-7, 741-754, (2007).
[4] M. T. McCulloch, G. Duxbury, N. Langford, Observation of saturation and rapid passage signals in the 10.25 micron spectrum of ethylene using a frequency chirped quantum cascade laser, Molecular Physics, 104.16-17, 2767-2779, (2006).
[5] Lagunov, V. V., I. V. Nikolaev, V. N. Ochkin, High-resolution and high-sensitivity absorption spectroscopy in external optical resonators with fast frequency tuning, Spectrochimica Acta Part A: Molecular and Biomolecular Spectroscopy, 246, 119060, (2021).

DOI: 10.24412/cl-35039-2022-22-193-193

High-Speed GaInAsSb/GaAlAsSb Photodetectors for Precision Diode Laser Spectroscopy

E.V. Kunitsyna[1], I.A. Andreev[1], G.G. Konovalov[1], A.A. Pivovarova[1], N.D. Il`inskaya[1], Yu.P. Yakovlev[1], Ya.Ya. Ponurovskii[2], A.I. Nadezhdinskii[2], A.S. Kuz'michev, D.B. Stavrovskii[2], M.V. Spiridonov[2]

1- Ioffe Institute, 26 Politekhnicheskaya str., 194021 St. Petersburg, Russia
2 - A.M. Prokhorov General Physics Institute of Russian Academy of Science, 38 Vavilov str., 119991 Moscow, Russia
kunits@iropt9.ioffe.ru

Diode laser spectroscopy (DLS) is one of the most dynamically developing fields of laser physics as applied to the challenges of analytical chemistry and gas analysis [1]. Recent advances in the technology of IR optopairs "diode laser – photodetector" and high-sensitivity IR absorption spectrometry result in a new generation of gas analytical systems. These systems are characterized by record spectral resolution and high operating speed.

Registration of laser radiation in the near- and mid-IR spectral ranges is one of the most important problems of laser physics. Photodetectors based on lead chalcogenides usually demonstrate the time constant of 100–400 μs. They are hardly applicable for operating with diode lasers that require significantly higher speed. Other widely applied IR photodetectors are InSb-based photodiodes [2]. However, cooling to 80–200 K is required for the effective operation of most InSb-based devices.

The uncooled high-speed photodetectors based on n-GaInAsSb/p-GaAlAsSb heterostructures have been developed for precision DLS. These heterostructures were LPE grown on n-GaSb(100) substrates doped with tellurium to a carrier concentration of $(1–5)\times10^{17}$ cm^{-3}. The active region was the epitaxial layer of the narrow-gap $GaIn_{0.22}AsSb$ solid solution (E_g = 0.53 eV). The $GaAl_{0.34}AsSb$ epitaxial layer (E_g =1.1 eV) was used as a "wide-gap window". Chips with diameters of the photosensitive area of 1.0 mm and 2.0 mm were made from the grown heterostructures by contact photolithography and liquid chemical etching. To protect the lateral surface of the mesa and *p–n* junction, anodic oxide was formed in the electrolyte solution (0.3% tartaric acid/ethyleneglycol in the ratio 1:2). The thickness of the oxide obtained at U = 60 V and j = 5 mA/cm^2 was ~0.3 μm. The Cr/Au/Ni/Au system and a galvanic Au layer were used as a contact system to the Al-containing epitaxial p-layer. The contact enhancement makes it possible to assemble photodiodes at elevated solder temperatures of 200–230°C. The contact to the n-GaSb(100) substrate was formed by sputtering the Cr/Au/Ni/Au system with subsequent sputtering of an additional Cr/Au layer.

The spectral sensitivity range of photodetectors with a photosensitive area diameter of 1.0 mm and 2.0 mm is 1.0−2.4 μm at T=300 K. The long-wavelength boundary of the spectral sensitivity is determined by the band-gap energy of the GaInAsSb active region. The sensitivity gradually decreases in the shorter wavelength part of the spectrum towards short wavelengths, which is associated with absorption at indirect-gap transitions in the layer of the Al-containing solid solution. So, the short-wavelength spectral sensitivity boundary is determined by the band-gap energy of the "wide-gap window". The current monochromatic sensitivity at the wavelength of 2.1 μm has a value of 1.0 A/W without bias. The capacity reaches 375 pF with a photosensitive area diameter of 1.0 mm and 800–5000 pF with 2 mm. The operating speed of the developed photodetectors is 30–45 ns with a diameter of 1 mm and 100–770 ns with a diameter of 2 mm. It is demonstrated, that these values are sufficient for operation of photodetectors as part of DL gas analyzers.

The modern gas analyzers based on diode lasers and developed GaInAsSb/GaAlAsSb photodetectors for medical screening diagnostics by analyzing the gas compositions of exhaled air, for control of impurity gases in the process of rectification of inorganic hydrides, control of methane leaks in gas pipelines, as well as for registration of exhaust gases of a moving car are presented.

[1] Ya.Ya. Ponurovskii, A new generation of gas analysis systems based on diode lasers, Analytics, vol.9(1), pp.68–74 (2019).
[2] B. W. Jia, K. H. Tan, W. K. Loke, S. Wicaksono, K. H. Lee, S. F. Yoon, Monolithic integration of InSb photodetector on silicon for mid-infrared silicon photonics, ACS Photonics, vol.5, pp. 1512–1520 (2018).

DOI: 10.24412/cl-35039-2022-22-194-194

Developing Compact LIDAR Systems: Size and Eye-Safety Matters

V.N. Lednev, M.Ya. Grishin, P.A. Sdvizhenskii, V.A. Zavozin, S.M. Pershin, A.F. Bunkin

Prokhorov General Physics Institute, Russian Academy of Science, Moscow, Russia
lednev@kapella.gpi.ru

LIght Detection And Ranging (LIDAR) systems were first suggested in early 1960-s when powerful pulsed lasers became available. However, large-sized, heavy and highly power consuming LIDAR systems required powerful aircraft vehicles to perform airborne remote sensing so the LIDAR technology was not widely used and mainly adopted for stationary systems. The progress in laser and detector production progress made it possible to develop compact and energy-efficient LIDAR systems. An eye-safety requirement is a mandatory condition for LIDAR application in real life so modern instruments should fulfil this requirement. A new generation of fully digital eye-safe LIDAR instrument was suggested in early 1990-s based on pulsed diode laser and single-photon avalanche photodiode [1]. Compact LIDAR development opens new perspectives for remote laser sensing of different objects like online control in agriculture [2] or aerosol studies in extraterrestial missions [3]. Here, we present the eye-safe digital LIDAR instrument operation principles as well as recent progress in its developments. Recent progress of compact LIDAR development to be installed at unmanned aircraft vehicles is discussed as well as LIDAR applications.

This work was supported by a grant of the Ministry of Science and Higher Education of the Russian Federation (075-15-2020-912) for the organization and development of a World-class research center "Photonics".

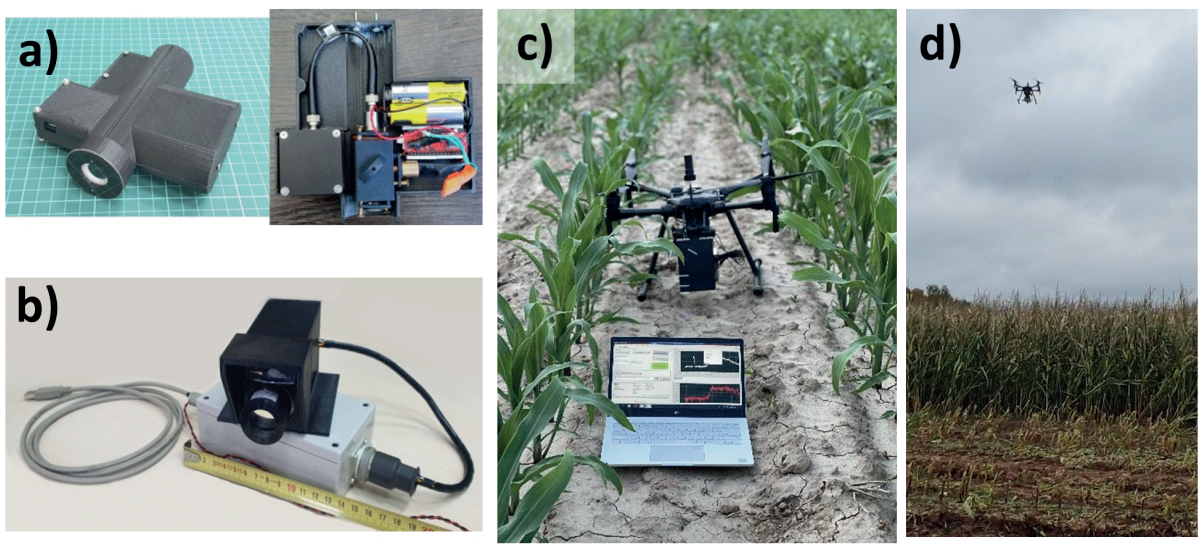

Fig.1 Compact fluorescence (a) and eye-safe (b) LIDAR systems developed at Prokhorov General Physics Institute of RAS. Compact LIDAR installed at a small drone (c) and during online monitoring of maize field (d).

[1] S.Pershin, et al. Spaceborn laser altimeter based on the single photon diode receiver and semiconductor laser transmitter, CLEO OSA vol. 10 p CFI1 (1991)
[2] Grishin, M. Ya, et al., Ultracompact Fluorescence Lidar Based on a Diode Laser (405 nm, 150 mW) for Remote Sensing of Waterbodies and the Underlying Surface from Unmanned Aerial Vehicles, Doklady Physics. vol. 66. No. 6. (2021)
[3] https://mars.nasa.gov/internal_resources/818/

DOI: 10.24412/cl-35039-2022-22-195-195

Elbrus activity sensing by eye-safe lidar based on diode laser proposed by Basov-Krokhin-Popov in 1960: to the 100th anniversary of Nikolai Basov

S.Pershin[1], V.Zavozin[1], M.Grishin[1], V.Makarov[2], S.Yakimenko[3], Ya. Ponurovsky[1], A. Ushakov[1]

1- Prokhorov General Physics Institute, Russian Academy of Sciences, Moscow, 119991 Russia
2- Space Research Institute, Russian Academy of Sciences, Moscow, 117133 Russia
3- Institute for Nuclear Research, Russian Academy of Sciences, Moscow, 117312 Russia
pershin@kapella.gpi.ru

In 1960 N. Basov, O. Krokhin and Yu. Popov [1] have proposed the physical principles of operation of injection diode lasers. Later Zhores Alferov has demonstrated that diode laser efficiency to 90% can be achieved [2] who shared the Nobel Prize in Physics in 2000. In 1991 [3] Russian scientists have opened a **new era** of an environmental sensing by eye-safe lidar (<1 μJ cm^{-2}) based on a pulsed GaAlAs diode laser with high (kHz) repetition rate. We have developed the new principle of lidar sensing based on single photon avalanche diode (SPAD). It allows us to use extremely low laser diode pulse energy (~1 μJ) and eye-safe energy density (<1 μJ·cm^{-2}) for environmental sensing without eyes protection. Actually, the Geiger mode of SPAD operating has only noise-proof digital circuits without analog preamplifiers. Note, the probability of a return photon registration per each laser pulse is 1. This feature allows us to sounding through multilayered clouds by lidar [4] or through fog and smoke, tree canopy and so on [5]. The most intriguing fact is that our lidar (among others from Europe, USA and Canada) won for the first time the NASA competition in 1996 and was involved in the NASA mission Mars Polar Lander-99 [6]. Remarkably, in Dec 03.1999 the NASA delivered the Lander to the Martian surface. So we have announced: "The Lidar of Russian Academy of Sciences is the "**First Lidar**" on the Martian surface. This is our contribution to collection of titles "First: sputnik, kosmonaut Gagarin, Leonov, Lunokhod,… Exciting applications of this new lidar principle were demonstrated (in the beginning of 2000s) in self-driving cars and other unmanned platforms with eye-safe lidars based on diode lasers and our principle [3].

Recently, we have installed our microlidar (weight ~380 g, Fig.1a) in the hot tunnel above the Elbrus volcanic chamber inside the Baksan Neutrino Observatory (Fig.1b) to monitor volcanic activity due to aerosol and gases variation.

Fig.1. (a) Microlidar, (b) BNO hot tunnel, (c) gas emanation in the hot tunnel: radon (1), H_2O (2) and aerosol (3).

We have revealed (Fig.1c) short bursts (~2 h) of aerosol backscattering over the seasonal decreasing trend coincide with radon emission (^{222}Rn) and with a pulsed increase (2-3%) in air humidity Around 300% jumps of lidar backscattering were detected for the first time in 21.10.2019 and periodical aerosol emanation in (7-11).10.2019. An inverted the temperature profile was measured in the BNO tunnel with high concentration of heavy magmatic gases ($^{12}CO_2$ and $^{13}CO_2$). Reversed air convection mechanism was proposed and discussed to explain the revealed features.

The authors gratefully acknowledge Russian Science Foundation for the financial support of the study (project no. 19-19-00712-P).

[1] N.Basov, O.Krokhin and Y.Popov, JETP, **11**(3), 720 (1960); Physics–Uspekhi, **3(**5), 702–728 (1961)
[2] Zhores Alferov, Nobel Prize lcture in Physics, (2000).
[3] S.Pershin, V.Linkin, V.Makarov, I.Prochazka and K.Hamal, 1991 Spaceborn laser altimeter based on the single photon diode receiver and semiconductor laser transmitter, CLEO OSA Technical Digest vol 10 (Baltimore, MD: Optical Society of America) p CFI1
[4] Pershin S.M., et al., Aerosol layers sensing by an eye-safe lidar near the Elbrus summit, Laser Phys. Lett., v.17(2), 026003, (2020).
[5] S. M. Pershin, M.Ya.Grishin, V. A. Zavozin et al., Lidar Sensing of Multilayer Fog Evolution in the Inclined Tunnel of the Baksan Neutrino Observatory, Bulletin of the Lebedev Physics Institute, , Vol. 46, No. 10, pp. 328–332 (2019).
[6] https://mars.nasa.gov/internal_resources/818/

DOI: 10.24412/cl-35039-2022-22-196-196

Fiber-optical Faraday current sensor with enhanced SNR

Y. Przhiyalkovskiy[1,2], N. Starostin[1,2], S. Morshnev[1,2], A. Sazonov[1,2]

1 – SPC Profotech, Skolkovo innovation center area, Bolshoi bulvar 42, bld. 1,, Moscow, 121205, Russia
2 - Kotelnikov Institute of Radio Engineering and Electronics (Fryazino Branch) of the Russian Academy of Sciences, Vvedensky Sq. 1, Fryazino, Moscow region, 141190 Russia
email address: yankus.p@gmail.com

At present, fiber optical Faraday current sensors are widely recognized in the power industry due to their high accuracy, easy installation, and immunity to electromagnetic interference [1]. However, given the fast reaction of the Faraday effect, the optical method of current measuring is also of interest for measuring low-amplitude current pulses, for example, in particle accelerators. To achieve the required sensor characteristics in this application, one thus should maximize the signal-to-noise ratio (SNR) and the sensitivity of the sensing coil.

In our work we design and investigate a fiber-optical current sensor with enhanced SNR for measuring current pulses (Fig. 1) [2]. The sensor is based on a reflective interferometer with the sensing spun fiber and has an additional reference optical channel for suppressing excess noise which is caused by beating of the spectral components of light [3]. The attained suppression of excess noise in the proposed sensor amounts to 15.3 dB.

To increase the sensor sensitivity, the number of fiber turns in a sensing coil should be maximized. While keeping the fiber length constant to ensure high time resolution of the sensor, this can be achieved by reducing the winding radius down to several millimeters. However the experiment shows that such strong bending of the fiber leads to a decrease in the interference visibility of the sensor and degradation of the SNR [2]. Mode coupling which occurs in the wound spun fiber makes the polarization state of light highly elliptical. So when light hits the mirror at the end of the fiber, each incident elliptically polarized mode excites both backward propagating polarization modes. If the winding radius is small, the incoherent components emerged in this way have significant amplitudes, which eventually results in a disturbance of the optical spectrum and, therefore, in low efficiency of noise suppression. Thus, for the radius of the sensing coil of 5 mm used in the experiment, the suppression coefficient reduces to 6 dB.

The theory shows, that if the winding radius change smoothly, polarization modes of the bent spun fiber adapt to the new radius with minimal coupling [4]. So to avoid the above degradation of excess noise suppression, we apply the modified configuration of the fiber winding in which the beginning and end 1-m segments of the spun fiber are wound spirally with change of the winding radius, respectively, from a large value to small and vice versa. Hence, the almost circular polarization of light is restored when it hits the mirror which prevents the emergence of incoherent waves there. As a result, the optical spectrum remains undisturbed and the excess noise suppression increases to 14.8 dB.

The work was carried out within the framework of the state task of the Kotelnikov Institute Radio Engineering and Electronics of RAS.

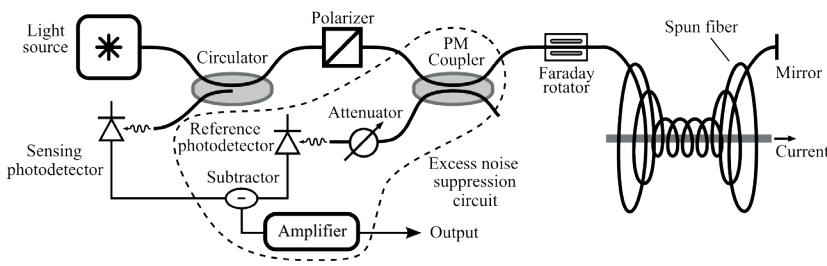

Fig. 1

[1] Bohnert, K., et al. "Optical fiber sensors for the electric power industry." *Optics and Lasers in Engineering* 43.3-5 (2005): 511-526.
[2] Gubin, V. P., et al. "A broadband Faraday fiber-optic current sensor with excess noise compensation." Results in Physics 18 (2020): 103286.
[3] Morkel, P. R., R. I. Laming, and D. N. Payne. "Noise characteristics of high-power doped-fibre superluminescent sources." *Electronics Letters* 26.2 (1990): 96-98.
[4] Przhiyalkovskiy, Yan V., et al. "Polarization Dynamics of Light Propagating in Bent Spun Birefringent Fiber." *Journal of Lightwave Technology* 38.24 (2020): 6879-6885.

DOI: 10.24412/cl-35039-2022-22-197-197

Interference method for the selection of homogeneous lines in the spectrum of a superluminescent source

S. Morshnev[1,2], N. Starostin[1,2], Y. Przhiyalkovskiy[1,2], A. Sazonov[1,2]

1 - Kotelnikov Institute of Radio Engineering and Electronics of RAS, Fryazino, Russia
2 - SPC Profotech, Skolkovo innovation center area, Bolshoi bulvar 42, Moscow, Russia
E-mail: morshnev@profotech.com

It is known [1,2] that an optical detector with an adjustable spectrum resolution δλ can play the role of a tunable spectral filter with a width δλ. An increase in the filter bandwidth δλ leads to a reduction in the coherence time of the received wave packet. In particular, it is so for the Yokogawa AQ6370C spectrum analyzer, which has a set of discrete spectral resolutions from δλ = 0.02 nm to δλ= 2 nm. By introducing a time delay between two orthogonally polarized wave packets and interfering them, we actually control the degree of overlap of wave packets using visibility of the interference pattern (IP). At the same time, the IP is observed on the spectral analyzer using a wavelength sweep. If the coherence time τ is determined by transmission spectrum of the filter, then an increase in the bandwidth δλ of the filter leads to a reduction in the coherence time τ, a decrease in the overlap of wave packets and, consequently, to a decrease in the visibility V, which is the same across the entire spectrum of the source. In this situation, the homogeneous structure of the source spectrum does not manifest itself, everything is determined by the spectral width of the spectral filter of the detector.

The width of the spectrum of the homogeneously broadened lines of the superluminescent Er-Yb light source can also limit the coherence time of the detected wave packets if the filter bandwidth becomes wider than the spectrum of the uniformly broadened line. In this case, the coherence time of the wave packet is determined by the homogeneous line width in this region of the spectrum. It is clear that in different regions of the spectrum, different homogeneously broadened lines may have different widths, which will entail different visibility values V(λ) for different wavelengths within the source spectrum. In a situation when the source spectrum determines the visibility function V(λ), and the width of the detector filter δλ is only greater than a certain value $\delta\lambda_o$, it can be argued that $\delta\lambda_o$ is a uniform width of the source line.

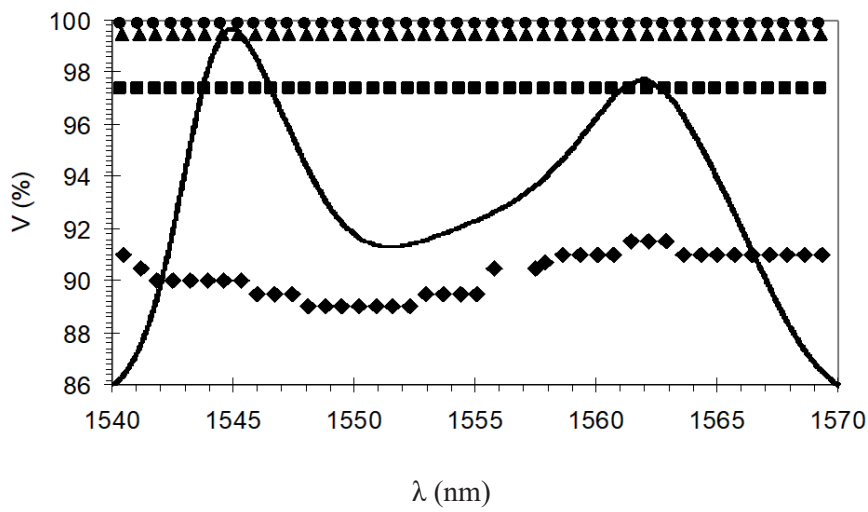

Fig.1. The dependence of visibility on the wavelength.
a) circles – δλ = 0.05 nm; triangles – δλ = 0.1 nm; squares – δλ = 0.2 nm; rhombuses – δλ = 0.5 nm.

From the analysis of Fig.1, it can be seen that up to the filter width δλ = 0.5 nm, there is not spectral dependence of the IP visibility, but its value decreases due to a reduction in the overlap of interfering wave packets. Starting from δλ > 0.5 nm, there is a spectral dependence of visibility within the boundaries of the inhomogeneous spectrum of the erbium source.We estimate the coherence time of the wave packet to be $\tau = 1.6 \times 10^{-11}$ s and the length of wave packet to be 4.8 mm >> λ in vacuum. The work was carried out within the framework of the state task of the Kotelnikov Institute Radio Engineering and Electronics of RAS.

[1] Mandel L., Wolf E., "Optical coherence and quantum optics",M., Fizmatlit, (2000).
[2] Mandel L., Wolf E., Proc. Phys. Soc., 80, 894, (1962)

DOI: 10.24412/cl-35039-2022-22-198-198

Dye's fluorescence amplification by nanostructures on various semiconductor thin films

Arthur D. Dolgopolov, Vladislav R.Gresko, Maksim M. Sergeev

ITMO University, Faculty of Nanoelectronics, Saint Petersburg, Russia
addolgopolov@itmo.ru

Fluorescence is used in the life sciences generally as a non-destructive way of tracking or analysing biological molecules by means of fluorescence. However, with constant dwarfing of measurements scale, it is also important to keep our analizing method updated, via inventing new technics, or reviewing existing ones with a different approach [1].

In this work, we observe properties of nanostructures with a submicron period and a several tens of nm relievo depth on the surface of semiconductor films that are obtained by the method of two-beam interference processing by pulsed laser emission. Such nanostructures were used to enhance the luminescence signal from organic compounds. In this work, it was suggested that the period of nanostructures can affect the luminescence intensity in the case when the spectral range of the luminescent emission is commensurate with the period. This study shows the effect of the resulting gratings on the luminescent properties of the dye rhodamine G6 and bromocresol purple. The nanostructure amplified the signal of rhodamine intensity several times, while the maximum amplification occurred at a wavelength near the grating period. At the same time, both the luminescence spectra of a solution of rhodamine and rhodamine on the initial untreated film differed from each other only slightly and had a maximum at a longer wavelength.

The material functionality of such applications is due to the combination of the effects of a semiconductor film with plasmonic NPs and a periodic nanorelief [2]. Thus, it is possible to improve the optical properties in a certain spectral range due to the complex action of several optical effects, which can be used in microanalysis and photocatalytic applications.

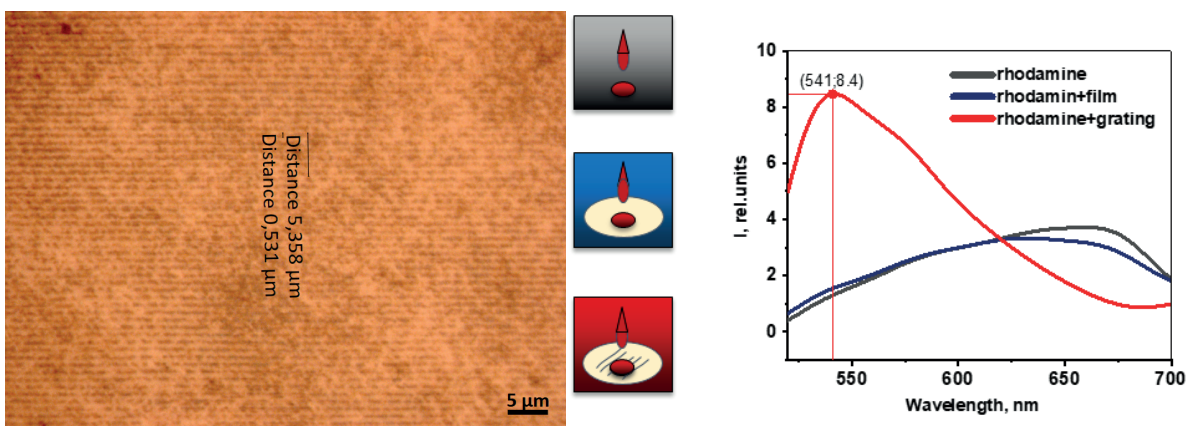

Fig.1 - (a) image of nanogratings before introduction to dye (b) fluorescence spectra relative to untreated film

The study is funded by the grant of Russian Science Foundation (project No. 19-79-10208).

[1] Hang Y., Boryczka J., Wu N. Visible-light and near-infrared fluorescence and surface-enhanced Raman scattering point-of-care sensing and bio-imaging: a review //Chemical Society Reviews. – 2022.
[2] Pietsch U., Holy V., Baumbach T. High-resolution X-ray scattering: from thin films to lateral nanostructures. – Springer Science & Business Media, 2004.

DOI: 10.24412/cl-35039-2022-22-199-199

Luminescent kinetics of the Quantum Dots inside Polymer with Different Refractive Indexes

I. Kalaev[1], A. Tarasevich[1,2,3], A. Arzhanov[1,2,3], K. Magaryan[1], A. Alentiev[4], S. Chirkov[4]

1 - Moscow Pedagogical State University, 29/7 Malaya Pirogovskaya str., 119435 Moscow, Russia
2 - Institute for Spectroscopy, Russian Academy of Science, 5 Fizicheskaya str., 142190 Moscow, Troitsk, Russia
3 - P.N. Lebedev Physical Institute of the Russian Academy of Sciences, 11 Fizicheskaya str., 142190 Moscow, Troitsk, Russia
4 - A.V.Topchiev Institute of Petrochemical Synthesis, Russian Academy of Science, 29 Leninsky prospect, 119991 Moscow, Russia
ka.magaryan@mpgu.edu

The actual problem in modern photonics is investigation of conduct of the single quantum emitter inside different matrices. More specific task is to provide experimental and theoretical research of the mutual influence of such emitters and local media. There is some progress in this task reflected in a few recent publications [1-3].

We report on the study of optical properties of the core/shell CdSe/CdS/ZnS quantum dots (QDs) inside commercial polymer – polyphenyleneoxide (PPO). PPO was chosen because of its ability to change its free volume when different temperatures are applied during film preparation. By changing the free volume of the polymer, its dielectric parameters, in particular the refractive index is altered. 7 samples with different volume were prepared in the temperature range of 20 – 50 °C.

QDs were embedded in all polymers during the process of synthesis with the same constant concentration. Then samples were characterized by luminescence and time-resolved spectroscopy.

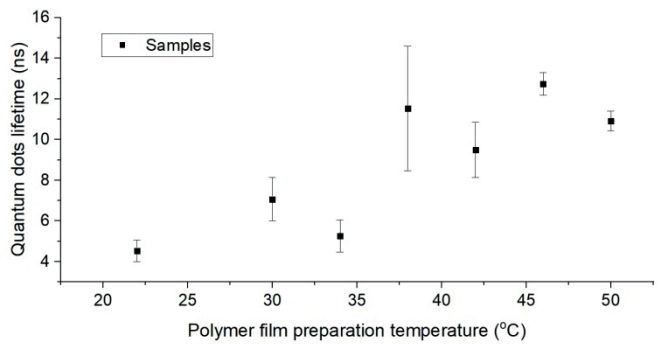

Fig.1. Dependence of the CdSe/CdS/ZnS quantum dots fluorescence lifetime on the temperature of crystallization of the polymer matrix-host.

We see that with increasing of the preparation temperature crystallinity degree of the PPO matrix decreases and therefore its refractive index changes (fig. 1). The fluorescence lifetime of the QDs also tends to increase successively.

The work was carried out within the framework of the State Assignment of the Moscow Pedagogical State University (MPGU) "Physics of Nanostructured Materials: Fundamental Research and Applications in Materials Science, Nanotechnology and Photonics" with the support of the Ministry of Education of the Russian Federation (AAAA-A20-120061890084-9) together with the Centre for Collective Use "Structural Diagnostics of Materials" of the Federal Research Centre of the Russian Academy of Sciences "Crystallography and Photonics". The authors are members of the Leading Scientific School of the Russian Federation (grant of the President of the Russian Federation NSh-776.2022.1.2).

[1] T.A. Anikushina, M.G. Gladush, A.A. Gorshelev and A.V. Naumov, Single-molecule spectromicroscopy: a route towards sub-wavelength refractometry, Faraday Discussions, vol. 184, pp. 263-274, (2015).
[2] N.A.Lozing et al., Stochastic superflares of photoluminescence from a single microdiamond with germanium-vacancy color centers: A general phenomenon or a unique observation, Physical Review B, vol.102, p.060301, (2020).
[3] O. Carion et al., Synthesis, encapsulation, purification and coupling of single quantum dots in phospholipid micelles for their use in cellular and in vivo imaging, Nature Protocols, vol. 2, pp. 2383–2390, (2007).

DOI: 10.24412/cl-35039-2022-22-200-200

Raman and hyper-Raman scatterings of light by TO phonons in a CdS crystal

L. Semenova

Prokhorov General Physics Institute of the Russian Academy of Sciences,
38, Vavilov Str., 119991, Moscow, Russia
sl@kapella.gpi.ru

In accordance with the selection rules, the Raman and hyper-Raman scatterings of light by E_1 and A_1 phonons in a CdS crystal with the wurtzite structure are allowed [1]. These optical phonon vibrations are split into longitudinal (LO) and transverse (TO) components. Resonant Raman scattering (RRS) by both LO and TO phonons was observed in CdS [2,3]. However, resonant hyper-Raman scattering (RHRS) by TO phonons was not found [4-6].

The present paper is devoted to a theoretical analysis of RRS and RHRS of light by TO phonons within the framework of the hydrogen-like Wannier exciton model. In so doing, for the valence band the wave functions, which were obtained in the work of Gutsche and Jahne [7], were considered.

The exciton-TO-phonon interaction leads to transitions between excitons with the same orbital quantum numbers. Thus, the main contribution in RRS is made by the sequence of intermediate virtual excitonic states *s*-*s*. For the scattering geometry used earlier in the experimental investigations [6], the hyper-Raman process involving two-photon transitions to the *s*-excitons of the A (the symmetry Γ_6), B and C (the symmetry Γ_1) series can take a place. At the first sight, it is analogous to RRS and could lead to an increase in the cross section near the two-photon resonance with the lowest exciton levels.

But RHRS of light by A_1(TO) phonons with the participation of A excitons is forbidden. The absence of a noticeable increase in the contribution of the hyper-Raman process involving two-photon transitions to A excitons to RHRS by E_1(TO) phonons near two-photon resonance with the $A_{n=1}$ exciton level can be explained by analyzing the obtained expression describing the indirect transition from the dipole-forbidden A exciton state of the *s*-type (Γ_6) [8].

The RHRS process involving two-photon transitions to the B and C excitons seems similar to RRS observed earlier [2,3]. However, the two-photon dipole transition can be described using both the two-band and three-band models [9]. And this can have a noticeable effect on the frequency dependence of the scattering cross section.

In general case, the RHRS process, which is described as two-photon dipole transition to a *p*-exciton state and then the indirect transition to the ground state, is also possible. The sequence of intermediate exciton states *s*-*p*-*p* conforms to it. However, an analysis of this process is difficult since it includes the weakly-forbidden dipole transitions. In this work, for RHRS by E_1(TO) phonons the scattering process involving two-photon transitions to A excitons of the *p*-type was considered as an example.

[1] S.J. Cyvin, J.E. Rauch, and J.C. Decius, Theory of hyper-Raman effects (nonlinear inelastic light scattering): selection rules and depolarization ratios for the second-order polarizability, J. Chem. Phys., vol. 43, pp. 4083-4095 (1965).
[2] J.M. Ralston, R.L. Wadsack, and R.K. Chang, Resonant cancelation of Raman scattering from CdS and Si, Phys. Rev. Lett., vol. 25, pp. 814-818 (1970).
[3] R.M. Martin and T.C. Damen, Breakdown of selection rules in resonance Raman scattering, Phys, Rev. Lett., vol. 26, pp. 86-88 (1971).
[4] Yu.N. Polivanov and R.Sh. Sayakhov, Resonant hyper-Raman scattering of light by optical phonons, JETP Lett., vol. 30, pp. 580-583 (1979).
[5] L.E. Zubkova, K.K. Ondriash, Yu.N. Polivanov, and K.A. Prokhorov, Multiphonon resonant hyper-Raman scattering, JETP Lett., vol. 57, pp. 348-351 (1993).
[6] V.A. Maslov, K.K. Ondriash, Yu.N. Polivanov, K.A. Prokhorov, L.E. Semenova, and Yu.L. Chuzavkov, Observation of the resonant hyper-Raman scattering of light in a CdS crystal using a tunable optical parametric oscillator, Laser Phys., vol. 6. pp. 132-143 (1996).
[7] E. Gutsche and E. Jahne, Spin-orbit splitting of the valence band of wurtzite type crystals, phys. stat. sol., vol. 19, pp.823-832 (1967).
[8] L.E. Semenova, Resonant hyper-Raman scattering of light by TO-phonons in a CdS crystal, XI Intern. Conf. on Photonics and Information Optics: Proceedings [in Russian] (Moscow: MEPhI), pp. 527-528 (2022).
[9] K.C. Rustagi, F. Pradere, and A. Mysyrowicz, Two-photon absorption in Cu_2O, Phys, Rev. B, vol. 8, pp. 2721-2732 (1973).

DOI: 10.24412/cl-35039-2022-22-201-201

Resonant hyper-Raman scattering of light by 2LO phonons in a CdS crystal

L. Semenova

Prokhorov General Physics Institute of the Russian Academy of Sciences,
38, Vavilov Str., 119991, Moscow, Russia
sl@kapella.gpi.ru

In experimental investigations of multiphonon resonant Raman scattering in a CdS crystal under excitation below excitonic resonances an intensity alternation with increasing number of excited longitudinal optical (LO) phonons was found where the even-order lines dominated [1]. This feature was qualitatively explained within the framework of the exciton model in accordance with which the odd-order lines could expect to dominate in hyper-Raman spectra [1,2]. It was later reported that resonant hyper-Raman scattering (RHRS) of light by 1LO and 3LO phonons was observed in CdS [2]. And in a study of RHRS in CdS with the use of a tunable laser an appearance of the 2LO line in hyper-Raman spectra under excitation near two-photon resonance with the 1s exciton state of the A series was found, and its intensity has grown with increasing the incident photon energy [3]. This RHRS by 2LO phonons was explained by the scattering mechanism involving two-photon dipole transitions to the B and C excitons of the *s*-type [4].

In present work, RHRS by 2LO phonons is considered, taking into account the valence band wave functions obtained by Gutsche and Jahne [5], i.e. mixing the *p*- and *d*-like wave functions is assumed to take a place in the top sub-band A and the deeper valence band *v'* of the symmetry Γ_9. The hydrogen-like Wannier excitons are supposed to be intermediate virtual states of an electronic system. The Fröhlich mechanism of the exciton-phonon interaction is taken into account.

The two-phonon RHRS process considered here involves two-photon dipole transitions to *s*-excitons of the B and C series and is, at first sight, analogous to Raman scattering by 2LO phonons. But, in accordance with the two-photon absorption theory [6,7], the two-photon dipole transitions to B and C excitons of the *s*-type can be occur via the intermediate virtual states which can be *p*-excitons belonging to same pair of the bands and *s*-excitons associated with the higher-lying conduction band or the deeper valence band *v'* (Γ_9). Values of the matrix elements of the dipole transitions in these bands are unknown.

The rough estimations performed has shown that taking into account the dipole transitions to the deeper valence band *v'* can affect the frequency dependence of the two-phonon RHRS cross section ($d\sigma/d\Omega$) and, under certain conditions, can lead to the fact that $d\sigma/d\Omega$ begins to increase sharply at excitation slightly below the two-photon resonance with the lowest exciton level.

[1] A.A. Klyuchikhin, S.A. Permogorov, and A.N. Reznitskii, Multiphonon processes in resonant scattering and exciton luminescence of crystals, Sov. Phys. JETP, vol. 44, pp. 1176-1186 (1976).
[2] L.E. Zubkova, K.K. Ondriash, Yu. N. Polivanov, and K.A. Prokhorov, Multiphonon resonant hyper-Raman scattering, JETP Lett., vol. 57, pp. 348-351 (1993).
[3] V.A. Maslov, K.K. Ondriash, Yu.N. Polivanov, K.A. Prokhorov, L.E. Semenova, Yu.L. Chuzavkov, Observation of resonant hyper-Raman scattering of light in a CdS crystal using a tunable optical parametric oscillator, Laser Phys., vol. 6. pp. 132-143 (1996).
[4] L.E. Semenova and K.A. Prokhorov, Two-phonon resonant hyper-Raman scattering treatment in a CdS crystal, Laser Phys. Lett., vol. 2, pp. 262-266 (2005).
[5] E. Gutsche and E. Jahne, Spin-orbit splitting of the valence band of wurtzite type crystals, phys. stat. sol., vol. 19, pp.823-832 (1967).
[6] G.D. Mahan, Theory of two-photon spectroscopy in solids, Phys. Rev., vol. 170, pp. 825-838 (1968).
[7] K.C. Rustagi, F. Pradere, and A. Mysyrowicz, Two-photon absorption in Cu_2O, Phys, Rev. B, vol. 8, pp. 2721-2732 (1973).

ALT'22

NONLINEAR AND TERAHERTS PHOTONICS

DOI: 10.24412/cl-35039-2022-22-203-203

Towards standardless calibration of the quantum efficiency of analog terahertz detectors

G.Kh. Kitaeva, P.A.Prukovskii, D.A. Safronenkov

Lomonosov Moscow State University, Leninskie Gory 1-2, Moscow 119991 Russia
gkitaeva@physics.msu.ru

We consider a possibility of measuring the quantum efficiency of sensitive elements of terahertz detectors using quantum-correlated pairs of optical and terahertz photons. Such pairs are generated via the nonlinear-optical process of spontaneous parametric down-conversion (SPDC) in strongly frequency non-degenerate regime [1]. Nowadays, the SPDC method of absolute calibration [2] is successfully applied to optical single-photon detectors and CCD cameras in frequency degenerate regime [3,4], but its extension to the terahertz range requires some specific modification.

Virtually none of the currently used terahertz detectors has the single-photon detection property. At the same time, our analysis of statistical distributions of the analog readings of antenna-coupled terahertz superconducting bolometer in the terahertz SPDC channel reveals the discrete nature of terahertz detection [5]. Similar features are observed in histograms of an analog photomultiplier tube placed in the optical SPDC channel [6]. We propose a modified SPDC quantum efficiency calibration method based on approximation of the histograms and applicable to both analog and single-photon detectors. Experimental verification of the method is carried out in the optical range using degenerate SPDC. We show a fairly good matching between the input photon numbers measured by a single-photon avalanche diode calibrated using the standard photon-counting approach, and by an analog photomultiplier tube calibrated using the proposed method. This result opens a possibility to calibrate terahertz analog detectors as well. A possible experimental scheme and the whole calibration procedure are discussed.

The work was done under financial support of the Russian Science Foundation (Grant No. 22-12-00055).

[1] G.Kh. Kitaeva, A.A. Leontyev, P.A. Prudkovskii, Quantum correlation between optical and terahertz photons generated under multimode spontaneous parametric down-conversion, Phys. Rev. A 101, 053810 (2020).
[2] D.N. Klyshko, On the use of two-photon light for absolute calibration of photoelectric detectors, Sov. J. Quantum Electron. 10(9), 1112–1117 (1980).
[3] S.V. Polyakov, A.L. Migdall, High accuracy verification of a correlated photon-based method for determining photoncounting detection efficiency, Opt. Expr. 15, 1390-1407 (2007).
[4] A. Avella, I. Ruo-Berchera, I.P. Degiovanni, G. Brida, M. Genovese, Absolute calibration of an EMCCD camera by quantum correlation, linking photon counting to the analog regime. Opt. Lett. 41, 1841-1844 (2016).
[5] P. Prudkovskii, A. Leontyev, K. Kuznetsov, G. Kitaeva, Towards Measuring Terahertz Photon Statistics by a Superconducting Bolometer, Sensors 21, 4964 (2021).
[6] D.A. Safronenkov, N.A. Borshchevskaya, T.I. Novikova, K.G.Katamadze, K.A.Kuznetsov, G.Kh.Kitaeva, Optics Express 29, 36644-36659 (2021)

DOI: 10.24412/cl-35039-2022-22-204-204

Transmission features of nonlinear Fabry-Perot interferometer with giant Kerr nonlinearity in THz frequency range

S.A.Kozlov, A.A. Gendrina, M.D.Shipov, M.V.Melnik, A.N.Tsypkin

ITMO University, Saint Petersburg, Russian Federation
Main author email address:tsypkinan@itmo.ru

Much attention has been paid to terahertz radiation in recent years. Features of THz radiationis quite surprising. For instance, relatively recently it was discovered that in the terahertz spectral range many materials demonstrate a giant low inertia nonlinearity, which ismuch larger than their nonlinearity in neighboring ranges[1-5].The report presents new data on the results of measuring the giant nonlinearity of materials with different methods. It is shown that according to the ratio of the magnitude of the nonlinear refractive index coefficient and the time of establishing a nonlinear response, materials with nonlinearity of avibrational nature in the terahertz spectral range demonstrate record values. This opens up new possibilities for terahertz nonlinear opticsand photonics.

For almost half a century, research has been carried out on optical bistability. It is a well-studied field, but there are still search for materials and systems that would allow the creation of near-ideal optical bistable devices. This report presents the results of the bistability features analysis of a nonlinear Fabry-Perot interferometer with media which refractive index nonlinearity is gigantic and low-inertia. It is shown that at high values of the radiation-induced change in the refractive index of the intracavity medium, its threshold length, at which bistable transmission is already observed, decreases significantly. At the same time, another threshold, small-scale smooth focusing, has not yet been reached. It is shown that the giant nonlinearity of the refractive index of the intracavity medium and the high value of its linear refractive index in the terahertz range make it possible to implement "resonatorless" nonlinear Fabry-Perot interferometers on solid-state plates with only Fresnel reflection. The figure shows the result of calculating the bistable transmission (dependence of the output intensity on the input one,)of terahertz radiation with a wavelength λ = 1.2 mm by lithium niobate crystal plates of different thicknesses (1mm – curve a), 2.21mm – curve b), 0.52mm – curve c)).

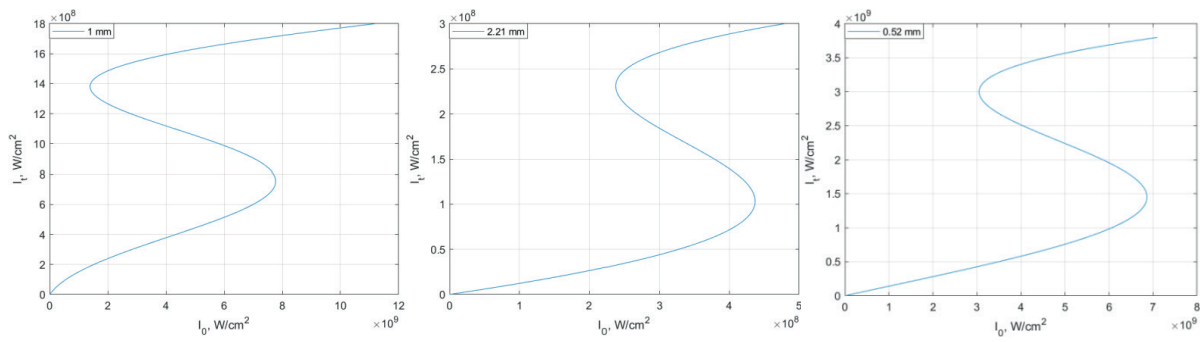

a) b) c)

Fig. 1: Curves of bistable transmission of the mirrorless Fabry-Perot interferometer

The report discusses the results of an experimental study of the transmission of quasi-monochromatic terahertz radiation from gyrotrons by these plates.

[1]Artser I. et al. Radiation shift from triple to quadruple frequency caused by the interaction of terahertz pulses with a nonlinear Kerr medium //Scientific Reports. – 2022. – T. 12. – №. 1. – C. 1-8.
[2] Tcypkin A.N. et al. Giant Third-Order Nonlinear Response of Liquids at Terahertz Frequencies // Physical ReviewApplied. 2021. Vol. 15. №. 5. P. 054009.
[3] Zhukova M., Melnik M., Vorontsova I., Tcypkin A. & Kozlov S. Estimations of low-inertia cubic nonlinearity featuredby electro-optical crystals in the THz range//Photonics 7, 98 (2020).
[4] Tcypkin, A. N. et al. High Kerr nonlinearity of water in THz spectral range. Optics Express 27, 10419–10425 (2019).
[5] Dolgaleva K., Materikina D.V., Boyd R.W. & Kozlov S.A. Prediction of an extremely large nonlinear refractive indexfor crystals at terahertz frequencies//PhysicalReviev A 92, 023809 (2015).

DOI: 10.24412/cl-35039-2022-22-205-205

Directional diagram of THz radiation from femtosecond filament in DC-biased and transition regimes

O.G. Kosareva[1,2], N.A. Panov[1,2], D.E. Shipilo[1,2], I.A. Nikolaeva[1,2], D.V. Pushkarev[1,2], G.E. Rizaev[2], D.V.Mokrousova[1,2], A.V. Koribut[2], Y.V. Grudtsyn[1,2], L.V. Seleznev[1,2], A.A. Ionin[2]

1-Faculty of Physics, Lomonosov Moscow State University, 119991, Moscow, Russia
2-P.N. Lebedev Physical Institute of the RAS, 119991, Moscow, Russia
kosareva@physics.msu.ru

The most efficient way to generate broadband THz radiation in air is a two-color (ω–2ω) filamentation [1]. At the same time, the THz radiation source based on the plasma channel biased by external electrostatic field (i.e. a single-color DC-biased filament) is free of the tedious ω–2ω pulse delay adjustment [2]. Besides, the directional diagram of THz radiation from the DC-biased plasma channel is characterized by the on-axis maximum [3]. The decrease of the conversion efficiency in a single-color filament as compared with the two-color one is compensated by the unlimited energy scalability when using terawatt peak power femtosecond laser sources producing multiple plasma channels [4].

In this work, we study THz generation during filamentation in the external electrostatic field (DC-biased single-color filamentation) [5, 6]. Directional diagram, frequency content, threshold of the external electrostatic field, providing for the transition from the conical to the on-axis THz emission, are studied experimentally using 744 nm single-color plasma channel and simulated based on the unidirectional pulse propagation equation ensuring frequency content from 0.01 THz to 3 PHz and angular divergence till 60°. Special consideration is given to the transition from the light pressure dipole radiation source at sub-THz frequencies to quadrupole source at higher frequencies in the unbiased plasma channel (filament) regime. This transition is observed in the measured 2D frequency-resolved far-field distributions of THz emission, which evolves from the conical one at 0.1–0.5 THz to the two-lobe one at higher frequencies [6].

In the experiment [5] with the DC field of E_{DC} = 10 kV/cm we focused the laser pulse (744 nm, 0.5 mJ, 90 fs) into the air gap between the plane electrodes. At the selected by the THz narrowband filters frequencies ν below 1 THz, a wide flat-top angular distribution was measured by a bolometer (Fig. 1). The simulations showed the transition of THz directional diagram from the flat-top to the conical one for ν > 8 THz due to the destructive interference of THz waves from the ionization front propagating with the superluminal velocity. At lower or the absence of the DC field, the transition from conical to on-axis emission was observed [6,7].

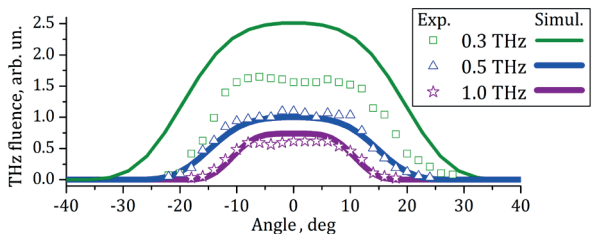

Fig. 1. Angular distributions of THz fluence obtained for three frequencies in the experiment (symbols) and simulations based on unidirectional pulse propagation equation (UPPE) [8] (lines).

We acknowledge the support from Russian Science Foundation (21-49-00023) and National Natural Science Foundation of China (12061131010).

[1] X.C. Zhang, A. Shkurinov, and Y. Zhang, "Extreme terahertz science" Nat. Photonics 11, 16-18 (2017).
[2] T. Löffler, F. Jacob, H. Roskos, "Generation of terahertz pulses by photoionization of electrically biased air," Appl. Phys. Lett. 77, 453-455 (2000).
[3] A. Houard, Y. Liu, B. Prade, V. T. Tikhonchuk, and A. Mysyrowicz "Strong enhancement of terahertz radiation from laser filaments in air by a static electric field" Phys. Rev. Lett. 100, 255006-1-255006-4 (2008).
[4] N. Panov, V. Andreeva, O. Kosareva, A. Shkurinov, V. A. Makarov, L. Bergé, and S. L. Chin "Directionality of terahertz radiation emitted from an array of femtosecond filaments in gases," Laser Phys. Lett. 11, 125401-1 - 125401-6 (2014).
[5] I.A. Nikolaeva, D. E. Shipilo, D. V. Pushkarev, G. E. Rizaev, D. V. Mokrousova, A. V. Koribut, Y. V. Grudtsyn, N. A. Panov, L. V. Seleznev, W. Liu, A. A. Ionin, and O. G. Kosareva "Flat-top THz directional diagram of a DC-biased filament", Opt. Lett. 46, 5497-5500 (2021).
[6] D. E. Shipilo, I. A. Nikolaeva, D. V. Pushkarev, G. E. Rizaev, D. V. Mokrousova, A. V. Koribut, Ya. V. Grudtsyn, N. A. Panov, L. V. Seleznev, W. Liu, A. A. Ionin, and O. G. Kosareva "Balance of emission from THz sources in DC-biased and unbiased filaments in air", Opt. Express 29, 40687-40698 (2021).
[7] G. E. Rizaev, D. V. Mokrousova, D. V. Pushkarev, D. E. Shipilo, I. A. Nikolaeva, N. A. Panov, L. V. Seleznev, O. G. Kosareva, and A. A. Ionin "Breakup of Axial Symmetry of Terahertz Emission from Single-Color Filament Plasma" JETP Letters 115, 699-702 (2022).
[8] M. Kolesik and J. V. Moloney, "Nonlinear optical pulse propagation simulation: From maxwell's to unidirectional equations," Phys. Rev. E 70, 036604-1-036604-11 (2004).

DOI: 10.24412/cl-35039-2022-22-206-206

THz emission from single metallic microdroplet targets irradiated with femtosecond laser pulses

A. V. Balakin[1], P. M. Solyankin[2], M. S. Krivokorytov[3,4], A. P. Shkurinov[1]

1- Faculty of Physics, Lomonosov Moscow State University, Moscow 119991, Russia
2- Institute on Laser and Information Technologies of the Russian Academy of Sciences—Branch of the Federal Scientific Research Center "Crystallography and Photonics" of the Russian Academy of Sciences, Shatura, 140700, Russia
3- Moscow Institute of Physics and Technology, Dolgoprudny, Moscow Oblast 141701, Russia
4 - Institute for Spectroscopy, Russian Academy of Sciences, Troitsk, Moscow 108840, Russia
a.v.balakin@physics.msu.ru

Here we present results of investigation of THz generation in liquid metal eutectic alloy (48% Sn, 52% In) microdroplets irradiated with femtosecond laser pulses. The single liquid-metal microdroplets with a diameter around 50 um were produced with special dispenser device as it has been described in our previous paper [1]. These microdroplets were falling down into vacuum chamber and their flowing was synchronized with the laser pump pulses from Ti:Sa regenerative amplifier. It provides possibility to supply a new microdroplet coming across each laser pulse, and to eliminate registration of any cumulative effects. A double-pulses excitation scheme with low-energy prepulse and more powerful second pulse, which was discussed indetails in [1], was applied to get efficient THz generation from the droplet.

In particular, one of worthwhile phenomenon investigated in our experiments was a study of the radiation pattern of THz emission from the single metallic microdroplet excited by ultra-short laser pulses. A special vacuum chamber made of a polypropylene tube transparent in THz, was designed to measure the THz radiation pattern in a wide range of angles (0°-150° relative to the laser pump beam direction). X-ray signal from the microdroplet target was measured simultaneously with the THz one in our experiments as well. A typical view of dependence of the THz signal from a microdroplet on the detection angle and energy of X-ray radiation is depicted in Fig.1. As one may see, it demonstrates a complicated multi-lobe structure with clear strong lobe directed in 60 degrees relative to the optical pump. We believe that observed behavior of the THz radiation pattern could be associated with an interference of contributions from the dipole and quadrupole currents, and the presence of opaque thick droplet could lead to effective decreasing of forwardly directed contribution into the THz signal. Also we compare this case with previously studied radiation pattern of THz emission from gas cluster jet irradiated with intense femtosecond laser pulses [2].

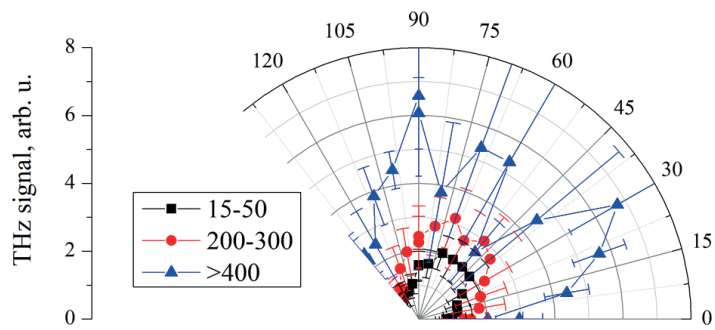

Fig. 1. Dependence of the THz signal from a microdroplet on the detection angle and energy of X-ray radiation. Droplet diameter is 50 μm.

This work was funded partly by RFBR and ROSATOM according to the research project № 20-21-00143, partly by the Ministry of Science and Higher Education within the State assignment FSRC "Crystallography and Photonics" RAS and in part by the Ministry of Science and Higher Education of the Russian Federation in framework of Agreement № 075-15-2022-830 from 27 May 2022.

[1] Solyankin P. M. et al. Single free-falling droplet of liquid metal as a source of directional terahertz radiation //Physical Review Applied, vol. 14, №. 3, p. 034033 (2020)
[2] Balakin A. V. et al. Directional terahertz beam generation under interaction of an intense femtosecond laser pulse with a cluster jet //JOSA B, vol. 38, №. 11, p.. 3515-3522 (2021).

DOI: 10.24412/cl-35039-2022-22-207-207

Anisotropic Photoconductivity and Terahertz Emission from Semiconductors

P. Ziaziulia[1], V. Malevich[2, 3]

1- Belarusian State University, Nezalezhnasti Ave. 4, 220030, Minsk, Belarus
2- Institute of Physics, National Academy of Sciences of Belarus, Nezalezhnasti Ave. 68, 220072, Minsk, Belarus
3- Belarusian State University of Informatics and Radioelectronics, P. Browki Str. 6, 220013, Minsk, Belarus
E-mail: v.malevich@ifanbel.bas-net.by

One of the methods for generating continuous wave terahertz (THz) radiation is the use of the photomixing effect in semiconductor excited by two optical beams with close frequencies [1, 2]. The photomixing effect arises due to the nonlinear nature of photoconductivity and, in the presence of a constant bias, leads to the generation of a photocurrent at the beat frequency. In this report we consider the anisotropic photoconductivity in a semiconductor excited by two-frequency optical radiation, as well as its contribution to the photocurrent at the beat frequency corresponding to the THz region. The interband anisotropic photoconductivity arises due to the anisotropy of the momentum distribution of electrons excited by polarized light and the energy dependence of the momentum relaxation [2] time and effective mass of the electrons. The response time of the anisotropic photoconductivity is very short, since it is determined by the electron momentum relaxation time, which for typical semiconductors is about 200 – 300 fs.

Let us consider a cubic semiconductor under interband excitation by the two-frequency linearly polarized optical radiation $\mathbf{E}(t)=\mathbf{E}_1\cos\omega_+ t+\mathbf{E}_2\cos\omega_- t$ with nearby frequencies $\omega_\pm=\omega\pm\Omega/2$. The constant electric field $\mathbf{F}$ is directed along the z-axis. The vectors $\mathbf{E}_1$ and $\mathbf{E}_2$ are assumed to be parallel to each other, lying in the xz plane and making an angle γ with the z-axis. Solving the kinetic equation for the component of the electron distribution function at the beat frequency Ω, we obtain expressions for the current density components:

$$j_z=\frac{e^2F}{3\pi^2}\frac{\alpha I}{\hbar\omega g(\varepsilon_0)}\left\{\frac{\tau_0}{1+i\Omega\tau_0}\frac{d}{d\varepsilon_{\mathbf{p}}}\left(p^2v_{\mathbf{p}}\frac{\tau_1}{1+i\Omega\tau_1}\right)-\frac{2}{5}P_2(\cos\gamma)\frac{\tau_2}{1+i\Omega\tau_2}V(\varepsilon_{\mathbf{p}})\right\}\Bigg|_{\varepsilon_{\mathbf{p}}=\varepsilon_0},$$

$$j_x=-\frac{e^2F}{10\pi^2}\frac{\alpha I\sin 2\gamma}{\hbar\omega g(\varepsilon_0)}\frac{\tau_2}{1+i\Omega\tau_2}V(\varepsilon_{\mathbf{p}})\Bigg|_{\varepsilon_{\mathbf{p}}=\varepsilon_0},\quad V(\varepsilon_{\mathbf{p}})=p^3\frac{d}{d\varepsilon_{\mathbf{p}}}\left(\frac{v_{\mathbf{p}}}{p}\frac{\tau_1}{1+i\Omega\tau_1}\right).$$

Here α is the optical absorption coefficient, I is the optical excitation intensity, $\varepsilon_{\mathbf{p}}$ is the energy of an electron with momentum $\mathbf{p}$, ε_0 is the excess energy of photoelectrons in the conduction band, $\mathbf{v}_{\mathbf{p}}=\partial\varepsilon_{\mathbf{p}}/\partial\mathbf{p}$ is the electron velocity, $g(\varepsilon)$ is the density of electron states in the conduction band, τ_0 is the recombination time of nonequilibrium electrons, $\tau_1(\varepsilon)$ and $\tau_2(\varepsilon)$ are the momentum relaxation times corresponding to the first and second spherical harmonics of the distribution function, $P_2(\cos\gamma)$ is the second-order Legendre polynomial.

In typical semiconductors the recombination time is usually much longer than the times τ_1 and τ_2. In the low frequency range ($\Omega\tau_0\ll1$) the anisotropic part of the photoconductivity is very small, since its relation to the normal (isotropic) photoconductivity is characterized by the parameter $\tau_2/\tau_0\ll1$. However, in the THz frequency range, when $\Omega\tau_0\gg1$, the anisotropic and isotropic parts of the photoconductivity can be comparable since their ratio is characterized by the parameter $\Omega\tau_2\sim1$. In THz photoconductive antennas used for photomixing, semiconductor layers with a subpicosecond lifetime are usually used [3]. Given that the carrier lifetime in such semiconductors $\tau_0\sim\Omega^{-1}$, we obtain that even in this case the anisotropic component of the photoconductivity is comparable to the value of the isotropic photoconductivity.

[1] S. Preu G. H. Döhler, S. Malzer, L. J. Wang, and A. C. Gossard, Tunable, continuos-wave Terahertz photomixer sources and applications, J. Appl. Phys., 109, pp. 061301-1-061301-56, (2011).
[2] V. Belinicher and V. Novikov, Nonequilibrium photoconductivity and influence of external fields on the surface photogalvanic effect, Sov. Phys. Semicond., 15, pp. 1138-1142, (1981).
[3] N. Burford and M. El-Shenawee, Review of terahertz photoconductive antenna technology, Opt. Eng., 56(1), pp. 010901-1-010901-20, (2017).

DOI: 10.24412/cl-35039-2022-22-208-208

Photogalvanic currents in α -Sn/Ge QW

V.N. Trukhin[1], I. A. Mustafin[1], F. V. Kusmartsev[2,3], A. Kusmartseva[2], Y. Liu[3], B. Zhang[3], Y. Luo[3]

1- Ioffe Institute, 19021, St Petersburg, Russia
2- Department of Physics, Loughborough University, UK
3- Nano-fabrication laboratory, MTRC, China
Email: valembr@mail.ru

In this report we present the results of an experimental study of photocurrents in nanostructures based on α-Sn/Ge quantum wells when they are excited by femtosecond optical pulses by the contact method and by recording the terahertz radiation induced by these photocurrents.

The studied samples were nanometer layers of Ge and α-Sn synthesized by electron-beam deposition on the surface of a silicon substrate with a top layer of SiO_2. The number of α-Sn/Ge quantum wells in the investigated nanostructures was 10, the width of the quantum wells were 4 nm, 6 nm, 8.5 nm, and 10 nm, respectively. The separation between the quantum wells was 10 nm.

Raman spectroscopy studies were carried out at room temperature in the "backscattering" geometry on a Horiba Jobin-Yvon T64000 spectrometer equipped with a confocal optical microscope. When measuring the laser spot of continuous radiation from a YAG: Nd laser (λ = 532 nm), it was focused in an area with a diameter of ~ 1 μm using a 100 × objective (NA = 0.9). The measurements were carried out using an optical pumping with a power in a range 0.04 - 1 mW. The key observation in the obtained Raman spectra is that, at the lowest pump power, an additional line in the 210 cm-1 region is observed, which is due to α-Sn mode. The mode disappears with increasing pump power. The observed disappearance of the line can be explained by the phase transition of α-Sn to β-Sn as the sample is heated with an increase in pump power.

The waveform of the THz pulse generated when the sample was excited by ultrashort laser pulses of femtosecond duration was recorded by terahertz time-resolved spectroscopy. During the study of samples containing α-Sn/Ge quantum wells with a width of 10 nm and 8.5 nm, it was found that when the polarization of the excitation light changes from TM to TE, the electric field of the THz radiation changes its sign and the dependence of the electric field of the THz radiation on the polarization vector rotation angle has a sinusoidal character. The sign of the electric field of the THz radiation excited by light with TM polarization corresponds to the movement of photoelectrons in the direction of light propagation. The amplitude of THz pulse is proportional to the intensity of excitation light. It was shown earlier that the observed dependences of the photocurrent on the polarization of light, the direction of the wave vector, and the intensity of the excited light are inherent in the drag current [1]. In samples with quantum well widths of 4 nm and 6 nm, the sign of the electric field of the THz radiation does not change when the polarization changes from TM to TE. At excitation by light with TE polarization the amplitude of THz pulse is less than at excitation of nanostructure by light with TM polarization. The amplitude of THz pulse is also proportional to the intensity of excitation light. Experiments on the study of photocurrents by the contact method showed a similar behavior of the corresponding dependences. The observed changes in the polarization dependences of the electric field of the THz radiation generated in α-Sn/Ge nanostructures when the width of quantum wells changes from 6 nm to 8. 5 nm appear to be related to the difference in electronic systems. Namely, nanostructures with α-Sn/Ge, 4 nm, and 6 nm quantum hole widths have the normal band structure of narrow-gap semiconductors, while nanostructures with α-Sn/Ge, 8.5 nm, and 10 nm quantum hole widths are two-dimensional topological insulators. Such a phase transition is predicted in the α-Sn/CdTe quantum well with the width of about 8 nm [2].

This work supported by the Russian Foundation for Basic Research and the Royal Society of London No. 21-52-10015.

[1] Trukhin V.N., Mustafin I.A., Gavrilova P.G., Kusmartsev F.V., Kusmartseva A., Liu Y., Zhang B., Luo Y., Generation of terahertz radiation in nanometer films:Ge/alpha-Sn, Proceedings of 45TH Int. Conf. Infrared, Millim., Terahertz Waves, IRMMW-THz, v.2020, pp. 915-915, 2020.
[2] S. Küfne, "Electronic and topological properties of low-dimensional α-Sn and HgTe structures", Dissertation (Ph.D.), 2015.

DOI: 10.24412/cl-35039-2022-22-209-209

Development of High-Power Frequency Tunable THz Band Gyrotrons for Spectroscopy Applications

M. Glyavin, A. Fokin, A. Tsvetkov, M. Morozkin, M. Proyavin, A. Fedotov, I. Zotova

Institute of Applied Physics RAS (IAP RAS), 46 Ul'yanov str., Nizhny Novgorod, Russia
glyavin@ipfran.ru

Development of a medium power (0.1-1 kW) frequency tunable sub-THz and THz band sources is highly demand for a number of spectroscpy applications including direct measurement of positronium hyperfine structure (Ps-HFS) [1] and sensitivity enhancement of DNP/NMR and RAD spectroscopy [2]. Nowadays, such level of sub-THz radiation power can only be achieved based on gyrotrons [3,4]. Significant widening of the tuning band can be provided in a gyrotron with a specially shortened normalized cavity length. In this case, a number of axial modes can be excited at the high power level due to the weaker sensitivity to the electron velocity spread. The experimental tests of such operation regime was successfully demonstrated at the 0.5 THz tube [5]. Record value of RAD spectromenter sensitivity has been obtained [6]. For Ps-HFS measurement gyrotron with output power 0.5-1 kW at the frequency of 203.4 GHz with the possibility of fine tuning in a band of 3-10 GHz has been developed [7]. Step by step frequency tuning based on the excitation of different operating mode has been obtained at 0.25 THz tube with output power level up to 100 kW in a pulse operation regime [8].

Other attractive method for tunable generation in gyrotrons is related to using an open confocal resonator when smooth frequency tuning is provided by mechanical variation of the distance between mirrors. However, the transverse structure of the operating mode in this case is rather non-uniform. As a result, when the gyrotron is conventionally powered by a tubular electron beam, the large part of electrons is located outside the caustic bounding the field area. Thus, the interaction efficiency is low. As a method of increasing the efficiency of confocal gyrotrons, it is possible to use the modified electron-optical systems injecting an electron beam in the form of two circular arcs. However, a simpler approach is related with using, for example, a double-confocal configuration proposed in [9].

We demonstrate that the number of confocal resonators can be increased to three while maintaining the selectivity of the operating mode excitation. Such a system provides high selective properties for the operating mode. Thus, the rather high efficiency can be achieved with using conventional tubular rotating beams. As shown in 3D PIC simulations, a 6-mirror (triple-confocal) gyrotron can provide 6-10 kW output power in the frequency range of 200-207 GHz. Indicated parameters is highly demand for applications including Ps-HFS.

The work is supported by the IAP RAS project #0030-2019-0027

[1] T. Yamazaki, A. Miyazaki, T. Suehara, et al., «Direct Observation of the Hyperfine Transition of Ground-State Positronium», Phys. Rev. Lett. 108, 253401 (2012); doi: 10.1103/PhysRevLett.108.253401

[2] M Koshelev, A. Tsvetkov, M. Morozkin et al., «Molecular gas spectroscopy using radioacoustic detection and high-power coherent subterahertz radiation sources», Journal of Molecular Spectroscopy, 331, 9-16 (2017); doi:10.1016/j.jms.2016.10.014

[3] T. Idehara, S. Sabchevski, M. Glyavin, S. Mitsudo. «The Gyrotrons as Promising Radiation Sources for THz Sensing and Imaging», Appl. Sci. 10, 980, 2020; doi:10.3390/app10030980

[4] A. Litvak, G. Denisov and M. Glyavin, «Russian Gyrotrons: Achievements and Trends», *IEEE Journal of Microwaves*, 1, 1, 260-268 (2021); doi: 10.1109/JMW.2020.3030917

[5] M. Glyavin, A. Kuftin, M. Morozkin *et al.,* «A 250-Watts, 0.5-THz Continuous-Wave Second-Harmonic Gyrotron», *IEEE Electron Device Letters*, 42, 11, 1666-1669 (2021); doi: 10.1109/LED.2021.3113022

[6] G. Golubiatnikov, A. Koshelev, A. Tsvetkov et al., «Sub-Terahertz High-Sensitivity High-Resolution Molecular Spectroscopy With a Gyrotron», *IEEE Transactions on Terahertz Science and Technology,* 10, 5, 502-512 (2020), doi: 10.1109/TTHZ.2020.2984459

[7] A. Fedotov, R. Rozental, I. Zotova et al., «Frequency Tunable sub-THz Gyrotron for Direct Measurements of Positronium Hyperfine Structure», *J Infrared Milli Terahz Waves* 3**9,** 975–983 (2018); doi:10.1007/s10762-018-0522-2

[8] A. Zuev, A. Fokin, A. Ananichev et al. «Realization of an Octave Frequency Step-Tuning of Sub-terahertz Gyrotron for Advanced Fusion Research», J Infrared Milli Terahz Waves, 42, 1131–1141 (2021); doi:10.1007/s10762-021-00832-4

[9] W. Fu, X. Guan and Y. Yana, «Harmonic terahertz gyrotron with a double confocal quasi-optical cavity», Physics of Plasmas 26, 043109 (2019) ; doi: 10.1063/1.5090471

DOI: 10.24412/cl-35039-2022-22-210-210

Terahertz-field-induced optical second harmonic generation and luminescence for material nonlinear diagnostic and terahertz beam visualization

S.B. Bodrov

[1]*University of Nizhny Novgorod, Nizhny Novgorod 603022, Russia*
[2]*Institute of Applied Physics, Russian Academy of Sciences, Nizhny Novgorod 603950, Russia*
sergey.bodrov@ipfran.ru, *bosbor@ufp.appl.sci-nnov.ru*

Terahertz-field-induced second harmonic generation (TFISHG) of optical radiation was used to investigate nonlinear properties of semiconductors (silicon), dielectrics (fused quartz, tellurite and chalcogenide glasses) and two-dimensional materials (graphene). In a case of transparent materials, the TFISHG technique allows finding the third-order susceptibility not only of homogeneous samples, but also can be used to determine the nonlinearity of hidden layers inside materials. Terahertz-field-induced optical luminescence from graphene is proposed and experimentally used for imaging of strong fields THz beams (>100 kV/cm). The visualization of local THz-field enhancement near a metal tip with a 2 um radius curvature was demonstrated.

DOI: 10.24412/cl-35039-2022-22-211-211

Analysis of the metabolites composition for the ENT organs tissues with high resolution THz spectroscopy

V.Vaks[1], V.Anfertev[1], A.Ayzenshtadt[1,2], M.Chernyaeva[1,3], E.Domracheva[1], K.Gavrilova[1,2]

1- Institute for Physics of Microstructures RAS, 603950, Russia, Nizhny Novgorod, GSP-105
2- Children's Municipal Clinical Hospital No.1, 603081, Russia, Nizhny Novgorod, Gagarina av., 76
3- Lobachevsky University, 603022, Russia, Nizhny Novgorod, Gagarina av., 23
elena@ipm.sci-nnov.ru

Recently, physical and physical-chemical methods of analysis, such as gas chromatography, mass-spectrometry, IR and THz spectroscopy, are becoming increasingly important in medical diagnostics. They allow you to identify substances, the so -called metabolites characteristic of a particular disease. The compilation of a metabolic profile will accelerate and facilitate the process of diagnosis of the disease, evaluate the stage and etiology, as well as predict the therapy. It is extremely relevant to study the state of ear-nose-throat (ENT) organs, since they are one of the main ways of penetrating into the human body of various infections, viruses, fungi, etc. However, there are no data on metabolites in the literature and the Human Metabolome Database in diseases of the ENT organs [1].

The work is devoted to the analysis of the metabolites composition for the ENT organs tissues with high resolution THz spectroscopy and comparing the composition of metabolites that appear during thermal decomposition of a relatively healthy mucosa, a sphenoid sinus polyp and a maxillary sinus cyst. The fast frequency sweeping spectrometer developed by the authors, operating in the range of 118-178 GHz, was used. The frequency range of 60 GHz is covered by the spectrometer in 30 sec. The sensitivity of the recorded absorption coefficient at a cell length of 1 m is from 10^{-7}cm^{-1} to $5*10^{-8}$cm^{-1}. [2, 3]

The identification of substances by absorption lines was carried out using electronic databases [4, 5].

To evaluate the whole metabolites, a qualitative analysis of the chemical composition for thermal decomposition products was performed and a comparison of the resulting spectra of substances and the number of absorption lines of a relatively healthy mucosa, a sphenoid sinus polyp and a maxillary sinus cyst in the frequency range of 60 GHz. If the concentration of the substance in the mixture under study is greater, the more weaker lines will be recorded in the spectrum at the equal conditions (temperature and pressure conditions).

The analysis of the results showed that in all samples there are substances such as methanol, propanediol, acetonitrile, butyronitrile, benzonitrile, methylmercaptan, azole, ethylene sulfide, carbonyl sulfide and sulfur dioxide. However, in the spectrum of a relatively healthy mucosa, the number of absorption lines of these substances is much less than in the spectra of the polyp and cyst, which indicates their lower concentration. Moreover, in the spectra of polyp and cyst appear absorption lines corresponding such a substances, as acetone, hydroxyaceton, digidroxyaceton, propionitrile, acrylonitrile, aminopropionitrile, hydroxyacetonitrile, aminoacetonitrile, methylbutironronitrile, propanal, benzaldehyde, glycolaldehyde, lactaldehyde, malone dialdehyde, monoethanolamine, alanine, pyridine, at that their concentration differ significantly. Besides, thermodecomposition products of cyst contain acetic acid and propenoic acid.

So, we can result, that using THz high resolution spectroscopy for analysis of the metabolites composition for the ENT organs tissues can be a powerful apparatus for metabolic diagnostics.

This research was funded by the Russian Science Foundation, grant No. 21-19-00357, https://rscf.ru/en/project/21-19-00357/.

[1] D.S. Wishart, Y.D. Feunang, A. Marcu, et al. HMDB 4.0 — The Human Metabolome Database for 2018, Nucleic Acids Res., vol. 46 (D1), pp. D608-617 (2018).
[2] V.L. Vaks, V.A. Anfertev, V.Yu. Balakirev, et al. High resolution terahertz spectroscopy for analytical applications, Physics Uspekhi, vol. 63, pp. 708–720, (2020).
[3] V. Vaks, A. Aizenshtadt, V. Anfertev, et al. Analysis of the Thermal Decomposition Products of Pathological and Healthy Tissues in Paranasal Sinuses: A High-Resolution Terahertz Gas Spectroscopy Study. Applied Sciences, vol. *11*, pp. 7562 (1-10), (2021).
[4] H.M. Pickett, E.A. Cohen, B.J. Drouin, et al. Submillimeter, Millimeter, and Microwave Spectral Line Catalog. JPL Molecular Spectroscopy, California Institute of Technology, http://spec.jpl.nasa.gov/ftp/pub/catalog/catform.html
[5] C.P. Endres, S. Schlemmer, P. Schilke, et al. The Cologne Database for Molecular Spectroscopy, CDMS, in the Virtual Atomic and Molecular Data Centre, VAMDC, J. Mol. Spectrosc., vol. 327, pp. 95–104, (2016).

DOI: 10.24412/cl-35039-2022-22-212-212

Technologies of Diffractive Optics for IR and THz Ranges

V. Pavelyev[1,2], B. Knyazev[3], M. Komlenok[4], K. Tukmakov[1], T. Kononenko[4], A. Reshetnikov[1], A. Agafonov[1], Yu. Choporova[3], N. Osintseva[3], V. Konov[4], V. Soifer[1,2], G. Kulipanov[3], N. Vinokurov[3]

1 - Samara National Research University, Moskovskoye Shosse 34, Samara, Russia, 443086
2 - IPSI RAS – Branch of the FSRC "Crystallography and Photonics" RAS, Molodogvardeyskaya 151, Samara, Russia, 443001
3 - Budker Institute of Nuclear Physics of SB RAS, Pr. Lavrentyeva 11, Novosibirsk, Russia, 630090
4 - Prokhorov General Physics Institute of the Russian Academy of Sciences, Vavilova str. 38, 119991 Moscow, Russia
pavelyev10@mail.ru

Technologies for silicon and diamond transmissive diffractive microoptics have been developed [1-6]. Silicon and diamond diffractive optical elements for focusing terahertz laser beam [1-3] as well for formation of terahertz laser beam with pre-given mode composition [4] and polarization state [5] have been fabricated and experimentally investigated. The experiments were carried out at a wavelength of 130-150 μm using the Novosibirsk Free Electron Laser [6]. Developed technologies are based on lithographic etching [1,4,5] and laser ablation [2,3]. The application of antireflection coating and antireflection structures for decreasing Fresnel losses is considered [6]. Technology of laser ablation was used for fabrication of high-effective infrared (λ=10.6 μm) diamond diffractive optics in before [7]. Besides, technology of micromilling was used for reflective terahertz free-form optics fabrication [8]. In the present talk the fabrication of photonics elements for far terahertz and millimeter ranges is considered. The perspectives of 3D printing application [9] as well as micromilling for fabrication of diffractive optics of submillimeter and millimeter ranges are considered.

The experiments were carried out at the Novosibirsk Free Electron Laser Facility, which is part of "the Siberian Synchrotron and Terahertz Radiation Center".

This work was supported by the Russian Science Foundation grant 19-72-20202.

[1] A.N. Agafonov, B.O. Volodkin, D.G. Kachalov, B.A. Knyazev, G.I. Kropotov, K.N. Tukmakov, V.S. Pavelyev, D.I. Tsypishka, Yu.Yu. Choporova, and A.K. Kaveev, Focusing of Novosibirsk Free Electron Laser (NovoFEL) radiation into paraxial segment. Journal of Modern Optics 63(11), 1051-1054 (2016). https://doi.org/10.1080/09500340.2015.1118163

[2] M.S. Komlenok, T.V. Kononenko, V.I. Konov, Yu.Yu. Choporova, N.D. Osintseva, B.A. Knyazev, V. S. Pavelyev, K.N. Tukmakov, V.A. Soifer, Silicon diffractive optical element with piecewise continuous profile to focus high-power terahertz radiation into a square area, *J. Opt. Soc. Am. B* **38**, B9-B13 (2021) https://doi.org/10.1364/JOSAB.425286

[3] M. Komlenok, T. Kononenko, D. Sovyk, V. Pavelyev, B. Knyazev, E. Ashkinazi, A. Reshetnikov, G. Komandin, V. Pashinin, V. Ralchenko, and V. Konov, Diamond diffractive lens with a continuous profile for powerful terahertz radiation//*Optics Letters*. -2021.- Vol.46, P.340-343. https://doi.org/10.1364/OL.414097

[4] Yu. Yu. Choporova, B. A. Knyazev, G. N. Kulipanov, V. S. Pavelyev, M. A. Scheglov, N. A. Vinokurov, B. O. Volodkin, and V. N. Zhabin, High-power Bessel beams with orbital angular momentum in the terahertz range. Physical Review A 96, 023846 (2017). https://doi.org/10.1103/PhysRevA.96.023846

[5] V.S. Pavelyev, S.A. Degtyarev, K.N. Tukmakov, A.S. Reshetnikov, B.A. Knyazev, Yu. Yu Choporova, (2021). Silicon subwavelength axicons for terahertz beam polarization transformation// *Journal of Physics: Conference Series*, 1745 (1), 012022 doi:10.1088/1742-6596/1745/1/012022

[6] Yu. Choporova, B. Knyazev, V. Pavelyev, Holography with high-power CW coherent terahertz source: optical components, imaging, and applications, *Light: Advanced Manufacturing*, Article number: 31 (2022), https://doi.org/10.37188/lam.2022.031

[7] T.V. Kononenko, D.N. Sovyk, P.A. Pivovarov, V.S. Pavelyev, A.V. Mezhenin, K.V. Cherepanov, M.S. Komlenok, V.R. Sorochenko, A.A. Khomich, V.P. Pashinin, E.E. Ashkinazi, V.G. Ralchenko, V.I. Konov, Fabrication of diamond diffractive optics for powerful CO_2 lasers via replication of laser microstructures on silicon template, Diamond and Related Materials, Volume 101, January 2020, 107656 https://doi.org/10.1016/j.diamond.2019.107656

[8] A.N. Agafonov, B.A. Knyazev, V.S. Pavel'ev, E.I. Akhmetova, and V.I. Platonov, Elements of the Terahertz Power Reflective Optics with Free-Form Surfaces. Optoelectronics, Instrumentation and Data Processing 55(2), 148-153 (2019). 10.3103/S8756699019020067

[9] A. Agafonov, A. Reshetnikov, I. Tzibizov, A. Shakhmin, (2021). The technology of manufacturing metal-dielectric photonic crystals for THz and millimeter ranges by 3D printing// *Journal of Physics: Conference Series*, 1745 (1), 012021 DOI:10.1088/1742-6596/1745/1/012021

DOI: 10.24412/cl-35039-2022-22-213-213

THz quantum cascade lasers with two-photon emission in the gain module grown by MBE and MOCVD

R.A. Khabibullin[1], S.S. Pushkarev[1], R.R. Galiev[1], D.S. Ponomarev[1], I.S. Vasil'evskii[2], A.N. Vinichenko[2], A.N. Klochkov[2], T.A. Bagaev[3], M.A. Ladugin[3], A.A. Marmalyuk[3], K.V. Maremyanin[4], V.I. Gavrilenko[4], D.V. Ushakov[5], A.A. Afonenko[5]

1- V.G. Mokerov Institute of ultra-high frequency semiconductor electronics of RAS, Moscow, Russia
2- National research nuclear university Mephi, Moscow, Russia
3- POLYUS Research Institute of M.F. Stelmakh, Moscow, Russia
4- Institute for Physics of Microstructures of RAS, Nizhny Novgorod, Russia
5- Belarusian State University, Minsk, Belarus
khabibullin@isvch.ru

The possibility of implementing two radiation transitions in the gain module for THz QCL has been shown many times [1,2]. However, the activation of these transitions is achieved at different bias points, which corresponds to the optimal alignment of energy levels for each transition. We propose to add an additional step to the ladder of energy levels in the gain module, equal to the energy of THz photon. Due to the low energy of THz photon, it becomes possible to design the gain module based on the conventional GaAs/$Al_{0.15}Ga_{0.85}As$ heterojunction with two-photon emission at one bias point.

A new lasing scheme with sequential two-photon emission in the gain module for terahertz quantum cascade laser (THz QCL) is proposed and experimentally demonstrated. Unlike the conventional lasing scheme with only one pair of laser levels, here electrons pass through an additional laser level, which is the lower laser level for the first radiation transition and upper laser level for the second one, forming a sequence "resonant tunneling – photon – photon – phonon" (see Fig. 1). The presence of two-photon emission in the gain module reduces the gain saturation with an increase in photon density, which should potentially increase the radiation power. An optimized two-photon design based on GaAs/$Al_{0.15}Ga_{0.85}As$ As four-quantum wells was developed using the balanced equation method [3,4] and grown by two epitaxial techniques – molecular beam epitaxy (MBE) and metal organic chemical vapor deposition (MOCVD). THz QCLs based on both MBE and MOCVD structures have a lasing frequency of 3.8 THz (see Fig. 2) and maximum operation temperature around 100 K.

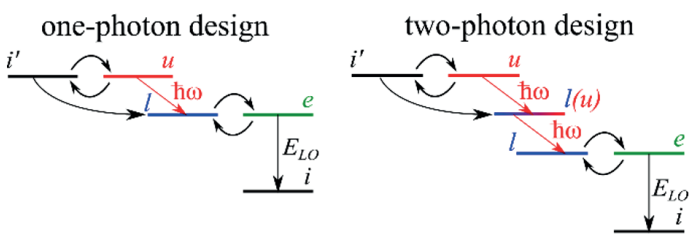

Fig. 1. Schematic diagram of one- and two-photon designs with resonant phonon depopulation mechanism of lower laser level.

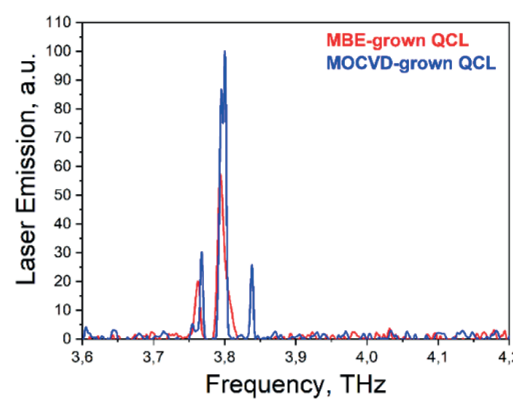

Fig. 2. Emission spectra of MBE- and MOCVD-grown THz QCLs with two-photon design.

[1] S. Kumar, C. Chan, Q. Hu, J. Reno, "A 1.8-THz quantum cascade laser operating significantly above the temperature of ħω/kB," Nature Phys., vol. 7, pp. 166–171, (2011).
[2] B. Wen, C. Xu, S. Wang, K. Wang, M. C. Tam, Z. Wasilewski, D. Ban, "Dual-lasing channel quantum cascade laser based on scattering-assisted injection design," Opt. Express vol. 26, pp. 9194–9204, (2018).
[3] D. V. Ushakov, A. A. Afonenko, A. A. Dubinov, V. I. Gavrilenko, O. Yu. Volkov, N. V. Shchavruk, D. S. Ponomarev, R. A. Khabibullin, "Balance-equation method for simulating terahertz quantum-cascade lasers using a wave-function basis with reduced dipole moments of tunnel-coupled states," Quantum Electronics, vol. 49, pp. 913–918, (2019).
[4] D. Ushakov, A. Afonenko, R. Khabibullin, D. Ponomarev, V. Aleshkin, S. Morozov, A. Dubinov, "HgCdTe-based quantum cascade lasers operating in the GaAs phonon Reststrahlen band predicted by the balance equation method," Opt. Express, vol. 28, pp. 25371–25382, (2020).

DOI: 10.24412/cl-35039-2022-22-214-214

Classification of chocolates by multivariate methods in THz spectroscopy

M. Khodasevich[1], A. Lyakhnovich[1], H. Eriklioğlu[2]

1 – B.I.Stepanov Institute of Physics, National Academy of Sciences of Belarus, Minsk, Nezavisimosti Ave., 68-2
2 – Middle East Technical University, Ankara, Turkiye
e-mail address: m.khodasevich@ifanbel.bas-net.by

Non-destructive and non-contact methods of diagnostics of the composition, quality and authenticity of food products are intensively developing in the world. Interest in these methods is due to the need for food safety and protection of the rights of consumers and producers. The THz frequency range has recently been added to the traditional UV, VIS and NIR spectroscopy. We study different types of chocolates (bitter, dessert, milk) from different manufacturers from Belarus, Russia, Turkiye and Ukraine. A description of the THz spectrometer used and measurement conditions is given in [1].

The aim of the work is to demonstrate the possibility of classifying chocolates by type and manufacturer by the "spectralprint" method [2]. Correction of transmission spectra baselines by the method of adaptive iteratively reweighted least squares with a penalty [3] is applied as a preprocessing procedure to the THz spectra. It allows to get rid of significant noise caused by Fabry-Perot effects and the presence of water vapor in the measuring path of spectrometer. The baselines of THz transmission spectra are used for multivariate analysis. Score plot in two-dimensional space of principal components [4] is shown in Figure 1 on the left. The symbols indicate the type of chocolates. Two principal components explain 95.6 % of the total variance of the baselines. The application of hierarchical cluster analysis [5] in this space makes it possible to classify 5 studied types of chocolates with precision (the ratio of true positive solutions of the classifier to the sum of true positive and false positive solutions) of 0.94 and recall (the ratio of true positive solutions to the sum of true positive and false negative solutions) of 0.93. The dendrogram of the classifier is shown in Figure 1 on the right where serial numbers correspond to the left figure. This figure is useful when analyzing cluster agglomeration and shows erroneous decisions of the classifier. The obtained precision and recall values are sufficient for practical application for the classification of chocolates. The applied methods are based on the a priori hypothesis of compactness of the location of objects in the space of the principal components of the baselines of THz transmission spectra of various types of chocolates.

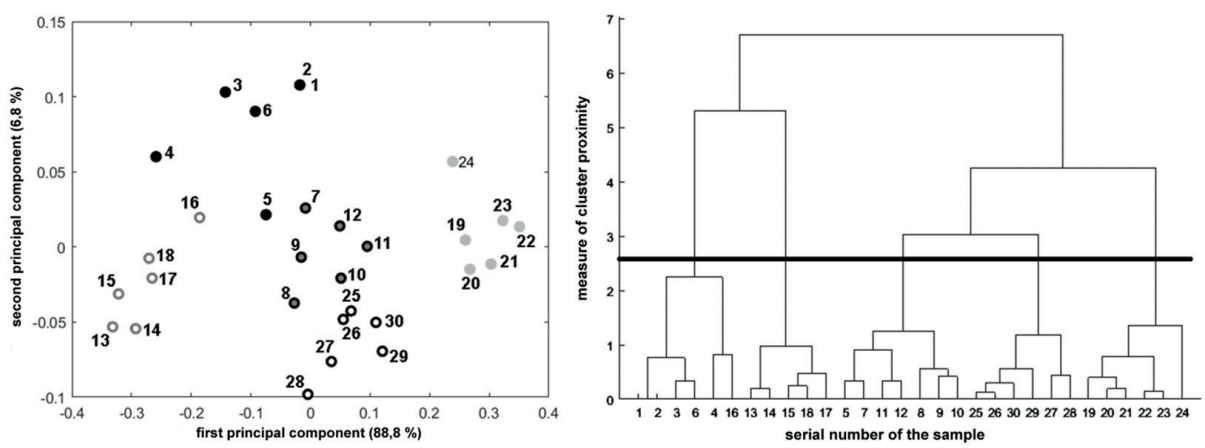

Fig. 1. Score plot in two-dimensional space of principal components of THz spectra baselines and dendrogram of hierarchical cluster analysis with selection of 5 types of chocolate.

[1] M. Khodasevich, A. Lyakhnovich, H. Eriklioğlu, Chocolate sample classification by preprocessed THz transmission spectra analysis, Journal of Applied Spectroscopy, vol. 89, pp 251-255 (2022).
[2] R. Ríos-Reina [et al.], Spectralprint techniques for wine and vinegar characterization, authentication and quality control: Advances and projections, Trends in Analytical Chemistry, vol. 134, pp. 116121:1-21 (2021).
[3] Z. M. Zhang [et al.], Baseline correction using adaptive iteratively reweighted penalized least squares, Analyst,vol.135, pp. 1138-1146 (2010).
[4] R. Bro, A.K. Smilde, Principal component analysis, Analytical Methods, vol. 6, pp. 2812–2831 (2014).
[5] T.W. Liao, Clustering of time series data – a survey, Pattern Recognition, vol. 38, pp. 1857–1874 (2005).

DOI: 10.24412/cl-35039-2022-22-215-215

THz generation in multi-terawatt laser plasma

M. M. Nazarov[1], P. A. Shcheglov[1], M. V. Chaschin[1], A.A.Tausenev[1,2], A.A. Garmatina[1], A.V.Mitrofanov[1,3], D. A. Sidorov-Biryukov[1,2,3].

1 - Kurchatov Institute National Research Center, Moscow 123182, Russia
2 - Physics Department, M.V. Lomonosov Moscow State University, Moscow 119992, Russia
3 - Russian Quantum Center, Skolkovo, Moscow Region 143025, Russia
Nazarov email address: nazarovmax@mail.ru

Powerful THz pulses are requested for the novel area of nonlinear optics in THz range, for accelerating charged particle bunches, for time-resolved experiments on matter manipulation. High-power THz radiation could be obtained from tera- and peta-watt class Ti:sapphire lasers if the problems of saturation and breakdown of materials were solved. One of the media free from saturation problems for conversion into THz at relativistic intensity and multiterawatt pulses is a metal foil (and a dense plasma above it surface). The other media is low-dense plasma in a low-pressure gas discharge, which is efficient and well studied for subterawatt, two-color pulses [1].

We experimentally compare the maximum energy of the obtained THz radiation in these two cases. To characterize the spatiotemporal dimensions of the plasma above the metal and the actual laser intensity, optical harmonics and X-ray radiation from the Cu target are also measured, which correlate with the THz output [2]. The observed effect of the foil thickness on the yield of all secondary radiation indicates the contribution of recirculating hot electrons in the thin foil [3]. While no saturation of the THz radiation output from the metal was observed up to intensities of 10^{18} W/cm^2, the resulting energy of 0.2 μJ is still less than in the case of THz generation in a low-pressure gas under two-color pumping. High-power THz pulses with an energy of 4 μJ and a spectral width of up to 6 THz obtained in the gas case unfortunately completely saturates at laser energies above 40 mJ under any optimization of the parameters of laser irradiation. The prospects of metal as a medium for conversion of laser pulses with energies of 0.5-7 J into THz is discussed. In addition, the spectrally bright Cu K_α X-ray radiation, which is best generated at subrelativistic intensity, is used for diffraction, that is, diagnostics with angstrom spatial resolution, all with femtosecond time resolution.

The work is partly supported by Ministry of Science and Higher Education of the Russian Federation in framework of Agreement No. 075-15-2022-830 and partly by RFBR grant N 20-21-00140.

Концевые сноски

1 M. M. Nazarov, A. V. Mitrofanov, D. A. Sidorov-Biryukov, et.al. JIMTW, 1-13.(2020).
2 M. M. Nazarov, P. A.Shcheglov, M. V.Chaschin, et.al. JPCS, 1692, 012018, (2020).
3 M. M. Nazarov, P. A.Shcheglov, A. A.Garmatina, et.al. Quant.Electron. in print, (2022).

DOI: 10.24412/cl-35039-2022-22-216-216

Ultrafast pump-probe spectroscopy of 1D van der Waals heterostructures

M. Burdanova[1,2], James Lloyd-Hughes[3]

1- Institute of Solid State Physics of the Russian Academy of Sciences, Chernogolovka, Russia
2-Center for Photonics and 2D Materials, Moscow Institute of Physics and Technology, Dolgoprudny, Russia
3- University of Warwick, Department of Physics, Gibbet Hill Road, Coventry, CV4 7AL, United Kingdom
Main author email address: burdanova.mg@mipt.ru

A novel class of 1D nanomaterials was created by building radial heterostructures, such as wafer scale, free-standing thin films of MoS_2 nanotubes grown outside BN nanotubes and carbon nanotubes[1, 2]. We examined the optoelectronic properties of atomically thin 1D van der Waals heterostructures comprising the single-walled carbon nanotubes wrapped by insulating BN layers and MoS_2 outer layers (MoS_2@BN@CNT). Here we will present the equilibrium properties of such materials (through optical absorption, Raman scattering, photoluminescence, FTIR and THz spectroscopy studies), and the dynamical properties of excitons and free charges (via optical pump-optical probe, and optical pump –THz probe spectroscopy). The radial heterostructure showed a unique THz photoconductivity that dynamically changed from anomalous (positive $\Delta T/T$, corresponding to negative photoconductivity) to normal (positive),driven by mobile free charges in the MoS_2 with a mobility comparable to high-quality 2D MoS_2. In addition, optical pump–white light probe spectroscopy revealed that excitons are the primary initial photoproduct in the MoS_2 nanotubes of the present vdW heterostructure. We discuss the co-existence of free charges and excitons in the heterostructure.

[1] M.G.Burdanova et al. Ultrafast optoelectronic processes in 1D radial van der Waals heterostructures: carbon, boron nitride and MoS_2 nanotubes with coexisting excitons and highly mobile charges. Nano Lett., 20, 5, pp. 3560–3567, (2020)
[2] R. Xiang et al., One-dimensional van der Waals heterostructures, Science, 367, 6477, pp. 537-542 (2020)

DOI: 10.24412/cl-35039-2022-22-217-217

Analysis of rodent's urine vapors with using THz high resolution spectrometer for revealing the markers of dysbacteriosis

V.L.Vaks[1,2], V.A.Anfertev[1], E.G.Domracheva[1], M.B.Chernyaeva[1,2], T.G, Shcherbatyuk[3], E.S.Zhukova[3]

1 - Institute for Physics of Microstructures RAS, 603950, Russia, Nizhny Novgorod, GSP-105
2- Lobachevsky University, 603022, Russia, Nizhny Novgorod, Gagarina av., 23
3- Nizhny Novgorod research institute for hygiene and occupational pathology», Rospotrebnadzor, Nizhny Novgorod, 603105 Russia, Semashko str., 20
elena@ipmras.ru

Nowadays there is a trend towards diagnosing diseases and pathologies, as well as the impact of therapy on the human body, based on identifying the metabolic profile of the disease, i.e. a set of metabolites – final or intermediate products of metabolism in the living body, specific for a given disease or pathology. The search for biomarkers is possible in exhaled breath, as well as in biological liquids (blood, urine, saliva, etc.), and this is often more informative, because substances may be present in high concentrations [1]. Preclinical trials of approaches to the treatment of diseases, including socially significant ones, such as dysbacteriosis, are carries out on rodents.

The thermal decomposition products content of the line of the urine samples of rats with artificially induced dysbacteriosis was studied in this work. A promising approach for studying multicomponent gas mixtures of various origins, including biological ones, is molecular absorption spectroscopy, in particular, nonstationary spectroscopy in the terahertz (THz) frequency range [2]. The advantages of the THz frequency range (100 GHz-10 THz) is the presence of absorption lines of the rotational spectrum, as well as low-frequency vibrational spectra of molecules. When radiation that has passed through a gaseous sample is detected, absorption lines are recorded in the spectrum, which are an unambiguous characteristic of specific substances. By the presence of these absorption lines, the conclusion about the presence of these substances in the studied multicomponent gas mixture can be done, and, therefore, potential markers of pathologies, diseases and markers that characterize the effects of various effects on a living organism, can be identified. A set of metabolites (see Figure) appeared during thermal decomposition of samples (healthy, with artificially induced dysbacteriosis, with various treatment regimens) was revealed, and the compositions of gaseous products were compared. The presented approach is promising for the development of a non-invasive research method that allows to identify markers that reflect the presence of dysbacteriosis, as well as to assess the impact on the rat's organism during the therapy.

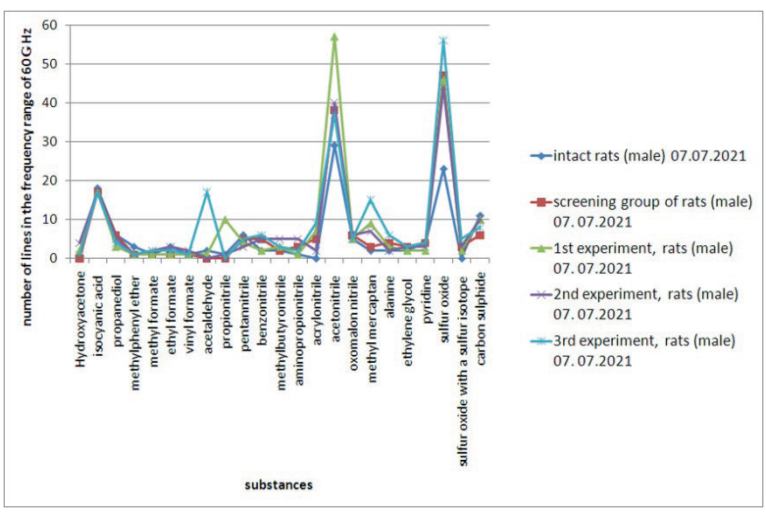

The authors acknowledge the support from Russian Scientific Foundation (grant 21-72-30020, https://rscf.ru/project/21-72-30020/).

[1] A. Amann, B. de Lacy Costello, M. Miekisch, J. Schubert et al. The human volatilome: volatile organic compounds (VOCs) in exhaled breath, skin emanations, urine, feces and saliva, J. Breath Res. vol.8, P. 034001 (17pp.) (2014).
[2] V. Vaks, V. Anfertev, V. Balakirev, S. Basov, E. Domracheva, A. Illyuk, P. Kupriyanov, S. Pripolzin, M. Chernyaeva. High resolution terahertz spectroscopy for analytical applications. Phys. Usp. vol. 63, pp. 708–720, (2020).

DOI: 10.24412/cl-35039-2022-22-218-219

Морфологические и фотоэлектрические исследования твердого раствора $(GaAs)_{1-x-y}(Ge_2)_x(ZnSe)_y$

С.З. Зайнабидинов, А.Й. Бобоев

Андижанский государственный университет им. З.М. Бабура, Андижан,170100 Узбекистан
e-mail: prof_sirojiddin@mail.ru

Качественный прорыв в области получения полупроводниковых наноструктур связан с эффектом самоорганизации полупроводниковых наноструктур в гетероэпитаксиальных полупроводниковых системах. Спонтанное появление на поверхности периодически упорядоченных структур и на эпитаксиальных пленках полупроводников охватывает широкий спектр явлений в физике твердого тела и в полупроводниковой технологии [1]. Появление упорядоченных массивов квантовых точек за счет эффекта самоорганизации играет важную роль в создании устройств, работающих на основе размерных эффектов. Поскольку параметр решетки Ge(a_{Ge} =5.6576 Å), а соединения GaAs(a_{GaAs}=5.6532 Å) и ZnSe(a_{ZnSe}=5.6676 Å) [2] имеет близкие значения, и они имеют одинаковую кристаллическую структуру (цинковая обманка), эти соединения являются перспективными материалами для получения высококачественных гетероструктур Ge/ZnSe/GaAs и непрерывных твердых растворов замещение типа $(GaAs)_{1-x}(ZnSe)_x$, $(Ge)_{1-x}(ZnSe)_x$ и $(Ge)_{1-x-y}(GaAs)_x(ZnSe)_y$ [2]. Качество таких гетероструктур - это один из ключевых моментов для производства оптоэлектронных устройств, таких как лазеры и светодиоды. В данной работе представлены результаты морфологических и фотоэлектрических исследований твердых растворов $(GaAs)_{1-x-y}(Ge_2)_x(ZnSe)_y$, выращенных на подложке *n*-GaAs, ориентированного по направлению (100) методом принудительного охлаждения.

Исследования поверхности твердого раствора $(GaAs)_{1-x-y}(Ge_2)_x(ZnSe)_y$ проводились с использованием атомно-силового микроскопа (АСМ) „Solver-NEXT“. На рис. 1-*a* показано трехмерное АСМ изображение эпитаксиальной пленки. Видно, что на поверхности образуются отдельные нанооствровки характерного размера. Анализ показал, что на этапе роста, нанооствровки ZnSe твердого раствора $(GaAs)_{1-x}(Ge_2)_x$, имеют геометрическую форму купола, т.е. так называемые *dome* – островки с характерным латеральным размером 55-60 нм, с круглым основанием. На рис. 1-*b* приведены результаты исследований локальной проводимости нанообъектов ZnSe на поверхности твердого раствора $(GaAs)_{1-x}(Ge_2)_x$ полученных методом контактной АСМ. Измерения локальных значений сопротивления растекания проводились параллельно с данными топографии. Из рис. 1-*b* видно, что светлым участкам соответствуют большие токи и имеют более низкое сопротивление растекания. Согласно полученным данным, нанооствровки ZnSe обладают повышенной проводимостью по сравнению с твердым раствором $(GaAs)_{1-x}(Ge_2)_x$. Это означает, что если квантовые точки из нанооствровков ZnSe (E_g=2,7 эВ) более широкозонные, чем GaAs (E_g=1,44 эВ) или Ge (E_g=0,67 эВ), то транспорт носителей через нанообъекты будет облегчен.

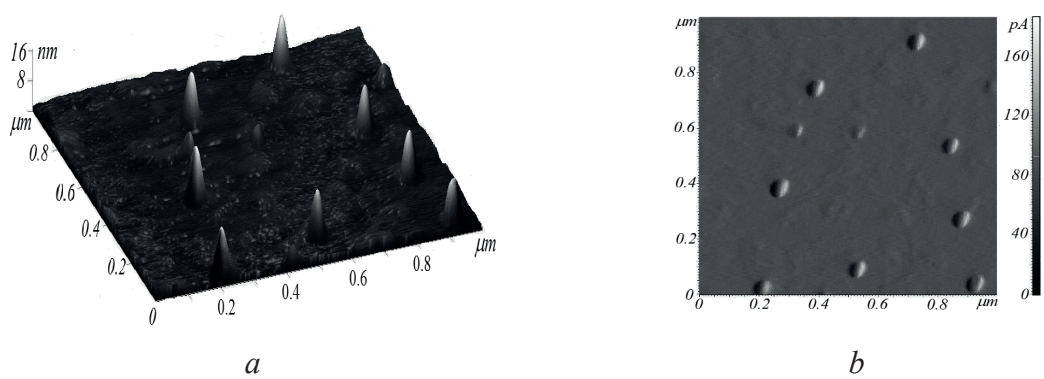

a *b*

Рис.1. Трехмерное изображение поверхности эпитаксиальной пленки $(GaAs)_{1-x-y}(Ge_2)_x(ZnSe)_y$ (а) и карта локальной проводимости нанообъектов ZnSe (б)

Люкс-амперные характеристики структур, полученные при освещении интегральным светом показали, что зависимость тока короткого замыкания ($I_{к.з.}$) от освещенности имеет нелинейную зависимость в начальном участке, т.е. увеличение величины падающего света приводит к волнообразному возрастанию $I_{к.з,}$ что может быть связано с изменениями параметров контактирующих полупроводников под влиянием потока светового излучения (время жизни неосновных носителей заряда, диффузионная длина. (Рис. 2). С ростом интенсивности

падающего света, ЭДС холостого хода стремился к насыщению, достигая при этом значения 0.6 В, что может быть связано с невозможностью уменьшения толщины переходного слоя между эпитаксиальной пленкой и подложкой под воздействием падающего света.

Измерение спектральной зависимости фототока в фотодиодном режиме (рис. 3), показало, что оно охватывает широкий интервал энергии падающих квантов от 1,07 эВ до 3 эВ.

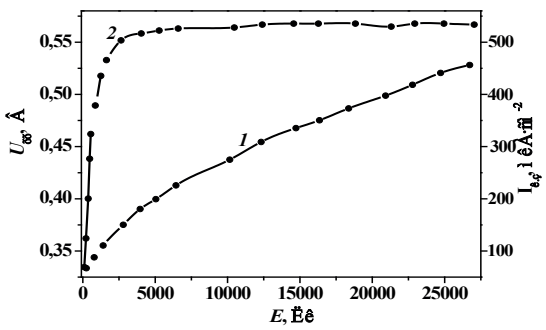

Рис. 2. Зависимости тока короткого замыкания (*1-кривая*) и ЭДС холостого хода (*2-кривая*) от освещенности интегральным светом.

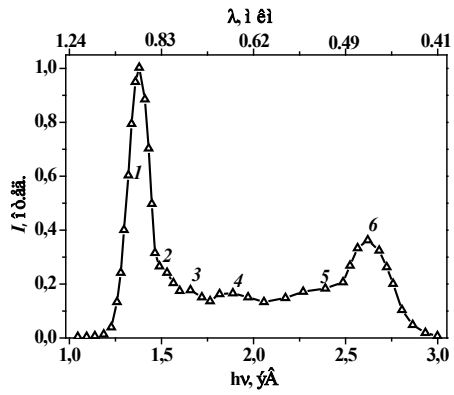

Рис. 3. Спектральная зависимость фототока структуры *n*-GaAs-*p*-$(GaAs)_{1-x-y}(Ge_2)_x(ZnSe)_y$ полученная в фотодиодном режиме.

Из рис. 3. видно, что спектр фоточувствительности гетероструктур в интервале энергий 1-3 эВ характеризуется шестью пиками с пиками с максимумами при энергиях фотонов эВ: *1*-при 1.37, *2*-1.47, *3*-1.65, *4*-1.88, *5*-2.3, *6*-2.62. Спектр начинается с энергии фотонов 1,07 эВ, который возможно, обусловлен энергией связи парных атомов Ge, которые частично замещают некоторые молекулы арсенида галлия и создают соответсвующий энергетический уровень [3]. Кроме того, примесные атомы германия самоорганизуются в нанокристаллиты в дефектоспособных областях арсенид галлиевой решетки [4], и они формируют собственный энергетический уровень с акцепторным характером [5]. При энергии фотонов 1,47 эВ наблюдается фотопик, соответствующий рекомбинации из зоны проводимости на акцепторные состояния в p-GaAs [6]. Следующий фотопик спектральной зависимости фоточувствительности наблюдается при 1,65 эВ, что возможно обусловлен со структурной щелью валентной зоны и изовалентними примесями соединений Ge-Se в слое GaAs [9]. Следующие фотопики, соответствующие энергиям фотонов 1.88, 2.3 и 2.62 эВ, возможно обусловлены соединениями GaSe (hv_{max} = 1.88 эВ), ZnAs (hv_{max} = 2.15 эВ) и ZnSe (hv_{max} = 2.69 эВ) с глубокими уровнями в валентной зоне арсенида галлия [4].

Таким образом, анализ данных АСМ показывает, что наноостровки ZnSe в твердом растворе $(GaAs)_{1-x}(Ge_2)_x$ имеют геометрическую форму *dome,* с латеральными размерами 55-65 нм и появление этих форм ZnSe наноостровков обычно объясняется релаксацией упругих напряжений в конфигурации *dome* фазы. В процессе роста эпитаксиальных пленок удалось создать достаточно плотный и однородный по свойствам ансамбль квантово-размерных объектов, обладающих, по сравнению с матрицей, более высокой проводимостью. Исследованы фотоэлектрические свойства *n*-GaAs-*p*-$(GaAs)_{1-x-y}(Ge_2)_x(ZnSe)_y$ гетероструктур, как в фотодиодном, так и в фотовольтаическом режимах. Выявлена, что спектральная зависимость фототока охватывает широкий интервал энергии падающих квантов от 1,07 эВ до 3 эВ.

[1] M. Funato, S. Fujita, and S. Fujita, *Bulletin of Materials Science*, vol. 18, no. 4, pp. 343–365, (1995).
[2] S.Z. Zainabidinov, A.S. Saidov, A.Yu. Leiderman, et al, , *Semiconductors,* vol. 50, no. 1, pp. 59–65, (2016).
[3] С.С. Хлудков. Вестник Томского Государственного университета общенаучный периодический журнал. № 285, 84 (2005).
[4] С.З. Зайнабидинов, А.Й. Бобоев, Ж.Н. Усмонов, Альтернативная энергетика и экология, № 10-12, 43 (2019).
[5] И.К. Полушина, Рудь В.Ю., Рудь Ю.В. Физика и техника полупроводников **33,** No.6, 697 (1999).
[6] Д.И. Блецкан, Й.Й. Мадяр, В.Н. Кабаций, Физика и техника полупроводников **40,** No.2, 142 (2006).

DOI: 10.24412/cl-35039-2022-22-220-220

Five-Fold Frequency Multiplication in MW-Level Gyrotrons as a Way to High-Power THz Radiation Sources

I. Zotova, G. Denisov, A. Malkin, A. Sergeev, I. Zheleznov, M. Glyavin

Institute of Applied Physics RAS (IAP RAS), 46 Ul'yanov str., Nizhny Novgorod, Russia
zotova@ipfran.ru

Multiple applications, including spectroscopy with high resolution, remote sensing, high-speed wireless communications, biomedicine, security and many others [1-3], require CW, compact and powerful radiation sources operating in the terahertz gap, i.e., at frequencies from 0.3 to 10 THz, to be developed. This problem still remains pretty much unresolved, as THz frequencies are "too low" for quantum devices and "too high" for classical electronics associated with radiation of rectilinear electron beams in slow-wave structures. Lack of powerful radiation sources is especially critical in the 1 to 2 THz band.

We propose the concept of high-power THz radiation sources based of fivefold frequency multiplication in high-power gyrotrons intended for plasma applications. The efficient excitation at the 5th cyclotron harmonic is due to the specific property of the eigenmodes of cylindrical waveguides, as a result of which the conditions of simultaneous electrodynamic resonance can be asymptotically satisfied at two selected *TE* modes suitable for multiplication effect. At the previous stage of research, the proposed approach was verified in the proof-of-principle experiment based on the setup of the fundamental harmonic 45 GHz/20 kW gyrotron [4]. In the experiment, the 5th harmonic excitation of $TE_{30,12}$ at the frequency of 225 GHz was obtained with power-level of 100 mW.

The possibility of reaching the THz range based on a fivefold frequency multiplication with a higher power level is associated with the use of higher frequency MW-level gyrotrons. However, this scheme may be limited by mode competition at the fundamental harmonic. Within the frame of time-domain averaged model, we demonstrate possibility of Watt-level 1.25 THz 5th harmonic excitation in a recently developed sub-MW 0.25 THz gyrotron with $TE_{19,8}$ operating mode [5]. The operating zone with efficient excitation of the 5th cyclotron harmonic can be significantly expanded when the gyrotron is locked by an external signal which suppresses parasitic oscillations [6].

The work is supported by the government contract of IAP RAS #0030-2019-0027 (Program "Development of equipment, technologies and research in the field of atomic energy use in the Russian Federation for the period up to 2024").

[1] E. Bründermann, H.-W Hübers and M.F. Kimmitt. Terahertz techniques. Springer Series in Optical Sciences, Springer, Berlin/ Heidelberg, 2012
[2] M. Tonouchi. "Cutting-edge terahertz technology", Nature Photon. 1, 97 (2007) doi: 10.1038/nphoton.2007.3
[3] S. Sabchevski, M. Glyavin, S. Mitsudo et al. "Novel and Emerging Applications of the Gyrotrons Worldwide: Current Status and Prospects", J Infrared Milli Terahz Waves, **42,** 715–741 (2021) doi: 10.1007/s10762-021-00804-8
[4] G. Denisov, M. Glyavin, A. Tsvetkov et al. "A 45-GHz/20-kW gyrotron-based microwave setup for the fourth-generation ECR ion sources", IEEE Trans. Electron Dev. 65, 3963 (2018) doi: 10.1109/TED.2018.2859274
[5] G. Denisov, M. Glyavin, A. Fokin et al. "First experimental tests of powerful 250 GHz gyrotron for future fusion research and collective Thomson scattering diagnostics", Rev. Sci. Instr. 89, 084702 (2018) doi: 10.1063/1.5040242
[6] V. Bakunin, G. Denisov and Yu. Novozhilova. "Principal enhancement of THz-range gyrotron parameters using injection locking", IEEE Electron Dev. Lett. 41, 777 (2020) doi: 10.1109/LED.2020.2980218

DOI: 10.24412/cl-35039-2022-22-221-221

Narrowband THz generation in nonlinear molecular crystals

A. Sinko[1,2]

[1]*Faculty of Physics, Lomonosov Moscow State University, Moscow, Russia*
[2]*Institute on Laser and Information Technologies - Branch of the Federal Scientific Research Center "Crystallography and Photonics" of the Russian Academy of Sciences, Shatura, Russia*
as.sinjko@physics.msu.ru

In the past years multicycle terahertz sources became very demanded in different fields of photonics, some of the main of which are: creating compact and convenient table-top free-electron lasers, where THz frequency range paves a way to higher field strength for electron acceleration and deceleration with significant excess of damage threshold depending on central frequency and pulse duration; developing narrowband sources for the efficiency and frequency resolution increase in THz nonlinear generation physics and resonant nonlinear spectroscopy. The most constructively convenient way to generate THz radiation is a nonlinear source usage. Certain molecular crystals have resonant phonon modes falling in the low-THz frequency range. Despite a widespread point of view that low-energy phonons negatively affect the generation of THz radiation, since first order and second order susceptibilities are affected by the high Q-factor phonon resonances, we can tune the conditions in such a way that the nonlinear conversion efficiency will be extremely high and noncritical phase matching conditions will be achieved only in a narrow spectral region around the phonon peaks.

Semiorganic molecular crystal guanylurea hydrogen phosphite $(NH_2)_2CNHCO(NH_2)H_2PO_3$ (GUHP) has several phonon resonances in the THz frequency range, which are defined by the molecular basis structure glued with hydrogen bonds and may be selectively tuned by the orientation and temperature of the sample [1-3]. We report on the nonlinear excitation the molecular phonon subsystem and multicycle THz pulse generation in GUHP crystal. The generated THz pulses are multicycle and thus have narrowband emission spectra, which width can be reduced up to 6.2 GHz, and the peak position may be tuned from 1.03 to 1.67 THz. Based on the THz-TDS and Raman experimental results we assume that the spectral properties of generated THz radiation in GUHP molecular crystal are determined by the stimulated Raman scattering on the both IR- and Raman- active vibrational resonances.

We have also investigated the possibility of narrowband THz generation in molecular crystals of phthalic acid: potassium, rubidium, cesium and ammonium acid phthalate. It turned out that, despite the same syngony and the presence of absorption peaks in the THz frequency range, the narrowband THz generation is possible only in crystals with all both IR- and Raman- active vibrational modes.

This work was supported by the Russian Foundation for Basic Research (projects 19-52-55004 and 20-32-90234) and by the Ministry of Science and Higher Education within the State assignment FSRC "Crystallography and Photonics" RAS.

[1] A. S. Sinko et al., "Molecular crystal (GUHP) for narrow-band pulsed THz generation with NIR femtosecond laser." 2021 46th International Conference on Infrared, Millimeter and Terahertz Waves (IRMMW-THz), 2021, pp. 1-2.
[2] A. S. Sinko et al., "Terahertz dielectric properties of guanylurea hydrogen phosphite crystal." 2021 46th International Conference on Infrared, Millimeter and Terahertz Waves (IRMMW-THz), 2021, pp. 1-2.
[3] Sinko, A., et al. "A monoclinic semiorganic molecular crystal GUHP for terahertz photonics and optoelectronics." Scientific reports 11.1 (2021): 1-13.

DOI: 10.24412/cl-35039-2022-22-222-222

Microsphere Sensors Based on Thermo-Optical Effect in Different Glasses: Modelling and Experiment

M.P. Marisova, A.V. Andrianov, E.A. Anashkina

Institute of Applied Physics, Russian Academy of Sciences, 46 Ulyanov St., Nizhny Novgorod, 603950, Russia
marisova.mariya@rambler.ru

Microresonators with whispering-gallery modes (WGMs) are now widely used in photonics [1].The thermo-optical effect in microspheres leading to WGM shifts can be used for sensing applications [2]. Here we study temperature microsphere sensors made of different glasses and transient nonlinear WGM shifts caused by partial thermalization of a laser pump.

The most common glass microresonator design is a fused silica (SiO_2) microsphere. However, investigating other materials could lead to the development of new microsensors with improved characteristics. In total, five optical glasses were considered: common silica (SiO_2), germanate (GeO_2), tellurite (TeO_2–WO_3–La_2O_3, TWL), and two types of chalcogenide glass (As_2S_3 and As_2Se_3).

Eigenfrequencies of an ideal dielectric microsphere can be obtained from the characteristic equations [3]. A variation in ambient temperature ΔT causes microresonator size and the refractive index of the glass to change due to the effect of thermal expansion and the thermo-optic effect, respectively. These two phenomena inevitably lead to thermally-induced WGM frequency shift. To describe this process numerically, we developed a computer code for solving the characteristic equation; temperature increase and glass dispersion were taken into account.

We found that in the considered parameter range (microsphere radius R=20…200 μm; temperature increase ΔT=0…100 K) the resulting WGM wavelength shift Δλ is an almost linear function of ΔT for modes near λ≈1.55 μm. The corresponding temperature sensitivity Δλ/ΔT is practically independent of R (Fig. 1a) (detailed explanation is given in [4]). The largest sensitivity is achieved for chalcogenide glass microspheres: 42.2 pm/K for As_2S_3 and 48.1 pm/K for As_2Se_3; it is several times larger than for common SiO_2 microsensors (13.4 pm/K). We also confirmed that for non-fundamental WGMs the differences are negligible.

The characteristic temperature relaxation time $\tau_{\Delta T}$ is another important parameter for sensing. To calculate $\tau_{\Delta T}$ we solved the heat equation numerically for an experiment-like geometry (Fig. 1b). It was found that $\tau_{\Delta T} \sim R^2$, as shown in Fig 1c for As_2S_3. This result coincides well both with the experiment and with the analytical solution for a uniformly heated ideal sphere [4].

This work was supported by the Russian Science Foundation, Grant No. 20-72-10188 (study of silica and tellurite microspheres) and by the Ministry of Science and Higher Education of the Russian Federation, Grant No. 075-15-2021-633 (study of germanate and chalcogenide microspheres).

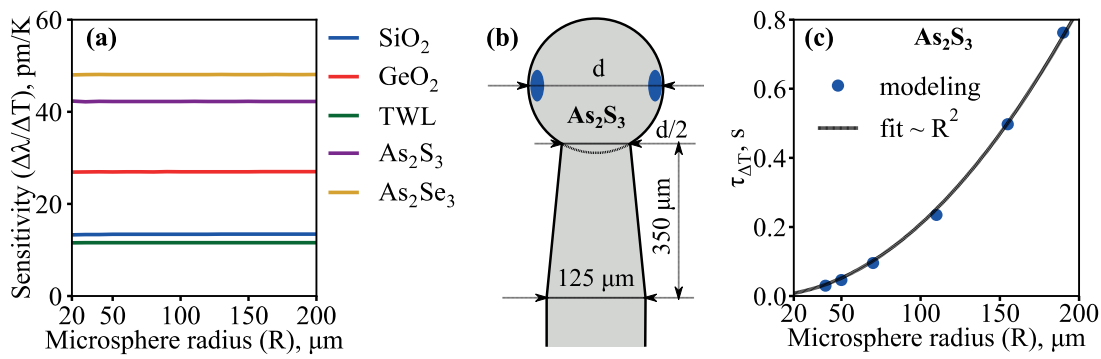

Fig. 1. (a) Calculated temperature sensitivity near λ≈1.55 μm as a function of microsphere radius for different glasses. (b) Scheme of the geometry used in simulations. Blue areas mark pump absorption regions. (c) Calculated temperature relaxation time $\tau_{\Delta T}$ as a function of R for As_2S_3 microspheres. Dashed line shows $\tau_{\Delta T} \sim R^2$ fit.

[1] T.J. Kippenberg, A.L. Gaeta, M. Lipson, M.L. Gorodetsky, Dissipative Kerr solitons in optical microresonators, Science, vol. 361, eaan8083, (2018).
[2] X. Jiang, A.J. Qavi, S.H. Huang, L. Yang, Whispering-Gallery Sensors, Matter, vol. 3, pp. 371–392, (2020).
[3] A.N. Oraevsky, Whispering-Gallery Waves, Quantum Electronics, vol. 32, pp. 377–400, (2002).
[4] A.V. Andrianov, M.P. Marisova, E.A. Anashkina, Thermo-Optical Sensitivity of Whispering Gallery Modes in As_2S_3 Chalcogenide Glass Microresonators, Sensors, vol. 22, 4636, (2022).

DOI: 10.24412/cl-35039-2022-22-223-223

Fundamental and practical properties of stretchable carbon nanotubes under ultrafast pump-probe spectroscopy

M. Paukov[2], A. Goldt[4], A. Nasibulin[4], James Lloyd-Hughes[3], A. Arsenin[2], V. Volkov[2], M. Burdanova[1,2]

1- Institute of Solid State Physics of the Russian Academy of Sciences, Chernogolovka, Russia

2 - Center for Photonics and 2D Materials, Moscow Institute of Physics and Technology, Dolgoprudny, Russia
3 - University of Warwick, Department of Physics, Gibbet Hill Road, Coventry, CV4 7AL, United Kingdom
4 –Skolkovo Institute of Science and Technology, Moscow

Main author email address: paukov.mi@phystech.ru

Devices which rapidly modulate THz beams are at high demand because of the advancement of communication systems such as 5G. In this work we report the fundamental and experimental results of optical-pump-terahertz-probe spectroscopy method applied to stretchable films of carbon nanotubes (CNT). It provides the information on the photo-induced conductivity of differently stretched CNT-films and the decay-time, which relies the behaviour of recombination of charge particles under the pump-light. Practical parameters of CNT such as modulation depth (MD), modulation speed (MS), energy modulation depth (EMD) for different relative stretching were also obtained. The experiment has shown that CNT possess highly effective characteristics, compared to previously studied materials. It makes them promising candidates for applications in the field of modulators of the terahertz signal, because at the same time it is possible to control their properties not only by the means of the intensity of light, but also by stretching.

DOI: 10.24412/cl-35039-2022-22-224-224

Angular structure of the optical-terahertz biphoton field

P.A. Prudkovskii

Lomonosov Moscow State University, Faculty of Physics, Moscow 119991, Russia
e-mail: vysogota@gmail.com

The structure of angular eigenmodes of an optical-terahertz biphoton field, which arises in the case of strongly non-degenerate parametric down-conversion, is theoretically investigated [1]. The azimuthal eigenmodes are obtained by diagonalizing the operator of the nonlinear interaction of electromagnetic field modes, which takes into account the anisotropy of the crystal quadratic susceptibility tensor [2]. It is shown that if the frequency of the idler terahertz radiation is sufficiently low, then the shape of the eigenmodes does not depend on the parametric gain. In this case, in the basis of angular eigenmodes, the scattering matrix has a simple form of the Bogolyubov transformations.

The dependence of the effective number of angular modes on the frequency of the terahertz idler radiation is calculated (Fig.1). In the case of small parametric gain, this number becomes the Schmidt modes number.

It is shown how the effective number and shape of the angular eigenmodes change when the terahertz idler radiation leaves the crystal through the side surface. The resulting angular structure of the optical-terahertz biphoton field is used to calculate the normalized correlation function of the intensities of the signal and idler radiation g_2 at different frequencies of the terahertz idler radiation and different values of the angular apertures of the detectors (Fig.2) [3].

This work was supported by the Russian Foundation for Basic Research (Grant № 20-02-00621A) and the Russian Science Foundation (Grant № 22-12-00055).

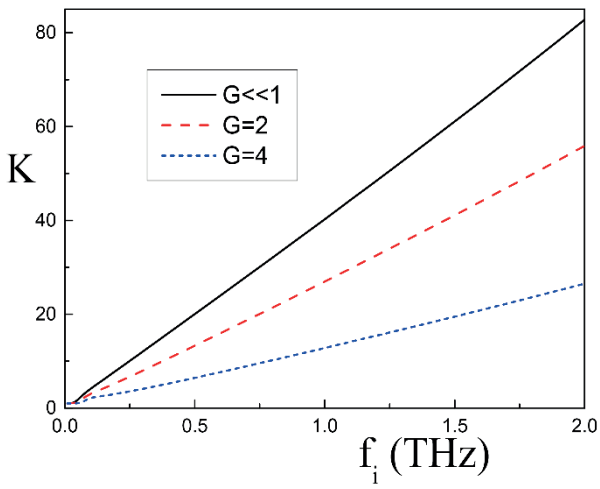

Fig.1. Dependence of the effective number of angular modes K on the frequency of terahertz idler radiation f_i for various parametric gains G.

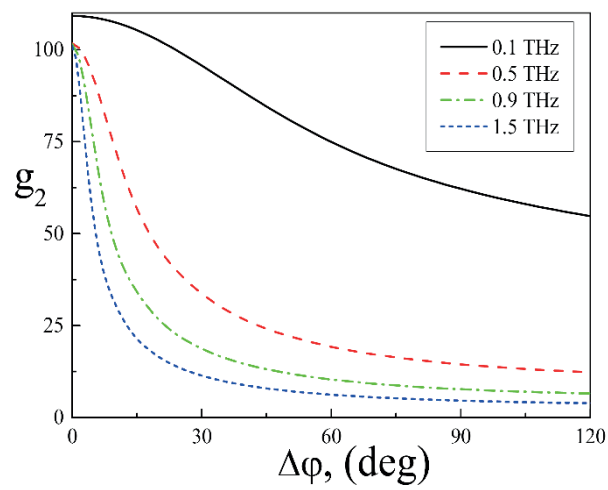

Fig.2. Dependence of the normalized correlation function of the signal and idler radiation intensities g_2 upon spontaneous parametric down-conversion on the angular apertures of the detectors Δφ at different frequencies of the terahertz idler radiation.

[1] G.Kh. Kitaeva, A.A. Leontyev, P.A. Prudkovskii, Quantum correlation between optical and terahertz photons generated under multimode spontaneous parametric down-conversion, Phys. Rev. A, vol.101, pp.053810(1-13) (2020).
[2] L.S. Dvernik and P.A. Prudkovskii, Azimuthal eigenmodes at strongly non-degenerate parametric down-conversion, Appl. Phys. B., vol. 127, p. 85(1-10), (2021).
[3] P.A. Prudkovskii, Correlation properties of an optical–terahertz biphoton field, JETP Lett., vol. 114, pp. 173–179, (2021).

ДЛЯ ЗАМЕТОК

ДЛЯ ЗАМЕТОК